Bioprocessing in Microalgae

A thesis submitted by

Chelsea Marie Brain

For the degree of Engineering Doctorate (EngD) in Biopharmaceutical Process Development

Biopharmaceutical Bioprocessing Technology Centre (BBTC)

School of Chemical Engineering and Advanced Materials (CEAM)

Newcastle University

Sponsored by Scottish Bioenergy Ltd.

March 2017

Abstract

This thesis is a portfolio of three projects carried out with Scottish Bioenergy Ltd, in the area of microalgae biotechnology.

The first small project saw the development of a rapid, simple and relatively low-cost technique based on UV absorbance for measurement of nitrate in two common freshwater and saltwater growth media. The test was successfully demonstrated in batches of *Chlorella*, measuring nitrate concentration as low as 40 μM and requiring only a 2 mL sample.

The second large project investigated the use of a narrow spectrum Light Emitting Diode (LED) with a maximum wavelength (λ_{max}) of 680 nm for the production of the high-value pigment phycocyanin in *Arthrospira* (*Spirulina*). The LEDs produced a substantial over 250 % increase in phycocyanin yield with no significant difference in growth rate in comparison to standard white LEDs, initially requiring an extended photoacclimation period. Although photobioreactor (PBR) systems incorporating the λ_{max} 680 nm would require increased investment in capital and operational expenditure, particularly relating to increased LED cooling requirements, increased product yield and profitability makes a powerful case for switching to longer wavelength red LEDs.

The third project was a feasibility study for the use of directed microevolution to generate a non-genetically modified copper-tolerant *Arthrospira* strain that may be used in a multi-process PBR system fed with distillery wastewater. Resistance 200-fold the typical optimal medium concentration was achieved. However, the extent of resistance was 3-fold lower than required and the length and unreliability made the process impractical for industrial use in generating resistant *Arthrospira* strains.

The projects provided a methodology to assist the company in future research and development, knowledge on the feasibility of a strain development technique and identified an exciting new business opportunity for production of a high-value product in artificially illuminated PBR systems.

Dedication

To my Grandma. Love you more.

Acknowledgments

I would like to acknowledge the following people and organisations during the EngD project. Thank you to Dr Gary Caldwell for his academic advice, support and supervision. David and Polly Van Alstyne and Scottish Bioenergy for providing financial support, experience in the business world and opportunities outside of academia. Dr Andrew Free, Rocky Kindt and Jennifer Lawson at the University of Edinburgh for collaborative work and expertise on microbial populations. Professors Elaine Martin and Gary Montague for their advice and support. The School of Marine Science and Technology (MAST), particularly David Whitaker for his technical help. The School of Chemical Engineering and Advanced Materials (CEAM) and staff and fellow students at the Biopharmaceutical Bioprocessing Technology Centre (BBTC) for their advice and support. The Scottish Association for Marine Science for advice and expertise on cultures and hosting enjoyable trips to Oban. Dr Kaveh Emami for teaching me about mass spectrometry. Dr Gavin Clark for his friendship and career mentoring. Louise Mackenzie for showing me how science can meet the arts. My Technology Transfer Team at the University of Surrey: Martyn Buxton-Hoare, Trevor Hartman, Jonathan Hodrien, Prof. Rob Yates, Dr Joana Nunes de Carvalho and Peter Lancaster for your encouragement. My family for your interest and love, particularly my Grandad who sadly did not live to see the completion of this thesis. Dr Matthew Abbott, my now husband, for his loving partnership. Thank you also to the EPSRC for funding.

The majority of funding enabling this research was provided by the EPSRC (Grant EP/G037620/1).

Contents

List of Figures

List of Tables

Abbreviations and Notation

Abbreviations

AD	Anaerobic digestion
ADP	Adenosine diphosphate
APC	Allophycocyanin
ATP	Adenosine triphosphate
BOD	Biochemical oxygen demand
CAPEX	Capital expenditure
CCA	Complementary chromatic adaptation
CCAP	Culture Collection for Algae and Protazoa
CCMP	Culture Collection of Marine Phytoplankton
CEO	Chief Executive Officer
CHP	Combined heat and power
COD	Chemical oxygen demand
CT	Constant temperature
DHA	Docosahexaenoic acid
DNA	Deoxyribonucleic acid
DO	Dissolved oxygen
DOM	Dissolved organic matter
DSP	Down Stream Processing
EngD	Engineering Doctorate
ESAW	Enriched Seawater, Artificial Water
FIT	Feed in tariffs
FSA	Food Standards Agency
GBP	Great British Pound
GM	Genetic modification or Genetically modified
GMM	Genetically modified microorganism
IB	Industrial biotechnology
IR	Infra red
JMM	Jarworski's Modified Medium

LED	Light Emitting Diode
MALDI-TOF	Matrix Assisted Laser Desorption Ionization Time-Of-Flight
MO	Microorganism
MS	Mass spectrometry
NCMA	National Centre for Marine Algae
OD	Optical density
OPEX	Operational expenditure
OTU	Operational taxonomic unit
PBP	Phycobiliprotein
PBR	Photobioreactor
PBS	Phycobilisome
PC	Phycocyanin
PCR	Polymerise chain reaction
POM	Particulate organic matter
PSI	Photosystem I
PSII	Photosystem II
PUFAs	Polyunsaturated fatty acids
R&D	Research & Development
RHI	Renewable heat incentives
RNA	Ribonucleic acid
ROCs	Renewable obligation credits
ROS	Reactive oxygen species
rRNA	Ribosomal ribonucleic acid
RSM	Random spontaneous mutation
SME	Small and medium-sized enterprise
STEM	Science, Technology, Engineering & Maths
STPBR	Stirred-tank photobioreactor
TAG	Triacylglycerol
TC	Total carotenoids
TNT	Trinitrotoulene

USD	US dollar
UV	Ultraviolet
UVR	Ultraviolet radiation
Vis	Visible
WFD	Water Framework Directive

Notation

Chl*a*	Chlorophyll *a*
Chl*b*	Chlorophyll *b*
Chl*d*	Chlorophyll *d*
Chl*f*	Chlorophyll *f*
Cu(II)	Cu^{2+} ions
Cyt b6-f	Cytochrome b6-f
Da	Dalton
EC_{50}	Half maximal effective concentration
Gt	Gigatonne
hv	Photon
kWh	Kilowatt hour
M	Molar
m/z	Mass/charge ratio
POM	Particulate organic matter
PQ	Plastoquinone
PQH_2	Plastoquinol
rpm	Revolutions per Minute
V	volume
vvm	Vessel volumes per minute
v/v	Volume/Volume
λ	Wavelength
λmax	The maximum wavelength
Δ	Change in

σ^2	Variance
μ	Mean

Chapter 1. Introduction

Prenote

This thesis is a portfolio of three projects carried out during an Engineering Doctorate partnership with Scottish Bioenergy Ltd in the area of microalgae biotechnology. The Engineering Doctorate (EngD) programme is distinct from a traditional PhD in that research is directed by a sponsor company in response to commercial needs. The EngD programme was developed on recommendations in the Parnaby Report (1990) which concluded "PhDs can be too narrow and academic for industry's needs". An EngD thesis, in-line with the philosophy of the EngD, can therefore cover a broader set of projects linked by an overarching topic area, where the research typically crosses disciplines.

The overarching theme of this thesis is microalgae biotechnology, therefore Chapter 1 begins by giving a broad introduction to microalgae biotechnology prior to the more specific literature reviews of the further chapters. The second part of Chapter 1 introduces the industrial context framing microalgae biotechnology as a part of UK Industrial Biotechnology strategy. Following on in the rest of Chapter 1 the principles of the EngD programme are described. The research journey directed by the commercial twists and turns of Scottish Bioenergy is then explained before introducing each chapter of the thesis.

1.1 Microalgae Biotechnology

1.1.1 Sourcing natural and renewable products

Microalgae (microscopic algae) is being increasingly explored and exploited as sustainable sources of food, feed, fuels and other biochemicals (Becker, 1994). There is also increasing interest in macroalgae (seaweeds) for similar purposes; however, throughout this thesis when referring to algae, it is microalgae and cyanobacteria (previously known as blue-green algae) alone that are being addressed. Reference to microalgae throughout this thesis will also incorporate cyanobacteria including the cyanobacterium *Arthrospira*. Some examples of products obtainable from microalgae are listed in Table 1.1.

Table 1.1. Commercial products that may be derived from microalgae. There is cross over as some products can fall into many product types (Santoyo, 2009, de Jesus Raposo, 2013).

Product Type	Products
Biofuels	Long-chain hydrocarbons, esterified lipids, hydrogen, biogas (methane)
Antimicrobials	Butanoic acid, methyl-lactate
Polyunsaturated Fatty Acids (PUFAs)	Docosahexaenoic acid (DHA), arachidonic acid (ARA), γ-linolenic acid (GLA), eicosapentaenoic acid (EPA)
Pigments	Carotenoids (astaxanthin, lutein, canthaxanthin, β-carotene, zeaxanthin, fucoxanthin), chlorophyll, phycobilins (phycocyanin, phycoerythrin, allophycocyanin),
Nutraceuticals and food/feed additives	Protein, amino acids, vitamins (vitamin C, K, B12, A and E, α-tocopherol), enzymes (superoxide dismutase (SOD), carbonic anhydrase, Coenzyme Q10), sterols (brassicasterol; stigmasterol, sitosterol), polysaccharides
Biopolymers	Poly-lactic acid, cellulose, polyhydroxyalkonates (s poly-3-hydroxybutyrate)
Chemotherapeutic agents	Fuco, violaxanthin
Photoprotectants	Mycosporin-like amino acids, pyropheophytin a
Other	γ-amino-butyric acid (GABA), okadaic acid, microcolin-A, biofertilisers, glycerol, squalene, phytoene, phytofluene, echinenone

The biodiversity of microalgae (marine and freshwater) is vast, with over 35,000 species described (Lee, 2008); many of which will be suited to the production of certain end-products. The importance of algae biodiversity for bioproduct development is far from being fully explored. The exploration for, and discovery of new algae strains as sources of products, particularly novel pharmaceuticals (or for particular purposes), is known as bioprospecting (Ratha and Prasanna, 2012). Some of these end-products are currently produced using land crops. Algae are considered to have a production advantage over conventional terrestrial crops as they are faster growing, have higher productivity per unit area (Dismukes, 2008), are more

efficient at utilising sunlight (Barbosa, 2003), and are tolerable of a wider range of growth conditions. Algae production is also not reliant on the use of limited arable land and, if used for biofuel production, avoids the food versus fuel argument (Tsoupeis, 2009).

Green algae and cyanobacteria are phototrophs which have the ability to perform photosynthesis. Heterotrophic algae generally lack the ability to photosynthesise and therefore rely on an organic carbon source for growth (Morales-Sánchez, 2015). The basic needs of phototrophic algae comprises chemical and physical factors: a source of nitrogen, inorganic carbon (CO_2/HCO_3), phosphorus, potassium plus small quantities of specific elements such as magnesium and sulphur in the presence of sunlight. The cells of eukaryotic green algae feature chlorophyll-containing chloroplasts or other photosynthetic pigments which absorb light and use electrons from the oxidation of water (via photosystems I and II in the thylakoid membrane) in the reduction of CO_2 to produce carbohydrate and other organic molecules (Alberts, 2002). Sugars, fatty acids and amino acids produced then contribute to the structure of the cell. It is also these 'renewable' products, derivable from algae, which can be commercially valuable.

Algae contain high quantities of protein which can be used as a supplement in animal feeds. Some strains also contain high levels of polyunsaturated fatty acids (PUFAs) such as omega-3 which is associated with decreased risk of heart disease when consumed in humans (Albert, 1998, Daviglus, 1997). Supplementation can increase the levels of PUFAs in animal products such as meat, fish, milk and eggs which could benefit public health (Abughazaleh, 2009, Franklin, 1991), as well as increasing farming productivity and quality of produce as has been demonstrated in chickens (Grigorova, 2005). Algae also produce pigments which can be used as natural colourants with additional anti-oxidant properties beneficial to human health. The best example are carotenoids which are typically red, orange or yellow in colour, and are used widely in the ceutical (pharma-, cosme- and nutri-) industries (Raja, 2007) and as additives in fish and poultry feed to enhance flesh and egg yolk colour (Pisal, 2005). The demand for naturally sourced pigments such as carotenoids is rising due to widening consumer health awareness and the preference for more natural products. Many of these can be naturally sourced from algae to maintain the natural status of some food products (Dominguez, 2013). Recognition of the inferior quality of some chemically synthesised carotenoids is also a driving force behind the increasing demand for natural pigments. For example, natural β-carotene, one of the most abundant carotenoids, contains a significantly higher ratio of 9-*cis*-β-carotene to all-*trans* isomer than in synthetically produced β-carotene. All-*trans*-β-carotene has lower anti-oxidant activity and other medically beneficial activities plus lower liposolubility. The ratio of *cis* to *trans* isomers is even higher in algae compared with other natural sources, therefore algae-

derived β-carotene is of a higher quality for health applications (Ben-Amotz, 1996, Levin, 1994, Palozza and Krinsky, 1992). The unicellular alga *Dunaliella salina* is a well-known producer of carotenoids, particularly β-carotene (Ben-Amotz, 1982) at yields of up to 14 % dry weight (Ben-Amotz, 1983, Aasen, 1969). However, high production occurs only under conditions of cellular stress, such as nitrogen starvation and high irradiance where growth slows and pigment accumulates. The need for stress conditions is also true for many lipid products (including precursors to biofuels) produced in algae, which can be problematic for continuous production when attempting to maintain high growth rates and product yields.

1.1.2 Photobioreactors and control

Current production methods using algae involve growth outdoors in open-ponds or raceways or in sealed photobioreactors (PBRs) of various designs, outdoors, or indoors using artificial light (Figure 1.1). It is recognised that PBRs can produce superior amounts of algae biomass as they can be more closely controlled and are less susceptible to contamination, so are preferred for the quality-assured production of commercially important products (Gupta, 2015). Most large scale algaculture currently takes place in the Far East and USA (Benemann, 2013) where there is a reliable source of solar energy year round, avoiding the need for artificial light. Outdoor cultivation on a large scale is uncommon in Britain, as climatic conditions are seen as unfavourable.

PBRs are designed and operated to meet the majority of the biological needs of algae and offer specific control to match the preferred conditions required by the particular strain under cultivation. Small volumes of supplemental CO_2 are required to reach high biomass concentrations. As the CO_2 composition of flue gas produced by burning fossil fuels (coal, oil and gas) is relatively low (approximately 4-14 %), this typically satisfies the CO_2 requirements of an algae culture (Kumar, 2011a, Zhang, 2015). Therefore, waste flue gas can be bubbled through cultures to supply CO_2. The CO_2 saturation level in the culture also depends on the culture temperature, as CO_2 is more soluble in water at lower temperatures (Piorreck, 1984) as well as the efficiency of the aeration method. During CO_2 supplementation, CO_2 dissolution in the culture lowers pH by the production of carbonic acid, and the presence of nitrogen (NOx) and sulphur oxides (SOx) in flue gas can produce sulphuric (H_2SO_4) and nitric (HNO_3) acids (Maeda, 1995); therefore appropriate buffering and pH control should be used, particularly as algae are sensitive to changes in pH. Also, low pH lowers the concentration of CO_2 dissolved in the culture according to Henry's Law (Doran, 2005) and so may affect the rate of CO_2 uptake by the algae if uncontrolled (Goldman, 1982, Azov, 1982). Additionally, accumulation of evolved oxygen from photosynthesis can be toxic to the culture (Torzillo, 1998).

Figure 1.1. Various types of algae cultivation systems. From top left to bottom right: polyethylene sleeves, open raceway, tubular photobioreactor and stirred tank photobioreactor. Images sourced top left to bottom right from: www.oilseedcrops.org, www.algaeindustrymagazine.com, www.personal.psu.edu, www.biooekonomie-bw.de.

Invading organisms or contamination by other algae species can inhibit culture growth through grazing or depletion of available nutrients. As PBRs are closed to the environment, there is a lower risk of an invasive species affecting productivity. When considering bacterial contamination however, it is not essential that algae cultures are completely bacteria-free, as the majority of the time the presence of bacteria is not problematic and can actually be beneficial to algae growth. The reason behind this may be the symbiotic relationships between bacteria and algae which are known to exist, where bacteria provide vitamins and micro-elements required by the algae through bacterial metabolism (Croft, 2005).

There are limits to light exposure as long periods of high intensity light can cause photoinhibition (Rubio, 2003, Torzillo, 2003) which causes problems for outdoor culturing as peak daily levels of solar irradiance are sometimes up to ten times higher than is normally required by algae (Gordon, 2007). In addition, it is questionable whether 24/7 illumination allows maximum productivity as algae have been shown to require light-dark cycles, although associated studies have shown mixed results (Zhang, 2001). Short intermittent periods of light and dark; appropriately named ‘the flashing light effect’ can increase productivity (Matthijs, 1996, Phillips Jr and Myers, 1954). Limitations on light penetration and availability can be caused by self-shading and therefore is dependent on the culture density, as well as mixing and

PBR geometry (Zhang, 2001). During algae cultivation mixing must occur at a rate to prevent the formation of dark zones and ensure light is received uniformly by the culture (Ogbonna, 1995), as photosynthetic processes cannot occur in low light levels and algae can be bleached if light exposure is too high (Carvalho, 2011). Also agitation ensures uniform distribution of heat in the culture and reduces settlement and fouling on the walls of the reactor, which if allowed to build up will block light penetration (Posten, 2009). Furthermore, agitation provides well distributed nutrients throughout the culture and as a result, well mixed reactors reach higher biomass yields (Eriksen, 2008, Wijanarko, 2008). There are numerous parameters to be controlled in algae culturing systems, and photobioreactors enable better control in production.

1.2 The UK Technology Roadmap

Realisation of the economic contribution of Industrial Biotechnology (IB) in the UK has prompted the UK government to invest in the IB sector. Investment has been in the form of part-funded Catapult centres and leasable facilities such as the National Biologics Manufacturing Centre (NBMC), located at the Centre for Process Innovation (CPI) in Darlington, in the North-East of England. Algae is a part of the IB landscape in the UK and organisations such as the Natural Environmental Research Council (NERC), Innovate UK (formerly Technology Strategy Board (TSB)), Knowledge Transfer Network (KTN), Algal Bioenergy Special Interest Group (ABSIG), Phyconet (BBSRC NIBB), NNFCC, and the Scottish Association for Marine Science (SAMS) are all organisations involved in developing algae biotechnology in the UK (Schlarb-Ridley, 2013) with the realisation of the numerous applications of algae biotechnology (Figure 1.2).

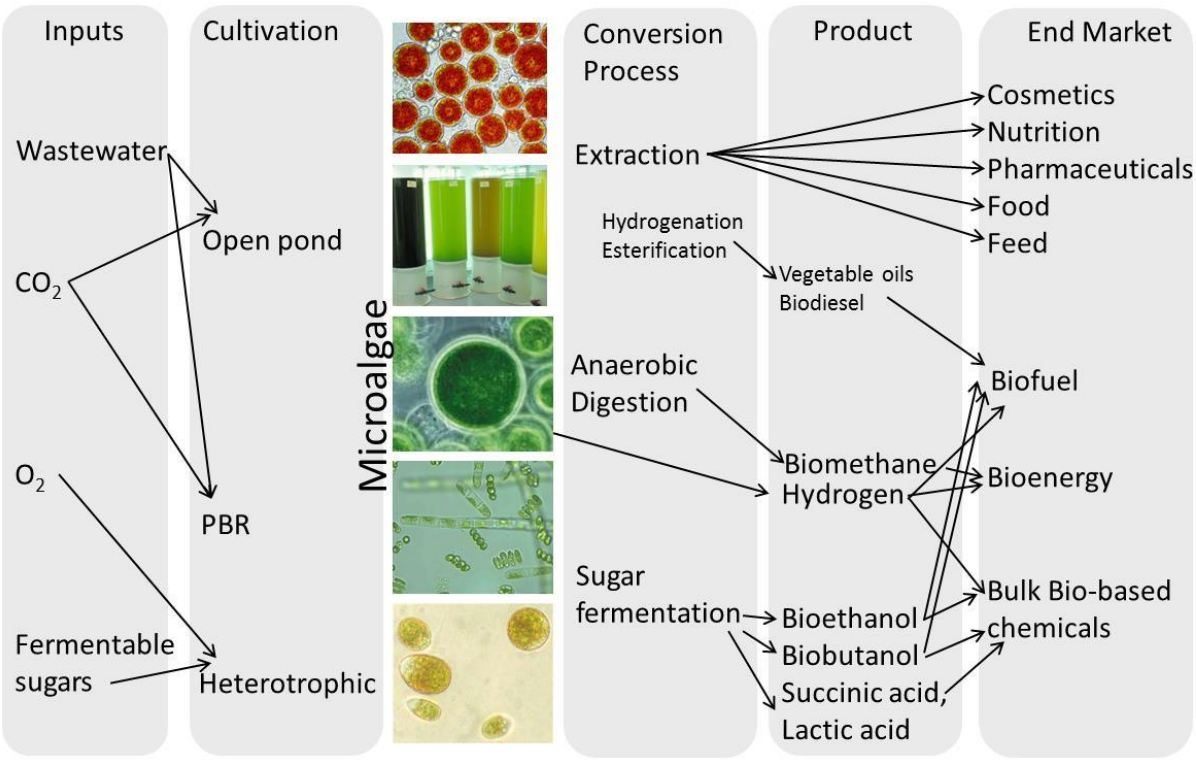

Figure 1.2. Possibilities for algae technology based on a presentation by Dr Michele Stanley (Phyconet, UCL, 2014). Images sourced from: http://mikrosvijet.wordpress.com/2013/03/23/haematococcus-pluvialis/, http://www.coastalwiki.org/wiki/Marine_Biotechnology_securing_alternative_sources_of_renewable_Energy, http://www.healthyfellow.com/770/best-of-chlorella-and-spirulina/, http://www.ongen.ca/ONGEN%20PROJECTS.html, http://abalgae.com/en/products/dunaliella/about.

UK research has played a huge part in the development of techniques and technologies in algae biotechnology, now adopted worldwide and combined with the UK's growing macroalgae industry. As an island nation, the UK is well placed to grow its microalgae segment of UK IB and fully exploit the commercial potential of algae biotechnology. High value bioactives such as pigments and antioxidants, bioremediation, fertiliser and feed production from microalgae are all aspects of algae biotechnology identified to be readily developed and now at a stage to take out in UK companies. These are therefore the most commercially promising in the short-term for the UK (Schlarb-Ridley, 2013). To assist in developing microalgae biotechnology, organisations are focusing on a number of key areas:

1. Encouraging academia-industry collaborative projects, the growth of expertise, developing multi-disciplinary people with broad knowledge of algae biotechnology as well as business skills, effective knowledge transfer through creating networks (Special Interest Groups) and opening-up funding pots particularly for micro-SMEs for training and research funding.

2. Ensuring pilot facilities are available with incubation space to grow algae-based businesses, to assist in the creation of producers, and avoid the 'Valley of Death' (House of Commons Science and Technology Select Committee, 2013), where technologies and businesses die out because of the lack of proof-of-concept funding. Pilot facilities also provide the necessary (scale-up) data, currently lacking, to near accurately model scale-up economics and financial feasibility and observe the effects of intensive and continuous cultivation, of which little is currently known about.
3. Engaging with the market through outreach events to promote the public understanding of the benefits of algae, particularly bioactives for health and wellbeing and also marketing the country's expertise to the world.

The algae market is notably under-developed in the West in comparison to the East and it is recognised that market uptake is one of the big hurdles to successful home-grown algae product businesses in the UK besides the economic/technical hurdles of production. Considerable marketing is required to penetrate the markets and for the public to accept paying a premium price for algae products.

There have been a number of reports looking at the challenges, opportunities, strengths and gaps in UK algae biotechnology from 2008 (Schlard-Ridley, 2011, Smith, 2010) and in 2011 the Algal Biotechnology Special Interest Group (AB-SIG) was set-up, funded by NERC and Innovate UK, hosted by Biosciences KTN, working with Government to drive UK algae biotechnology. They commissioned the 2013 report (Schlarb-Ridley, 2013) with a focus on commercialisation and now work assisting algae biotechnology projects connecting academia with industry, creating networks and advising and facilitating business – all movements identified and required to grow UK algae biotechnology.

For high-value products such as pigments, technologies in the UK need to become price competitive with Asian imports. Relationships between universities and interested enterprises are therefore vital for the UK to get into the high-value market, and integrated systems involving bioremediation could be a way to reduce production costs to create price-competitive products. However, when it comes to natural and organic consumer care products (rather than ingredients) western brands dominate the increasing Asian market (Organic Monitor, 2015), and the competitive landscape is seen as difficult for Asian companies.

1.3 The Engineering Doctorate

The Engineering Doctorate (EngD) was established by the Engineering and Physical Sciences Research Council (EPSRC) in 1992. The scheme aims to address the skills shortage in the UK engineering industry, highlighted in the Parnaby Report of 1990 (Parnaby, 1990), required to support the UK remaining ahead in advanced science and technical capability. The EngD is distinct from, and complementary to the traditional PhD, which has been criticized for a lack of industrial relevance in preparing for the challenge of working in industrial environments and accused of being too narrow and academic for industry's needs (Godfrey, 2012). The EngD student works with an industrial partner on industrial projects and problems, providing experience to the student in industrial interaction and industry-focused research whilst at the same time meeting business needs; addressing also the hurdle of UK knowledge (traditionally generated in universities) not being transferred effectively into industry to benefit the UK. Although EngD programmes can differ between EngD Centres, the EngD programme at the Biopharmaceutical Bioprocessing Technology Centre (BBTC), Newcastle University combines three and a half years of postgraduate research working with an industrial sponsor company with around 15 taught modules including technical Masters-level subjects, complementing the research area and also covering broad aspects of business, management and intellectual property. Such transferrable skills are now considered essential for careers in industry. Additionally, universities have begun to incorporate these subjects into traditional PhD programmes in recognition that such exposure can better equip students for careers in the UK science and engineering sector as well as enhance academic careers.

As the majority of STEM doctorate students find careers outside of academia (Figure 1.3), there is the responsibility for universities to provide adequate training to equip students for these roles.

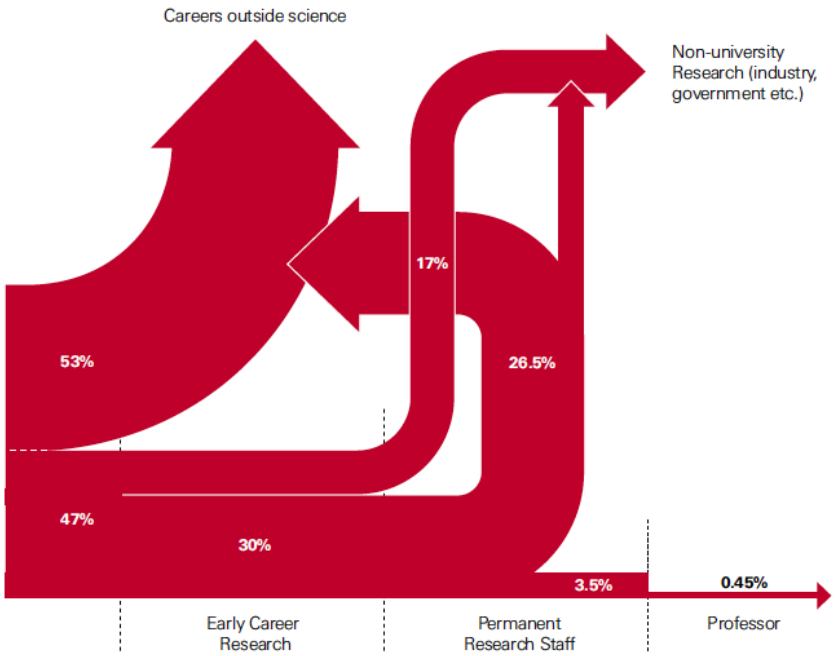

Figure 1.3. Illustration of the transition points in typical academic scientific careers following a PhD (The Royal Society, 2010).

The EngD programme also seeks to cross disciplines (EPSRC, 2011) and projects can sit between subjects; for example, microbiology and chemical engineering for bioprocessing, where taught technical modules assist in this. The exposure to industry and commercial realities gives the student an appreciation and understanding that research direction can change rapidly in product-led industry. With this, EngD students usually submit a thesis by portfolio demonstrating a breath of related projects.

The EngD scheme runs alongside and in hand with the changing vision and direction of UK universities. Traditional roles of UK universities were limited to research and teaching. Recently, a 'third mission' has developed associated with engaging knowledge users and promoting technology transfer (Gulbrandsen and Slipersæter, 2007) to create maximum impact from research (Research Councils UK, 2014). Such interactions, which are best demonstrated in Germany's Fraunhofer Model (Reid, 2010, Wessner, 2013) drive innovation and the economy. The aims of the EngD programme and universities 'third mission' is aligned with UK industry roadmaps covering all areas of science and technology, including the UK industry roadmap for algae biotechnology. Here, academia-industry collaborations, knowledge transfer and the creation of a workforce with broad knowledge across disciplines, including an understanding of the complications of business and academia interaction are sought.

1.4 Scottish Bioenergy Ltd

Scottish Bioenergy is a small enterprise formed in 2007 which operates in the field of algaculture. The company is specifically concerned with the design and operation of inexpensive microalgae photobioreactors (PBRs) for the production of biochemicals from microalgae. Their systems are multi-process using waste carbon dioxide emissions and/or various wastewaters from different industrial activities. Microalgae use carbon dioxide (CO_2) and inorganic nitrogen: nitrate (NO_3^-), nitrite (NO_2^-), ammonia (NH_4^+) and phosphates for growth. Some wastewaters contain a high concentration of inorganic nitrate and phosphate and these pose a huge environmental risk because of the high biochemical and chemical oxygen demand (BOD/COD) and risk of eutrophication if leaked into local water sources; therefore they are costly to dispose of. These wastewaters can be used as a nutrient source for the algae while simultaneously treating the effluent for discharge (Hammouda, 1995, Fedler, 2006). As well as treating wastewater with algae, phosphate is recovered, which is an important finite resource (Steen, 1998). Scottish Bioenergy systems therefore simultaneously facilitate carbon capture, wastewater treatment and element recovery (Figure 1.4). These systems align with the EU Water Framework Directive (WFD) (European Parliament, 2000) which looks to improve the quality of surface and ground water. The Nitrates Directive (European Council, 1991) forms part of the WFD, specifically addressing nitrates which the EU recognises can be problematic for human health and the environment. The Nitrate Directive looks to reduce nitrates in waters through monitoring, reporting and proposing best agricultural practices.

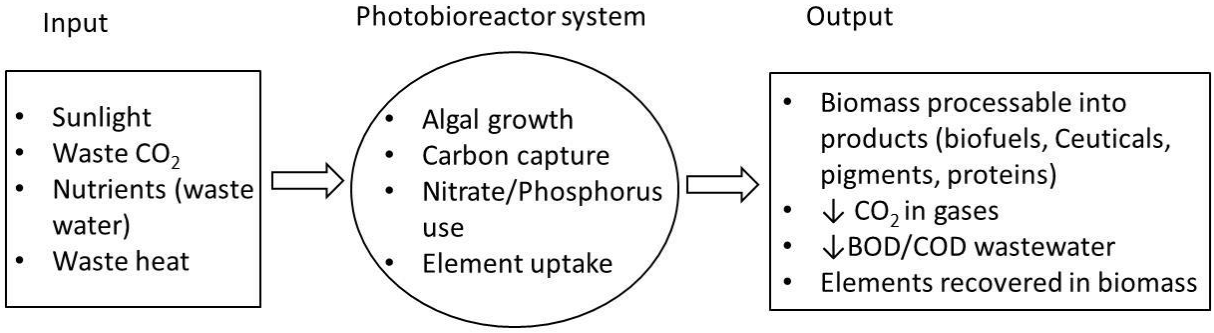

Figure 1.4. Schematic of multi-process systems achievable in microalgae photobioreactors.

The company is now in the late development phase of its systems and is completing testing at its scale-up facility at the Roslin Institute, University of Edinburgh. The company has a Research and Development strategy of actively seeking partnerships with universities in the UK and Ireland to work on joint projects, giving the company access to equipment and expertise

which would otherwise be unaffordable to a small company. Here the company recognises the great benefit of industry-academia collaboration to the business. This strategy also encourages dialogue between similar research groups at the partner universities.

1.5 Commercially-driven Research and Thesis by Portfolio

The current Scottish Bioenergy EngD project was carried out at Newcastle University, working between the School of Chemical Engineering and Advanced Materials and the School of Marine Science and Technology. During the start of the project, at the end of 2010, Scottish Bioenergy were a company interested in the production of biofuels from microalgae. The company recognised that the economics of a microalgae-based biofuel production process could be increased to a business-viable level through the development of a multi-process system, as demonstrated in Figure 1.4. The company also had a patent application (Van Alstyne, 2009) originally claiming a modular microalgae photobioreactor system for biodiesel production operating on multiple-processes. The early vision of the company was to develop algae biotechnology specifically in the North of England and Scotland and to demonstrate that this technology could create viable businesses in colder places, not just in equatorial regions. Early systems were set-up and tested at the Glenturret Whisky Distillery in Crieff, Scotland. Here, pot ale, a wastewater from the whisky distilling process, was used as a nutrient source for the microalgae. Pot ale contains nutrients such as nitrate and ammonia which can support microalgae growth. Large volumes of pot ale are produced, approximately eight litres for every litre of whisky (Mohana, 2009), which not only has a high BOD/COD but also contains a high amount of copper (up to 6 ppm) from the copper whisky stills (Graham, 2012). The characteristics of pot ale make it difficult to dispose of and it sees limited permitted uses as a land fertiliser and animal feed, and is mainly treated using anaerobic digestion (AD) (Dionisi, 2012) at a cost to the distillery. During the earliest feasibility study pot ale was used as a feedstock for a modular photobioreactor system which also used the CO_2 from waste flue gas and heat from the distilling process for microalgae growth. Strains of microalgae (mainly *Chlorella* and *Scenedesmus*) from a water source local to the distillery were used to inoculate the PBR system and the indigenous nature of the strains meant they were particularly hardy to the lower temperatures in winter. The feasibility study demonstrated that not only could the microalgae reduce the BOD/COD of pot ale but also that uptake of copper by the microalgae could remove the hazardous metal (Rai and Gaur, 2001) making the pot ale safe to return to rivers and sea or for use in crop watering.

Even though such systems provided free sources of feedstock for microalgae production, the processing costs and amounts of biodiesel obtainable from microalgae biomass, along with the

price that could be achieved for the sale of biodiesel still arrived at an unviable business model. Between 2005-2009 the number of algae-to-energy start-ups tripled (Rosenthal, 2011), but the surge of both commercial and scientific interest in algal oils and biofuels worldwide around 2010 began to tail-off (Figure 1.5) as companies realised they had been misinformed by over interpretation of the scientific literature on microalgae biofuels. Extrapolated data from lab-scale studies gave impressive numbers, but on a large-scale this was unrealistic and unachievable. The economics of biofuel production using microalgae just did not add up based on the current technology, particularly through the high cost of production associated with dewatering and extraction of the desired products (Robertson, 2011). Companies realised that massive investment was required to develop higher efficiency dewatering and processing techniques, as well as faster growing and higher lipid producing strains before microalgae biofuel production can become an economic process. With the lowering oil prices it is becoming even more difficult to achieve a microalgae-derived biofuel that competes with today's fossil fuels, when microalgae biofuels still can't compete with first-generation biofuels (those derived from starch, sugar, animal and vegetable fats). Scottish Bioenergy recognised this was not an environment that microalgae biofuel SMEs can thrive in and so during the early phases of the EngD project the company began looking for more promising and potentially profitable microalgae-derived products.

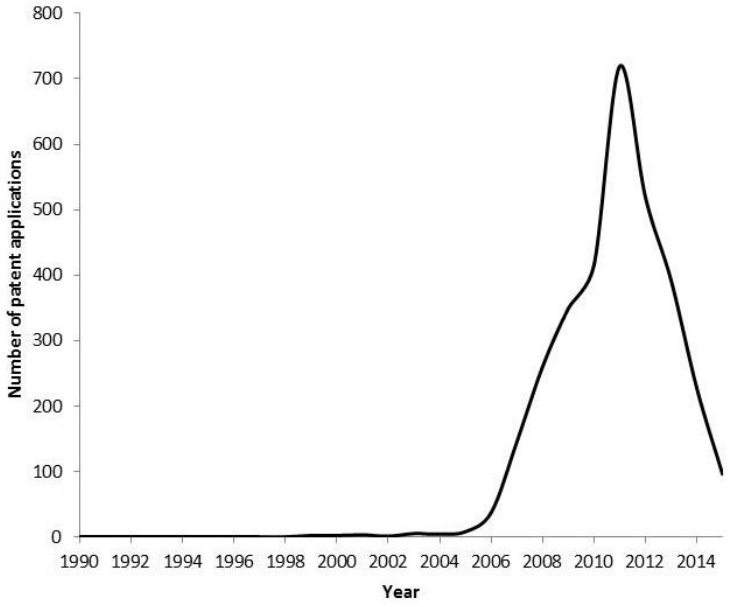

Figure 1.5. Patent applications filed between 1990-2015 on biofuel production using microalgae. Figure composed using patent data retrieved by PatSnap software searching all patent databases on 6th March 2016 produced in Microsoft Excel 2007. Search terms used [All: "microalgae AND biofuel"].

The company therefore began looking for possible viable multi-process operational models for production of higher value products, particularly a model which could support the use of artificial illumination, in the form of LEDs, to avoid the high variability in productivity experienced at Glenturret caused by seasonal fluctuations in light level and temperature. Artificial illumination would offer a better element of control for year round consistent production.

The company observed an opportunity in operating PBRs synergistically with AD facilities containing combined heat and power (CHP) units for treatment of AD wastewater (Figure 1.6). AD effluent could be used as a nutrient source for microalgae growth along with waste CO_2 from the burning of biogas in the CHP unit to provide a supply of inorganic carbon and reduce the plant's CO_2 emissions (Deublein, 2011). At the time, and still, AD facilities with CHP units are entitled to generous Government tariffs such as Renewable Obligation Credits (ROCs), Feed In Tariffs (FITs) and Renewable Heat Incentives (RHI) (NNFCC, 2011), which were guaranteed for 20 years. Here money is paid back to the AD facility depending on the amount of power they return to the national grid and heat produced. The AD facility therefore is paid for the energy they produce, which could be used to provide artificial light for continuous growth and maintenance of an optimal culture temperature for year round maximum production. Along with concurrent wastewater treatment in the reduction of BOD/COD in the AD effluent, money can be made from the sale of high protein and omega-3-containing microalgae biomass for supplementation of animal feeds. The system was an attractive proposition to UK dairy farmers who had recently invested in AD systems as the add-on to their system had the potential to provide a cheap source of protein supplementation for their cows, at a time when high protein price was, and still is, increasing production costs for dairy farmers worldwide (Johnson Jr, 1991, Stallings, 2011).

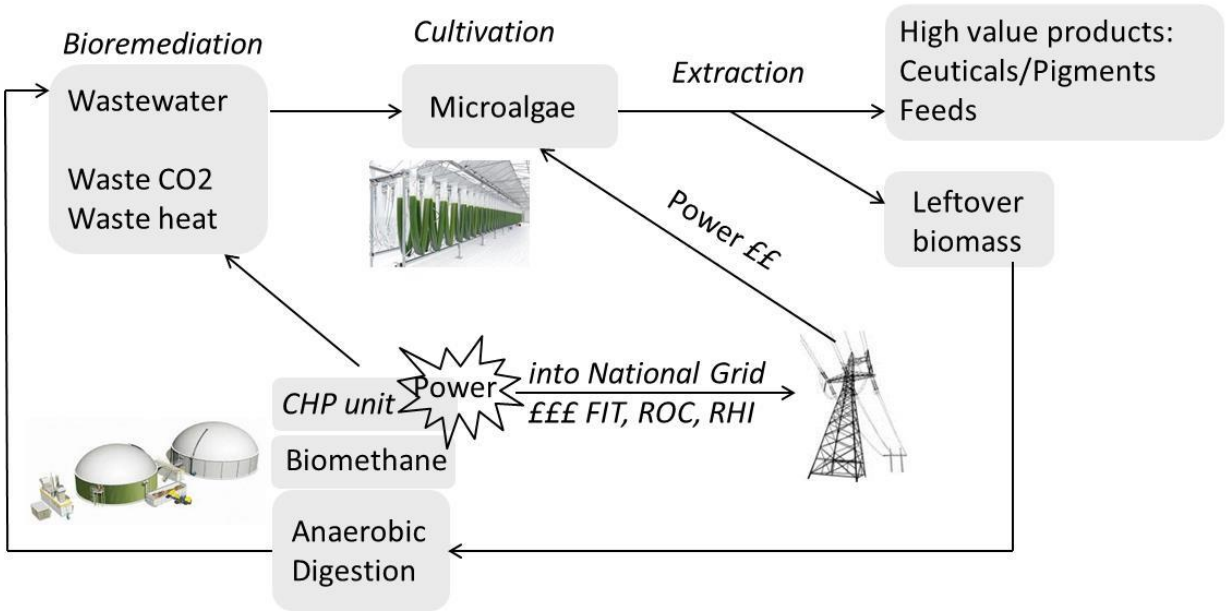

Figure 1.6. Schematic of the proposed Scottish Bioenergy AD-PBR synergistic system. Graphics sourced from: www.seai.ie, www.pintrest.com and www.canstockphoto.com.

The system, however, hit upon a regulatory problem. The Food Standards Agency (FSA) would not allow the production of algae biomass for supplementation of animal diets when the biomass was grown on a nutrient source which came from animal waste. This would therefore rule-out employing the system on farms, where the AD unit would be fed by animal slurry. Furthermore, the FSA ruled-out synergistic operation with an AD facility fed by household waste, if meats were included as a feedstock (which most are). This decision by the FSA vastly limited the market for synergistic AD-PBR systems, preventing the development of the proposed system moving forward. Additionally, there was always the risk that changing government policy relating to subsidies for renewables, in this case FIT and RHI, would affect the viability of the business model.

A year into the project the company was looking for a new direction to focus innovation. They needed a product that could support an artificially illuminated system required for process stability, from lessons learned at the Glenturret distillery. As a researcher new to the field of microalgae, and after a period of reassessment, *Arthrospira* stood out as an interesting organism, not least because of the early and interesting research into the properties of a particular pigment, phycocyanin, which *Arthrospira* is known to contain in high quantities. The filamentous nature of this cyanobacteria offered a simpler dewatering process as the large filaments of ~5 mm in length mean that *Arthrospira* cultures can be filtered through a fine mesh to obtain a wet biomass, unlike smaller unicellular microalgae like *Chlorella* or *Dunaliella*. The high value of phycocyanin (at higher purity) and increasing use in common products made *Arthrospira* a good candidate in the company's quest for a fresh endeavour. The company

supported the idea to re-focus the EngD project on high value pigment production and got on board with *Arthrospira*. The company turned to artificial illumination and existing interest in the School of Marine Science and Technology by Dr Gary Caldwell surrounding the use of long wavelength LEDs to identify an opportunity to test the effects of long wavelength LEDs on the growth and phycocyanin content of *Arthrospira*. Knowing the growth (productivity)-enhancing effects that long wavelength LEDs can have on microalgae, it was of interest to know if similar effects on productivity would be seen in *Arthrospira*, which may offer benefits in a production process using artificial illumination.

This identification of *Arthrospira* as a potential new product combined with the company's maintained interest in whisky distillery wastewater as a feedstock for photobioreactors also influenced an additional project. The company was interested in developing a strain of *Arthrospira* which could grow in conditions of high copper, such as that experienced in pot ale, but wanted to avoid genetic modification because of risks of regulatory barriers which they had previously experienced. Microevolution is the evolutionary change within a species or small group of organisms over a short period of time and cultures can be 'microevolved' through directed microevolution and selection, after a short-period of exposure to a certain environment or selection pressure, for an advantageous genetic mutation (Gonzalez, 2012, Luria and Delbrück, 1943). The suggestion to attempt this through microevolution was accepted and it was thought this work would also be an opportunity to test the feasibility of using such a process to develop other wastewater-tolerant strains of microalgae and cyanobacteria, and therefore may have broader applications.

There was also a simple side-project earlier in the Scottish Bioenergy project, undertaken during the period of reassessment, to develop a simple and quick method of measuring nitrate concentration in microalgae cultures. The company lacked in-house 'there-and-then' nitrate monitoring in their early testing, which could have shed light on problems experienced in particular batches and they thought this a valuable additional tool in their development and understanding of the photobioreactor systems and processes. A method of determining nitrate concentration quickly and easily using simple laboratory equipment already available to the company: a spectrophotometer and centrifuge was developed in two standard media and demonstrated using the common microalga *Chlorella.* This technique could then be applied by the company to monitor the nitrate levels in their photobioreactors, at no extra cost using the simple equipment they had access to.

This thesis is therefore a portfolio of three projects carried out in partnership with Scottish Bioenergy. Chapter 2 explains the development of a simplified spectrophotometer-based test to measure nitrate concentration in algae cultures, developed in standard Jarworski's and f/2 Medium and tested with batches of *Chlorella vulgaris.* Chapter 3 and 4 describe the experimentation with long wavelength red LEDs for phycocyanin production in *Arthrospira platensis* where the discovery was made that LEDs of a maximum emission wavelength (λ_{max}) of 680 nm increase the content of phycocyanin in *Arthrospira* biomass by over 250 %. Chapter 5 extends the results of Chapter 3 and 4 considering industrial application. Chapter 6 explores growth of *Arthrospira* on a high copper wastewater and the development of a copper tolerant strain through directed microevolution. The portfolio is concluded in Chapter 7.

Chapter 2. Development of a Spectroscopic Technique for Nitrate Measurement in Microalgae Cultures

2.1 Introduction

Nitrogen is the second most important nutrient for phytoplankton after carbon. Phytoplankton are responsible for approximately 70 % of nitrogen assimilation on Earth, mainly in the form of nitrite and nitrate (NO_2 or NO_3), ammonia and ammonium (NH_3 or NH_4) or other reduced sources (Raven, 1993). Additionally, some cyanobacteria have the ability to directly fix atmospheric nitrogen (N_2) into a usuable form (NH_3) (Zehr, 2011). Nitrogenous compounds are taken-up into cells by diffusion and/or active transport. Nitrate, as one of the main nitrogen sources for microalgae, has been well studied (Sanz-Luque, 2015). In nature, nitrate concentrations can range from 50-500 µM N L^{-1} (Collos and Berges, 2009). Nitrite is also present, but at much lower concentrations of up to 2 µM N L^{-1}. Both compounds can be toxic above 1000 µM N L^{-1}.

Inside the cell nitrate is reduced to nitrite and then ammonium by the enzymes nitrate and nitrite reductase (Figure 2.1). Two pathways exist for ammonium assimilation – 1. reductive amination of α-ketoglutamate, catalysed by glutamate dehydrogenase, to form glutamate and 2. glutamate plus ammonium to form glutamine, catalysed by glutamine synthetase. Glutamate synthase then catalyses the transfer of glutamine amido group to α-ketoglutarate to produce two molecules of glutamate, where one is recycled back. Glutamate forms the basis of amino acids – the building blocks of proteins (Collos and Berges, 2009).

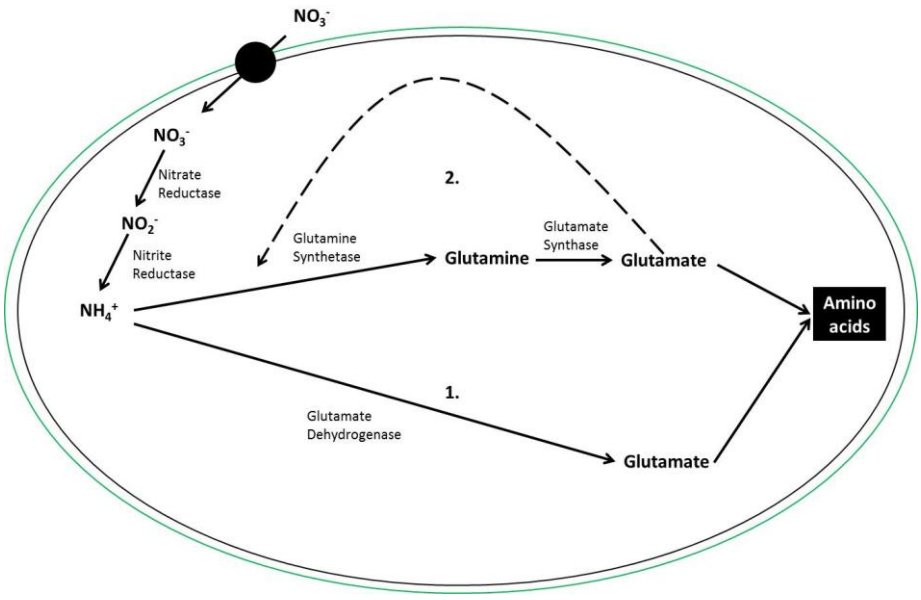

Figure 2.1. Nitrate metabolic pathways in microalgae.

Nitrates in the medium are depleted as the culture grows due to nitrogen becoming locked within the algae biomass. Nitrate limitation can restrict growth and biomass production through reduced protein synthesis and photosynthesis. Consequently, nitrate limitation can also see the reduction in certain products of interest, sometimes through depletion as products are recycled as a protein source in times of starvation; phycobiliprotein pigments are examples (de Loura, 1987). It is therefore important to monitor nitrate levels in algae cultures to avoid nutrient deficiency and consequences on productivity, whether that be biomass or levels of particular higher value products of interest. Conversely, nitrate limitation can cause carbohydrates and lipids to accumulate in microalgae. Under conditions of nitrate starvation microalgae cell division slows and cells divert energy to fatty acids for storage (typically triacylglycerol or TAG) (Breuer, 2012), which would normally be used in cell membrane synthesis. This is noted in numerous species, including *Chlorella*, and the process has been well reviewed by Sharma et al. (2012). Nutrient starvation is used widely in increasing lipid content in microalgae, particularly TAG for biodiesel production or polyunsaturated fatty acids (PUFAs) as nutraceuticals. Other biochemical products will accumulate under conditions of nitrate starvation including β-carotene in *Dunaliella* (Pisal, 2005). Production systems for these starvation products typically involve a two-phase process of high-nitrate biomass generation followed by a product-focused starvation period. This can be done through normal depletion of nitrate triggering the starvation phase (progressive limitation) or transfer of cells from a nitrate-rich to nitrate-poor medium (abrupt limitation) to begin starvation (Millán-Oropeza, 2015). In these production systems, nitrate monitoring also enables identification of starvation phases required for accumulation of such products.

Normal laboratory techniques for measuring nitrate concentration in algae cultures use lengthy colorimetric titration procedures involving numerous chemicals (Jones, 1984, Wood, 1967, Morris, 1963). Widely-used titrations involve use of the Cadmium Column Reduction Method (Strickland and Parsons, 1968) and preparation of the column can be time consuming. Samples higher than 10 mL are also required, as small volumes are used for washing/rinsing the column; therefore titrations are not practical for small batches where there is limited sampling volume. Field test kits, working on colour indicators (colorimetric assays) are commercially available. Although faster than titration methods, such kits only indicate broad concentration ranges and have higher limits of detection; they are therefore not practical for precise measurement of low nitrate concentrations (Turner Designs). Nitrate electrodes can be used to determine ionic nitrate concentrations, however the equipment is expensive and pH-dependable, therefore readings can be inaccurate with varying pH (Spellman, 2009) as occurs in microalgae cultures.

Real time continuous flow analysers are available, but again the equipment is expensive and unsuitable for small sampling frequencies (Jodo, 1992). The methods as described above could not be practically applied for accurate monitoring of low nitrate concentrations (<1 mM) in small-scale experiments, involving a number of readings over time, particularly where sample volume was restricted.

Alongside sufficient sensitivity and low sample volume requirements, Scottish Bioenergy was looking for a nitrate monitoring technique that was rapid, relatively low cost, and simple to perform given the standard laboratory equipment available to it. Such a method would be applied in smaller-scale experiments and also likely for monitoring larger-scale pilot systems. A challenge was set forming a miniature-project to attempt to develop a simple, rapid and low cost method for measurement of nitrate in microalgae cultures for use by the company. From initial research, Collos et al. (1999) outlined a method to monitor nitrate in phytoplankton cultures without the need for chemical addition, based on UV absorption (range 190-230 nm) by nitrate ions. The method first involves screening the medium components to determine UV absorbance and identify any potential interference in the selection of a particular wavelength in the UV range to be used for measurement. After, a calibration is performed using nitrate standards made up in the chosen medium. For measurement, samples are filtered followed by absorbance reading of the supernatant by UV spectrophotometry at the selected wavelength. Nitrate concentration can be determined using the produced calibration curve. Collos et al. (1999) demonstrated the method in Enriched Seawater, Artificial Water (ESAW) Medium (Harrison, 1980) for six marine phytoplankton including *Synechococcus* and *Isochrysis* for nitrate concentrations above 40 µM N L^{-1}. The group also showed the method to be in good agreement with standard colorimetric methods. Despite this simplified and rapid method, titration still remains the preferred and standard method for nitrate determination for sensitivity and discrimination – i.e. no real risk of interference from organic matter, nitrite, iron, chloride and iodide. However, the UV method may benefit certain applications where simplicity and rapidity may be of higher importance than sensitivity and where any interference risks have been limited. After discussing the Collos et al. method with Scottish Bioenergy, it was concluded that it could be a valuable R&D tool if it was successfully applied to the specific media and cultures of interest.

For simplicity, economy and speed, a modification to the Collos et al. method could involve centrifuging the cultures to remove organic matter as opposed to filtering using Whatman glass-fiber filters (GF/F). Centrifugation at a low enough speed to not damage the cells but high enough to form a pellet would be a satisfactory processing method if it can be demonstrated

that few cells or organic matter are retained in the supernatant *(Dr Yves Collos, personal communication).* Here, such a test would involve the use of two pieces of standard laboratory equipment which the company had access to: a UV/Vis spectrophotometer and a microcentrifuge. Modifications were made to the Collos et al. method and applied for nitrate monitoring using *Chlorella vulgaris* and *Dunaliella salina,* both species of commercial interest to Scottish Bioenergy.

2.2 Experimental Details and Method

2.2.1 Screening of medium components

Jarworski's and f/2 Media were prepared according to the recipes provided by the Culture Collection for Algae and Protazoa (CCAP) (www.ccap.ac.uk). Firstly, solutions of each medium component at their requisite concentrations were made and the UV absorbance measured to determine the level of interference from each component. The absorbance of both autoclaved (121 °C, 15 minutes) and non-autoclaved media with and without $NaNO_3$ were measured to determine any differences in absorbance caused by the autoclaving procedure. Absorbance was measured at 210 and 220 nm at room temperature against fresh deionised water (older deionised water can have a higher UV absorbance) using a Cary 100 UV/Vis Spectrophotometer (Varian, UK) and quartz cuvettes, as standard plastic cuvettes absorb in the UV range. Cuvettes were washed with deionised water and then a small volume of sample in between samples to ensure there was no contamination by the previous sample, or dilution caused by any remaining wash water.

2.2.2 Calibration

Sodium nitrate ($NaNO_3$) is commonly used as a nitrate source in many microalgae growth media, including both Jarworski's and f/2, so here the UV absorbance of $NaNO_3$ is used to indicate the nitrate level for monitoring. A $NaNO_3$ calibration curve was produced (0 M- ~ 0.001 M) against fresh deionised water. $NaNO_3$ (obtained from Sigma Aldrich) standards were produced by serial dilution of $NaNO_3$ stock and added to medium lacking the $NaNO_3$ component. The standards were autoclaved and absorbance scanned as described in 2.2.1. Absorbance spectra were plotted using Microsoft Excel 2007 and calibration curves produced through regression analysis.

2.2.3 Microalgae strain and culturing conditions

Chlorella vulgaris (CCAP 211/63) was obtained from CCAP and batch cultured in Jaworski's Medium as recommended by CCAP modified with the removal of $Ca(NO_3)_2$, and addition of $CaCl_2$ as described in 2.3.1 and Appendix 1. Microalgae were cultured in 1 L borosilicate bottles

with foam stoppers covered with aluminium foil to prevent evaporation and contamination. Eight hundred millilitres of sterile medium was inoculated with 10 % volume/volume (v/v) microalgae culture of density ~$2x10^{10}$ cells/L at logarithmic growth. Cultures were aerated using an eight-outlet air pump (Eco Air 8 Variable Control Air Pump), each outlet connected by 3 mm diameter silicon tubing (Thermo Fisher Scientific) to a glass pipette (5 mL) running to the bottom of the bottle. An in-line-valve/flow meter (Cole-Parmer) and 0.2 μm HEPA filter (Thermo Fisher Scientific) were used to control air-flow and ensure a sterile air supply. Air was provided at 70 mL per min (~0.875 vvm) and cultures were maintained at 18 °C (± 1°C) irradiated with a mixture of cool white and warm white fluorescent light at and an average light intensity of 105 μmol m^{-2} $s^{-1}$with an 16:8 light:dark cycle. Bottle positions were rotated daily to prevent positional bias on light exposure. During the experiment 4 mL samples were extracted for analysis daily after mixing from each batch culture. All equipment was sterile and inoculation and sampling was performed under aseptic conditions. Four biological repeat cultures were grown over 11 days until stationary phase.

2.2.4 Growth measurement

Microalgae growth was measured daily at similar times by direct cell counts taken using an improved Neubauer haemocytometer with a Leitz Dialux 20 light microscope at x400 magnification. Cell counts were taken as an average of 10 x 0.004 mm^2 (0.4 μl) squares.

2.2.5 Nitrate measurement

2 mL volumes of culture were centrifuged at 3000 g for five minutes (Sigma 1-15 microcentrifuge) to remove cells, particulates and suspended organic matter and the supernatant was used for analysis. Absorbance of the samples was measured at 210 nm; if required samples were diluted until the absorbance fell into the range of 0.2-1.5 (linear part of the calibration curve) for accuracy. Nitrate concentration was calculated from the mean of three technical replicates using Equation 2.1, where absorbance *x* is multiplied by the dilution factor if dilution is required.

Equation 2.1: $y = 8048.9x + 0.141$

Where *y* is the concentration of $NaNO_3$ (M), *x* is the absorbance at 210 nm.

All results were recorded in Microsoft Excel 2007 and analysed using Matlab (2010).

2.3 Results

2.3.1 Interference from medium components

Most medium components had a negligible absorbance at 210 nm (Figure 2.2). Calcium nitrate ($Ca(NO_3)_2$), a second nitrate source in Jaworski's Medium, had high absorbance as expected at 210 nm. The recipe for Jarworski's Medium was changed to remove the $Ca(NO_3)_2$ component and supplemented with a higher amount of $NaNO_3$ to account for the nitrate lost through $Ca(NO_3)_2$ removal. $NaNO_3$ stock concentration (stock 8) was increase to 1.44 g/ 200 mL and 19 g/ 200mL of calcium chloride ($CaCl_2$) was added as an alternative calcium source (stock 1). Details of media and modifications can be found in Appendix 1. $NaNO_3$ would then be solely responsible for significant changes in absorbance at 210 nm correlating to nitrate concentration.

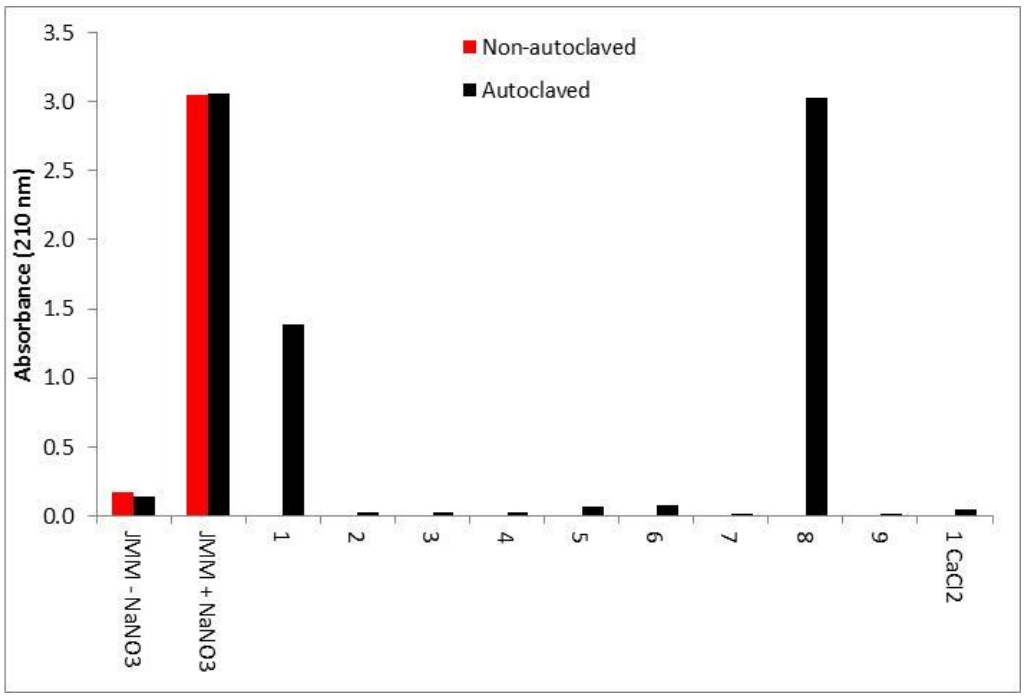

Figure 2.2. Absorbance at 210 nm of Jarworski's Medium and Jarworski's Modified Medium (JMM) components. Numbers 1-9 represent original stock solutions 1: $Ca(NO_3)_2$, 2: KH_2PO_4, 3: $MgSO_4$, 4: $NaHCO_3$, 5: EDTAFeNa, $EDTANa_2$, 6: H_3BO_3, $MnCl_2$, $(NH_4)6Mo_7O_{24}$, 7: cyanocobalamin, thiamine HCl, biotin, 8: $NaNO_3$, 9: Na_2HPO_4 (details of medium can be found in Appendix 1). $CaCl_2$ is the replacement stock solution 1 in JMM. Absorbance for autoclaved and non-autoclaved JMM with and without the addition of $NaNO_3$ is also shown.

As shown in Figure 2.2 the absorbance of all individual medium components in JMM was negligible in comparison to absorbance by $NaNO_3$ at 210 nm. Therefore components would not contribute to absorption in samples to an extent which would affect the accurate measurement

of $NaNO_3$ concentration through UV absorption. Interestingly, there were slight differences in absorbance in autoclaved compared with un-autoclaved medium (Figure 2.2).

2.3.2 Calibration of Jarworski's Medium

The 200-250 nm region of the absorbance spectra for the calibration series of standards with increasing nitrate concentration, along with the derived absorbance calibration curve at 210 nm can be seen in Figure 2.3. Absorbance spectra (Figure 2.3a) show a clear relationship between increasing $NaNO_3$ concentration and increasing absorbance within the region of 200-230 nm. At the higher $NaNO_3$ concentrations (0.00025-0.001 M) noise in the absorbance spectra was seen between the 200-215 nm wavelengths.

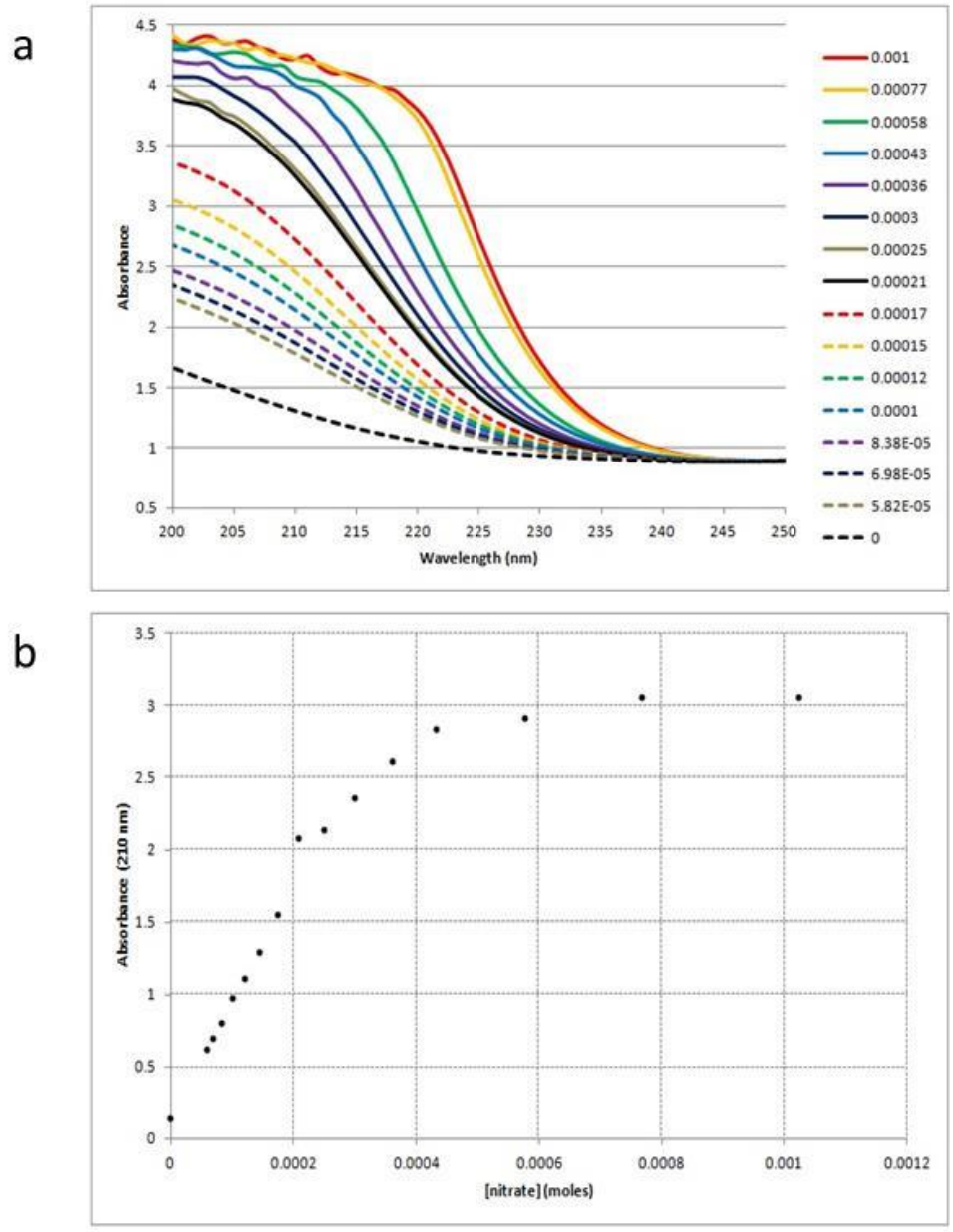

Figure 2.3. Absorbance spectra (200-250 nm) for $NaNO_3$ standards in Jarworski's Modified Medium (JMM) (a). Absorbance (210 nm) versus $NaNO_3$ concentration in JMM (b).

Collos et al. (1999) suggested 210 and 220 nm for use in spectroscopic nitrate measurement. Here, 210 nm was selected for JMM as absorbance (intensity) was highest at this wavelength, which should allow better 'resolution'.

The calibration curve (Figure 2.3b) becomes non-linear at an absorbance of around 2 at 0.0002 M $NaNO_3$. Non-linearity at concentrations above ~0.0002 M $NaNO_3$ also corresponds to the concentrations showing noise in the absorbance spectra at wavelengths below 215 nm. Absorbance data for these concentrations were therefore excluded and the linear part of the curve (0-0.00017 M $NaNO_3$) was used to derive an equation through linear regression, explaining the relationship between absorbance (210 nm) and $NaNO_3$ (M), for use in a spectroscopic nitrate measurement method for JMM (Figure 2.4). This equation (see Equation 2.1 in 2.2.5) can be used to accurately determination $NaNO_3$ concentrations in samples whose absorbance falls within the range of 0.2-1.5. Samples with absorbance values at 210 nm above 1.5 must be diluted so that absorbance at 210 nm falls within this range. The calculated concentration can then be multiplied by the dilution-factor to derive the $NaNO_3$ concentration.

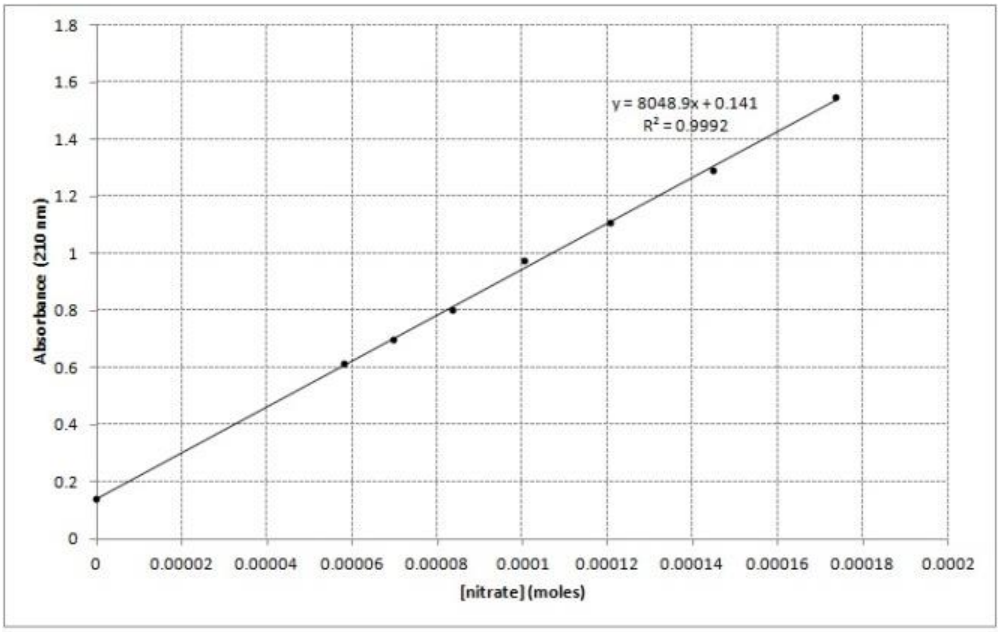

Figure 2.4. Calibration curve and derived linear equation for use in spectroscopic nitrate measurement in Jarworski's Modified Medium.

2.3.3 Calibration of f/2 Medium

The absorbance of all individual medium components tested, as background, was negligible and would not contribute to absorption in samples to an extent that would affect accurate $NaNO_3$ measurement (Figure 2.5). There was a small amount of absorbance by filtered seawater, likely caused by the small concentration of nitrates (~2-5x10^{-5} M according to Sharp et al. (1982)) already present in seawater. Interestingly, autoclaving slightly increased the

absorbance in seawater and f/2 Medium (with and without nitrate), likely caused by precipitation during the autoclaving procedure. Here, precipitates are formed which can interfere and increase absorbance in the medium.

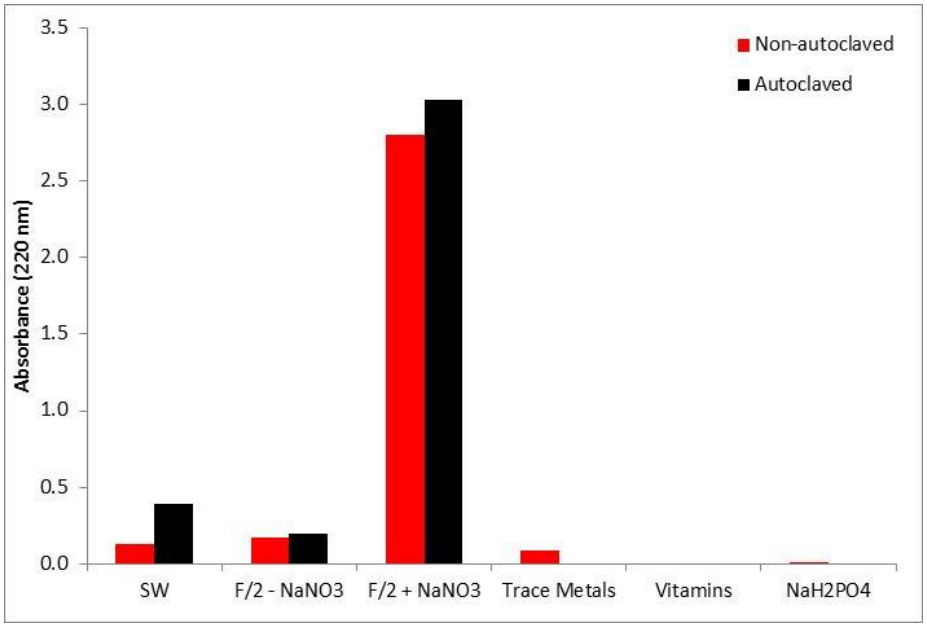

Figure 2.5. Absorbance at 220 nm of f/2 Medium components. Trace metal solution contains: $EDTANa_2$, $FeCl_3$, $CuSO_4$, $ZnSO_4$, $CoCl_2$, $MnCl_2$, Na_2MoO_4. Vitamin solution contains: cyanocobalamin, thiamine HCl, biotin (details of medium can be found in Appendix 1). Absorbance for autoclaved and non-autoclaved filtered seawater and f/2 with and without the addition of $NaNO_3$ is also shown.

The 200-250 nm region of the absorbance spectra for the calibration series of standards with increasing nitrate concentration, along with the derived absorbance calibration curve at 220 nm are given in Figure 2.6.

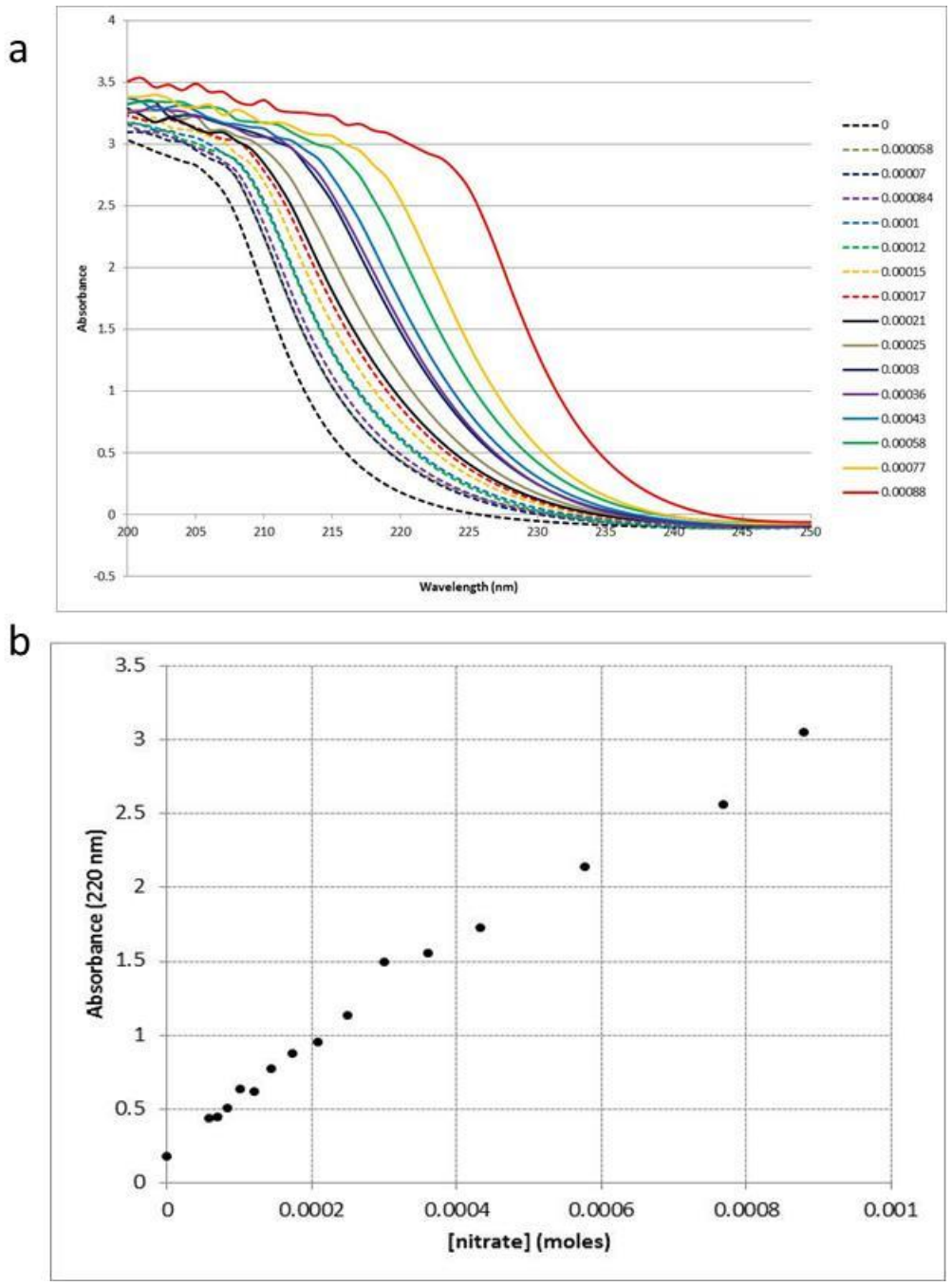

Figure 2.6. Absorbance spectra (200-250 nm) for $NaNO_3$ standards in f/2 Medium (a). Absorbance (220 nm) versus $NaNO_3$ concentration in f/2 Medium (b).

The absorbance spectrum shows a clear relationship between increasing $NaNO_3$ concentration and increasing absorbance within the region of 210-230 nm (Figure 2.6a). There is considerable noise in the majority of spectra above 210 nm. This noise is more extensive than seen with JMM, likely caused by the presence of halogen compounds or sodium chloride (Collos, 1999). Similar noise is also present in the absorbance spectra of the higher $NaNO_3$ concentrations (0.00036-0.00088 M) and for this reason these standards were removed from the calibration. Unlike in JMM, where 210 nm was used for nitrate absorption, because of the noise in the spectra around 210 nm, 220 nm was used. Absorbance at 220 nm for each $NaNO_3$ concentration

was plotted to create a calibration curve (Figure 2.6b) which suggests that 220 nm should give a good resolution for $NaNO_3$ concentration determination.

From Figure 2.6b it can be seen that the calibration curve becomes non-linear at an absorbance of around 1.5 at 0.0004 M $NaNO_3$. Absorbance data for these concentrations were therefore excluded and the linear part of the curve (0-0.0003 M $NaNO_3$) was used to derive an equation through linear regression, explaining the relationship between absorbance (220 nm) and $NaNO_3$ (M), for use in a spectroscopic nitrate measurement method for f/2 Medium (Figure 2.7 and Equation 2.2).

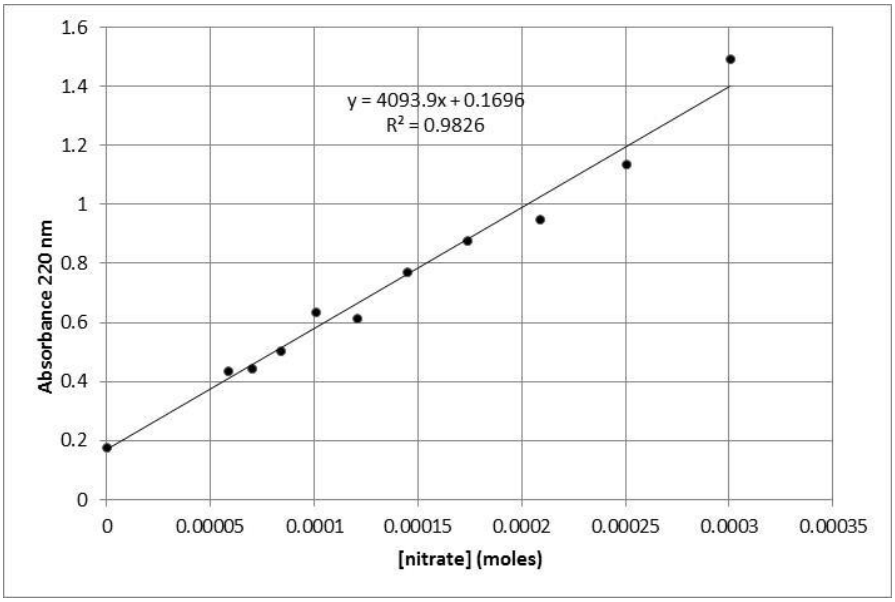

Figure 2.7. Calibration curve and derived linear equation for use in spectroscopic nitrate measurement in f/2 Medium.

Equation 2.2: $y = 4093.9x + 0.196$

Where *y* is the concentration of $NaNO_3$ (M), *x* is the absorbance at 220 nm. Absorbance *x* should be multiplied by the dilution factor if dilution is required.

Equation 2.2 can be used for accurate determination of $NaNO_3$ concentrations in samples whose absorbance falls within the range of 0.2-1.5. Samples with absorbance values at 220 nm above 1.5 must be diluted so that absorbance at 220 nm falls within this range. The calculated concentration can then be multiplied by the dilution-factor to derive the $NaNO_3$ concentration.

2.3.4 Demonstration of spectroscopic nitrate measurement in Chlorella

The method of nitrate measurement in JMM was then used to track the nitrate concentration during four (repeat) batch cultures of *C. vulgaris*. Samples were taken daily over 11 days and nitrate was measured in 2 mL samples through centrifugation and absorbance of supernatant at 210 nm, requiring dilution early on in the batch. Culture density and corresponding nitrate concentration over the 11 day batch is shown in Figure 2.8.

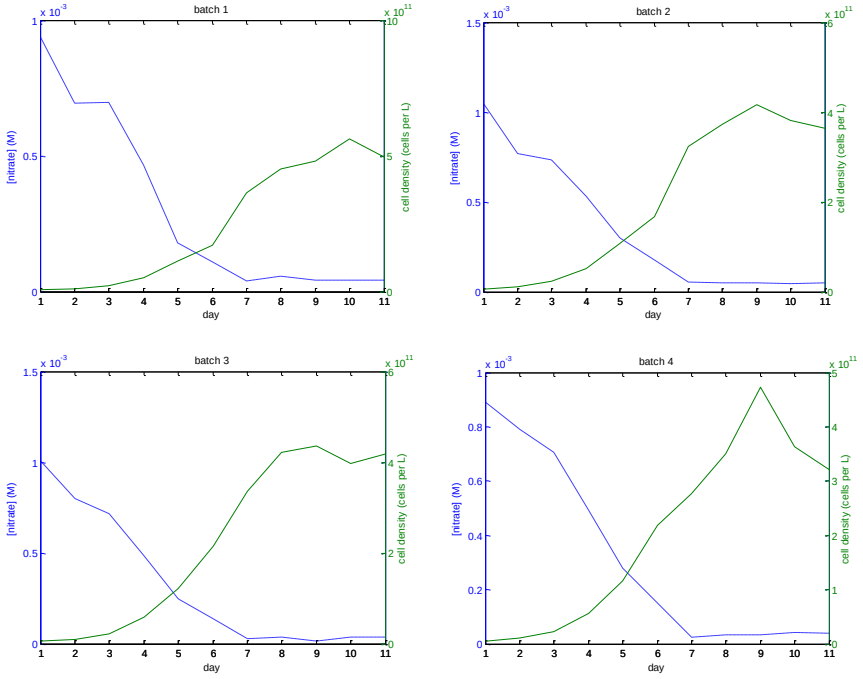

Figure 2.8. Nitrate concentration in the four batch cultures over a period of 11 days plotted against cell density.

Supernatant samples analysed under the microscope before UV absorbance measurement did not show the presence of any *Chlorella* or debris, demonstrating that the centrifugation technique was sufficient to remove suspended organic matter and particulates. Nitrate concentrations at the start of the culture (~1 mM) matched the expected concentration given the $NaNO_3$ concentration of JMM. Nitrate concentration in the batches decreased rapidly from ~1 mM to ~0.2-0.3 mM by day five, during the logarithmic growth phase. Upon the cultures reaching stationary growth, there was little nitrate remaining in the culture and the detection limit (~40 μM) for nitrate was reached at day seven in all of the cultures.

2.4 Discussion

At the beginning of this mini-project the company was looking for a nitrate monitoring method which was simple, fast, required low sample volumes and where costs were low, given the current equipment the company had access to, but which also had the accuracy and sensitivity for use with the concentration ranges of nitrate in common microalgae media.

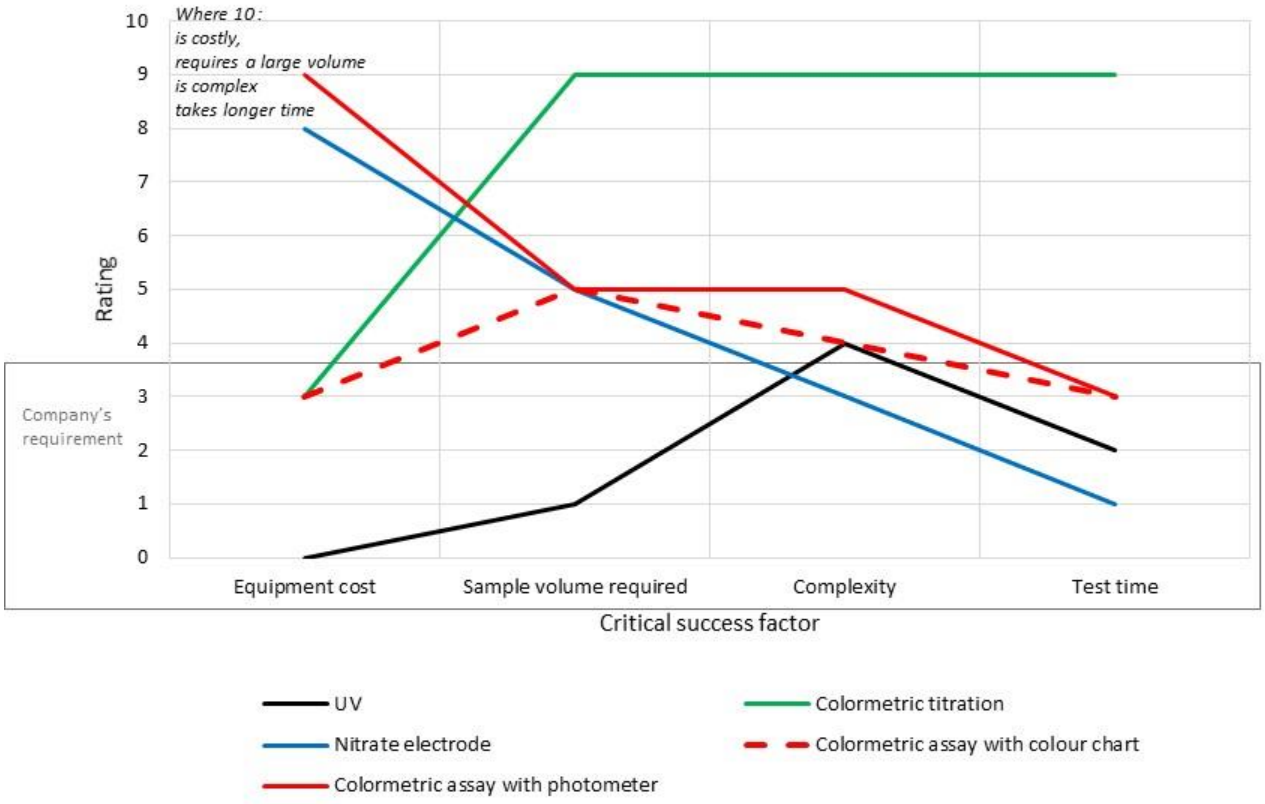

Figure 2.9. Value curves for five commonly used nitrate tests. Tests are rated for four critical success factors which are features of a nitrate test particularly valued by the company at the start of the project. The grey box shows the company's rating requirement.

In Figure 2.9 the UV method is compared with four other commonly used nitrate tests. The comparison is made based on the four features identified to be most important when developing a test for use by the company (critical success factors) at the start of the project. The critical success factors are rated using Vernier Nitrate Ion-Selective Electrode and Vernier labquest interface system, Palintest photometer 7100 kit with nitrate reagent starter pack, Cadmium-copper column (titration) method by Strickland and Parsons (1968) and Palintest SK200 field kit as examples, where information is based on Standard Operating Procedures in the instruction manuals. Equipment is costed based on supplier quotes and only on requirement of any additional equipment necessary not already available in the company's laboratory at the time (excluding lab disposables). Filtration of samples is not costed. Figure 2.9 shows that the UV method best meets the company's requirements for a relatively low-cost, simple, fast test where low sample volume is required.

The Vernier Nitrate Electrode must be used with a datalogger (Vernier labquest interface system) at an equipment cost of nearly £1000, requiring a 10 mL sample to take a reading to nitrate concentration. Apart from setting the interface and calibrating the electrode taking a

reading is straight forward and readings can be taken in a few minutes. Cadmium-copper column colormetric titrations do not require expensive equipment, only standard laboratory equipment, a number of chemicals for preparation of solutions and a column. However large sample volumes (100 mL) are needed to wash and run through the column and preparation of solutions and column, requiring multiple steps, makes this method complex and lengthy, taking a number of hours. Colormetric field kits such as the Palintest SK200 can be purchased for around £200 and are simple to use with the addition of colour indicators to 10 mL samples to be compared against colour charts within 15 minutes. The problem with colormetric assays when used with colour charts is that comparison is done by eye meaning only broad concentration ranges of samples can be determined so there is little sensitivity in the tests and they are not suitable for monitoring small concentration changes. To solve the sensitivity problem these colormetric assays can be used with special photometers (for example Palintest photometer 7100) to provide a digital reading of nitrate concentration based on colour absorbance. The photometer however increases the equipment cost significantly by 100s of pounds. Given the company already had access to standard laboratory equipment including a spectrophotometer and quartz cuvettes, no additional equipment would have to be purchased in the use of the UV method for measuring nitrate concentration and only 2 mL of sample is required for three repeats readings, a much lower volume than is required for other nitrate tests. The complexity of the UV method is in the dilution of the sample so that the absorbance falls within a particular range which puts the complexity proportionate to colormetric assay tests with a five minute time saving from experience using the UV method.

Although the UV method to monitor nitrate may be inferior in accuracy and sensitivity to other tests such as colorimetric titration (Collos, 1999), it is superior overall in its simplicity, speed, and low volume sample requirement and suitably accurate and sensitive within the range of the nitrate concentrations which are currently used in a number of common microalgae media for monitoring nitrate levels.

The adequacy of the UV technique for other applications is of course dependent on the accuracy and sensitivity in the required experiments. Firstly, if measurement of nitrate concentrations below 40 μM are required then this technique may not be suitable, dependent on the background absorbance of other components of the medium of interest, which in these experiments was ~40 μM. Secondly, there will also be a limit to the maximum nitrate concentration measureable by this method. Absorbances higher than those used to derive the linear equation (0.0003 for f/2 and 0.00017 for JMM) cannot be used in the equation to calculate nitrate concentration as the equation assumes a linear relationship between absorbance and nitrate concentration which is

not true at higher absorbances (Burke, 2001). Typically, dilutions are required to obtain an absorbance within the linear range, and here errors can be created by dilution increases with a larger dilution factor at higher nitrate concentrations. Therefore at high nitrate concentrations measurements can contain large error.

Use of JMM as a modified version of Jarworski's Medium should not have any detriment on cultures as $CaCl_2$ is a commonly used calcium source in a number of standard medias (Becker, 1994) including EG:JM, a freshwater medium (CCAP). However, the inability to change medium components which interfere with UV absorbance of nitrate, will prevent the use of this method for nitrate measurement. Experiments with JMM and f/2 Media in this chapter show that the method can be used with both freshwater and saltwater media. Use of the method for JMM was also demonstrated in *Chlorella*. Nitrate levels throughout the batch cultures followed the expected depletion trend. Upon the culture reaching the stationary growth phase, there was little nitrate (below detection limit) remaining in the culture. Growth uses a fixed amount of nitrate available in the medium and nitrate was therefore depleted. At stationary phase, nitrate had depleted beyond the detectable limit. Here perhaps nitrate is the limiting factor and a causal factor of stationary growth. The measurement technique has shown to be sufficient for application.

Although in the experiments with *Chlorella* centrifugation at low speed as a method of separating cells, suspended organic matter and particulates was sufficient, there may be particular cultures for which centrifugation will not suffice. It is important to check, when setting up such a method, whether cells remain in the supernatant after centrifugation. From experience, particular microalgae can be difficult to pellet. Of particular mention is *Arthrospira* where gas vacuoles can keep some filaments in suspension even after high-speed centrifugation (10-15 g). This technique using centrifugation for filtering is therefore not applicable to *Arthrospira*. Care should also be taken that centrifugation is not carried out at speeds high enough to damage cells and release cell components into the supernatant which could affect absorbance. *Dunaliella* can be more difficult to pellet than *Chlorella*, given their high lipid content and buoyancy and it is tempting to increase centrifugation speed. However, their lack of a cell wall makes them susceptible to damage at high centrifugation speeds (Borowitzka, 1989). Dissolved Organic Matter (DOM) is the fraction of organic matter that can be sized 300,000-100 Da or <0.1 µM, much smaller than Particulate Organic Matter (POM) which includes microalgae and bacteria (Mostofa, 2013). Microalgae are known to release DOM into the culture medium during normal growth (Puddu, 2003). Algae exudates mainly comprises carbohydrates and also nitrogen compounds (Aluwihare and Repeta, 1999). As DOM is known

to absorb UV (Mostofa, 2013), the presence of DOM in samples could affect the accuracy of nitrate concentration determined by this spectroscopic method. In experiments by Mostafa et al. (2013) DOM concentration increased over the batch time of *Chlorella vulgaris* and *Dunaliella tertiolecta* cultures in a PBR reaching a maximum of 37-times the levels contained in medium. Given the range (and sensitivity) of this method, a 37-times increase in DOM and associated interference may be trivial in comparison. This would depend on the accuracy required from the technique. As DOM release by microalgae is also known to increase under conditions of stress, particularly restricted supply of nutrients, interference effects may be higher for use in nitrate monitoring cultures under stress conditions and so applications should be carefully considered (Obernosterer and Herndl, 1995). Filtering would not avoid DOM interference given the such small particle size.

After further experimentation with filtration equipment, Collos et al. recommend using syringe filters (Pall-Gelman Acrodisc 25 mm, 0.2 μM HT Tuffryn membrane) *(Dr Yves Collos, personal communication).* Although syringe filtering will increase disposable costs, it is quicker than basic filter paper and doesn't require larger samples for washing of the membrane so sample size required remains small if volumes are limiting in experiments.

Apart from the speed and simplicity of this spectroscopic method, the requirement for small volumes is of great value in small-scale batch experiments where sampling volume is limited. As no more than 10 % of culture volume can be taken for sampling (Doran, 2005) in experiments of 500 mL volumes where daily sampling is required over 11 days, a maximum of only 4.5 mL samples can be taken. A maximum sample volume of 2 mL was required in these experiments for nitrate concentration determination, which suits such set-ups and sampling volume limitations. After centrifugation this volume provided ~0.5 mL for washing of the cuvette and 3 x 0.5 mL technical replicates for measurement of UV absorbance. Additionally, where dilutions are required, smaller volumes can be used.

Finally, there has been much interest in this technique for nitrate measurement by fellow researchers at Newcastle University. Although the technique is inferior in accuracy and sensitivity to colorimetric titration methods, in certain situations the accuracy and sensitivity offered is acceptable for the purpose and the merits in ease of use and small sample volume requirement are easily recognisable, especially for application to multiple small-scale experiments where nitrate concentration data is of value. The knowledge of this method has not only been passed onto the company for use in small-scale experimentation, but also a number

of PhD and post-doctoral researchers have successfully adapted the technique for simplified and rapid nitrate monitoring in their own research.

Chapter 3. Enhancing Phycocyanin Production in Arthrospira platensis using Long Wavelength Red Light

3.1 Introduction

3.1.1 Photosynthesis in microalgae and cyanobacteria

Approximately 3 billion years ago, cyanobacteria-like organisms were responsible for the 'Big Bang of evolution' (Barber, 2008). They evolved cellular apparatus that could capture visible solar radiation (300-700 nm), allowing the extraction of electrons from water (H_2O) and the reduction of carbon dioxide (CO_2) to energy-rich carbohydrates, releasing oxygen (O_2) as a by-product (Srivastava and Neilan, 2013). This event began the accumulation of oxygen in Earth's atmosphere, creating aerobic conditions suitable for the development of more advanced life forms based on aerobic metabolisms.

Cyanobacteria (formerly classified as blue-green algae) still contribute important amounts of O_2 to the atmosphere – providing an estimated 50-80 Gigatonne (Gt) of O_2 per year and fixing 20-30 Gt of CO_2 into biomass; around 20-30 % of global primary photosynthetic productivity (Srivastava, 2013). Many cyanobacteria species are also capable of fixing atmospheric nitrogen (N_2) using specialised heterocyst cells (Zehr, 2011) and some can grow using anoxygenic photosynthesis, using hydrogen sulphide (H_2S) as an alternate electron donor to H_2O (Cohen, 1986).

The mechanism of oxygenic photosynthesis in cyanobacteria resembles that of eukaryotic algae and higher plants. The light processes of photosynthesis can be broken-down into four steps as shown in Figure 3.1.

1. Light capture by photosynthetic pigments;
2. Photosystem energy conversion;
3. Electron transport and oxidation of H_2O coupled with the evolution of O_2 (Photosystem I and Photosystem II and electron carriers plastoquinones, Cyt b6-f and plastocyanin);
4. $NADP^+$ reduction to NADPH and phosphorylation of adenosine diphosphate (ADP) to adenosine triphosphate (ATP) (ferredoxin-NADP oxidoreductase ATP synthetase).

These four steps occur in the thylakoid membrane with metabolic processes involving inorganic carbon and nitrogen occurring in the stroma through enzyme activity.

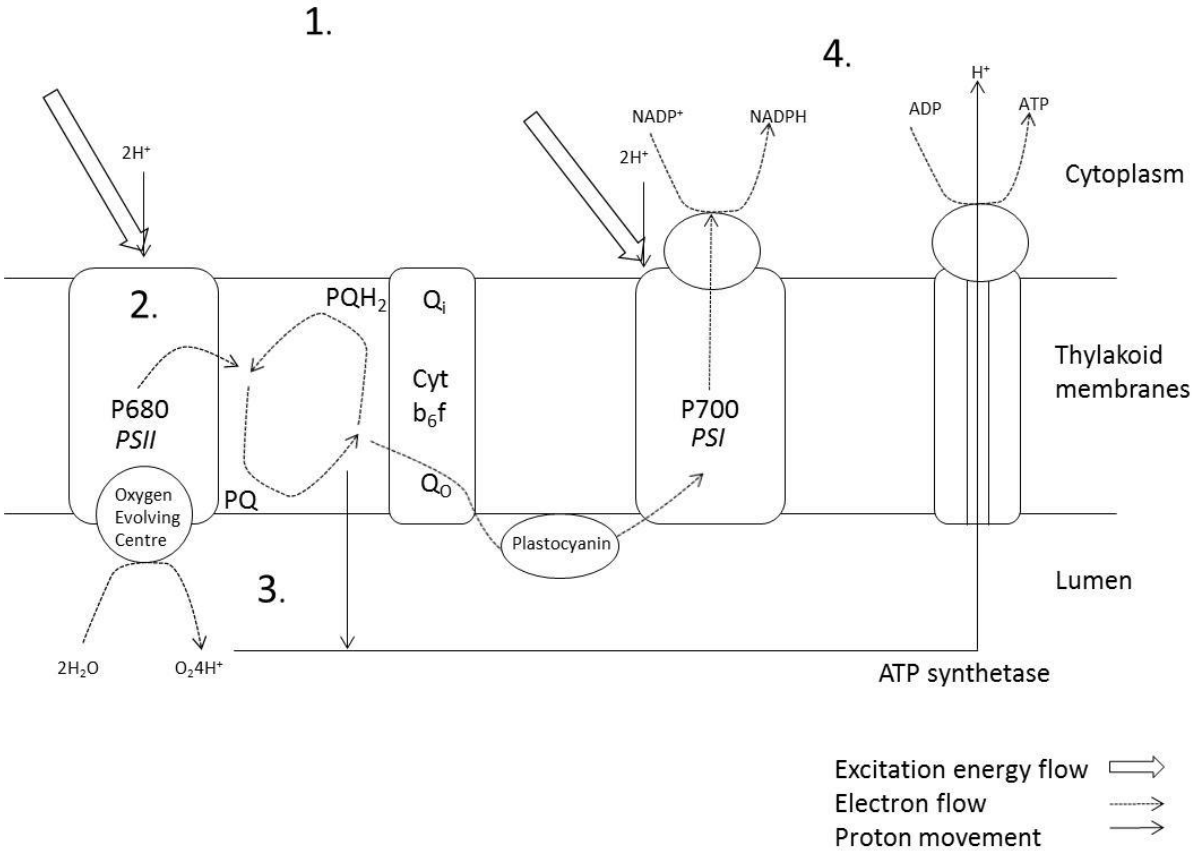

Figure 3.1. Simplified schematic of the energy conversion process in photosynthesis. P680 and P700 represent the reaction centre Chl*a* of photosystem II (PSII) and photosystem I (PSI) respectively. Plastoquinol (PQH_2) and plastoquinone (PQ) are the respective oxidation and reduction site of cytochrome b6-f (Cyt b6-f). Light is captured by photosynthetic pigments (1) and photons channeled to PSII where they are converted to electrons (2) for oxidation of H_2O producing O_2 (3) and reduction of $NADP^+$ to NADPH and phosphorylation of ADP to ATP (4). Energy flow to PSII is greater than PSI. Production of NADPH and ATP contributes to CO_2 fixation and carbohydrate production.

In step 1, photons of light are captured and converted to excitation energy by pigments located in (or attached to trans-membrane proteins in, and present on the outside of) the thylakoid membrane. The main pigment in this process is chlorophyll *a* (Chl*a*) (Björn, 2009). Chl*a* absorbs light in the regions 200-500 and 650-700 nm, showing two absorbance peaks with maximum wavelength (λ_{max}) 465 nm and 665 nm (Figure 3.2). In addition to Chl*a*, most but not all cyanobacteria contain carotenoids and phycobilins which function as accessory pigments in this step 1 of photosynthesis, absorbing wavelengths of light that are not absorbed by Chl*a*. Carotenoids are a group of fat-soluble pigments coloured from pale yellow to deep red with an absorption maxima in the region of 400-500 nm (Figure 3.2). Carotenoids are present in cyanobacterial cytoplasmic membranes for photoprotection in high irradiance conditions (Masamoto, 1999), but also in the thylakoid membranes complexed to proteins as

accessory pigments in photosynthesis. The most abundant carotenoids are α-, β-and γ-carotene, lycopene, lutein, zeaxanthin, and astaxanthin. Well-known examples of carotenoids found in eukaryotic unicellular microalgae are the production of the orange pigment β-carotene by *Dunaliella salina* (Pisal, 2005), and red astaxantin production in *Haematococcus pluvialis*, both under conditions of cellular stress (Solovchenko and Chekanov, 2014).

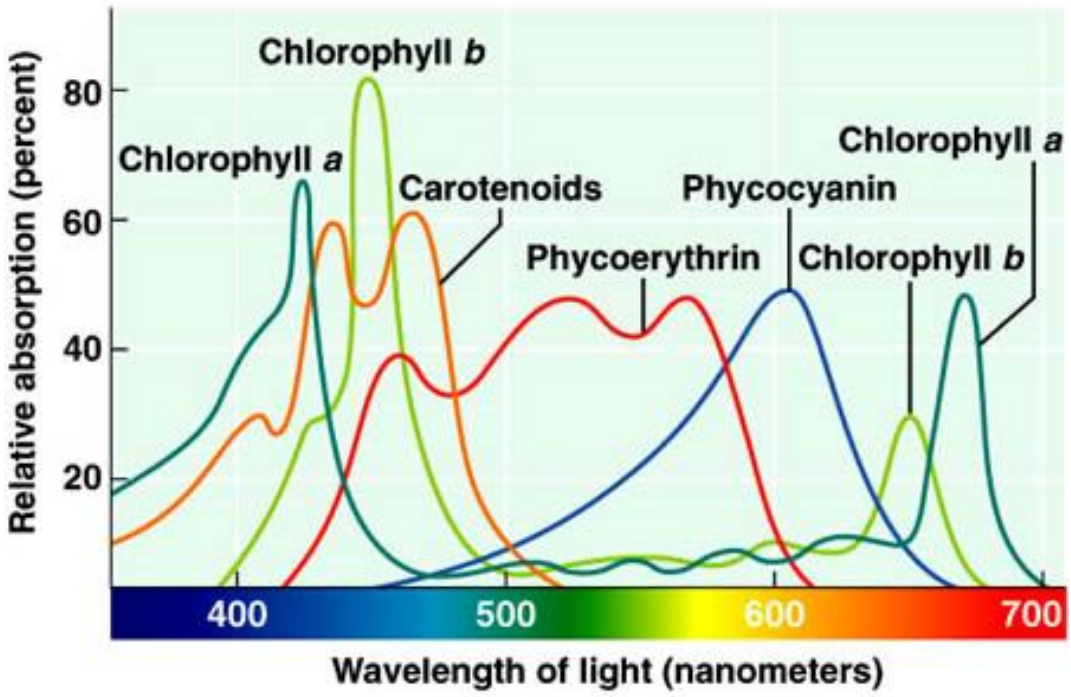

Figure 3.2. Absorbance spectra of multiple photosynthetic pigments. Chl*a* (in acetone) λmax 430 and 664 nm, phycocyanin 615-640 nm, allophycocyanin 650-655 nm and phycoerythrin 495-655 nm. Image sourced from http://www.citruscollege.edu/lc/archive/biology/Pages/Chapter06-Rabitoy.aspx.

Phycobilins are chromophore molecules formed from open chains of four pyrrole rings (tetrapyrole) (unlike chlorophyll whose pyrroles are arranged in a ring with a metal atom in the centre) (Figure 3.3). Phycobilins attach to water-soluble proteins to create phycobiliproteins, the most common being the blue pigments phycocyanin, allophycocyanin, and the red pigment phycoerythrin. These phycobiliproteins are found in mixtures and variations in photoautotrophs. Phycocyanin, phycoerythrin and allophycocyanin absorb at λ_{max} 620 nm, 565 nm (with an additional absorption peak at 498 nm) and 655 nm respectively (Figure 3.2).

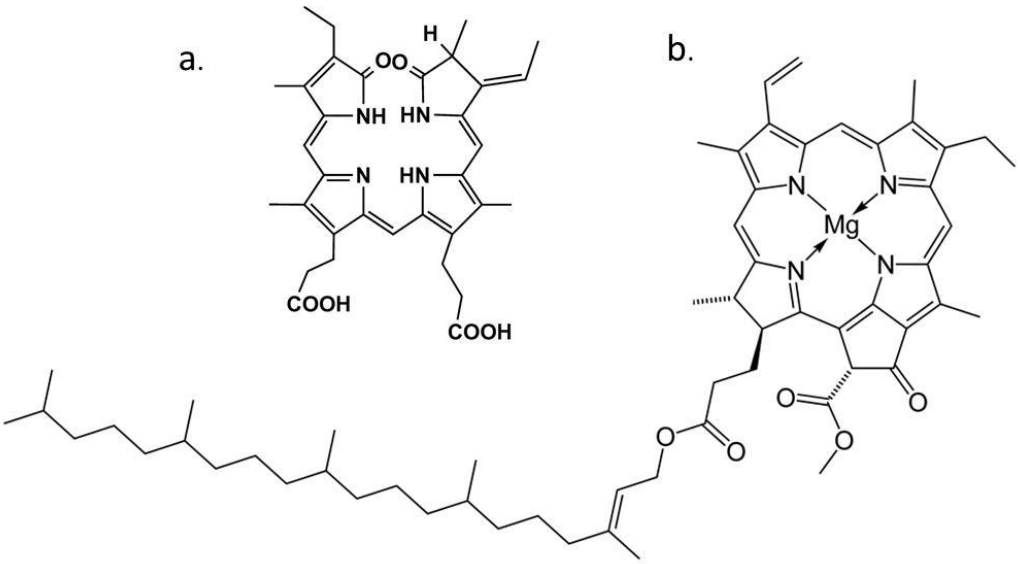

Figure 3.3. The structures of phycocyanobilin (a) and chlorophyll *a* (Chl*a*) (b). A Chl*a* molecule has 4 pyrroles arranged in a ring around a central manganese (Mg) atom. Differently, phycobilins are formed from a chain of four pyrrole rings. Images sourced from https://commons.wikimedia.org/wiki/File:Chlorophyll-a-2D-skeletal.png and Zhao et al. (2007).

There are also other types of chlorophyll, with chlorophyll *b* (Chl*b*) commonly present in photosynthetic eukaryotic algae and higher plants, but not cyanobacteria. Chl*b* is more water soluble that Chl*a* and absorbs in different regions (λ_{max} 450nm and 650 nm) (Figure 3.2).

In cyanobacteria, both photosynthetic (in the presence of light) and respiratory (in the absence of light) reactions take place on the same thylakoid membrane, whereas in eukaryotic microalgae, for example, photosynthesis and respiration takes place in separate organelles; the chloroplast and mitochondria respectively.

During exposure to ultra-violet radiation (UVR) in normal daylight and sources of artificial light, Reactive Oxygen Species (ROS) are produced in cyanobacteria. ROS (a type of free-radical) are high energy molecules containing oxygen produced during normal biochemical reactions or through exposure to ionising radiation such as UVR. ROS contain an unpaired electron making them highly-reactive molecules, meaning they can react with lipids, protein and nucleic acids causing high amounts of cellular damage if they accumulate. As well as the benefits of absorbing the maximum amount of light for photosynthesis, contributing to cellular growth and maintenance of vital processes for life, cyanobacteria must control and optimise the amount of light they absorb so that cells do not accumulate ROS to damaging levels.

3.1.2 The chemistry of phycocyanin and the phycobilisome

Phycocyanin is a blue pigmented phycobiliprotein – a chromophore – produced in prokaryotic cyanobacteria as well as certain eukaryotes including the rhodophytes, cryptomonads and glaucocystophytes. In *Arthrospira* (*Spirulina*) *platensis*, phycocyanin is complexed with another phycobiliprotein – allophycocyanin – which together function as a light-harvesting apparatus known as the phycobilisome (Figure 3.4). Phycobilisomes attach to the surface of the thylakoid membrane on the cytoplasmic side and are normally much larger than the photosystems. The phycobilisome absorbs specific wavelengths of light which cannot be utilised by chlorophyll, thereby increasing the efficiency of photosynthesis.

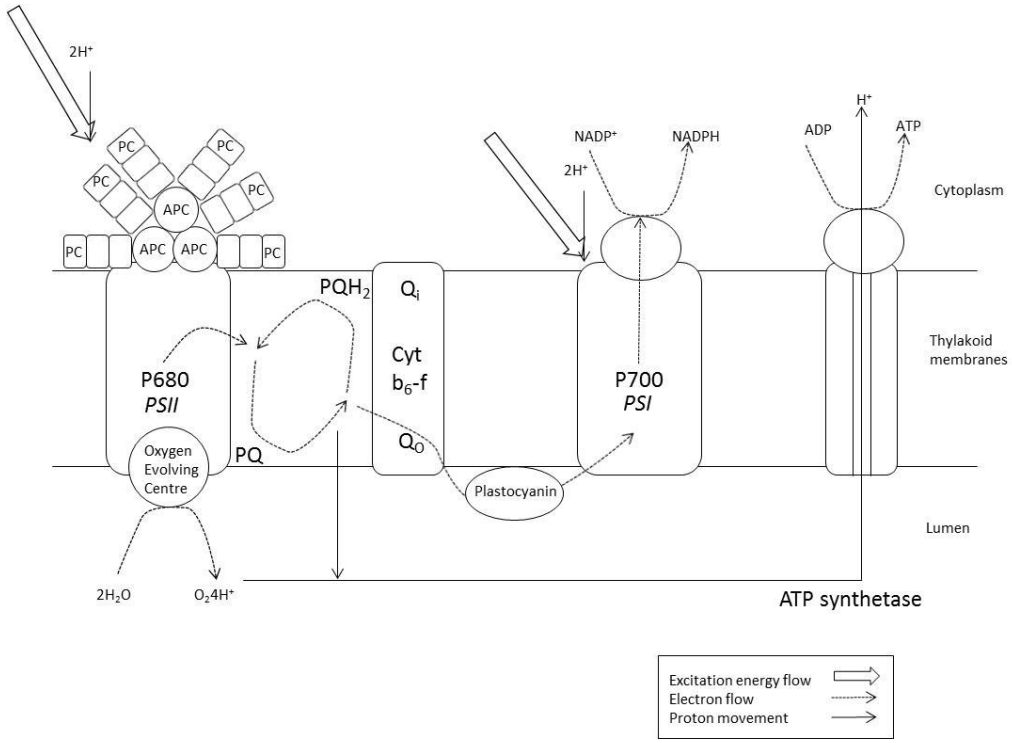

Figure 3.4. Schematic of a typical cyanobacterial thylakoid membrane containing photosystems I (700 nm) and II (680 nm) and the phycobilisome consisting of a tricylindrical core of allophycocyanin (APC) at the base of the phycobilisome and six phycocyanin (PC) rods extending from the core (as described by Nomsawai et al. (1999)). Each core is composed of 2-3 stacked discs. Phycocyanin absorbs maximally at 610-620 nm and allophycocyanin at 650-655 nm. Note that although the phycobilisome is shown attached only to PII, phycobilisomes have mobility and can be redistributed to PI.

Phycocyanin rods of stacked disks, 6-10 in number comprising of 2-3 discs, covalently attach to the allophycocyanin core of the phycobilisome via colourless linker proteins (Figure 3.5). Electron micrographs take by Ducret et al. (1996) can be seen in Figure 3.6. In other cyanobacteria and eukaryotes (namely Rhodophyta) the phycobilisome also contains phycoerythrin which forms the outer disks of the rods. Phycoerythrin is an advantageous

accessory pigment at ocean depth where mainly green light is available (Falkowski and Raven, 2007).

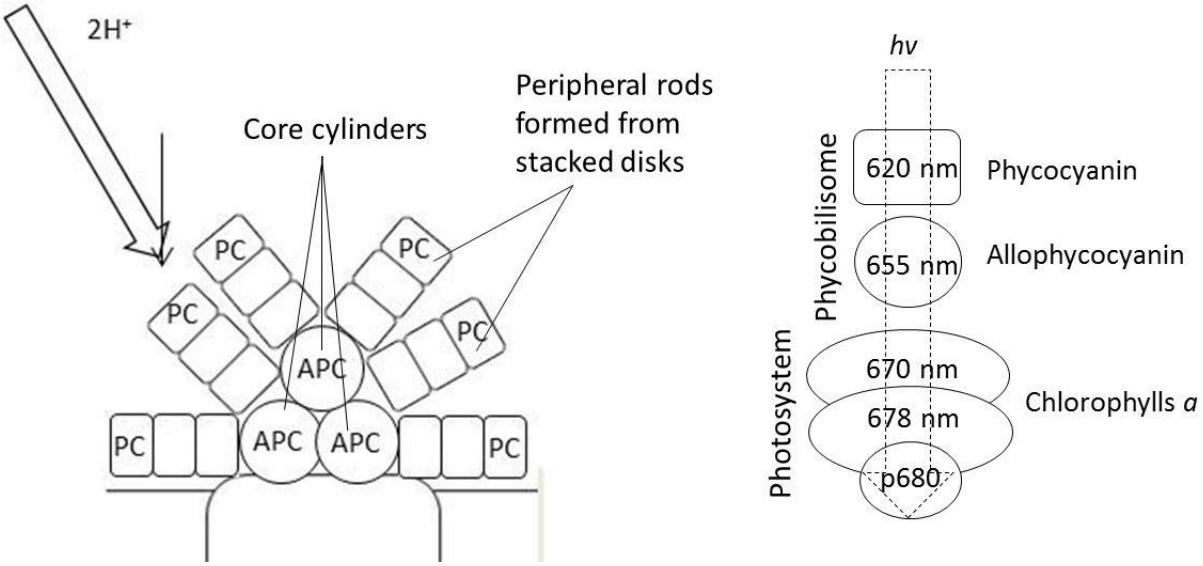

Figure 3.5. The phycobilisome of *Arthrospira* (left) and schematic of excitation energy transfer steps in the phycobilisome and PSII reaction centre (right). The phycobilisome is formed of an allophycocyanin (APC) core and peripheral rods of phycocyanin (PC) (left). The absorbed photon (hv) is transferred through the phycobilin pigments phycocyanin and allophycocyanin in the phycobilisome and Chl*a* molecules until it reaches the PSII reaction centre.

Phycocyanin and phycoerythrin are composed of a number of α- and β-subunits, each having a protein backbone to which bilins are covalently bound. The major chromophore contained within phycoerythrin is phycoerythrobilin and the major chromophore within phycocyanin is phycocyanobilin; this common form of phycocyanin is known as c-phycocyanin, however the chromophores can contain other minor bilins such as phycourobilin and phycobiliviolin (Glazer, 1985).

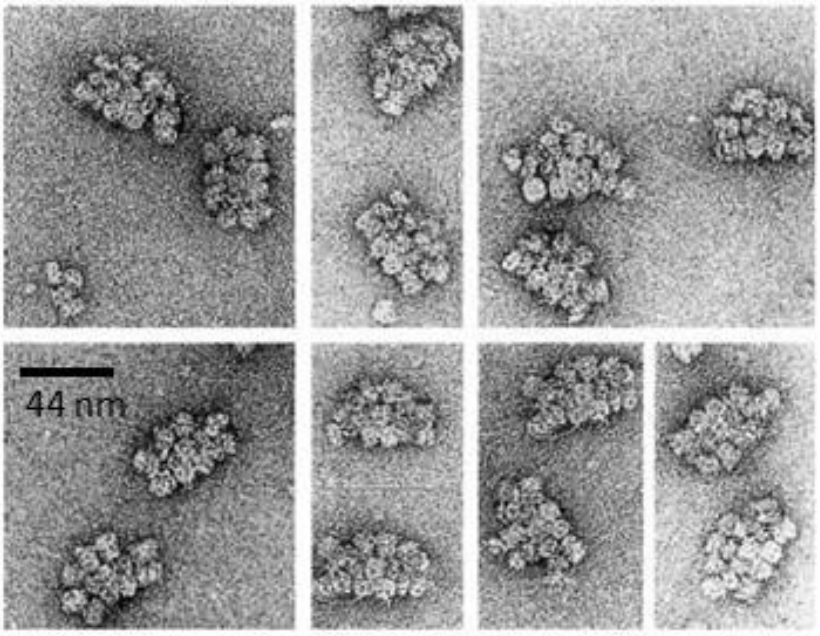

Figure 3.6. Electron microscope images (Ducret, 1996) of intact hemi-discoidal phycobilisome from the cyanobacterium *Anabaena sp.* PCC 7120 (magnification x228000). 6-8 rods can be seen originating from the allophycocyanin core. Although detail is difficult to see, the rods form a complex pattern around the core. Rods are formed of 2-3 discs of measured dimensions 5-6 nm width, 10-12 nm length.

Early studies believed that phycobilisomes were structurally associated with PSII only, and that energy was transferred to PSI through Chl*a* – known as the 'Spill-over Model'. Later, the phycobilisome core was shown to interact directly with PSI, as it does with PSII (Su, 1992, Mullineaux, 1992) in what is known as the 'Mobile Antenna Model', and although still not fully understood, it is widely accepted that although PBSs are primarily associated with PSII, they are mobile and can be redistributed to PSI to regulate the efficiency of excitation energy transfer between the two photosystems. In *A. platensis* phycobilisomes mainly interact with PSI as there are around 5.7-fold more PSI to PSII (Rakhimberdieva, 2001). Rakhimberdieva et al. (2001) showed that around 80 % of phycobilisomes transfer energy to PSI trimers and monomers compared with the 20 % of phycobilisomes which are bound to PSII.

The ultrastructure of the phycobilisome can depend on the conditions to which the cyanobacterium is exposed, particularly the quantity and quality of light. In low light the phycobilisome can increase in size by increasing the number of disks per rod, or number of rods; conversely, in high light the phycobilisome can reduce in size, even losing all of the peripheral rods (Nomsawai, 1999). In the case of cyanobacteria which contain both phycocyanin and phycoerythrin in the phycobilisome rods, the phycocyanin to phycoerythrin

ratio can vary in response to light quality (Glazer, 1982). Additionally, the total number of phycobilisomes can change. All of these features demonstrate the adaptability of the cyanobacterial phycobilisome to maximise the yield of usable light for photosynthesis, whilst minimising damage to the photosynthetic apparatus.

3.1.3 Commercial landscape for phycocyanin

Over the past decade the consumer demand for more natural products in food, nutraceuticals and cosmeceuticals has driven global interest and research into 'blue biotechnology' in these industries (Scott, 2014). Phycocyanin is increasingly being exploited as a natural food colourant, replacing synthetic dyes such as Brilliant Blue FCF, which has been associated with health problems (Weber, 1979). Phycocyanin is particularly suited as a food colourant due to its high water solubility and stability over a large pH range (Sarada, 1999, Chaiklahan, 2012). At high purity phycocyanin is also used as a biochemical tracer in immunoassays, microscopy and cytometry, taking advantage of its fluorescent properties. Additionally, phycocyanin is exploited in the 'ceutical industries for its anti-oxidant, anti-arthritic and anti-inflammatory properties together with other associated health benefits (Piñero Estrada, 2001, Gonzalez, 1999, Romay, 2003, Romay, 1998, Benedetti, 2004). There is ongoing research into the therapeutic properties of phycocyanin for medical use, particularly for immunomodulation, anti-viral and anti-cancer therapies (Belay, 2002, Chiu, 2006, Hayashi, 2006, Roy, 2008).

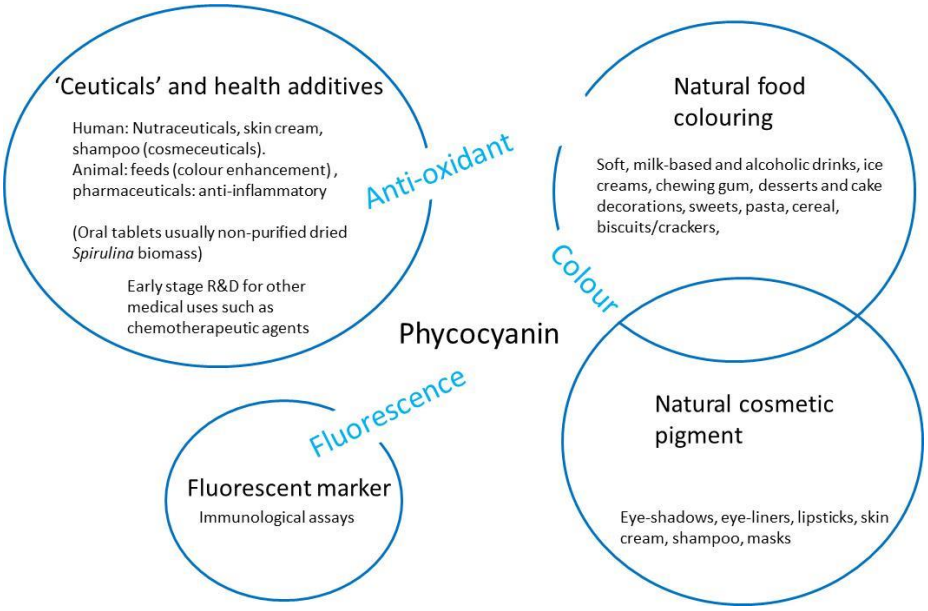

Figure 3.7. Graphic of the main phycocyanin markets and associated properties exploited.

There are many uses for phycocyanin and the main markets take advantage of either one or more properties of the pigment from colour, anti-oxidant activity or fluorescence (Figure 3.7).

The demand for natural food colourings in the food processing industry is expanding. This is driven by public demand for natural food colourings following increasing concerns of the effects on health of artificial colourants, e.g. 80 % of US and UK parents are concerned about the use of synthetic food colourings (Crawford, 2015), and this change in opinion and preference for natural food colourings is pushing manufacturers to switch to using natural food colourings in their products, driving the demand for algae-based pigments such as phycocyanin. Many global food manufacturers have made public commitments to and are removing artificial colourants from some or all of their products including Mars, Nestlé USA, Kraft, Campbell's, General Mills, Frito-Lay, Kellogg's and Mondelez International (Wollan, 2016). The 2014 global natural food colour market represented 54.9 % of the total food colour market, expected to grow to 60 % by 2020 (Algae Industry Magazine, 2015), with a particular and rapidly growing demand for phycocyanin blue food colouring, where demand is expected to rise five times by 2020 (Future Market Insights, 2016). The approval of spirulina-derived phycocyanin in 2013 by the US Food and Drug Administration, after years of safety testing and petition by Mars, made spirulina-derived phycocyanin the first natural blue colourant to be approved for use in the US which has fed the increasing demand for phycocyanin (United States Government Publishing Office, 2013).

The sale price of phycocyanin is dependent on purity, where purity is typically graded in three bandings based on the pigment:protein ratio measured at an absorbance of A620/A280. Below 0.7 phycocyanin purity ratio is classified as food grade, up to 3.9 is reactive grade and above 4 is analytical grade (Rito-Palomares, 2001). The lower end of the reactive grade banding (0.8-2.4 purity) is usually graded as suitable for cosmetics. Food and cosmetic grade phycocyanin is used mainly for its colour, reactive grade phycocyanin is of a quality to be used as biomarkers and in gel electrophoreses and analytical grade phycocyanin can be used therapeutically. Phycocyanin is often sold as lyophilised, water-soluble powder and the higher the purity of phycocyanin, the higher the cost. Figure 3.8 shows the price of phycocyanin sold at different purities in various amounts by five manufacturers. At a purity classified as food grade the price of phycocyanin ranges from £0.12-0.18 per g. At a reactive grade purity the price of phycocyanin ranges from £0.26-5,000 per g. Analytical grade phycocyanin can sell for £0.2-

113 per mg. The price is also heavily dependent on the amount purchased as buying in bulk (kg instead of mg) at higher grades can reduce the unit price, sometimes by nearly 6-times.

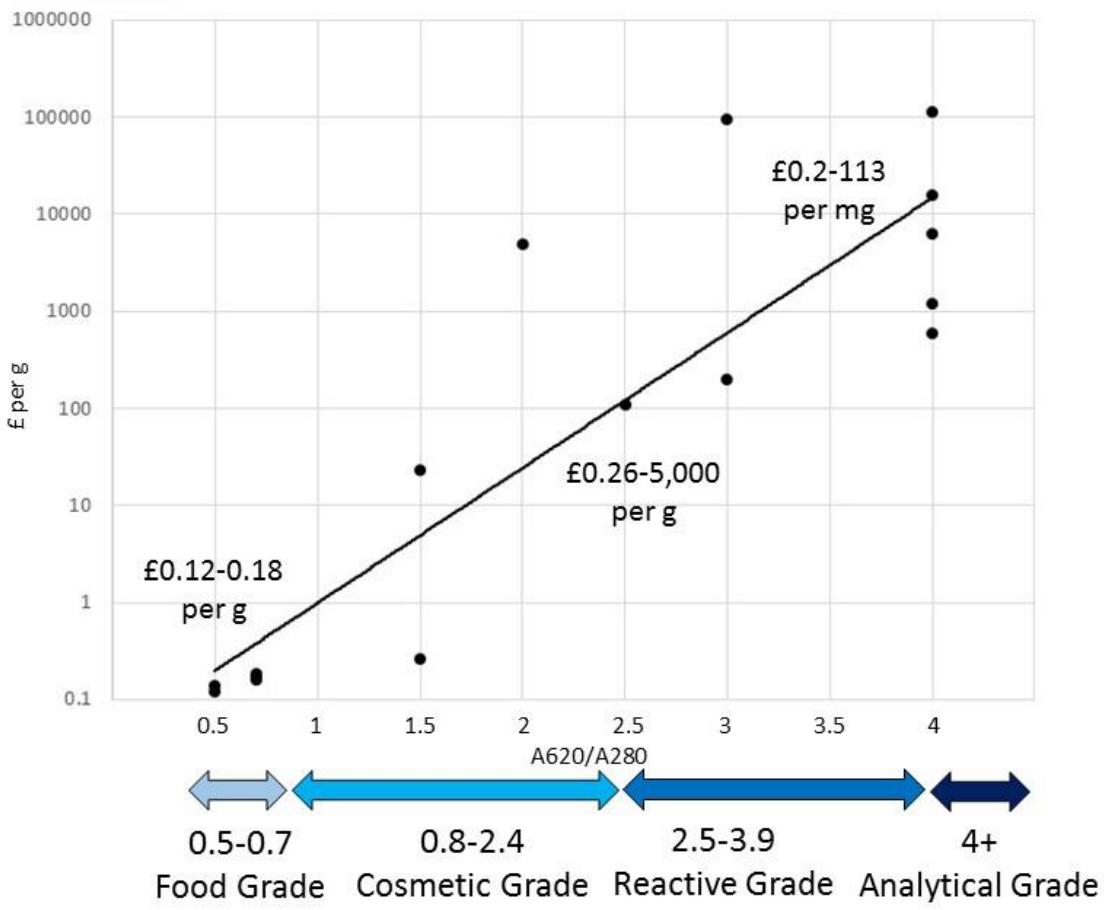

Figure 3.8. Scatter plot of the price of phycocyanin of various grades sold by five manufacturers: Soley Institute (Turkey), Delhi Nutraceuticals PVT (India), Shaanxi Fuheng (FH) Biotechnology Co. (China), Qingdao Haosail Science Co. (China), Sigma Aldrich (UK). Conversion from 1.25 USD to 1 GBP as of exchange rate 7th February 2017.

Cyanobacteria are widely used in aquaculture for phycocyanin production, with eukaryote sources showing potential for future exploitation. Among the cyanobacteria the genus *Arthrospira* (formerly known as *Spirulina* and still commercially known as 'Spirulina') is the most commonly cultured genus; however, phycocyanin has been extracted from other genera such as *Aphanizomenon* and *Anabaena* (Bekasova, 1979). The main species in culture are *Arthrospira platensis* and *A. maxima*.

The majority of *Arthrospira* farms in the supply of phycocyanin are located in China, India and the USA (Figure 3.9). Although there exists a large number of companies globally selling *Arthrospira* and/or phycocyanin products, most are formulation and distribution companies

who source their *Arthrospira*/phycocyanin powders from production companies in Asia (mainly China), India and the US. However there are a small number of companies within Europe who produce their own *Arthrospira* for formulation, packaging and sale, as a unique selling point to promote a natural, home-grown, high quality and trusted product.

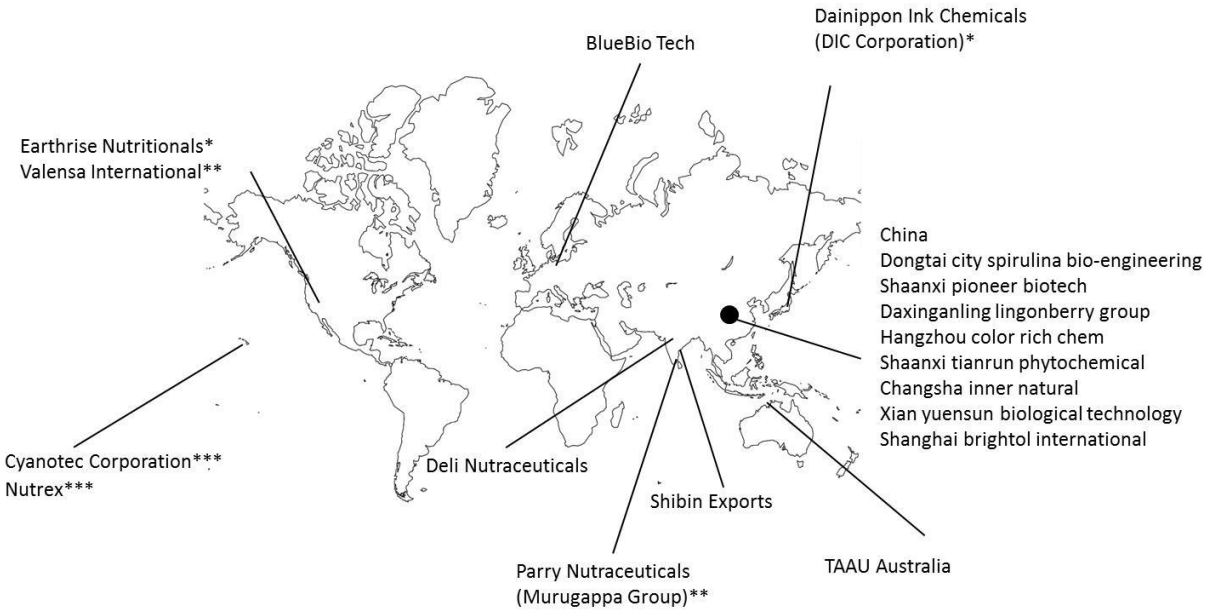

Figure 3.9. Map of the largest Spirulina and phycocyanin producers worldwide. Matching * represents manufacturer-distributer partnerships. Companies listed were active on the date 1st April 2014. Map image sourced from: www.mappery.com.

Parry Nutraceuticals (part of the Murugappa Group), India have a 130 acre *Arthrospira* farm. Their products include SpiruBlu and SuperBlu (phycocyanin powders). The company is partnered with US-based firm Valensa International which produce Pur-Blue^{TM}, SpiruZan® and BlueMax^{TM}, products which are formulated using material from Parry's Indian production facility. Dainippom Ink Chemicals (part of the DIC Corporation, Japan) have two *Arthrospira* farms (Japan and Thailand) with the capability of reportedly producing 800 tonnes of dried *Arthrospira* per year. The company produce products: LinaBlue® with LinaBlueA and LinaBlueHGE (which are improved products with increased blue-colour intensity and stability). This company is partnered with Earthrise, a US company with a reported world's largest 108 acre *Arthrospira* farm based in California. Earthrise also have a number of associated European companies including Green Valley, Germany who re-package/brand and sell their products. Sapphire Energy have production facilities in California and New Mexico and are investigating *Arthrospira* for oils and fuels using a strain licenced from Earthrise.

Cyanotec Corporation (Hawaii) have production facilities on the Kona Coast, Hawaii, producing the notable Hawaiian strain *A. pacifica.* Nutrex Hawaii is a subsidery of Cyanotec. These companies produce *Arthrospira* in numerous powder, tablet and capsule formulations.

There are also a large number of Chinese and Indian companies selling phycocyanin (powder) on international trade websites (Alibaba at http://www.alibaba.com/), although the company websites do not list a phycocyanin product only *Arthrospira* powders with average reported production capabilities of around 1000 kg per month. Australian Spirulina (TAAU) has a production facility in Darwin boasting the highest quality *Arthrospira* formulations with lowest bacterial contamination in the world. All production facilities of these large companies listed above are open air ponds or race-ways.

There also exists multiple European health companies providing phycocyanin/*Arthrospira* products; however, nearly all of these companies obtain their raw materials from large suppliers in China, India and the US or low-tech small farms in Africa or Asia. BlueBio Tech International GmbH, as an exception, provide analytical grade phycocyanin from their algae production facility in Elmshorn, Germany. There is also a significant number of *Arthrospira* production companies based in France; however, a number of these are social enterprises or charities funding small production facilities in Africa with the aim to improve the health and life prospects of the local population, for example Spirulina du Burkina. Some of these French companies are also low-tech family micro-farms in the south of the country selling *Arthrospira* food products locally, for example In'Spir. Spiralps farm *Arthrospira* in Valais, Switzerland in a controlled greenhouse environment for production of fresh health drinks.

Two interesting companies as members of the European Algae Biomass Association (EABA) are Algaenergy (Spain) and Microlife SRL (Italy). Algaenergy are involved in R&D activities and production of high quality, contaminant-free *Arthrospira* for nutritional and cosmetic purposes. Microlife srl produce *Arthrospira* for addition into its range of food and health products, suggesting their traditional method of drying in noodles allows fast drying at low temperatures, preserving more of the beneficial health properties of its *Arthrospira* products.
In the late 1980s, UK-based company Blue Green - Biotech (now dissolved) founded by Steve Skills produced *Arthrospira* biomass from anaerobically digested agricultural waste in a 1000 L closed and artificially illuminated PBR (Skill, 2013). Biotechna Ltd (Luton) developed a re-circulating helical photobioreactor known as BIOCOIL PBR for production of *Arthrospira*

using AD liquor, patented in 1987 (Robinson, 1993). Both these early companies had difficulty in creating a commercially viable business. All Seasons Health (Hampshire) produce *Arthrospira* tablets and are the only company in the UK to provide Certified Organic *Arthrospira* (Soil Association). *Arthrospira* are however currently imported from India and Taiwan for formulation.

3.1.4 The physiology of Arthrospira

Arthrospira is a free-floating filamentous cyanobacterium with spiral-shaped filaments or trichomes (Figure 3.10).

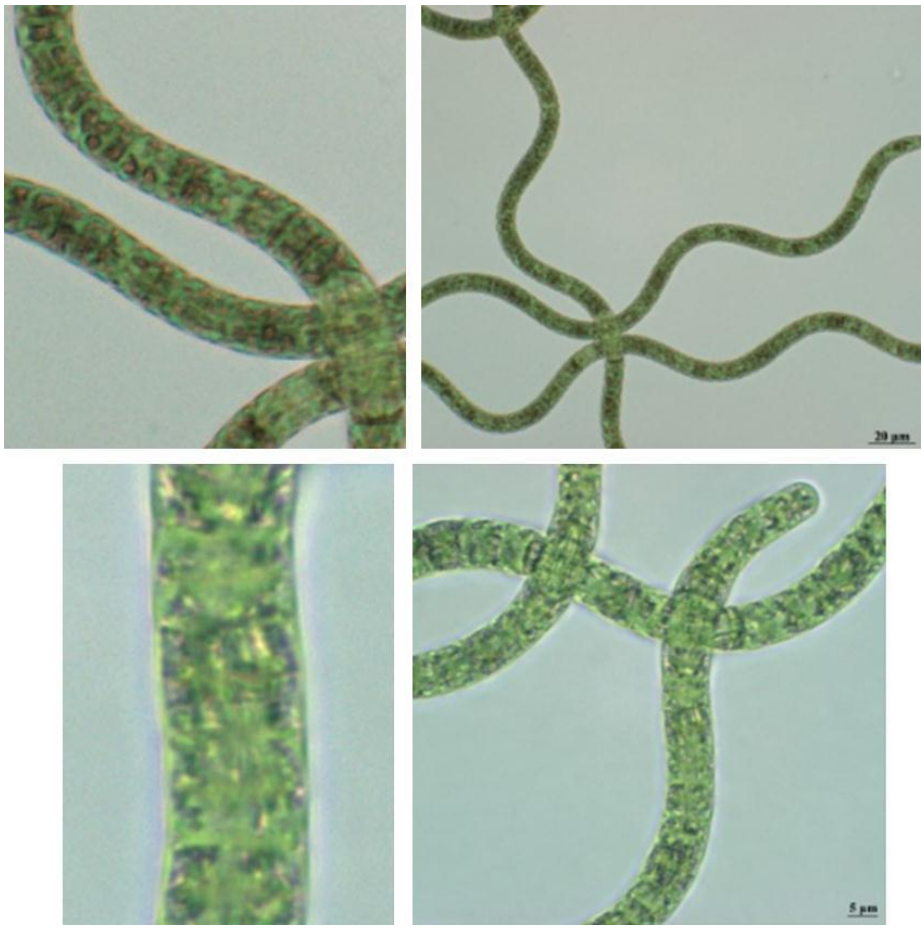

Figure 3.10. Microscope images at various magnification taken of *Arthrospira platensis* (Oerst.) Geitler strain CCMP1295 deposited with the Bigalow Laboratory culture collection (images taken from https://ncma.bigelow.org/ccmp1295).

In addition to its high phycocyanin content, which can be up to 20 % dry weight, *Arthrospira* also contains high amounts of other nutraceuticals such as vitamins and polyunsaturated fatty acids (PUFAs), and is high in protein (Vonshak, 1997). For this reason *Arthrospira* biomass is a salable product; however, pure phycocyanin - depending on purity - has a considerably higher market price.

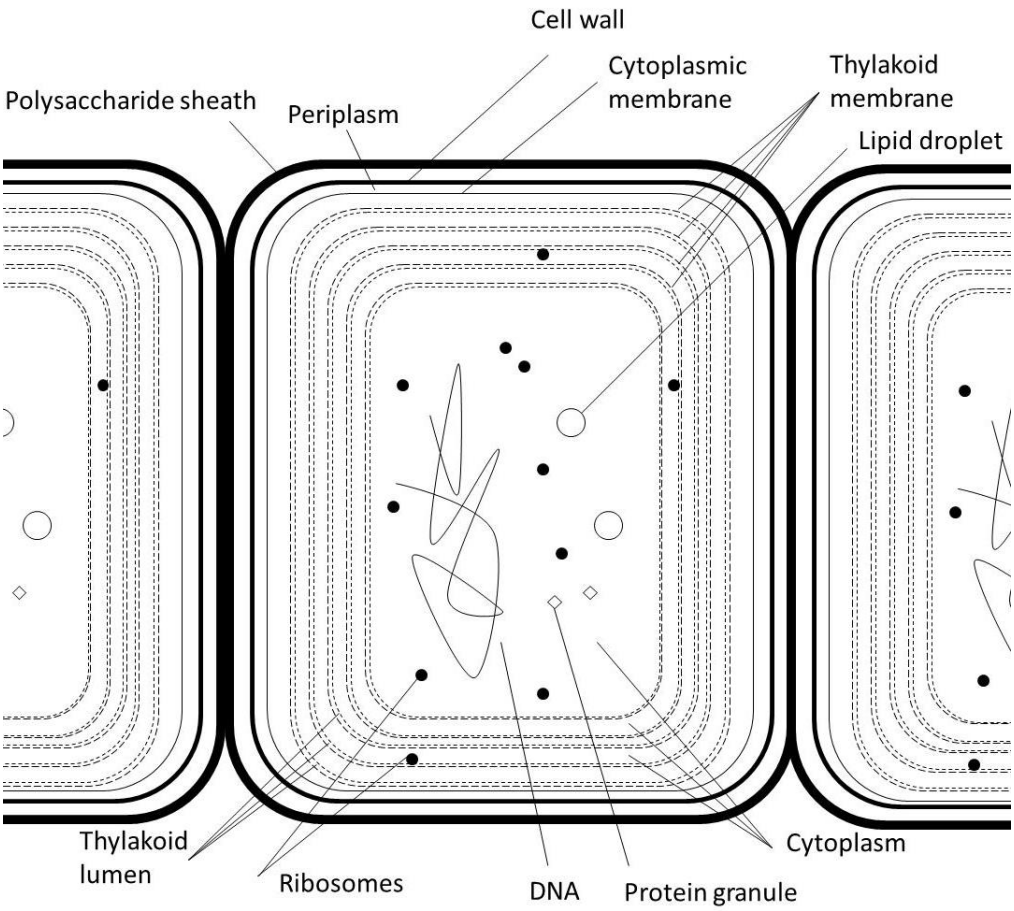

Figure 3.11. Diagram of a typical *Arthrospira* cell. The thylakoid membranes involved in photosynthetic and respiratory processes contain photosynthetic pigments including chlorophyll *a*. The cytoplasmic membrane, involved only in respiration, contains carotenoids. Protons are brought into the thylakoid lumen, the space between a pair of thylakoid membranes, in photosynthetic and respiratory electron transport, creating a proton gradient which drives the synthesis of ATP.

The morphological features of *Arthrospira* are varied and are linked to environmental factors. Typically, *Arthrospira* forms left-handed helical trichomes of variable length and degree of coiling. The cells of the trichome are broader than long with a typical width of 3-12 μm (Gershwin and Belay, 2007) and transverse cross-walls are visible under a normal light microscope. The cells lack membrane-bound organelles with the DNA, ribosomes, protein granules and lipid droplets floating in the cytoplasm. The cells are surrounded by an outer membrane which forms a murein-based cell wall, and an inner cytoplasmic membrane separating the cytoplasm from the periplasm (Figure 3.11). There are multiple pairs of thylakoid membranes, which do not stack to form grana as they do inside the chloroplasts of higher plants and algae.

Arthrospira require a higher concentration of nitrate (typically 33-fold higher), than other typical commercially cultured microalgae, which is normally supplied through the addition of sodium nitrate to media. This is because, unlike other filamentous cyanobacteria, *Arthrospira* lack heterocyst cells and are therefore non-diazotrophic (unable to fix nitrogen). Nitrogen-limited cultures show pigment bleaching, in a process that is referred to as chlorosis (Allen and Smith, 1969, Lau, 1977) and phycocyanin can be degraded by protease activity (Carr, 1988).

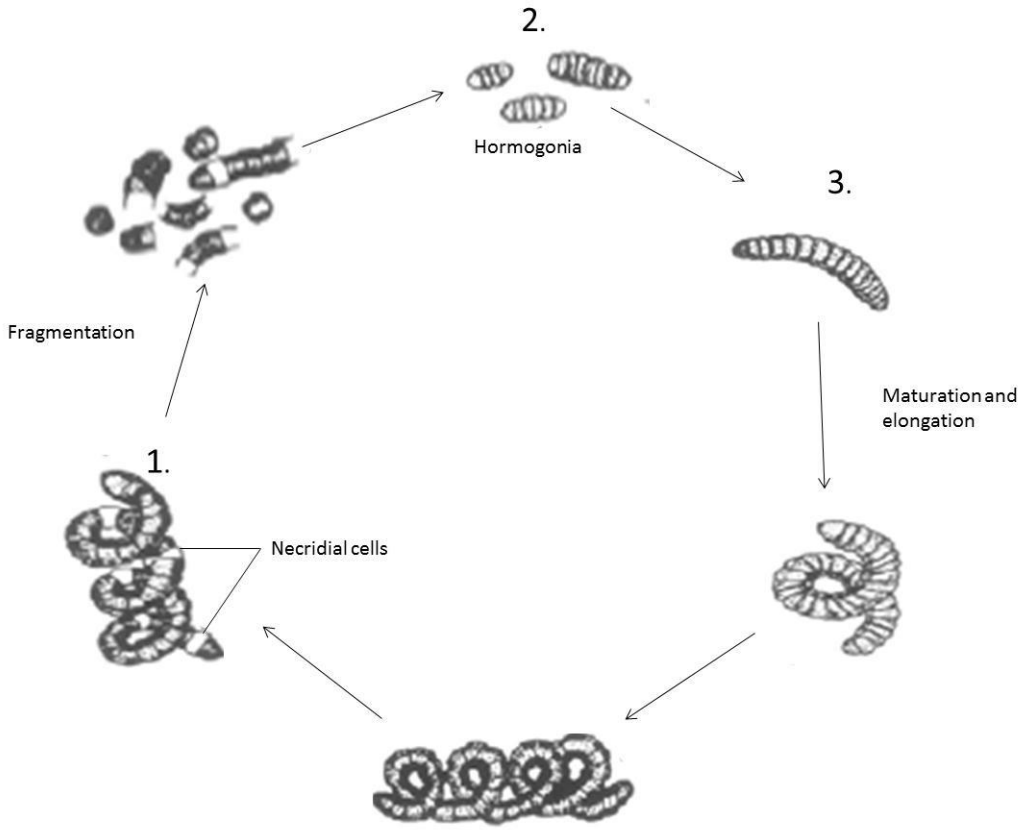

Figure 3.12. Life-cycle of *Arthrospira* modified (Ali and Saleh, 2012). *Arthrospira*, like many filamentous cyanobacteria reproduce through trichome fragmentation and formation of hormogonia.

Arthrospira reproduces asexually by binary fission through trichome fragmentation and formation of hormogonia (Figure 3.12). Mature trichomes fragment through the formation of specialised necridia cells (1.) that undergo lysis providing bioconcave separation discs (Gershwin and Belay, 2007). Fragmentation of the trichome produces hormogonia: 2-4-cell chains (2.), which then lose attached necridial cells and become rounded at the distal ends (Ali and Saleh, 2012). Hormogonial cell enlargement and trichome elongation (3.) through binary fission produces new trichomes.

3.1.5 The move towards efficient lighting

The typical approach to the cultivation of *Arthrospira* is using open ponds or raceways; however, this type of cultivation requires large areas of land and limits cultivation in countries with low daylight levels. The incorporation of efficient artificial illumination (e.g. light-emitting diodes (LEDs)) into more intensive cultivation methods using closed photobioreactors, could facilitate production industries in non-equatorial countries and where land is restricted. As productivity is determined by light intensity in microalgal cultures, the use of artificial illumination allows better control over production (avoiding diurnal and seasonal fluctuations). However, the use of artificial illumination may only be appropriate for high value products, such as phycocyanin, due to the economics of associated energy costs (Blanken, 2013). As photoautotrophs are restricted to utilising only those wavelengths of light absorbed by their photosynthetic apparatus, the efficiency of artificial light can be increased by matching light sources to the organisms' photosynthetic capability. As LEDs can be manufactured to emit light in narrow emission spectrums, they are ideal for producing efficient artificial lighting arrays, reducing waste light and further increasing the photosynthetic efficiency. This property has made them increasingly popular in horticulture and aquaponics artificial illumination systems (Massa, 2008, Morrow, 2008). Lighting arrays for plant growth incorporating blue and red LEDs tuned to Chl*a* absorbance are now commonplace.

3.1.6 Adaptation to light

As water molecules absorb in the red region of the electromagnetic spectrum, limitations for photosynthesis occur naturally in these wavelengths. Light scattering of shorter wavelengths also occurs by suspended material resulting in the provision bias of blue-green wavelengths in nature (Kirk, 2000). Environmental factors therefore determine light availability forcing photoautotrophs to adapt to the quality and quantity of available light. Some phycobilisome-containing photoautotrophs exhibit a phenomenon called complementary chromatic adaptation (CCA) wherein the phycocyanin to phycoerythrin ratio is altered in the rods in response to different light quality by modulating pigment synthesis (Bennett and Bogorad, 1973, Bogorad, 1975, Tandeu de Marsac, 1977). This process is photoreversible. CCA was first observed by Engelmann in 1902 (Engelmann, 1902) when cyanophyte cells became increasingly blue-green or red-brown under red and green light respectively, with increasing rates of photosynthesis after the colour change. The genetic aspects of CCA have been studied in the cyanobacteria *Calothrix sp.* PCC7601, *Fremyella diplosiphon* and *Synechococcus sp.* (Kirk, 2000), which are closely related to *Arthrospira* (Figure 3.13). Three gene sets encoding phycocyanin apoprotein

(α- and β-) subunits have been identified with the expression regulated chromatically in two out of these three gene sets and genes encoding linker proteins have also been identified (Grossman, 1993). CCA has since being shown to be widespread in cyanobacteria (Kehoe, 2010). In addition to changes in pigment ratio, changes in response to a difference in light quantity can include modulation of the size and number of rods in the phycobilisome (Nomsawai, 1999). Nomsawai et al. (1999) showed in *Arthrospira* that under low and high quantities of light the number of phycocyanin discs per rod can vary from 1.7-2.2, and the number of rods per phycobilisome can vary from 4.5-5.8, with the number of discs per phycobilisome varying from 7.7-12.9.

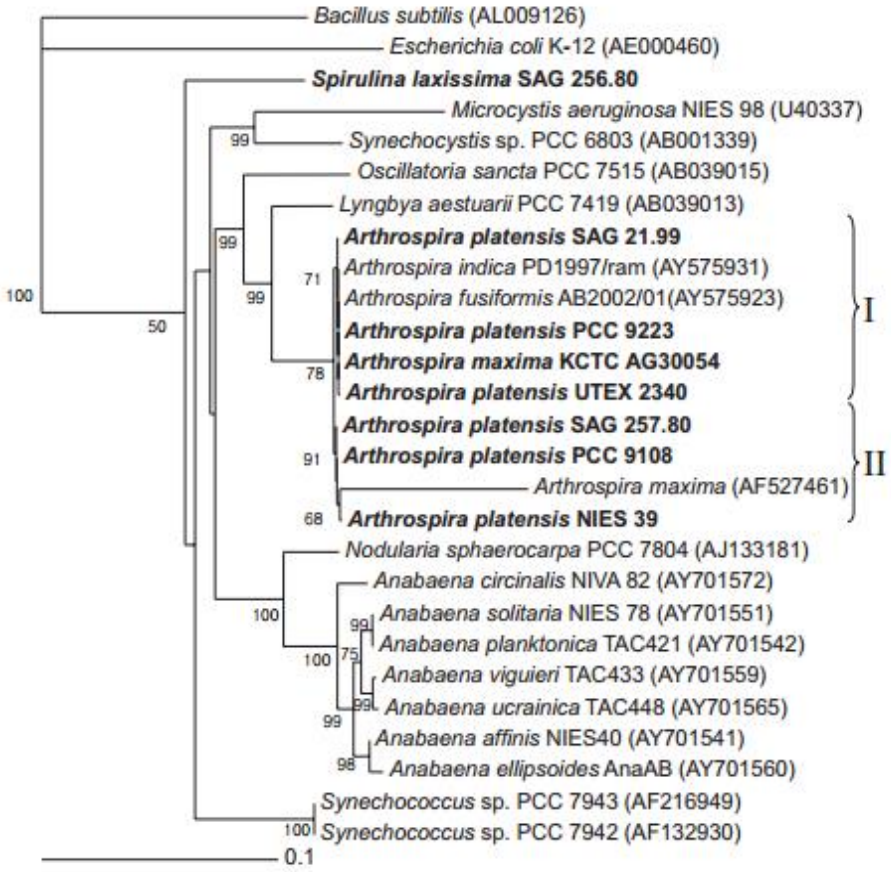

Figure 3.13. Neighbour-joining tree showing relationships among *Arthrospira* strains and other cyanobacteria from 16S rRNA gene sequence analysis; taken from (Choi, 2012).

Although changes in pigment ratio is attributed to CCA in numerous photoautotrophs, Babu et al. (Babu, 1991) demonstrated that CCA is not applicable to *A. platensis*. In phycoerythrin containing photoautotrophs, both phycoerythrin and phycocyanin undergo changes in synthesis (at the gene expression level) in response to light quality. Phycoerythrin and phycocyanin are enhanced under green and red light respectively. Babu et al. (1991) showed that phycocyanin

does not undergo major changes in synthesis in response to light quality, as it does for light quantity. Instead, it is changes in the phycocyanin chromophore that are attributed to adaptation. Under green light the presence of the chromophore phycobiliviolin was enhanced in the α-subunit of phycocyanin. *Arthrospira* is therefore a non-chromatin adapting photoautotrouph. There have been a number of studies following on from Babu et al. (1991) demonstrating that *A. platensis* can be manipulated to increase phycocyanin content by the application of certain light wavelengths, with additional effects on productivity and these are summarized below in Table 3.1.

Wang et al. (2007) found *A. platensis* biomass productivity was higher when cultured under red light (620-645 nm), compared with white (380-760 nm) and other monochromatic light and presented calculations demonstrating that the use of red light would be economically beneficial to photoautotrophic production, as energy to biomass conversion is more efficient. Farges et al. (2009) also modelled *A. platensis* productivity under polychromatic blue/red and monochromatic red light. There were comparable biomass productivities under the two light types, proving an increased energy-to-biomass conversion efficiency under monochromatic red light, through lower electrical power consumption. Despite maintaining biomass productivity, phycocyanin content decreased by 2-fold under red monochromatic light. Using light filters, Walter et al. (2011) achieved a higher phycocyanin content and biomass productivity under white light, compared with red, yellow, green and blue monochromatic light.

Table 3.1. Summary of light studies on *A. platensis*. Details of light wavelengths presented where available as range or emission maximum (max). White light assumed to be standard where details not available. Effects on biomass productivity and phycocyanin content are compared with white light and shown as increased (↑), decreased (↓) or same (─).

Study	Light colour	Wavelength (nm)	Biomass productivity	Phycocyanin content
Wang, 2007	red	620-645	↑	not measured
	yellow	587-595	↓	
	green	515-540	↓	
	blue	460-475	↓ lowest	
	white	380-760	─	
Farges, 2009	red	626 max	─	↓
	red + blue	640 max, 470 max	─	─
Chen, 2010	red	620-645	↑ highest	↑ *
	yellow	587-595	↓	↓
	green	515-540	↓	↑
	blue	460-475	↓ lowest	↑ highest
	white	380-760	─	─
Walter, 2011	red	475-600	↓	↓
	yellow	400-475	↓	↓
	green	400-475, 550-700	↓	not measured
	blue	525-700	↓ lowest	↓
	white	standard	─	–
Akimoto, 2012	far-red	700-780	↓ lowest	↑
	red (longer)	620-700	↑ highest	↓ lowest
	red	600-650	↓	─
	yellow	570-600	↓	↑
	green	500-570	↓	↑
	blue	400-500	↓	↑ highest
	fluorescent white		↓ *	↑ *
	white LED	standard	─	─
Markov, 2014	red	620 max	↑	↓

	yellow	590 max	–	↓
	green	525 max	↓	↑
	blue	475 max	↓ lowest	↑ highest
	Pink	440 max, 620 max	↑ highest	↓ lowest
	white	standard	–	–

**Not statistically significant.*

Chen et al (2010a) showed *A. platensis* cultures have higher biomass yields under red (620-645 nm) light, compared with white and other monochromatic light. Phycocyanin content was highest under blue light, and slightly higher under red compared with white light, although not a statistically significant increase. Markou et al. (2014) showed that biomass productivity was higher under pink and red light compared with white light and other monochromatic colours. Significantly lower phycocyanin content was found under pink and red light, but a high phycocyanin content was found under blue light. Both Chen et al. and Markou et al. acknowledged an inverse relationship between biomass productivity and phycocyanin yields under the different light regimes and suggested the effect may be a result of slower growth under blue light, thereby directly limiting the amount of recycling/metabolysis of phycocyanin as a nitrogen source (Carr, 1988) - therefore increasing phycocyanin content. Alternatively, they suggest that the relationship may be an effect of light limitation (as pigment levels are known to increase under light-limiting conditions) to allow capture of the maximum amount of light for photosynthesis; therefore, in these examples blue light would equate to a 'dark environment for photoautotrophs'. Either way, both groups put forward the case for the preferred, beneficial use of blue light for phycocyanin production in *A. platensis.*

The use of longer wavelengths of light for microalgae cultivation has demonstrated the achievement of higher biomass productivity and pigment yields under certain narrow bands. In studies by Akimoto et al. (2012) three types of red light were tested against other monochromatic light and white fluorescent and LED light. A standard red LED was used along with longer wavelength red LEDs of 620-700 nm and 700-780 nm. Interestingly, biomass productivity was highest under 620-700 nm light, with minimal biomass productivity under 700-780 nm light. Contrastingly, phycocyanin content (measured as phycobilisome/Chl*a*) was highest under blue light (comparing well to similar studies) and 700-780 nm furthest red light. Phycocyanin content was lowest under 620-700 nm red light and both sources of white light therefore contributing to the support of a biomass productivity-pigment content trade-off in

culture, and a relationship that perhaps requires further attention and investigation for optimisation of closed high-value pigment systems using photoautotrophs.

These earlier short-term studies hinted at the potential for manipulating the biomass productivity and phycocyanin content of *A. platensis*, additionally allowing decreased power consumption in an artificially illuminated high-value product production system using longer wavelengths of light. The current work focused on the longer-term effects of culturing *A. platensis* using longer wavelength red light than the wavelengths emitted by standard red LEDs - specifically those wavelengths approaching near-infra red.

3.2 Experimental Details and Method

3.2.1 Equipment

3.2.1.1 Infors photobioreactor system

Arthrospira platensis was cultured in a modified Labfors 4 benchtop bioreactor (Infors HT, UK) (Figure 3.14). Modifications were made by Infors to the basic system following a particular specification to create a stirred tank photobioreactor (STPBR) system suitable for culturing photoautotrophs. The STPBR consisted of a 3 L volume glass vessel with water jacket using heated and chilled water, with temperature probe for temperature control. Cooling water was provided by a connected chiller unit (FL601 Recirculating Cooler, Julabo, UK). Water was heated by the base unit of the STPBR system (Figure 3.14). A motorised impeller, with hydrofoil blades, allowed for controlled mixing of the culture medium. CO_2 was delivered using sterile air filtered using a 0.45 µm in-line filter and orifice sparger placed under the impeller. Air flow was controlled with a mass flow meter (Cole-Palmer, UK). An air outlet condenser was fitted and cooled using water from the chiller unit to reduce medium evaporation. Dissolve oxygen (DO) was monitored using a DO probe (Finesse, Switzerland). pH was monitored using a pH probe (Mettler Toledo, Leicester) and pH correction fluid supplied to the vessel through peristaltic pumps. The glass vessel was surrounded by a steel jacket of interchangeable LED light strips powered by an external driver transformer. Another feature of the STPBR system was a sampling port for aseptic culture sampling. The glass vessel and tubing, correction fluid pumps and bottles could be removed when connected together from the base unit for sterilisation by autoclave. pH, DO, and temperature were monitored online over selectable periods. Light intensity, photoperiod, pH, temperature, aeration and mixing was controlled through a connected work station running Iris Parallel Bioprocess Control Software version 5.2 (Infors HT, UK).

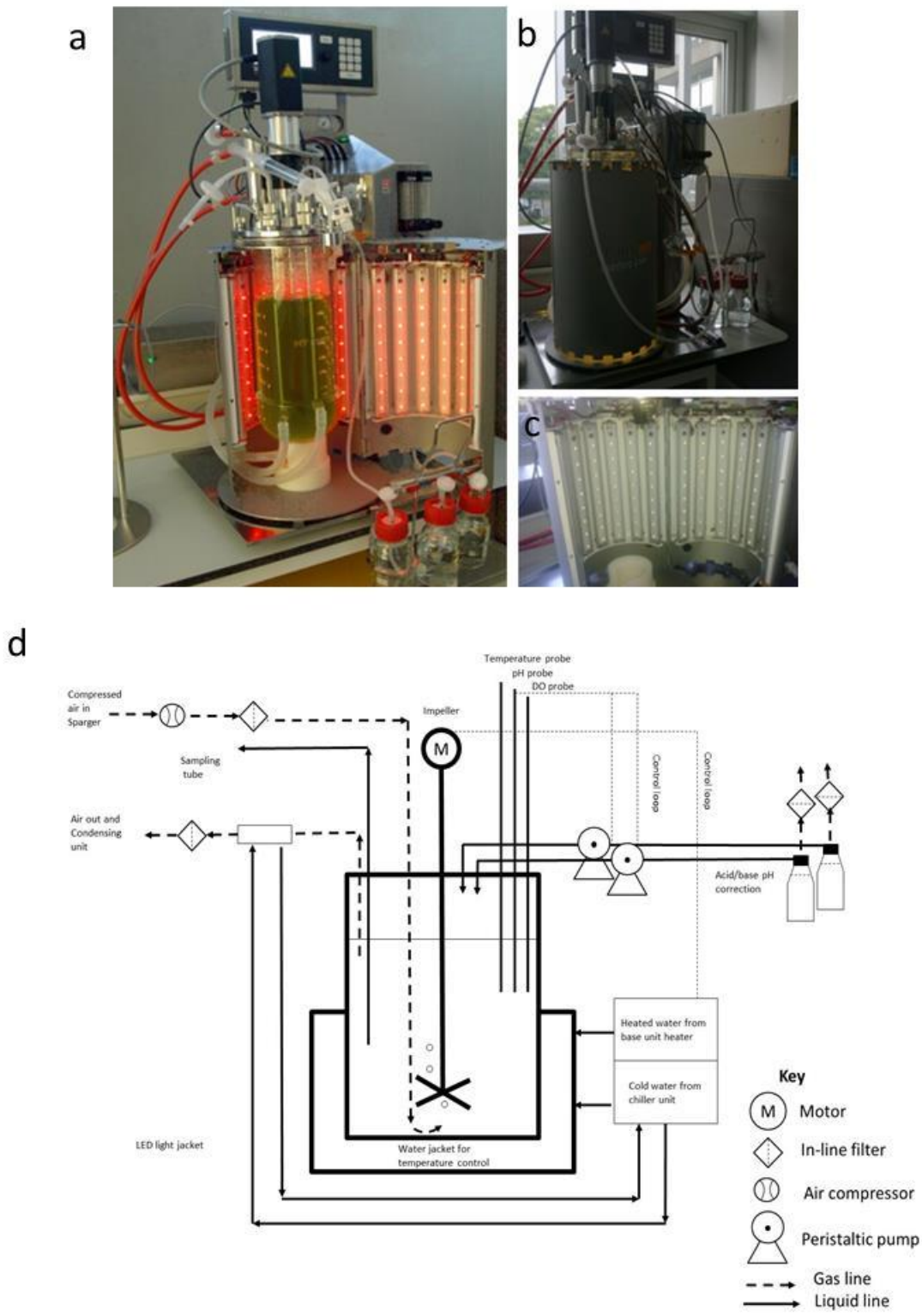

Figure 3.14. The Infors stirred-tank photobioreactor system. The system consisted of a 3 L glass vessel with temperature regulating water jacket, impeller, sterile air inlet flow control and sparger with air outlet condenser and online pH monitoring (d). The glass vessel was surrounded by a jacket of interchangeable LED light strips, shown with red (a) and white (c) LED jackets and closed jacket during normal operation (b).

3.2.1.2 Light-emitting diodes (LEDs)

White LEDs (Lumitronix Barre LED High-Power SMD 600 mm, 12 V) were kindly provided by Prof. Chris Howe, University of Cambridge. λ_{max} 680 nm red LEDs (Epitex high power top LED SMB680-1100-02-I) were purchased from Infors HT, UK. The λ_{max} 680 nm red LEDs emit light at a longer wavelength than standard red LEDs (Figure 3.15).

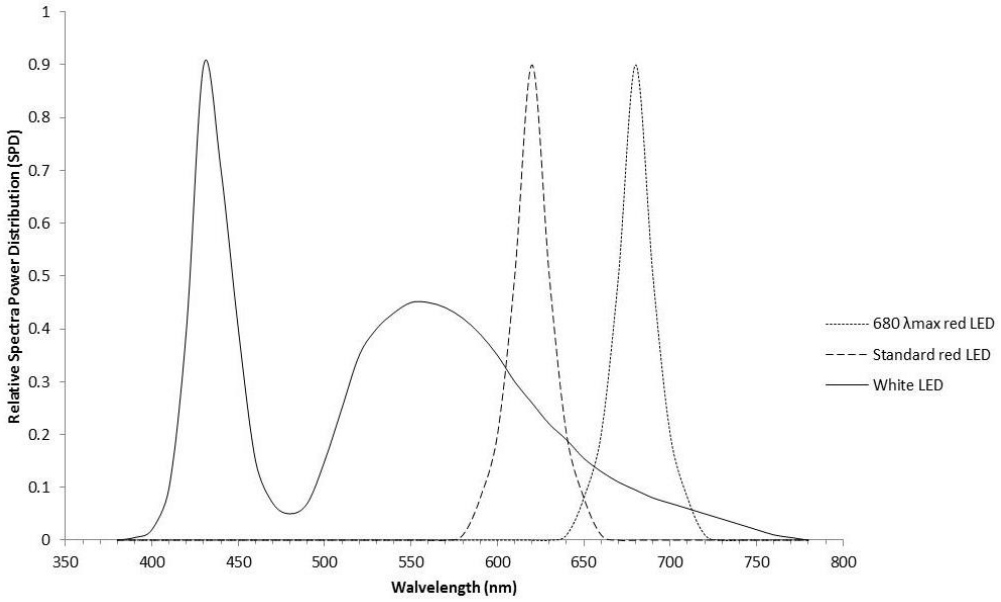

Figure 3.15. Standard white (solid line), standard red (dashed line) and 680 λmax red (dotted line) LED emission spectra. Standard white and 680 λ_{max} red LEDs were used for batch culturing. The red LEDs had a narrow emission spectra at a longer wavelength than standard red LEDs which typically emit at 620 λ_{max}.

The LEDs strips could be individually added to or removed from the light jacket. Power was regulated using a driver transformer as electrical properties change with temperature, and the power level (%) was controlled (through pulse width modulation) remotely through the Iris software. Power level (%) was calibrated to light intensity (μmol m^{-2} s^{-1}) for both the white and red LEDs (Figure 3.16). A LI-250 light meter (LI-COR Environmental, UK) was positioned in the centre of the STPBR glass vessel and the light jacket closed to simulate a running STPBR. Background light levels (from natural daylight entering from the open top and bottom of the light jacket) at 0 % power was below 0.2 μmol m^{-2} s^{-1}. Light intensity was recorded in triplicate at each increasing power level using the 15 second averaging feature of the LI-250 light meter. Light was selected to be provided at 45 μmol m^{-2} s^{-1}, achieved through operating red and white LEDs at 8 % and 3 % respectively.

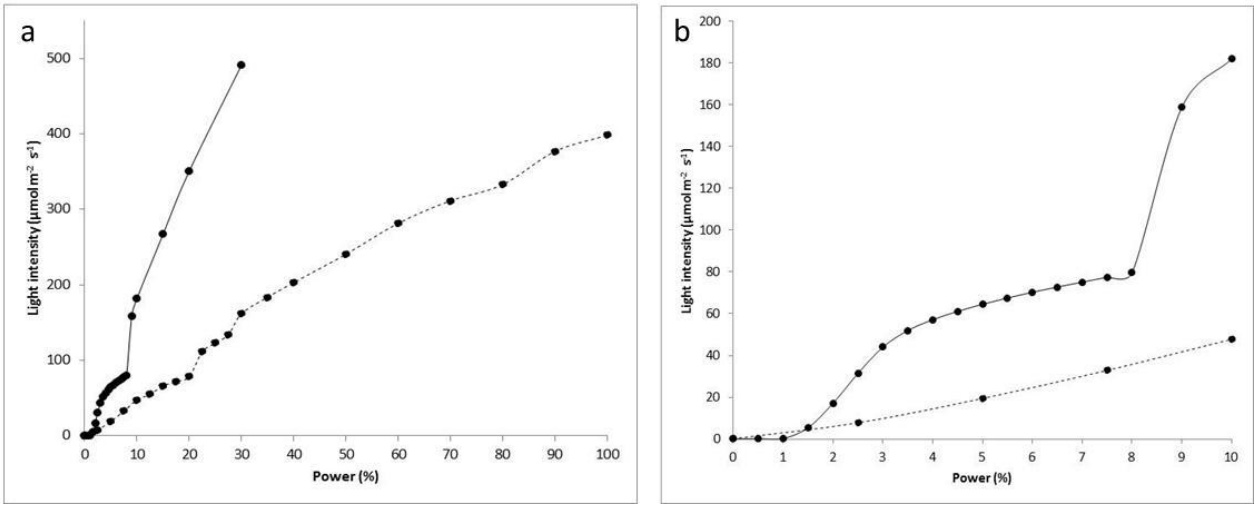

Figure 3.16. Light intensity-power curves for white (solid lines) and red (dashed lines) LEDs in the Infors STPBR as read by LI-250 light meter (LI-COR). (a) Light intensity curves for power outputs of up to 100 % for red and 30 % for white LEDs. (b) Light intensity curves for power outputs up to 10 % for both red and white LEDs. Points are means of triplicate readings. Error bars not shown as they were negligible.

3.2.2 Cyanobacteria strain and culture conditions

Arthrospira platensis (CCMP 1295) was obtained from the Provasoli-Guillard National Centre for Marine Algae and Microbiota (NCMA; https://ncma.bigelow.org/) (formerly the Centre for Culture of Marine Phytoplankton) and batch cultured following the guidance on the Culture Collection of Algae and Protozoa (CCAP) website (www.ccap.ac.uk) using sterile f/2 Medium (Guillard and Ryther, 1962) supplemented with 29.4 mM/ 2.5 g/L $NaNO_3$ (Raoof, 2006) and adjusted to pH 8. Media was made with 1 µm filtered, UV sterilised natural seawater and autoclaved in the glass vessel of the STPBR. Master and working stock cultures were maintained in a constant temperature (CT) room at 18 °C (± 1°C) containing cool white and warm white fluorescent lighting tubes (Figure 3.17) at approximately 105 µmol m^{-2} s^{-1} and 18:6 light:dark cycle.

The sterile media (2.25 L) was inoculated with 0.5 L of *A. platensis* stock culture at an optical density (OD) of 0.11-0.12 at 750 nm under aseptic conditions. Successive red light batches were seeded using inoculum from the previous batch (the inoculant of which was, when necessary, stored in the CT room). Cultures were grown at 30 °C (± 0.5°C) with a 18L:6D photoperiod with a mean illuminance of 45 µmol m^{-2} s^{-1}, impeller speed 200 revolutions per minute and supplemented with compressed sterile-filtered air (~0.03 % CO_2) supplied at 0.08 L per min (0.03 vessel volumes per min) through an orifice sparger.

pH, temperature and DO were monitored online every 10 minutes. pH was monitored using a Mettler Toledo probe that was calibrated before sterilisation ahead of each run using pH 8 and pH 10 buffers as recommended by Infors HT, UK. DO was monitored using a Finesse probe recording DO in the culture as a percentage of the starting culture conditions. Calibration of the DO probe was performed after sterilisation. For calibration, the STPBR was set to the culturing conditions as described above and monitored until standard culturing parameters were reached, and the DO value at those conditions recorded at 100 %. Eight milliliter samples were taken aseptically on days 1 (inoculation), 3, 6, 7, 10, 13 and 14 for analysis.

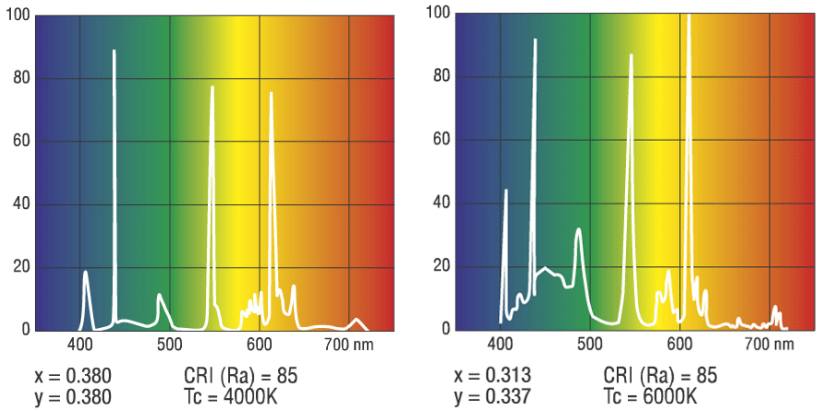

Figure 3.17. Spectral profile for constant temperature room fluorescent tube lighting that comprised a combination of Sylvania-Havells (F58W/865) Daylight Delux (right) and Cool White (F85W/840) (left) lights. Images taken from http://webassets.havells-sylvania.com/Legacy/SylvaniaLamps/spectral/DAYLIGHT_DELUXE_860.gif and http://webassets.havells-sylvania.com/Legacy/SylvaniaLamps/spectral/COOLWHITE_DELUXE_840.gif.

3.2.3 Growth measurement

Optical density (OD) was used alongside direct filament counts as a proxy for growth. Culture ODs were measured at 750 nm (Griffiths, 2011) from 500 µl triplicate samples using a Cary 100 UV/Vis Spectrophotometer (Varian, UK) corrected with f/2 Medium. Filament counts were performed using a Sedgewick rafter counting cell and Olympus BH-2 brightfield microscope at x100 magnification. Filaments present in 10 individual 1 µl squares of triplicate samples were counted and an average used for statistical analysis. Because of the difficulty and potential inaccuracies in counting such organisms (as noted by Lawton et al. (1999)) filaments were only counted if: 1. over half of the filament was located in the square, to avoid double counting 2. the filament spiral contained over 2 complete turns, to eliminate fragments. Growth rates were calculated as increase in OD 750 nm day^{-1} according to Equation 3.1:

Equation 3.1: $\text{Growth rate} = \frac{N2-N1}{t2-t1}$

Where N2 is the mean OD (750 nm) on day t2, N1, mean OD on day t1 and t1 to t2 is the period for which the gradient of the growth curve was maximal.

Growth rates were not reported as specific growth rate (Andersen, 2005) as there was an absence of logarithmic growth.

3.2.4 Morphological assessment

The total lengths of at least 20 filaments were measured to assess any changes in trichome morphology. Images were taken using a Leitz Dialux 20 light microscope and EasyGrab software with analysis performed using ImageJ software. Image size was calibrated using graticules at 630 pixels mm^{-1}. Again, filaments were only measured if the filament spiral contained over two complete turns.

3.2.5 Pigment analysis

Pigment extraction was based on the method from Zhang and Chen (1999). Samples of 5 mL were harvested by centrifugation at 3000 g for 10 minutes (Sigma 3K18C centrifuge) in pre-weighed glass tubes. Cells were washed once in deionised water and the wet biomass determined. The pellet was then resuspended in 3 mL 0.05 M sodium phosphate buffer (pH 7). Cells were disrupted by a freeze/thaw cycle (-20 °C) over 1 hour and sonicated for 3 minutes at 6 microns amplitude (Soniprep 150, MSE). Samples were then centrifuged at 10,000 g for 30 minutes (Sigma 1-15 microcentrifuge) and the absorbance of the supernatant scanned over 200-800 nm by spectrophotometer (Cary 100 UV-Vis spectrophotometer, Varian) using a quartz cuvette. In a typical absorbance spectra of pigment extracts from *Arthrospira* (Figure 3.18) the phycocyanin absorbance peak is visible at about 620 nm. First and second Chl*a* absorbance peaks are visible at about 430 and 662 nm respectively.

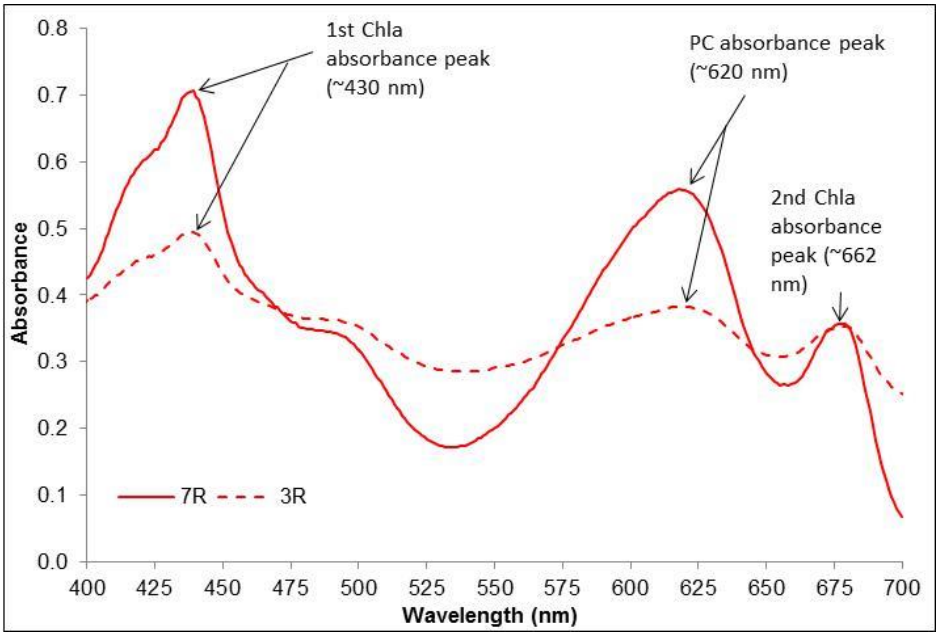

Figure 3.18. An example absorbance spectra of pigment extracts from *Arthrospira*, demonstrated using spectra from high and low phycocyanin concentration extracts. Spectra have been normalised at the second Chl*a* absorbance peak.

Sodium phosphate buffer (0.05 M) was used as a blank and the phycocyanin concentration and purity calculated using the method by Bennett and Bogorad (1973) (Equation 3.2) and Boussiba and Richmond (1979) (Equation 3.3), respectively. In calculation of phycocyanin concentration using the method by Bennett and Bogorad one must take into account in the calculation the presence of allophycocyanin and absorbance by allophycocyanin at 655 nm, which is not normally a visible peak in the spectra.

Phycocyanin concentration was analysed in triplicate at day 14 (or when growth reached OD 0.33). Extraction yield was calculated as below in Equation 3.4 using dry weight biomass and phycocyanin concentration.

Equation 3.2: $\text{PC (mg/mL)} = \frac{A_{620} - 0.474(A_{655})}{5.34}$

Equation 3.3: $\text{PC purity} = \frac{A_{620}}{A_{280}}$

Equation 3.4: $\text{PC extraction yield (mg PC/g biomass)} = \frac{\text{PC x V}}{\text{B}}$

Where PC is the phycocyanin concentration (mg/mL), A, absorbance at the wavelength denoted by the subscript number, V, volume of solvent (mL) and B, dry biomass (g).

Phycocyanin was also expressed as phycocyanin per cumulative filament length in 1 mL of culture using Equation 3.5.

Equation 3.5: Phycocyanin per cumulative length in 1 mL $= \frac{\text{PC}}{(\text{L} \times \text{CC})}$

Where PC is the phycocyanin concentration (mg/L), L, average filament length in the sample and CC, average filament count per mL

3.2.6 Statistical analysis

Data analysis was performed using both Microsoft Excel 2007 and GraphPad Prism version 6.07 for Windows. In the assessment of the differences in growth rate, filament length, biomass, and phycocyanin concentration, purity and yield under red compared with white light, three runs under red light (1-3R) and three runs under white light (1-3W) are used for statistical comparison. Growth rate was calculated as the steepest part of the curve from a minimum of 3 data points. Error was calculated as the average of the standard deviations of all OD values used in the growth rate calculation. Growth rates were averaged for red (1-3R) and white (1-3W) light conditions and error calculated as the standard deviation of growth rates. A two-tailed un-paired T-test not assuming equal standard deviations (Welch's Correction) was used to compare growth rates under red and white light with a p value <0.05 deemed to be a significant difference in GraphPad Prism. For filament length data the reduction in filament length on inoculation was calculated by the % decrease in average filament length between the initial average length taken on day 1 (time 0) to the lowest filament length recorded in the period of days 1-6 after inoculation, which happened to be either the second or third reading. For % increase over the batch calculation, % increase was calculated from the lowest value after inoculation to the end value. For filament length, dry weight, phycocyanin concentration, yield and puritya two-tailed un-paired T-test not assuming equal standard deviations (Welch's Correction) was used to calculate the significance of the difference with a p value <0.05 deemed to be a significant difference. Welch's correction was used as standard deviations were not assumed to be equal under the two light conditions given acclimation under red light. Asterisks indicate the level of statistical significance where p<0.05 =*, p<0.005=**, p<0.0005=***. The significance of the difference between the growth rate and phycocyanin yield in each individual batch 1R-7R compared with the mean under white light was calculated using a two-tailed un-paired T-test and significance levels are indicated by asterisks in the figures.

3.3 Results

3.3.1 Selection of culturing conditions

During the first few runs in the STPBR using conditions of lower mixing (60 rpm), higher air flow rate (0.4 L per min or 0.146 vvm), lower operating temperature (18 °C), lower nitrate concentration (standard f/2 Medium with no nitrate supplementation) and white LED light (45 $\mu mol\ m^{-2}\ s^{-1}$), problems with bleaching and fragmentation (Figure 3.19) of the culture occurred along with reduced trichome width and low levels of phycocyanin production (no observable phycocyanin absorbance peak in sample extracts).

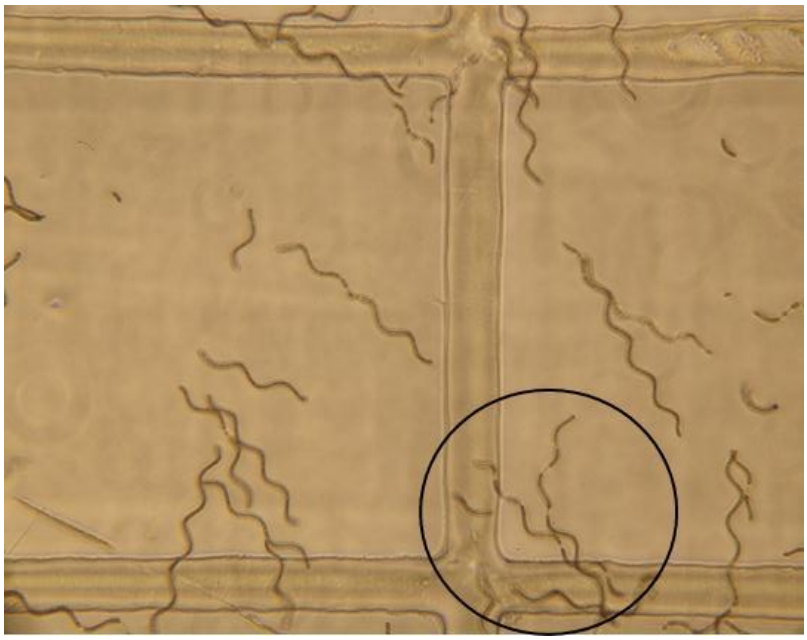

Figure 3.19. Microscope image showing trichome fragmentation, noticeable between days 12-14 in the STPBR, indicating damage. Filaments with obvious damage are circled.

During these early runs the DO levels rose rapidly over the 14 day batch period, through oxygen evolution during photosynthesis and accumulation of oxygen in the culture. High DO likely leads to the production of reactive oxygen species (ROS), and the damage observed through oxidative damage of lipids, proteins and DNA (Nishiyama, 2005, Foyer and Noctor, 2005, Halliwell, 2003). Accumulation of DO and associated bleaching and fragmentation were reduced by changing the operating temperature and impeller speed to 30 °C and 200 rpm respectively (Doran, 2005).

3.3.2 Batch details

A total of 10 batches were successfully completed: seven under red light (labelled 1-7R) and three under white light (labelled 1-3W). The complete culturing order (independent of light type) was: Batch 1R, 2R, 1W, 2W, 3W, 3R, 4R, 5R, 6R and 7R. Data from each batch is presented individually, as the acclimation effects observed could not be visualised by combining data. The culture failed to grow in the first 20 days during the first trial batch under red light (data not shown); however, growth was observed after day 20, suggesting that acclimation had occurred. This culture was subsequently used as the inoculant for batch 1R.

Although only runs 1-3R and 1-3W were used for statistical comparison in the assessment of the differences in culturing under red compared with white light in this chapter, data from batches 4-7R is displayed in the figures alongside the data from batches 1-3R and 1-3W to most clearly show the acclimation effects of successive culturing.

3.3.3 Growth

Batch 2R, as one of this first red light batches, experienced an approximate 13 day lag phase (Figure 3.20). The inoculant from 1R was stored in the CT room for approximately one month prior to inoculation of 2R. Batch 3R also showed slower growth compared with subsequent red light batches. Batch 2W also experienced slow growth after day 10.

The average maximum growth rate under red light (0.028 ± 0.009 ΔOD d^{-1}) was approximately 22 % higher than under white light (0.023 ± 0.009 ΔOD d^{-1}) (Figure 3.21) which, when compared using a Two-tailed un-paired T-test with Welch's Correction, is not significantly higher ($p=0.2857$). From the growth curves in Figure 3.20, there is a visible pattern in the consecutive batches 4R-7R in that the final OD increased with each consecutive culture.

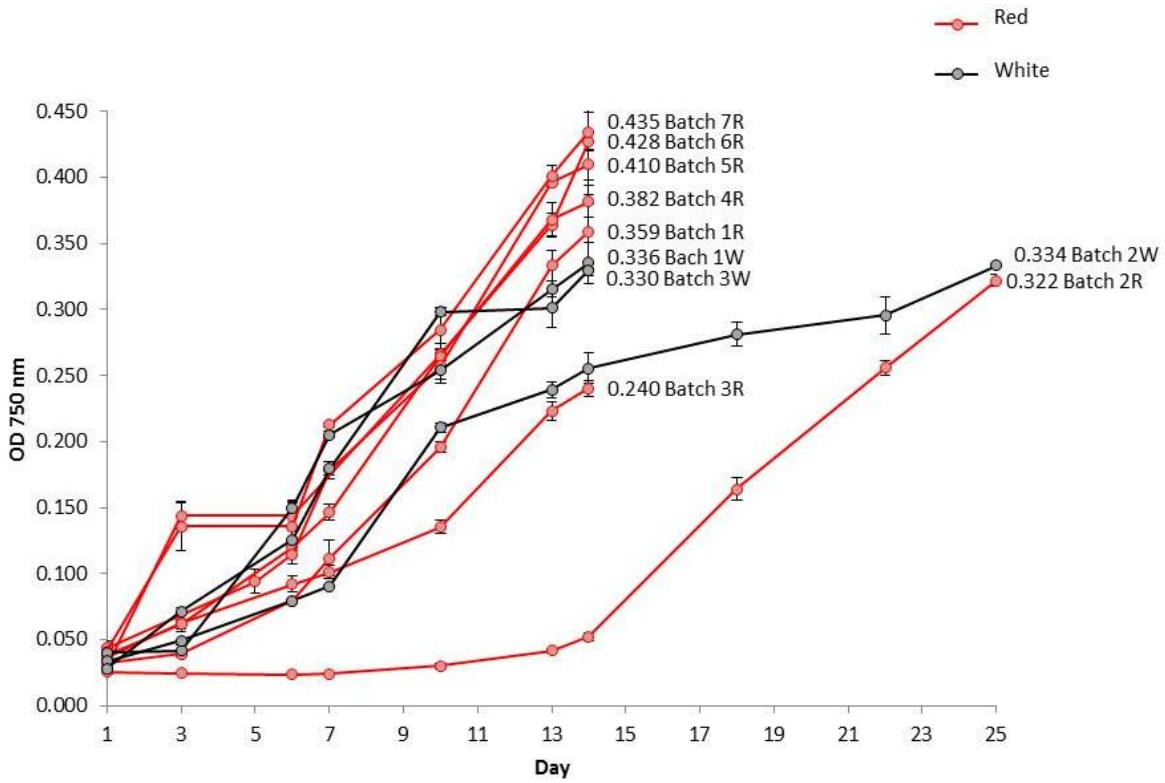

Figure 3.20. Growth curves of replicate batches measured at OD 750 nm cultured under red (red line) and white (black line) light. Each point is mean ± standard deviation, n = 3. The final OD 750nm of each batch and batch number is labelled.

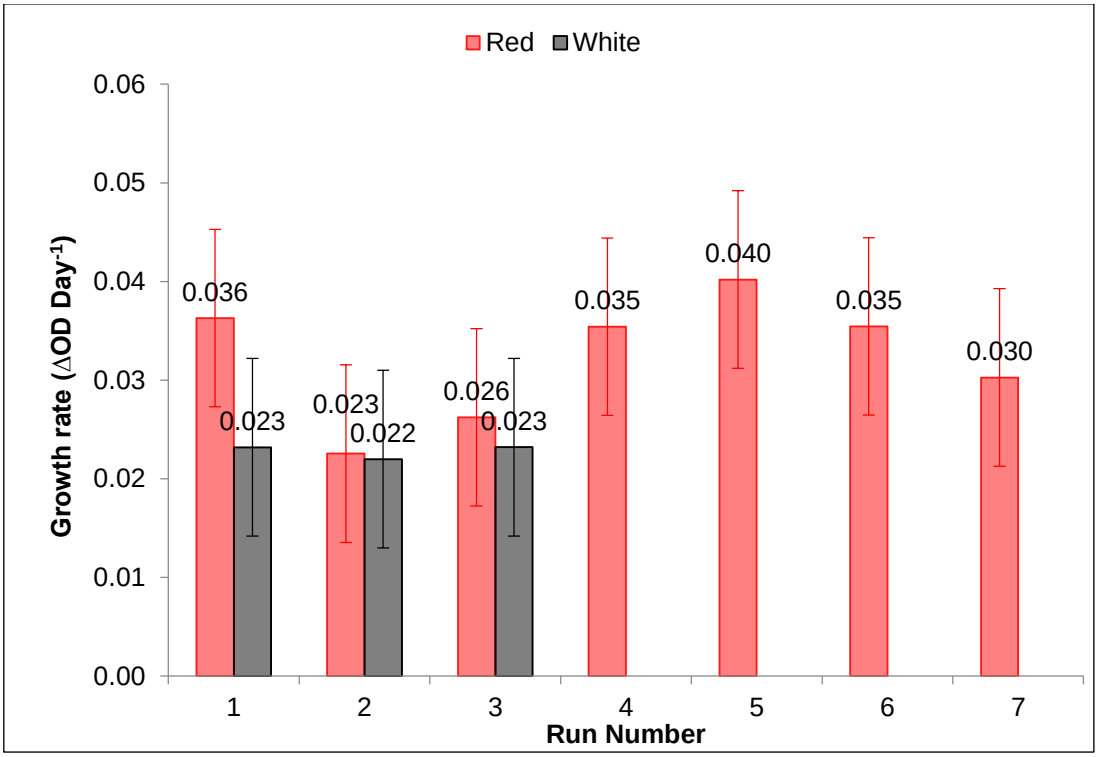

Figure 3.21. Maximum growth rates represented graphically for the batches. Growth rates were calculated from the maximum gradient of the slope of the growth curves from a minimum of three data points. Error is ± standard deviation.

a.

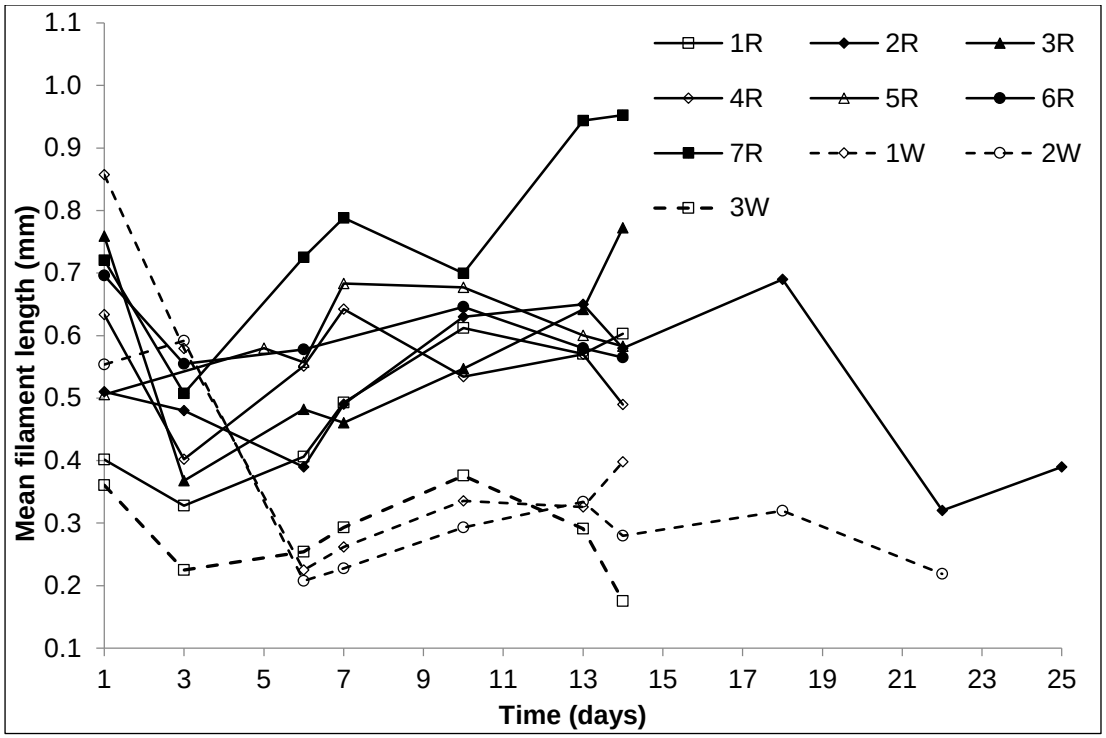

b.

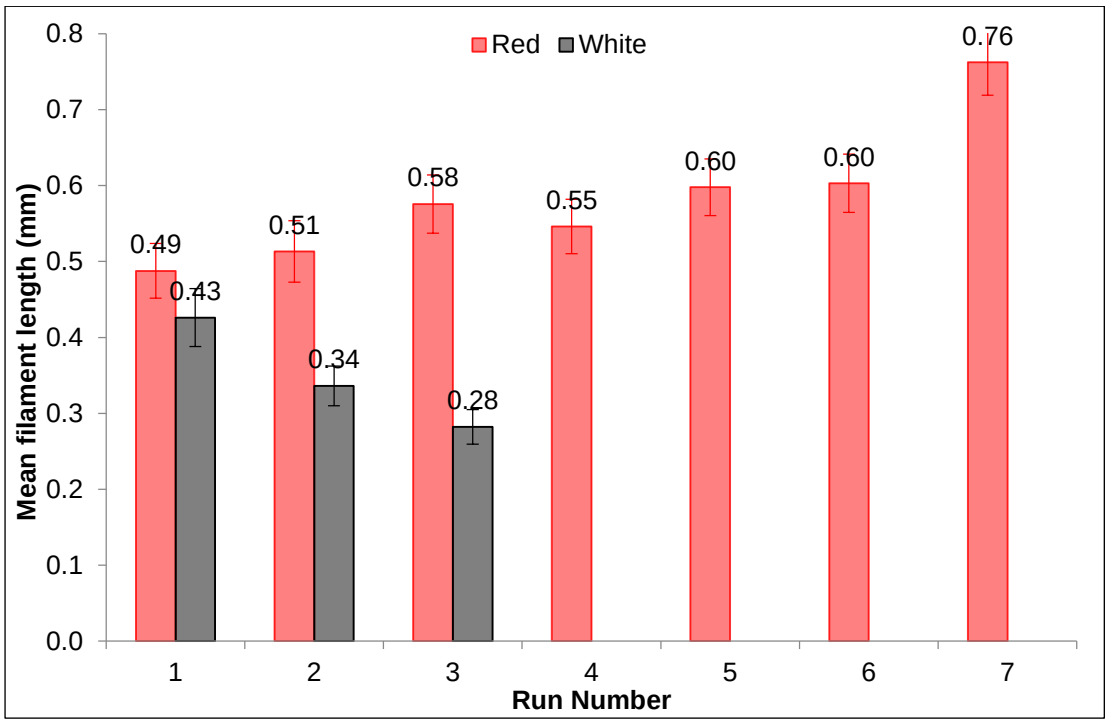

Figure 3.22. Filament length over time (a) and mean filament length (b) across the 10 batches. (a) Each point represents the mean of at least 20 measured filaments. (b) Mean ± standard deviation for filament length over the entire batch culture period.

Filament length reduced rapidly after inoculation, on average by 40 % when calculated across all batches, before slowly increasing (Figure 3.22a) in the majority of batches. This reduction did not occur in batch 5R and in batch 2W reduction was observed between reading 2 and 3 between days 3 and 6. The reduction in filament length after inoculation was pronounced in those batches cultured under white light (average 60 %); and whereas filament length began to increase after day 3 in red light batches, the filament length under white light continued to decrease until day 6. *Arthrospira* filaments were on average 51 % longer in those batches cultured under red (mean length 0.53 mm) compared with white light (mean length 0.35 mm) (Figure 3.22b) which, when compared using a Two-tailed un-paired T-test with Welch's Correction, is significantly higher (p=0.0347*). The lengths of *Arthrospira* filaments in the final batch samples were also on average 119 % longer in those batches cultured under red (0.59 mm) compared with white light (0.27 mm). There were no other obvious morphological differences observed between *Arthrospira* cultured under red light compared with white light. There was also a general trend that filament length increased slowly over the culture period. This filament length increase over the culture period was on average 47 % across all the batches (excluding batches 2R, 1W and 3W where this trend wasn't seen).

3.3.4 Pigment analysis

The individual absorbance spectra for the 10 batches are shown in Figure 3.23 with peak absorption values at 620 nm given in Table 3.2. Spectra were normalised at the second Chl*a* absorbance peak, at 680 nm, which was calculated to be the specific wavelength at which the Chl*a* absorbance peak occurred in the majority of batch spectra.

Figure 3.23 also shows an interesting blue-shift in the second Chl*a* peak for batches cultured under white light. Here the Chl*a* peak occurred at a shorter wavelength at around 673 nm, instead of 678 nm in the absorbance spectra of those batches cultured under red light, giving a blue shift of 5 nm, and can be seen clearly in Figure 3.24(a) and Table 3.3. No additional absorbance peaks were observed at wavelengths above the second Chl*a* peak (Figure 3.24(b)). Interestingly, the second Chl*a* peaks for the three earliest batches cultured under red light (1R, 2R and 3R) are skewed towards the shorter wavelengths in comparison to the later red light batches (Figure 3.24(a)). However, on closer inspection of the absorbance maxima (Table 3.3) there is no obvious trend between maxima shifting and batch number.

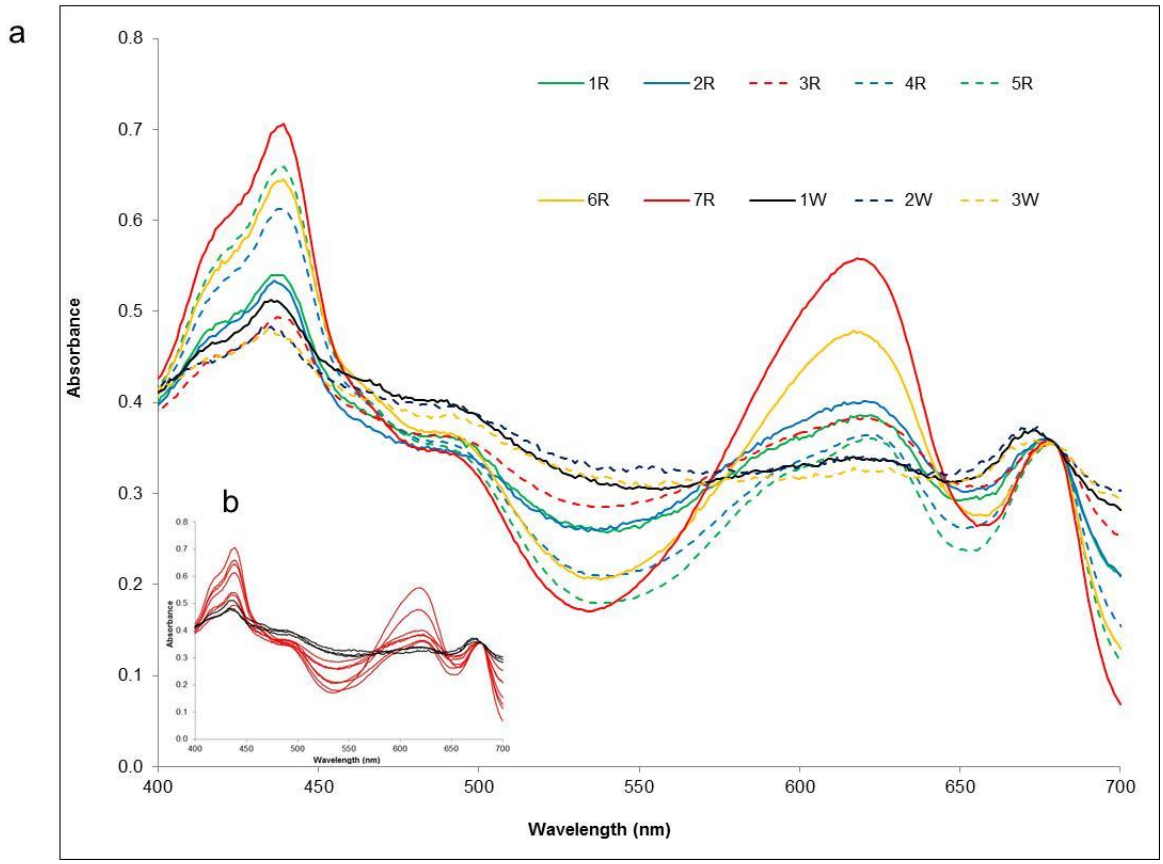

Figure 3.23. Absorbance spectra of pigment extracts from all batches normalised against the second Chl*a* absorbance peak (680 nm). (a) Spectra from individual batches and shown in window (b) coloured according to culturing light type (red light = red line, white light = black line).

Table 3.2. Absorbance values at 620 nm (phycocyanin) in the batch extracts. Error is presented in brackets expressed as mean ± 1 standard deviation.

		Absorbance 620 nm	Mean
Batch	1R	0.236 (0.021)	0.211 (0.011)
	2R	0.249 (0.007)	
	3R	0.148 (0.005)	
	1W	0.117 (0.012)	0.064 (0.007)
	2W	0.057 (0.007)	
	3W	0.019 (0.003)	
	4R	0.262 (0.021)	
	5R	0.311 (0.037)	
	6R	0.388 (0.034)	
	7R	0.558 (0.023)	

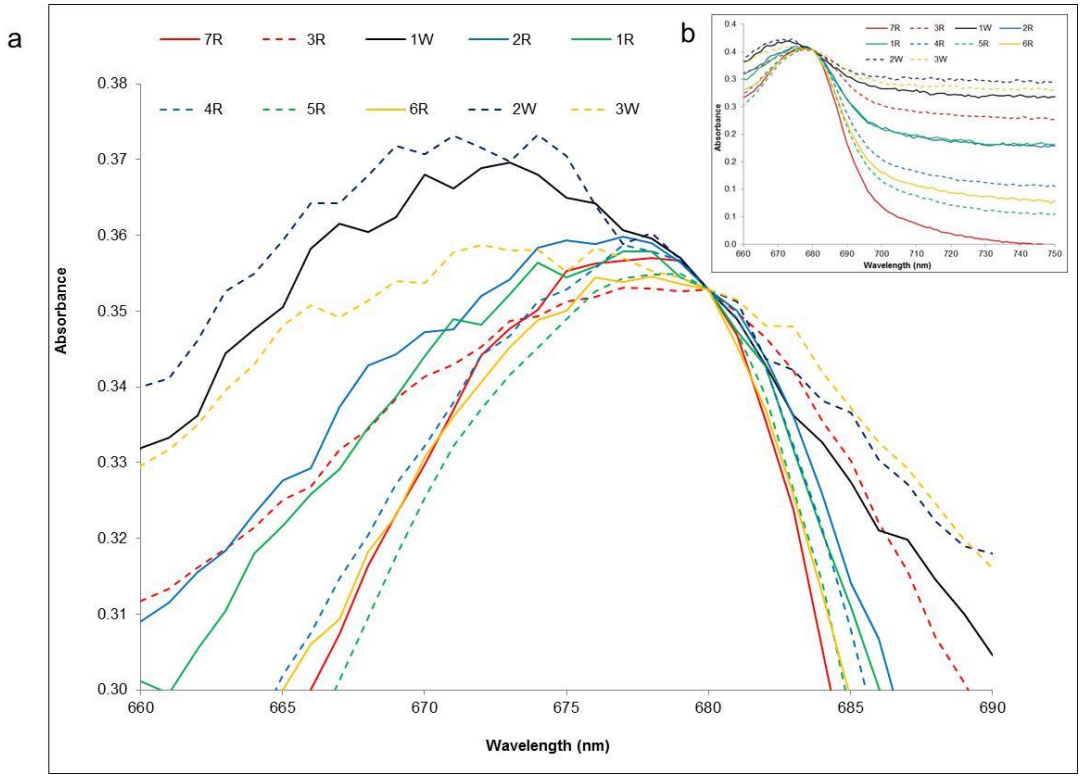

Figure 3.24. (a) Second Chl*a* absorbance peak of batch extracts, (b) absorbance of batch extracts at longer wavelengths between 650-750 nm.

Table 3.3. Absorbance maximum of second Chl*a* peak in batch extracts.

Light	**Batch number**	**Second Chl*a* absorbance maximum (nm)**
White	1	672-673
	2	671-674
	3	672-676
Red	1	677-678
	2	674-677
	3	677-680
	4	677
	5	678-679
	6	678
	7	677-679

The batches cultured under red light were a richer blue in colour compared with batches cultured under white light (Figure 3.25).

Figure 3.25. Visual colour differences between the cultures from the end of batch 1W (left) and 2R (right). Mean OD reading from the bottled cultures at the time the photo was taken were similar at 1W=0.332 (± 0.007), 2R=0.321 (± 0.01).

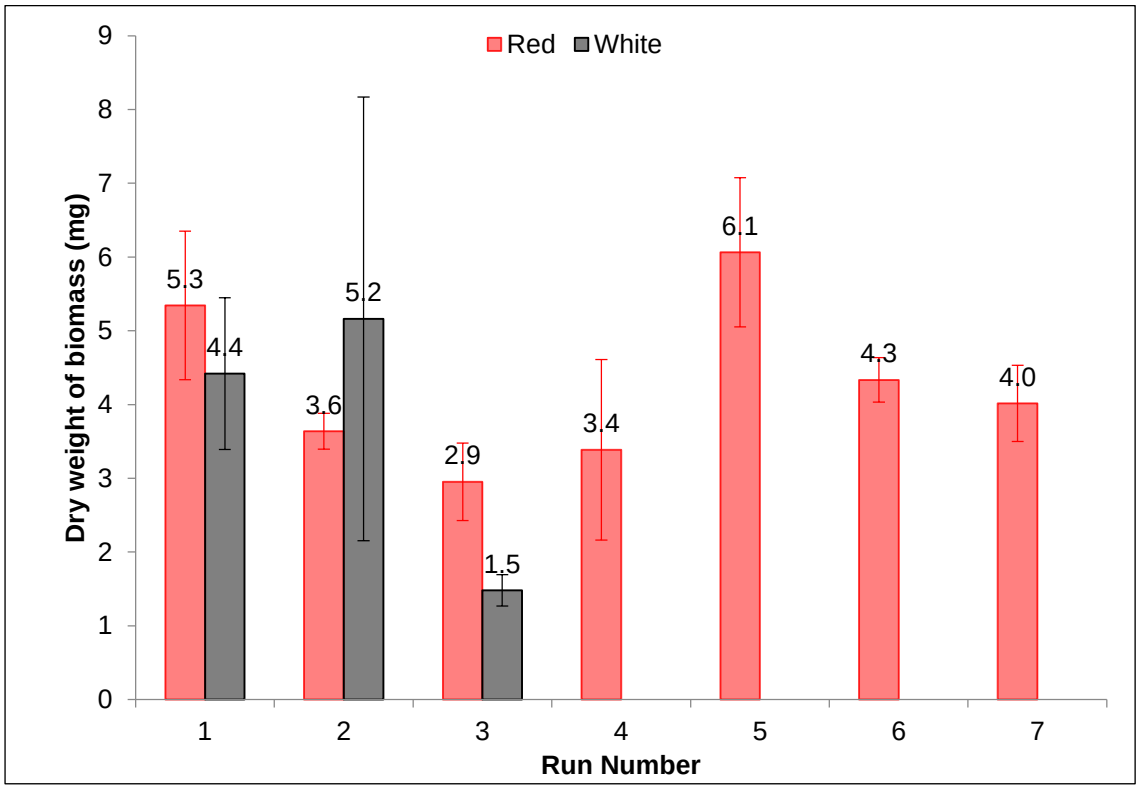

Figure 3.26. Dry weight (mean ± standard deviation) of biomass in the 5 mL samples. Measurements were calculated from three technical replicates.

The 7.8 % increase in mean dry weight biomass obtained from batches cultured under red light (3.977 ± 0.592) compared with white light (3.688 ± 1.417) was not significant (Figure 3.26) (p=0.871 using a Two-tailed un-paired T-test with Welch's Correction).

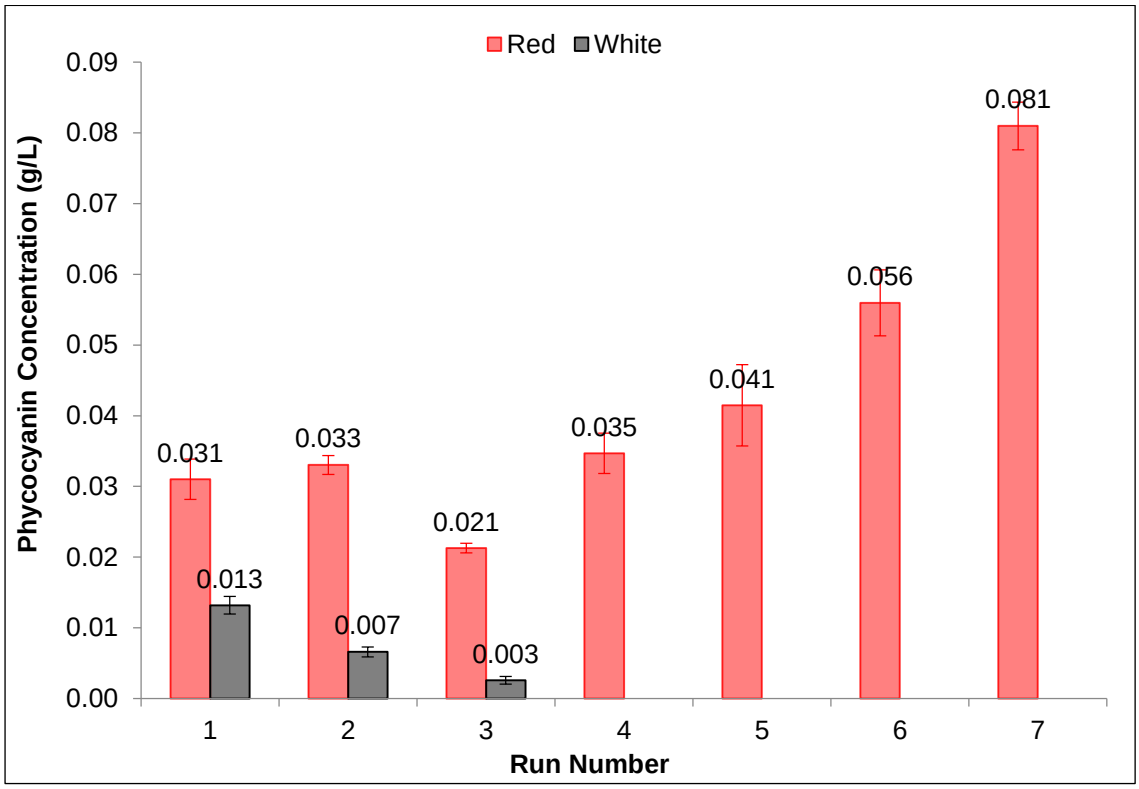

Figure 3.27. Mean ± standard deviation phycocyanin concentration (g/L) of the extracts measured by spectrophotometer according to the method of Bennet and Bogorad (1973), (Equation 3.2). Measurements were taken from three technical replicate samples.

Phycocyanin concentration was higher on average in batches cultured under red light (0.028 ± 0.002 g/L), compared with white light (0.007 ± 0.001 g/L) (Figure 3.27), giving a 300 % significant concentration increase under red light (p=0.0134* using a Two-tailed un-paired T-test with Welch's Correction). Mean phycocyanin yield (Figure 3.28) was higher in red light batches (22.496 ± 3.554 mg/g) compared with white light (6.37 ± 1.417 mg/g), a 253 % significant increase in yield (p=0.0126* using a Two-tailed un-paired T-test with Welch's Correction). In batches 4R-7R, which were cultured consecutively, there was a clear trend of increasing phycocyanin yield. The phycocyanin yield in each individual batch 1R-7R was significantly higher when compared with mean phycocyanin yield under white light and the significance level is indicated by asterisks in Figure 3.28 and the increase in phycocyanin yield observed under red light in batch 7R, compared with white light was a remarkable 864 %.

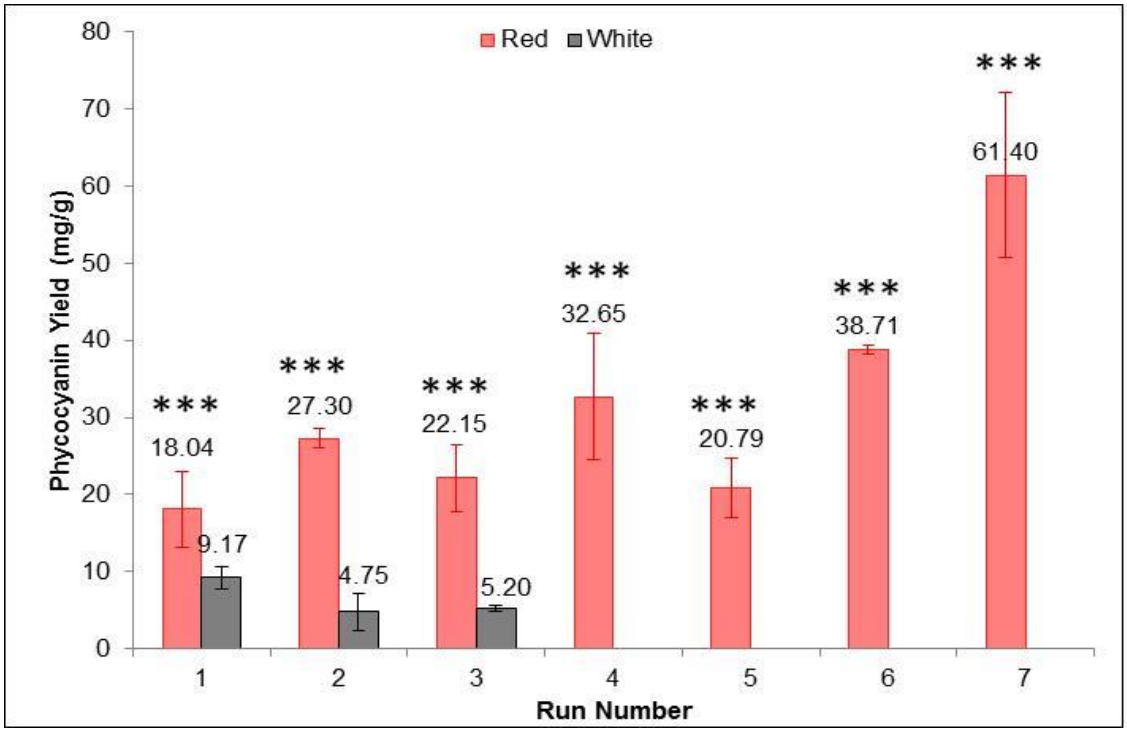

Figure 3.28. Phycocyanin yield (mean ± standard deviation) at the termination of each batch. Yield is expressed as mg phycocyanin per g dry biomass as calculated using the phycocyanin concentration (g/L) results from the triplicate extracts and a value of dry weight biomass from the samples (Equation 3.4). Significance of difference in yield between white and each individual red batch indicated by asterisks where *** = $p<0.0005$.

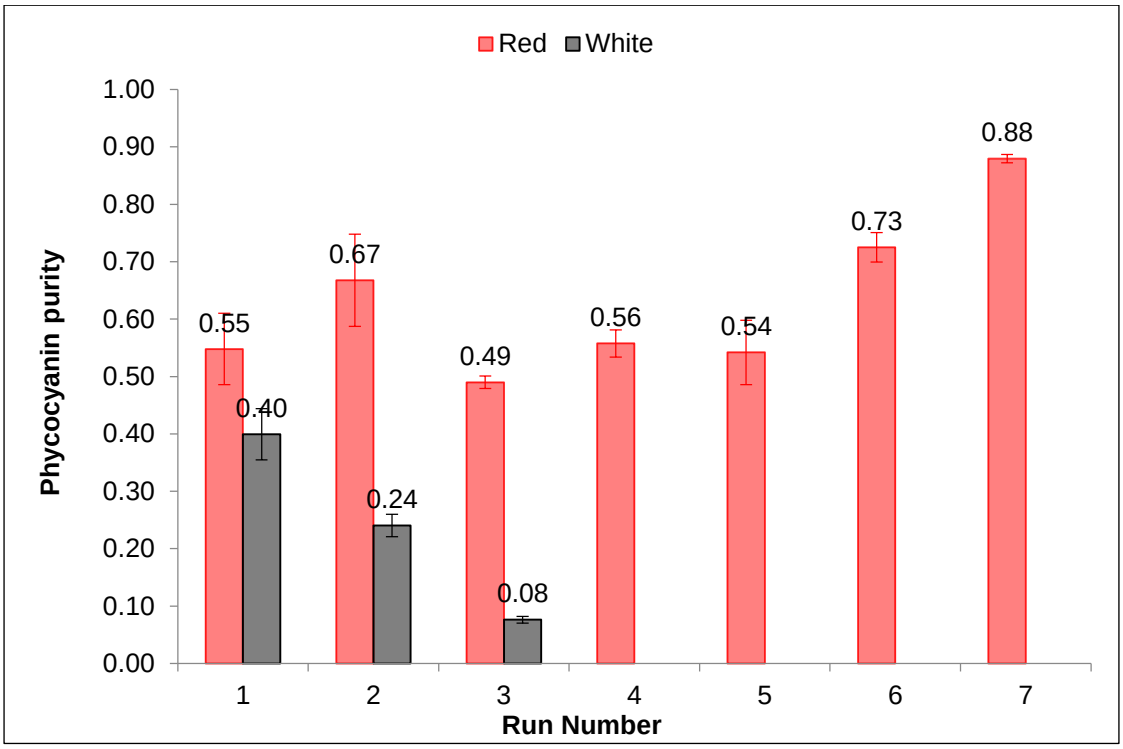

Figure 3.29. Phycocyanin purity (mean ± standard deviation) of the extracts measured by spectrophotometer according to the method of Boussiba and Richmond (1979) (Equation 3.3). Measurements were taken from 3 technical replicates.

Phycocyanin purity was higher in red light batches (0.569 ± 0.051) than in white light (0.239 ± 0.023), an 138 % increase, but not significantly higher using a p value of <0.05 (p=0.0504 using a Two-tailed un-paired T-test with Welch's Correction) (Figure 3.29). In batches 4R-7R, which were cultured consecutively, there was a trend of increasing phycocyanin purity.

According to Pearson's correlation coefficient R, the square root of the R^2 value shown in Figure 3.30a, there is a very strong (0.908) positive relationship between phycocyanin yield and average filament length (Evans, 1996). There is a strong positive (0.787) relationship between phycocyanin yield and final filament length in the batches (Figure 3.30b).

Using the filament counts per volume (Figure 3.31a) phycocyanin was also expressed in a novel way (Figure 3.31b) as mg of phycocyanin per cumulative length of filaments in 1 mL, calculated according to Equation 3.5. This was an attempt at reporting the mass of phycocyanin contained in the total length of cells present in 1 mL of culture. Because *Arthrospira* are filamentous the lengths and cell counts alone do not provide quality information on how much 'cell' there is in a sample; however when combined they can. It was of interest to see if this new measure could provide interesting information about the phycocyanin content of 'cell'. Unfortunately, this measure suffers from high error as calculations are based on highly variable cell length data, so concluding this is not an informative measure.

a.

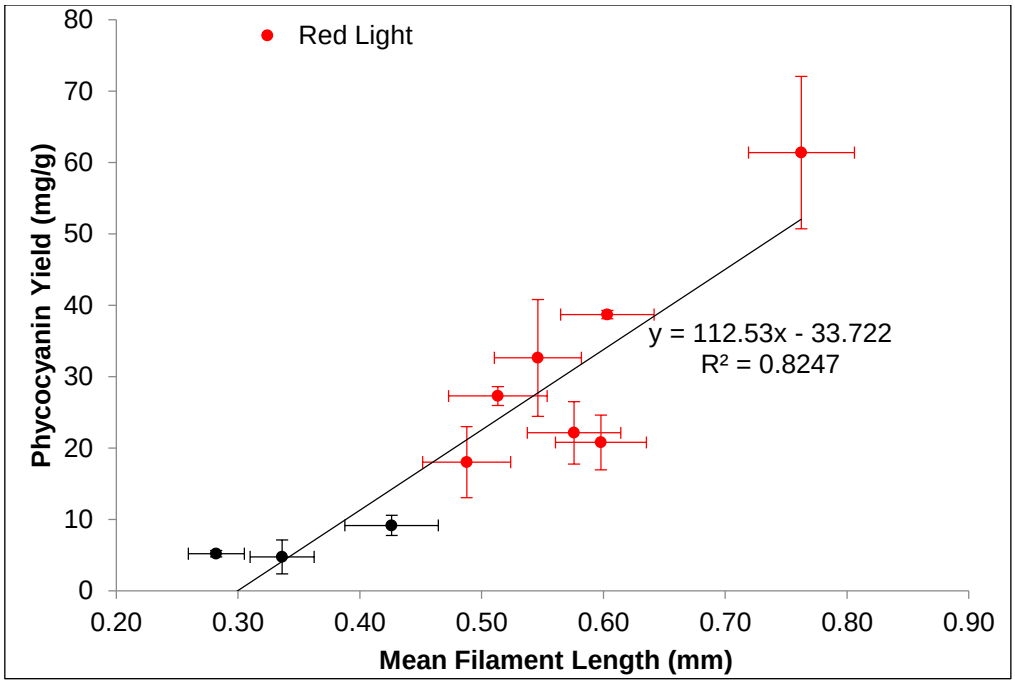

b.

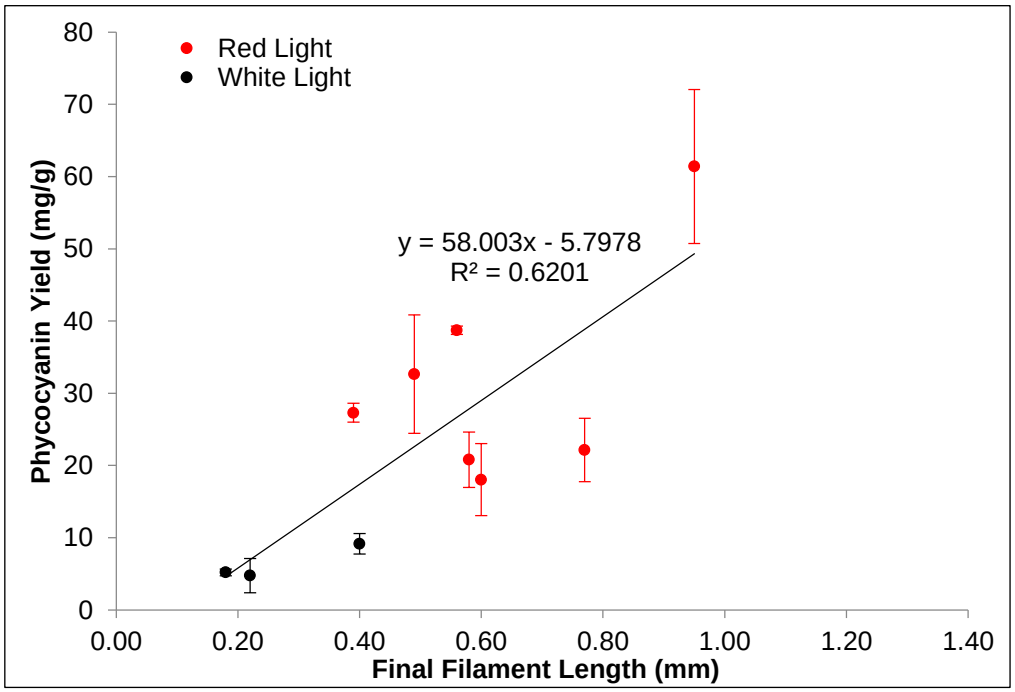

Figure 3.30. Phycocyanin yield (mg/g) plotted against mean filament length (whole of batch) (a) and final filament length (end of batch) (b). Data is shown as mean ± standard deviation. The coefficient of determination (R^2 value) and linear equation of the line-of-best-fit are labelled. Error is not shown for (b) for figure clarity as the error was large, as expected with the variation in filament length in the sample.

a.

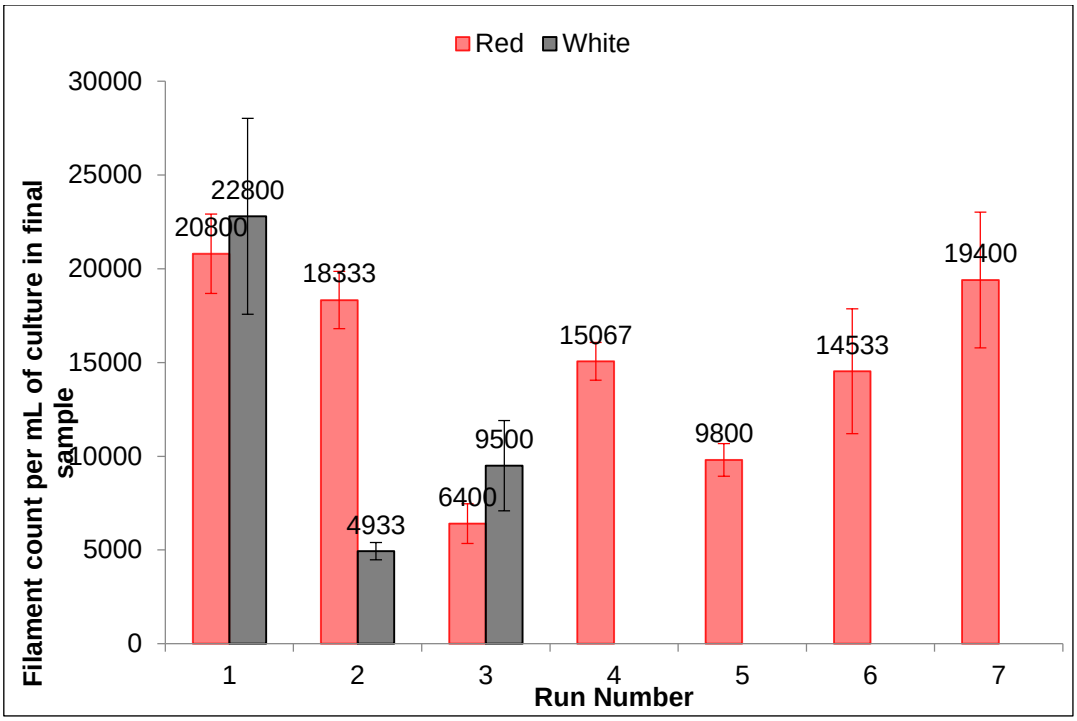

b.

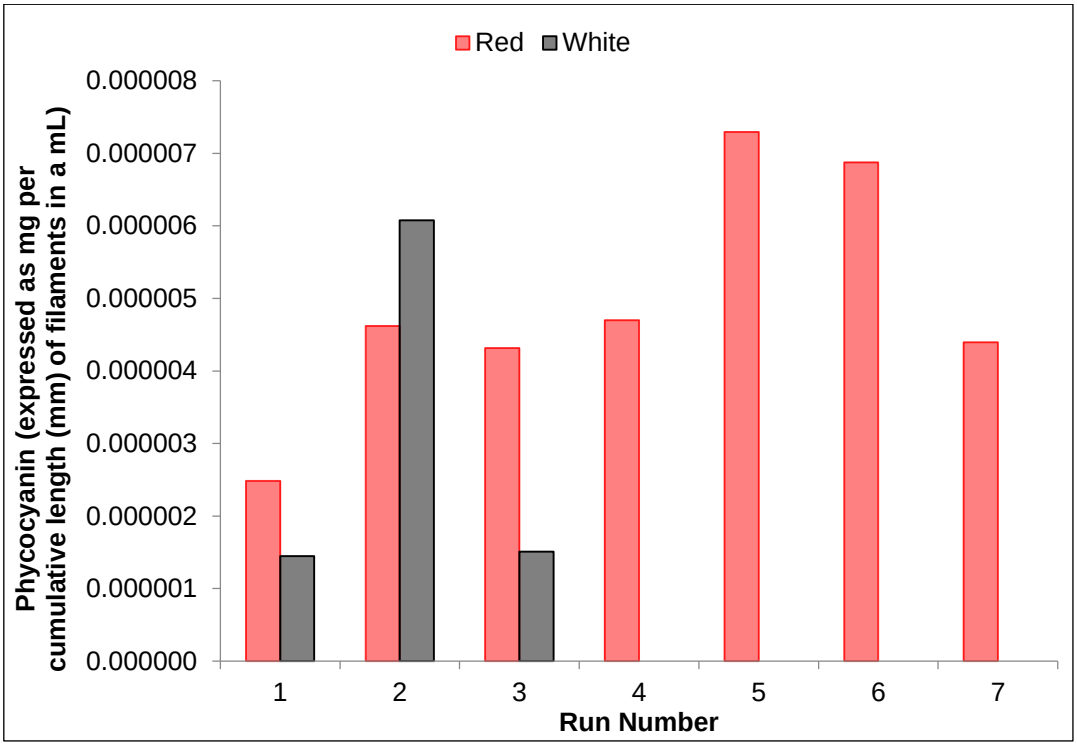

Figure 3.31. (a) Mean filament count (± standard deviation) per mL of sample at the end of the batch and (b) phycocyanin expressed as mg per cumulative length of filament in a mL of sample.

3.4 Discussion

3.4.1 Main findings

Culturing of *Arthrospira platensis* under λ_{max} 680 red light requires acclimation to enable the culture to utilise the light type. This acclimation phase took approximately 14 days under the conditions of these experiments. This acclimation was also (quickly) reversible if acclimated cultures were removed from red light conditions.

There was a 22 %, but not significant, increase in growth rate of *Arthrospira* measured by OD under red light compared with standard white light. There was a surprising significant over 250 % increase in phycocyanin yield under red light compared with white light. Average and final filament length of *Arthrospira* was 51 % higher under red light compared with white light.

Furthermore, acclimation seems to be a constantly active process observable through the continual batch culturing of *Arthrospira* cultures under red light resulting in progressive increases in phycocyanin yield and increases in final culture OD of *Arthrospira* batches. Although extraction procedure has a large impact on phycocyanin concentration, purity and yield, these increases under red light mean that even using a crude extraction method, reactive-grade purities of phycocyanin were obtainable (Below 0.7 phycocyanin purity ratio is classified as food grade, above 0.7 to 3.9 is reactive grade and above 4 is analytical grade (Rito-Palomares, 2001)).

Other effects observed during the experiments were that conditions in the STPBR caused fragmentation of the filaments upon inoculation, likely through high shear created from the impeller; however, filament length increased throughout the batches reaching lengths similar to those in the inoculant, thus this was unlikely problematic.

3.4.2 Chromatic acclimation

The narrow band wavelengths tested in this thesis have generated surprising results, not observed before. Given the lower energy of light at longer red wavelengths compared with white light, the use of λ_{max} 680 nm light in artificially illuminated PBR systems would not only achieve higher yields of high-value phycocyanin, but would also achieve more efficient energy to biomass conversion (Wang, 2007).

Previous studies have shown that trade-offs are made between biomass productivity and pigment yield when using monochromatic light to culture *Arthrospira*. In this thesis it is demonstrated that culturing *A. platensis* under λ_{max} 680 nm light significantly increases

phycocyanin yield without any detriment to productivity (compared with culturing under standard white light).

Although direct comparisons cannot be made with other studies, as red wavelengths of light previously used to culture *Arthrospira* have been of shorter wavelengths, it seems to have been assumed that the effects of red light used at longer wavelengths would be similar to previous observations reported in the literature, except for those wavelengths of light approaching far-red which cannot be utilised by photoautotrophs. Although Walter et al. (2011) showed white light to be most effective for *Arthrospira* productivity and phycocyanin yield compared with 475-600 nm red light, the results presented in this thesis demonstrate that longer wavelength red light (660-700 nm) is more effective in achieving a higher phycocyanin yield whilst maintaining high biomass productivity. In contrast to Walter et al. a number of other studies have reported increased *Arthrospira* productivity cultured under 620-645 nm red light compared with white light (Chen, 2010a, Markou, 2014, Wang, 2007) although with reduced phycocyanin yield (Markou, 2014) (or no significant increase in phycocyanin yield, in the case of Chen et al.). Moreover, the same studies did in fact report highest phycocyanin yield under blue light (Markou, 2014, Chen, 2010a). It was suggested that blue light may increase phycocyanin yield by limiting growth and recycling of phycocyanin for a nitrogen source in the cultures (Chen, 2010a), or by creating a light-limiting environment, causing natural increases in pigments – a well-known response to increase energy-capture for photosynthesis (Markou, 2014).

The closest study to which the findings of this thesis can be compared is that by Akimoto et al. (2012). They tested three regions of red light for the culture of *Arthrospira*: 600-650 nm (standard), 620-700 nm (long-wavelength red) and 700-780 nm (near-infra red), against other monochromatic and white LEDs. The highest productivity was observed under long-wavelength red LED (final OD_{750} 0.93), the culture having an OD_{750} 0.17 higher than the OD obtained through culturing under standard white LEDs (final OD_{750} 0.76), although there was no significance calculation reported. Both the growth rate (calculated as $\Delta OD\ day^{-1}$) and biomass yield was slightly higher under λ_{max} 680 nm light compared with standard white LEDs in the present work, but neither were significant increases.

Furthermore, in contrast to this thesis, Akimoto et al. reported that the phycocyanin content was lowest under 620-700 nm red light, but higher under 700-780 nm red light compared with

standard white LEDs (being highest under blue light). Trade-offs between biomass productivity and pigment yield were again seen by Akimoto et al.

Long-term culturing (over 700 hours) under monochromatic light, albeit at a shorter wavelength (λ_{max} 620 nm standard red LED) than used here, was performed by Farges et al. (2009). However, only a handful of long-term monochromatic culturing studies have ever been performed on *Arthrospira*, and none using such long wavelengths as in this study. Long-term (3,500 hours, constituting approximately 30 5-day batches) culturing under standard red LEDs produced a steady growth rate over the batches, but showed a mean two-fold decrease in phycocyanin content, although the trend in phycocyanin content over time was not reported. Current work showed that phycocyanin yield increased by 3.4-fold over the 7 batches (approximately 2,350 hours) cultured under λ_{max} 680 nm red light demonstrating continual chromatic acclimation. This chromatic acclimation was also quickly reversible. At the beginning of the experiments, chromatic acclimation was also required to enable *Arthrospira* to utilise the λ_{max} 680 nm red light.

Chromatic acclimation has remained largely unexplored in *Arthrospira*. Chromatic acclimation to enable *Arthrospira* to utilise red light was obvious from the large lag phase observed in the first trial batch. From experience, acclimation to conditions such as increased mixing or increased temperature, for example, normally only takes a maximum of a few days, before the lag phase disappears; however, acclimation to a new light type can take much longer. Long lag phases also observed in early batch 2R after storage of the inoculant (from batch 1R) in the CT room demonstrates that chromatic acclimation in *Arthrospira* is (quickly) reversible. During storage the culture underwent acclimation to the white light conditions of the CT room and then re-acclimation to the red light upon inoculation of the STPBR batch 2R. Acclimation continued throughout subsequent batches. This thesis has shown that chromatic acclimation can increase phycocyanin production while maintaining stable growth. An open question remains as to the extent that the phycocyanin content can be increased through continual chromatic acclimation over longer-term culturing, and whether the culture will become unstable.

It is possible that continued acclimation to the red light occurring with each generation of *Arthrospira* is accountable for increasing the efficiency of utilisation of red light (productivity), seen as a higher final OD achieved in each consecutive batch (excluding 2R and 3R). Maximum growth rate based on change in OD 750nm per day was used as a measure of growth. This is

because *Arthrospira* filament count is not an accurate measure of growth, as filaments can vary in size. The OD 750 nm therefore gives an accurate calculation of biomass present per volume of culture, and enables growth measurements to be taken accurately from small volumes of culture, which cannot be achieved through testing wet and dry weight. However, with an OD-based maximum growth rate calculation there is less information to extract on productivity compared with cell-counts typically used in (non-filamentous) microalgae cultures. Although a pattern of increasing final OD is observed in consecutive red light batches, this is not reflected in OD-based growth rates.

The phycocyanin increases observed in this study contrasts with earlier suggestions that monochromatic light that increases phycocyanin is the result of light limitation (Markou, 2014). The interesting phenomena of blue-shifting, where the second Chl*a* peak shifted by approximately 5 nm, from 678 to 673 nm under white light has been observed before and is an associated feature of cellular stress. Sudhir et al. (2005) recorded blue-shifting of the second Chl*a* peak by approximately 4 nm, from 680 nm to 676 nm in fluorescence emission spectra of salt-stressed *A. platensis* caused by the loss of chlorophyll protein (47 kDa) and core membrane linker-protein (94 kDa) that attach phycobilisomes to thylakoids. As the chlorophyll/linker proteins are important in maintaining phycobilisome structure and energy transfer, these stress-induced structural changes result in the decreased energy transfer from chlorophyll/phycobiliproteinto the PII reaction centre. Decoupling of the phycobilisome during high irradiance (or short-term stress) is assumed to be a strategy to prevent photo-oxidative damage to photosynthetic reaction centres after exhaustion of all other light adaptation responses (Tamary, 2012); however, there is currently a gap in understanding the phycobilisome decoupling mechanism.

Whereas the current study measured fluorescence, the relationship between Chl*a* absorbance and fluorescence can mean that similar shifts can be seen in both absorbance and fluorescence spectra (Chen, 2010b). Chlorophyll *f* (Chl*f*), discovered and characterised by Chen et al. had an *in vitro* absorbance and fluorescence peak red-shifted (706 and 722 nm respectively), compared with all other chlorophylls from oxygenic phototrophs. Their findings suggested that oxygenic photosynthesis can be extended further into the infra-red region. Their observation led from culturing stromatolites (Western Australia, Shark Bay), under near-infra red (λ_{max} 720 nm) light. It is also known that chlorophyll *d* (Chl*d*) can replace Chl*a* in the photosystem of the cyanobacterium *Acaryochloris marina* (Miyashita, 1996) and related organisms (Itoh, 2015, Gan, 2014), extending the range of the light spectrum that can be harvested. Chl*d* and Chl*f*

absorbance peaks are 447-455.5 and 688-697 nm (dependent on extraction solvent) and 439.5-440 and 698-707 nm (dependent on extraction solvent) respectively (Li and Chen, 2015). In Gan et al. (2014) the appearance of an absorbance peak at λ_{max} 706 and 720 nm in the cyanobacterium *Leptolyngbya* sp. cultured under 700-750 nm red light, indicated the production of Chl*d* and Chl*f* during photoacclimation. As additional absorbance peaks were not observed at wavelengths above the second Chl*a* peak in this thesis, *Arthrospira* did not produce new forms of chlorophyll (Chl*d* or Chl*f*) during photoacclimation under λ_{max} 680 nm red light. Nevertheless, in the experiments of Gan et al. (2014) it is interesting to see small shifts (3-5 nm) in the second Chl*a* absorbance peaks in red light photoacclimated cultures, which are likely caused by remodelling of the photosynthetic apparatus during photoacclimation.

Guikema and Sherman (1983) also reported a blue-shift in the second Chl*a* absorbance peak from 678 to 673 nm in iron-starved, chlorophyll/phycocyanin depressed cells of the cyanobacteria *Anacystis nidulans.* This was attributed to the loss of longer wavelength chlorophylls (also known as red or low-energy chlorophyll), specifically forms Ca670 and Ca680 in PSI (ÖQuist, 1971, Karapetyan, 2014). Such longer wavelength chlorophylls of PSI can be irreversibly bleached by illumination with high-intensity white light (Cometta, 2000).

Although there can be no certain conclusion as to the exact cause of the 5 nm shifting of the second Chl*a* absorbance peak, it could be the result of loss of longer wavelength chlorophylls through conditions under white light or a de-coupling of the phycobilisome from PSII, which is unlikely given that the intensity of white light during the experiments, and therefore photo-stress, was not particularly high compared with similar set-ups reported in the literature. A more likely explanation is that the shift indicates a remodelling of the photosynthetic apparatus during photoacclimation under the λ_{max} 680 nm light, despite a trend in peak shifting with red batch number photoacclimation being absent.

3.4.3 Filament length and fragmentation

Fragmentation of *Arthrospira* trichomes have been noted under conditions of high DO or light through ROS production, leading to oxidative damage of lipids, proteins and DNA (Nishiyama, 2005, Foyer and Noctor, 2005, Halliwell, 2003). Additional culture changes caused by this type of damage are narrowing of the trichome, and colour change from green to yellow (chlorosis) caused by bleaching of both chlorophyll and phycocyanin (Ma and Gao, 2010, Singh, 1995, Marquez, 1995, Tomaselli and Margheri, 1981). These effects were seen during the trial runs

for selection of culturing conditions in the STPBR, using low mixing, temperature and nitrate concentration. Fragmentation of mature trichomes is also the method by which *Arthrospira* reproduces. *Arthrospira* has previously been shown to be sensitive to shear stress, caused by mechanical mixing, demonstrating breakage of trichomes under such conditions (Mitsuhashi, 1994, Mitsuhashi, 1995). Moving from a low shear flask environment to a high turbulence and shear photobioreactor environment likely caused the reduction in trichome length observed in the batches of these experiments. Substantial agitation is required in photobioreactor systems for efficient gas exchange and even light exposure to maintain healthy cultures. Trichome length of *Arthrospira* increases with normal growth where the number of cells per filament increases, and filaments fragment during asexual reproduction, increasing filament number. The increase in trichome length after the initial length decrease upon introduction into the PBR suggests that *Arthrospira* adapted to the conditions of high shear and the impeller speed was not problematic long-term, similarly observed by Mitsuhashi et al. (1995). Perhaps the lower average and final length of trichomes observed under white light were caused by photodamage. Taking this explanation, it may be that red light, specifically longer-wavelength red light as such used in these experiments, causes less photodamage. As red light provides lower energy photons to the photosynthetic apparatus, reducing the production of free-radicals (specifically ROS) which are associated with trichome fragmentation. Further, a decreased level of intracellular ROS would preserve the highly reactive phycocyanin pigment. Given the findings of these experiments and the scientific knowledge behind light electromagnetic spectrum energetics and cellular biochemistry, culturing under higher wavelengths of light (where possible) could be extremely beneficial in the production of high-value reactive products, such as pigments, as demonstrated here for phycocyanin.

Chapter 4. Effects of culturing Arthrospira platensis under Long Wavelength Red Light

4.1 Introduction

This chapter expands on the analysis of samples obtained from the experiments of Chapter 3. In this chapter samples are analysed for Carotenoid and Chlorophyll *a* (Chl*a*) yield, Phycocyanin:Chl*a* ratio in assessing whether light limiting effects contributed to the increased phycocyanin yield seen under red light in Chapter 3, and Carotenoid:Chl*a* ratio to determine whether nutrient limitation was present. pH throughout the batches in the experiments of Chapter 3 is analysed and mass spectral data is presented to look at differences in the protein composition of whole cell samples of *Arthrospira* cultured under red and white light. Observations of differences in the leaching properties of biomass produced under red compared with white light are investigated along with observations in the autoflocculating properties of the culture. Information on the microbial population in the culture over time in the batches of Chapter 3 is evaluated.

4.2 Experimental Details and Method

4.2.1 Pigment analysis

Pigment extraction was as described in 3.2.5. Chlorophyll *a* (Chl*a*) and total carotenoid (TC) concentration and yields were calculated as follows according to Equations 4.1, 4.2 and 4.3 (Markou, 2014, Lichtenthaler, 1987):

Equation 4.1: $\text{Chl}a\,(\text{mg/L}) = 16.82(\text{A}_{665}) - 9.28(\text{A}_{650})$

Equation 4.2: $\text{TC}\,(\text{mg/L}) = \frac{1000(\text{A}_{470}) - 1.91\text{Chl}a - 95.1[36.92(\text{A}_{650}) - 16.54(\text{A}_{665})]}{225}$

Equation 4.3: $\text{Chl}a\,/\,\text{TC yield}\,(\text{mg/g}) = \frac{\text{Chl}a}{1000(\text{TC})} \text{x} \frac{\text{V}}{\text{B}}$

Where A is absorbance at the wavelength denoted by the subscript number, V, volume of solvent (mL), B, dry biomass (g), Chl*a*, chlorophyll *a* concentration (mg/L) and TC, total carotenoid concentration (mg/L).

4.2.2 MALDI-TOF MS analysis

Twenty milligrams of the sample matrix (α-cyano-4-hydroxycinnamic acid; HCCA, Bruker Daltonics, Germany) was prepared by mixing 1 ml of 50 % acetonitrile: 2.5 % trifluoro-acetic

acid (Sigma-Aldrich, UK). The matrix was vortexed and saturated by a 30 minute incubation at 25 °C in an ultrasonic water bath at 100 % power (Grant instruments, UK) with a second vortex at 15 minutes. The matrix was then centrifuged at 14,000 g for 1 minute (Sigma 1-15K microcentrifuge) and 50 µl aliquots prepared fresh for use.

1 mL samples of each culture (batches 2R and 1W) were centrifuged at 14,000 g for 5 minutes and the pellets washed twice with deionised water and stored at -80 °C. Prior to spotting onto the MALDI target plate, samples were thawed on ice and resuspended in 50 µl deionised water. Samples were mixed 1:1 with HCCA matrix and four 2 µl technical replicates were spotted onto a MTP 384 ground steel MALDI target plate (Bruker Daltonics, Germany) and air dried at room temperature.

Mass spectrometry was done using an UltraFlex II MALDI-TOF TOF mass spectrometer (Bruker Daltonics, Germany) with fuzzy control of laser intensity. Ion source 1 was set at 25 kV and ion source 2 was set at 23.5 kV with a laser frequency of 50.0 Hz, a detector gain of 1,650 V and a gating maximum of 1,500 Da. Spectra were recorded in the positive linear mode for the mass range 2,000 to 20,000 *m/z*. Each spectrum was obtained by averaging 100 laser shots acquired in automatic mode. For data acquisition, validation measurements were performed in Auto Execute mode. The spectra were externally calibrated using the Bacterial Test Standard (Bruker Daltonics, Germany). The standard consisted of seven ribosomal proteins from *Escherichia coli* with added RNase A and myoglobin to cover a range of ca. 3637 to 16957 *m/z*. Four independent samples of each culture were placed on four separate spots on the steel target plate. Each sample spot was read twice thereby producing eight spectra per culture. The quality and mass accuracy of the peaks were examined using FlexAnalysis software (Bruker Daltonics, Germany). The eight spectra were overlain and a consensus spectrum generated which was added to the database for each sample.

4.2.3 Population analysis

Samples taken throughout the batch for the 10 batches were frozen in 15 % sterile glycerol at -80°C for subsequent population analysis, carried out by Andrew Free, Rocky Kindt and Jennifer Lawson at the University of Edinburgh. Population analysis was carried out by illumina sequencing of the 16S ribosomal RNA (rRNA) gene (Degnan and Ochman, 2012). DNA was extracted from the samples using Ultraclean Soil DNA Isolation Kit (MO BIO Laboratories, Inc.) with the amount of sample used was proportional to OD. DNA was eluted in PCR-grade water and stored at -20 °C and PCR performed first to amplify 16S rRNA gene,

followed by a second round for amplification of the V3 region of the gene and addition of illumine chip adapters and multiplex barcodes. PCR products were cleaned-up by running amplicons via agarose gel electrophoresis followed by excision under UV and purification using Promega Wizard Gel and PCR Cleanup System. DNA was quantified using a PicoGreen fluorescence-based assay and used to make a mastermix of barcoded amplicons at equimolar ratios for Illumina Hiseq and Miseq sequencing (Edinburgh Genomics, UK). Downstream data processing was performed in QIIME (http://qiime.org/) with sequences in FASTA format. Sequences were firstly separated according to original samples into libraries using barcodes added during the PCR step and any sequences of poor quality (Phred quality score<19) excluded. V3 amplicons were just over 250 base pairs (bp) long and read pairing was performed to join matching reads together (minimum overlap 200 bp) and sequences shorter than 240 bp filtered out. Chimeras (multiple templates amplified during PCR) were removed using Greengenes (http://greengenes.secondgenome.com/downloads) and then aligned and clustered to reference sequences and assigned operational taxonomic units (OTUs). Reads were output as a table of OTUs and corresponding number of hits per sample and converted to relative abundances.

4.2.4 Leaching tests

Samples from runs 1R (where R = red LEDs) and 1W (where W = white LEDs) stored at -80 °C (mean OD after defrost: white: 0.463, red: 0.467) were defrosted on ice and 1 mL transferred to 10 pre-weighed Eppendorf tubes to create 10 repeats for each light condition. Tubes were re-weighed and samples then centrifuged (10,000 g for 5 minutes), to obtain a pellet which was washed once and resuspended in 1 mL deionised water, vortexed and stored upright in a dark part of the CT room (18 °C). Samples were vortexed daily for 5 seconds until day 5 where samples were centrifuged before analysis of the supernatant by scanning visible spectrophotometry and phycocyanin concentration, yield and purity calculated as described in 3.2.5. Phycocyanin yield data for extracted: 3 technical replicates of phycocyanin yield from batches 1R and 1W and leached: 10 repeat samples from batches 1R and 1W was used for analysis. PC yield Red Extracted:PC yield Red Leached and PC yield White Extracted:PC yield White Leached ratios were calculated for all combinations giving two sets of 30 values which were compared using a Two-tailed un-paired T-test not assuming equal standard deviations (Welch's Correction).

4.2.5 pH data filtering

A moving average filter was used to remove noise in the online pH batch data caused by variation in pH during daily illumination/dark periods. Here, a new filtered value is derived from adjacent unfiltered data points taking into account the previous filtered data point (Smith, 1997). The mathematics behind the filter is explained in Equation 4.4.

Equation 4.4: $\mathrm{Xnew} = \left(\frac{-1-2\mathrm{T}}{1+2\mathrm{T}}\mathrm{Xold}\right) + \frac{\mathrm{Ynew}}{1+2\mathrm{T}} + \frac{\mathrm{Yold}}{1+2\mathrm{T}}$

Where, X_{new} is the new filtered value, X_{old} is the previous filtered value, Y_{new}, the current unfiltered value and Y_{old}, the previous unfiltered value.

The power of the filter can be adjusted, where a higher number of data points in the window has a larger smoothing effect on the data.

4.2.6 Statistical analysis

Data analysis was performed using both Microsoft Excel 2007 and GraphPad Prism version 6.07 for Windows. In the assessment of the differences in carotenoid and Chl*a* yield under red compared with white light, three runs under red light (1-3R) and three runs under white light (1-3W) are used for statistical comparison. For total carotenoid concentration and yield, phycocyanin:Chl*a* ratio, total carotenoid:Chl*a* ratio a two-tailed un-paired T-test not assuming equal standard deviations (Welch's Correction) was used to calculate the significance of the difference with a p value <0.05 deemed to be a significant difference. Welch's correction was used as standard deviations were not assumed to be equal under the two light conditions given acclimation under red light. Asterisks indicate the level of statistical significance where $p<0.05$ =*, $p<0.005$=**, $p<0.0005$=***.

4.3 Results

4.3.1 Pigment analysis

Although only runs 1-3R and 1-3W were used for statistical comparison in the assessment of the differences in culturing under red compared with white light on carotenoid and Chl*a* yield in this chapter, data from batches 4-7R is displayed in the figures alongside the data from batches 1-3R and 1-3W to allow a clear comparison.

Carotenoid yield was higher under red light (151 ± 23.6 mg/100 g) batches than white light (137 ± 41.8 mg/100 g) (Figure 4.1), a 10 % increase under red light. The increase was not significant (p=0.773 using a Two-tailed un-paired T-test with Welch's Correction).

Chl*a* yield was higher in batches cultured under red light (1.02 ± 0.16 mg/g), compared with those cultured under white light (0.95 ± 0.3 mg/g) (Figure 4.2), a 7 % increase under red light. This increase is not significant (p=0.822 using a Two-tailed un-paired T-test with Welch's Correction).

There was a positive correlation between phycocyanin and Chl*a* concentration (Figure 4.3a) and phycocyanin:Chl*a* ratio (Figure 4.3b) under red light was consistently higher and significantly higher on average (p=0.0155* using a Two-tailed un-paired T-test with Welch's Correction) when compared with white light.

The carotenoid:Chl*a* ratio (although not an exact indicator) is a relative index of nutrient limitation where usually higher ratios show nutrient limitation (Schitüter, 1997). The similarity of the ratios in all batches (Figure 4.4) demonstrates that there was no significant nutrient limitation effects during the experiments (p=0.576 using a Two-tailed un-paired T-test with Welch's Correction). The mean ratios for batches cultured under red and white light were 150 ± 4 and 142 ± 7 respectively.

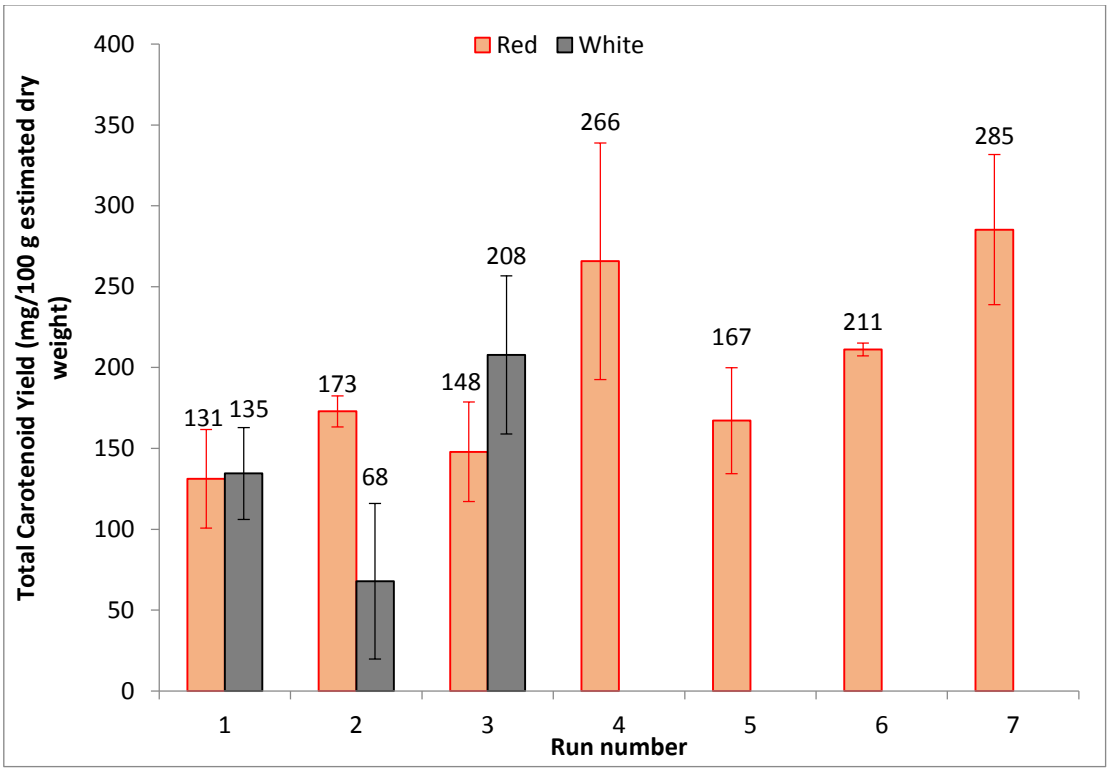

Figure 4.1. Total carotenoid yield (mean ± standard deviation) at the termination of each batch.

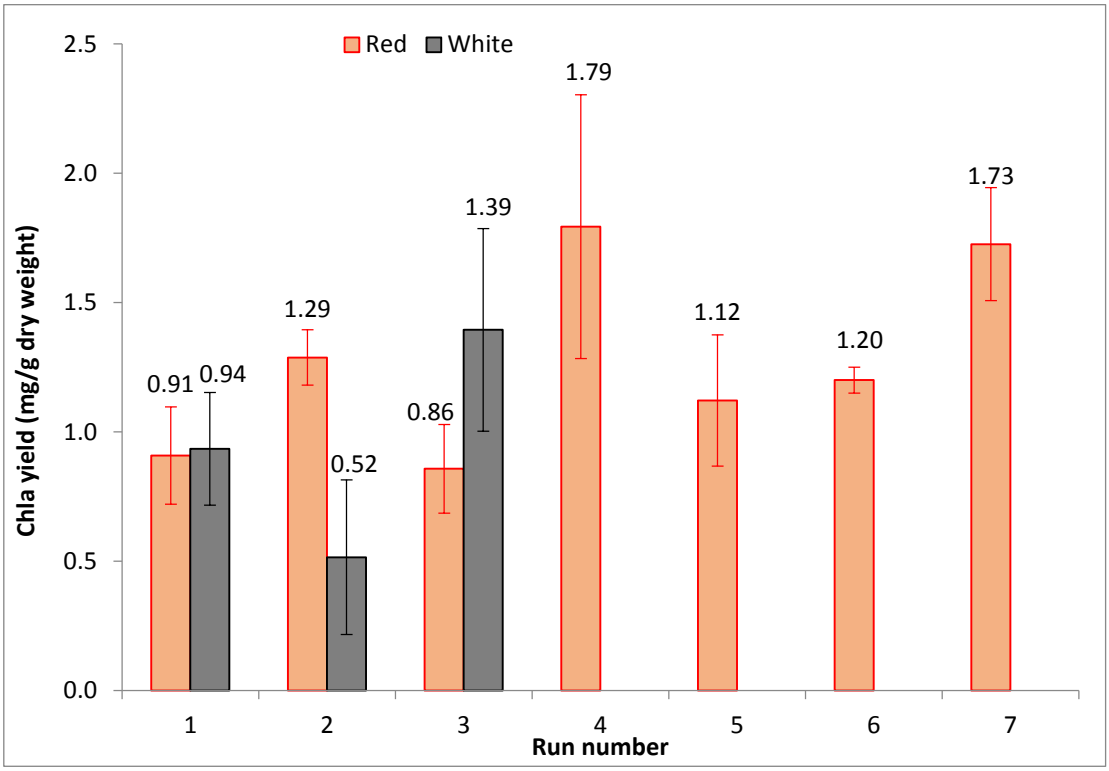

Figure 4.2. Chl*a* yield (mean ± standard deviation) at the termination of each batch.

a.

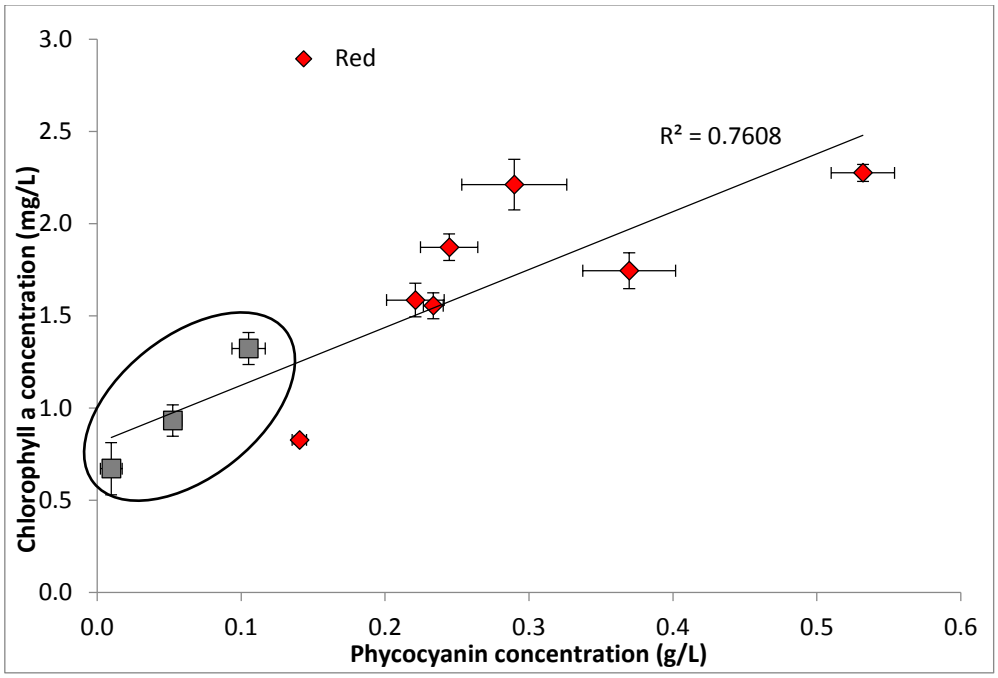

b.

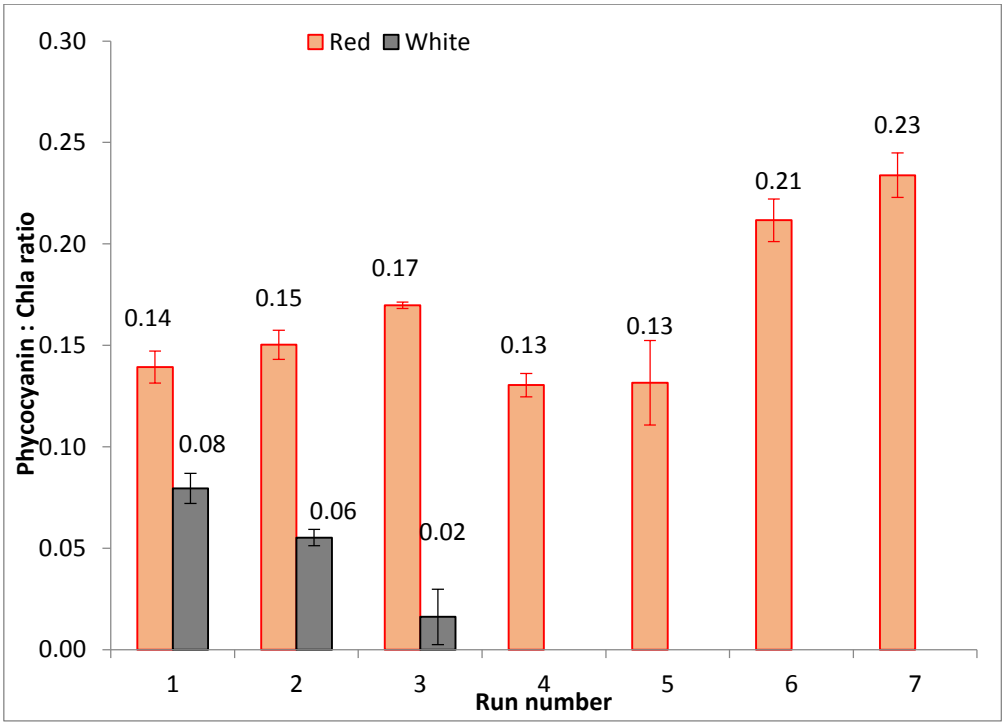

Figure 4.3. Relationship between Chl*a* and phycocyanin concentration at the termination of each batch (a). The plots of the batches cultured under white light can be seen circled closest to the Y-axis. Phycocyanin:Chl*a* ratio (b).

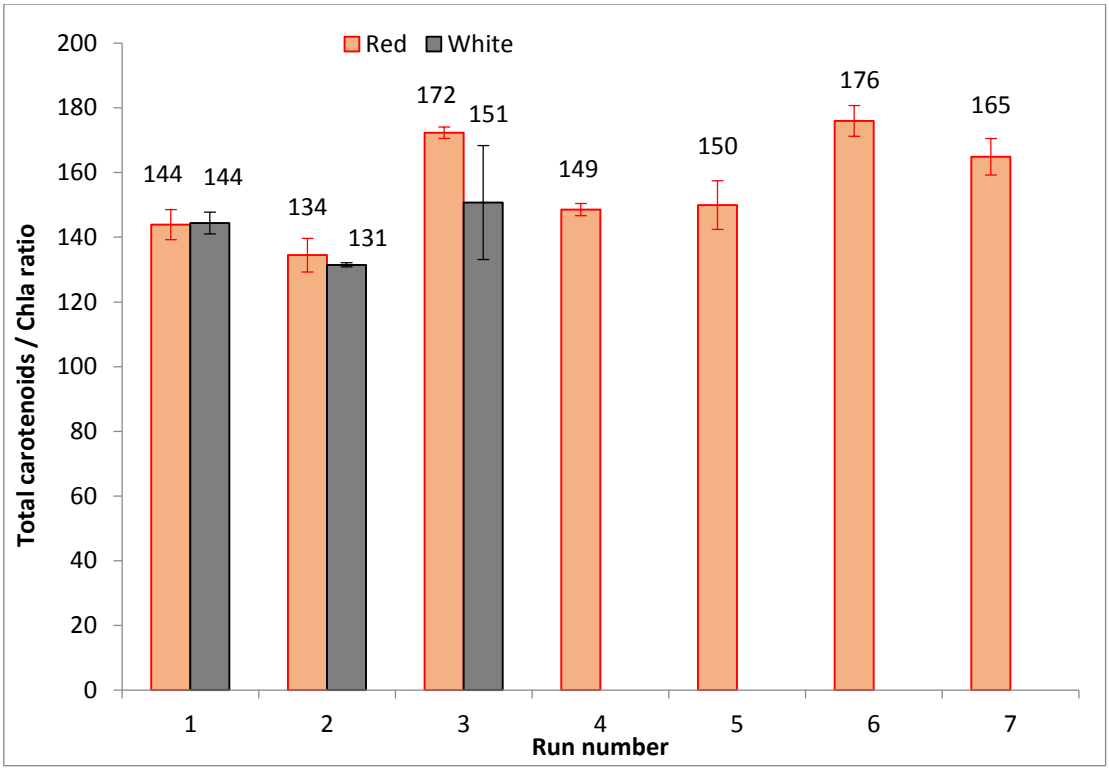

Figure 4.4. Carotenoid:Chl*a* ratio at the termination of each batch.

4.3.2 pH

The pH of the batches varied with the light cycle (Figure 4.5). Typically, pH increased during the illuminated period and decreased in darkness, giving an average daily variance in pH of around 0.5. This is expected in such cultures during normal diurnal cycles. During exposure to light, photosynthetic processes increase pH. Conversely, in the dark, the cells switch to respiratory processes, decreasing pH of the culture (Falkowski and Raven, 2007). Batches 7R, 6R and 3R showed a pattern of continued pH increase and decrease during illumination and dark periods respectively. Interestingly, the other batches only exhibited this behaviour at the start of the batch before pH began to plateau. As the change in pH is caused directly by production of certain metabolites in either photosynthesis or respiration, the fall in pH during illumination indicates a slowing or stopping of basic metabolite production and photosynthesis, indicating possible photoinhibition (Falkowski and Raven, 2007). This photoinhibition-effect was present in batches 1R (after day 11), 2R (after day 21 of 25), 4R (after day 8), 5R (after day 8), 1W (after day 4), 2W (after day 5 of 23), and 3W (after day 6), as seen in Figure 4.5.

a.

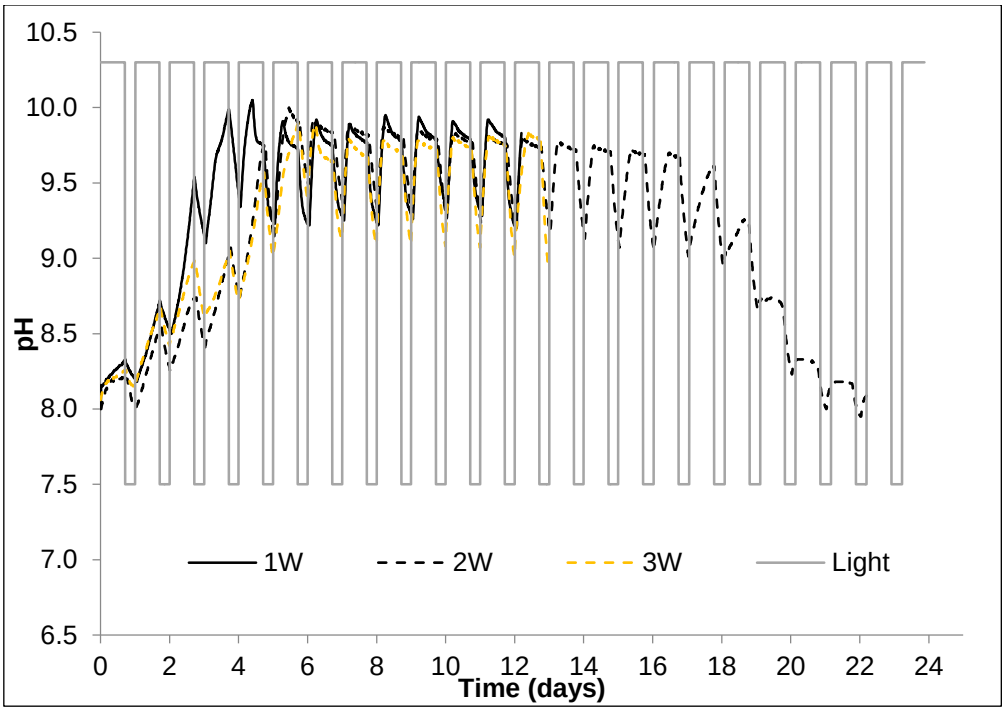

b.

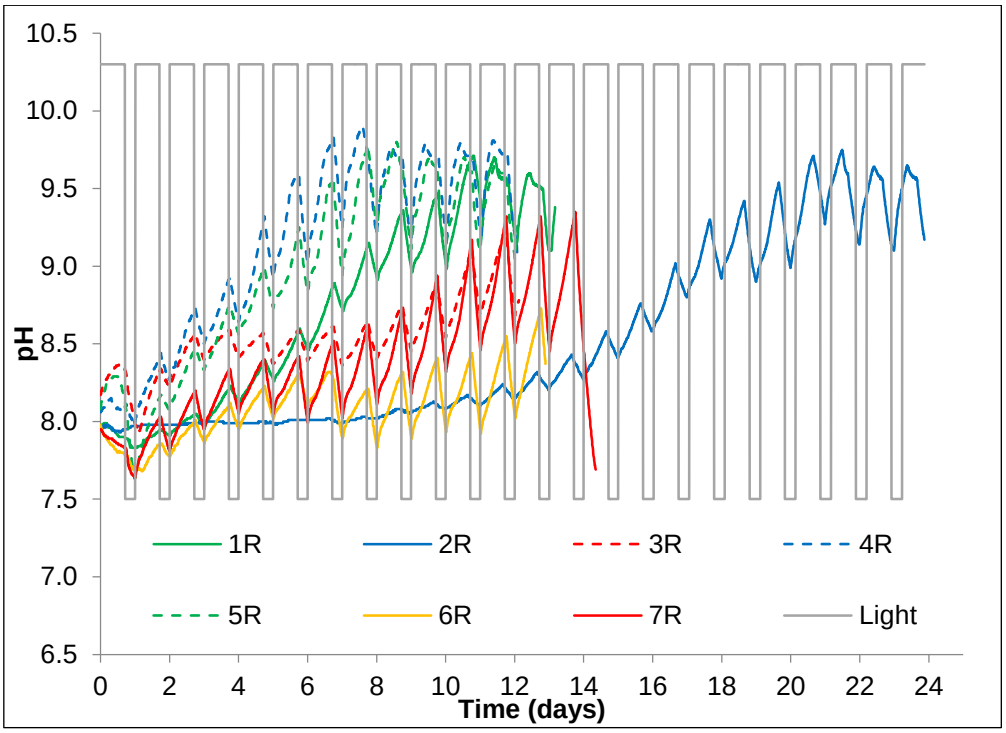

Figure 4.5. pH throughout the batches under white (a) and red (b) light.

Indication of photoinhibition occurs earlier and is more pronounced in the three batches cultured under white light (Figure 4.5). Photoinhibtion was not observed in batches 6R and 7R – the cultures with the highest phycocyanin yield and observed acclimation to red light.

Through filtering out the diurnal cycles, the pH trends generally increased throughout the batch runs (Figure 4.6). Batches began at approximately pH 8 with the majority increasing to a pH of around 9-9.5 at day 6 (excluding 2R which followed the same trend after a 14 day growth lag phase).

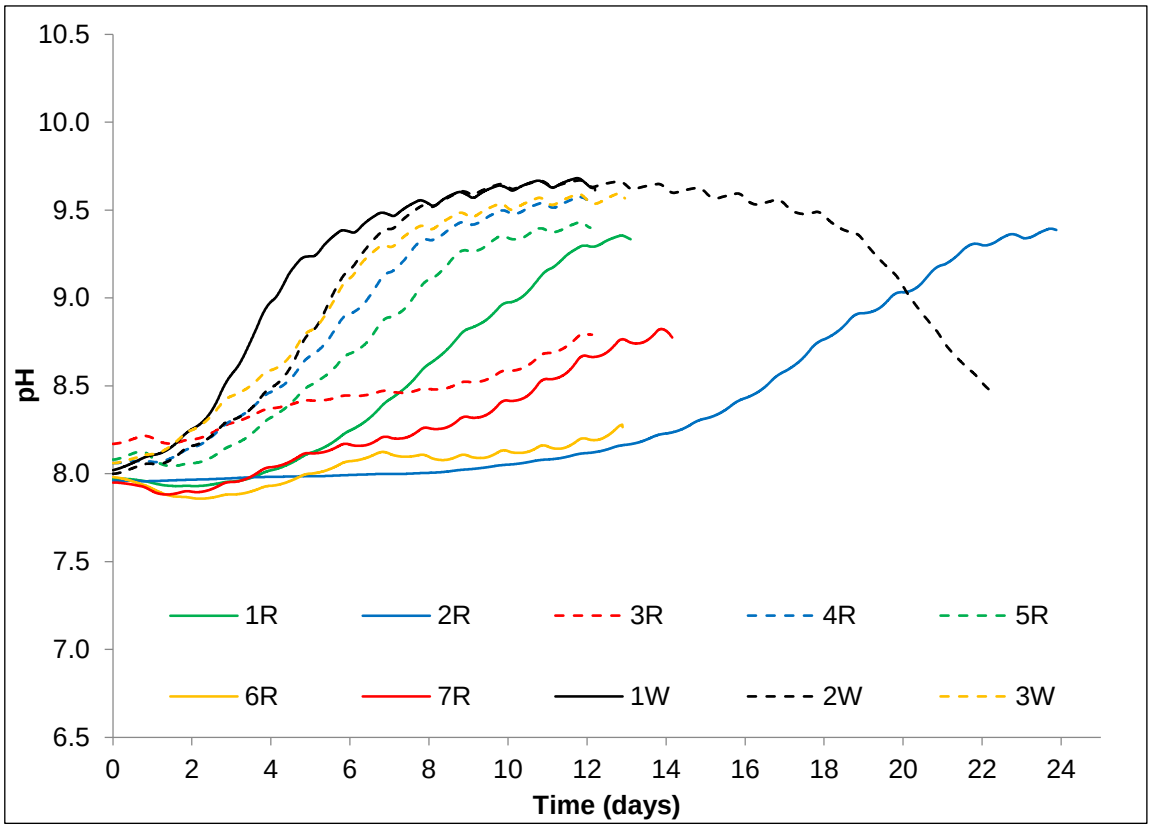

Figure 4.6. pH throughout the batch cultures. Data has been filtered using a time moving average filter to remove pH variation attributed to illumination/dark periods.

pH levels in white light runs rose sharply between days 3 and 7 and maintained a pH of around 9.5 until the end of the batch; apart from 2W where pH began to drop slowly after day 14 and then dropped sharply after day 19. Overall, the pH in white runs were typically higher than the majority of red light runs. Of those runs cultured under red light, 4R and 5R showed the fastest rate of pH increase from days 3 to 7, increasing to a pH of 9.4-9.5 at the end of the run (Table 4.1). The pH in 1R increased rapidly after day 6 to give a final pH of 9.38. The pH in 2R, which displayed a growth lag phase of 14 days, increased rapidly from days 16-21 to give a final pH

of 9.17. The pH of batches 3R, 6R and 7R did not increase as rapidly nor reach as high a final pH as in other batches, although all batches experienced a similar daily variance in pH.

Table 4.1. Final pH recorded at the end of each batch

Run	Final pH	Batch end time (Days)
1W	9.83	12.19
2W	8.09	22.19
3W	8.96	12.97
1R	9.38	13.17
2R	9.17	23.87
3R	8.78	12.13
4R	9.09	12.07
5R	9.26	12.08
6R	8.37	12.90
7R	7.69	14.35

4.3.3 Mass spectra

Matrix Assisted Laser Desorption Ionisation Time of Flight Mass Spectrometry (MALDI-TOF MS) was used to analyse the protein composition of whole cell samples of *Arthrospira* cultured under red (2R) and white (1W) light. The protein-mass spectra obtained are presented in Figure 4.7 and were highly reproducible (replicate spectra are shown in Appendix 2).

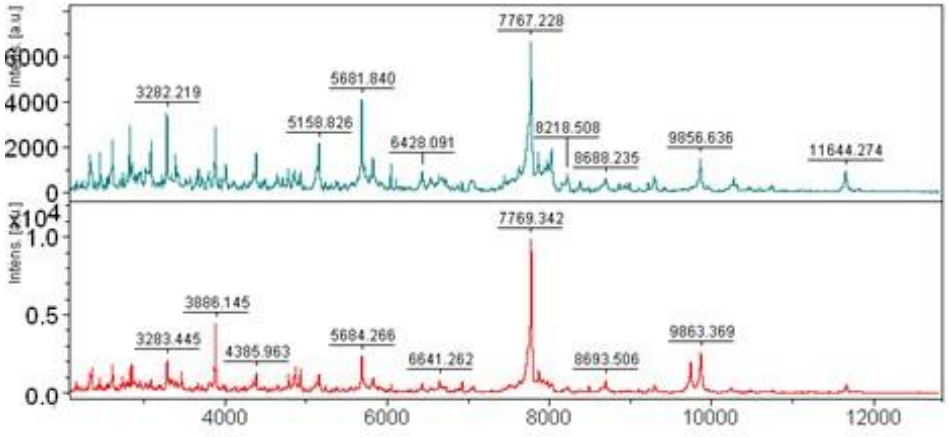

Figure 4.7. MALDI-TOF mass spectra showing protein-mass spectral patterns of *Arthrospira* cultured under red (bottom) and white (top) light.

Mass spectra from the two light conditions were broadly similar with common peaks at approximately *m/z* 7767, 5681, 3282, and 3883. However, the common peak at approximately *m/z* 5681 was higher in *Arthrospira* cultured under white light, relative to the other common peaks, whereas the common peak at approximately *m/z* 7767 was higher in *Arthrospira* cultured under red light, relative to the other common peaks identified. The peak at approximately *m/z* 4389 was much larger in *Arthrospira* cultured under white light in comparison to other common peaks. A peak was present at approximately *m/z* 5157 in *Arthrospira* cultured under white light but not under red light. There was also an additional peak at *m/z* 9733 in *Arthrospira* cultured under red light.

Although as expected there are numerous common *m/z* peaks under the two light conditions, there are notable differences in peak intensity. There was also a major peak present under white light that was absent under red light. This mass spectral data indicates that there are differences in abundant proteins when *Arthrospira* is cultured under red light in comparison to white light.

4.3.4 Leaching differences

When discarding the samples prepared for mass spectral analysis, it was observed that the tubes containing pellets suspended in distilled water from the red light batch were a stronger blue colour compared with those cultured under white light (Figure 4.8). Phycocyanin leaching was investigated further to determine whether this was simply a direct reflection of the difference in biomass phycocyanin yield.

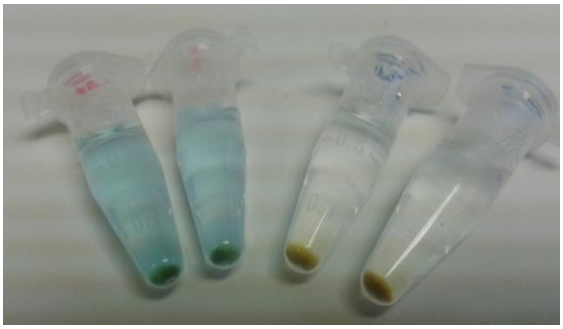

Figure 4.8. MS samples observed during disposal. A stronger blue colour was present in tubes containing *Arthrospira* pellets from the batch cultured under red light (left) compared with white light batch (right).

a.

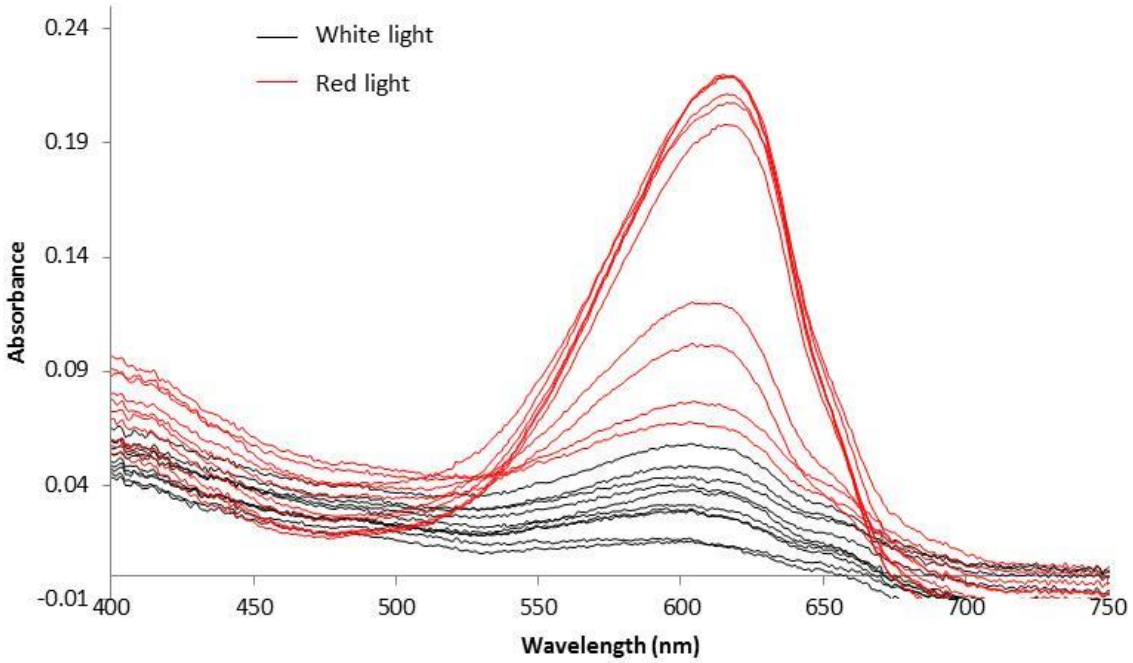

b.

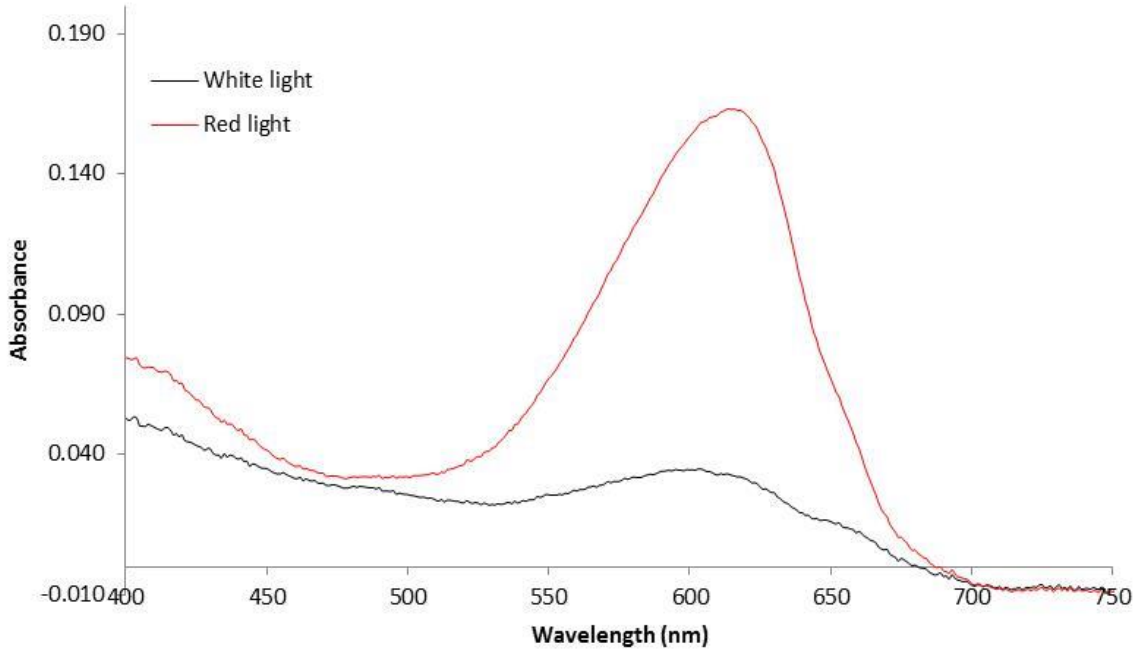

Figure 4.9. Individual (a) and mean (b) phycocyanin absorbance peaks for leached samples cultured under red and white light.

Table 4.2. Mean (± standard deviation) phycocyanin concentration, yield and purity for solutions containing leached and extracted phycocyanin (through standard sonication method) in samples cultured under red (1R) and white light (1W).

	Leached		Extracted	
	White light	Red light	White light	Red light
Phycocyanin concentration (mg/mL)	0.005 (+/- 0.002)	0.025 (+/- 0.011)	0.013 (+/- 0.001)	0.031 (+/- 0.003)
Yield (mg/g)	0.167 (+/- 0.079)	0.771 (+/- 0.349)	9.17 (+/- 1.414)	18.04 (+/- 4.986)
Purity	0.206 (+/- 0.077)	0.627 (+/- 0.259)	0.4 (+/- 0.044)	0.55 (+/- 0.062)

The variance in the leached phycocyanin concentrations in the samples cultured under red light was much higher ($\sigma^2 = 1.1 \times 10^4$) than in the samples cultured under white light ($\sigma^2 = 3 \times 10^7$), which can be seen in Figure 4.9. The leached phycocyanin concentration and yield from the red light culture were, respectively, 400 % and 362 % higher than the white light culture (Table 4.2). In comparison, the extracted phycocyanin concentration and yield showed a respective 139 % and 97 % increase under red light. The ratios of extracted phycocyanin yield to leached phycocyanin yield for biomass produced under red light was 31, significantly lower when compared with the ratio of 72 under white light (p=0.0001*** using a Two-tailed un-paired T-test with Welch's Correction) This indicates that a higher amount of phycocyanin leached from the biomass cultured under red light, compared with white light-cultured biomass, which cannot be explained by the difference in actual phycocyanin contained within the biomass. Hence, the stronger blue colour observed in the leached red light samples was not a direct result of the increased phycocyanin content, but rather caused by increased leaching properties of the red light produced biomass.

4.3.5 Other observations

During batch 6R, autoflocculating properties of the culture were observed from around day 7 (Figure 4.10). Microscopical inspection revealed small crystals on the *Arthrospira* filaments in the auto-flocculating culture which were absent in the culture of batch 5R (Figure 4.11).

Figure 4.10. Photograph of samples from cultures 5R and 6R.The culture from batch 6R showed auto-flocculating properties (right) unlike the culture of batch 5R (left).

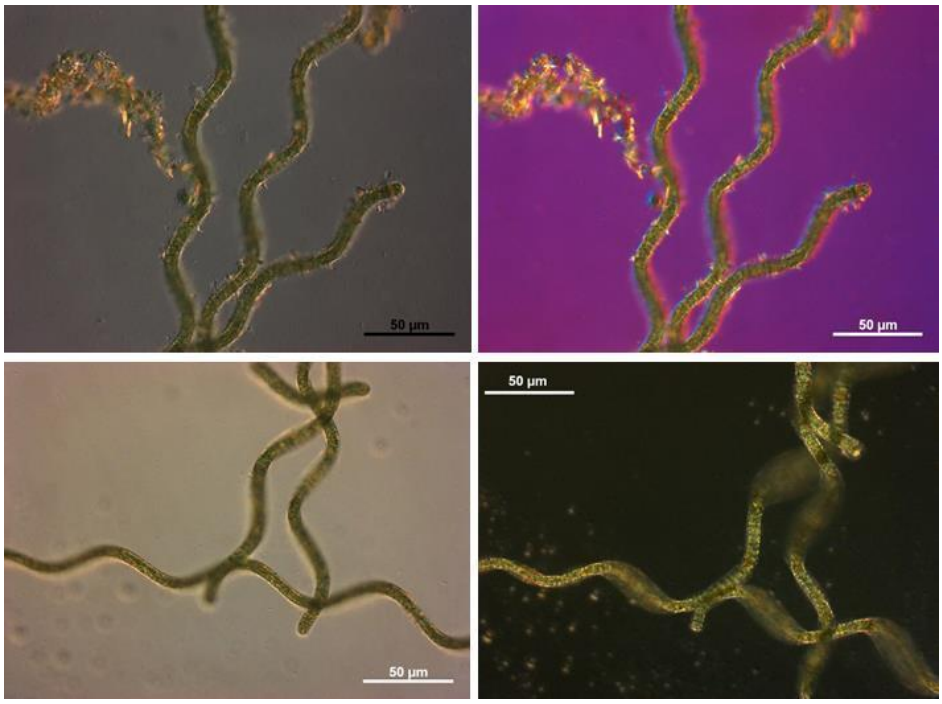

Figure 4.11. Microscope images of *Arthrospira* from batches 6R (top) and 5R (bottom). Top left image was taken using a lambda plate filter.

4.3.6 Microbial population

Investigation into the population in the culture over time in the batches through llumina sequencing of the 16S ribosomal RNA gene revealed *Arthrospira* was the dominant species throughout the batches along with a strong presence of *Muricauda* and *Halomonous*, both halophilic bacteria (Figure 4.12). *Halomonas* is most noticeably abundant in red runs 1R and 2R and becomes less abundant in subsequent batches cultured under red light.

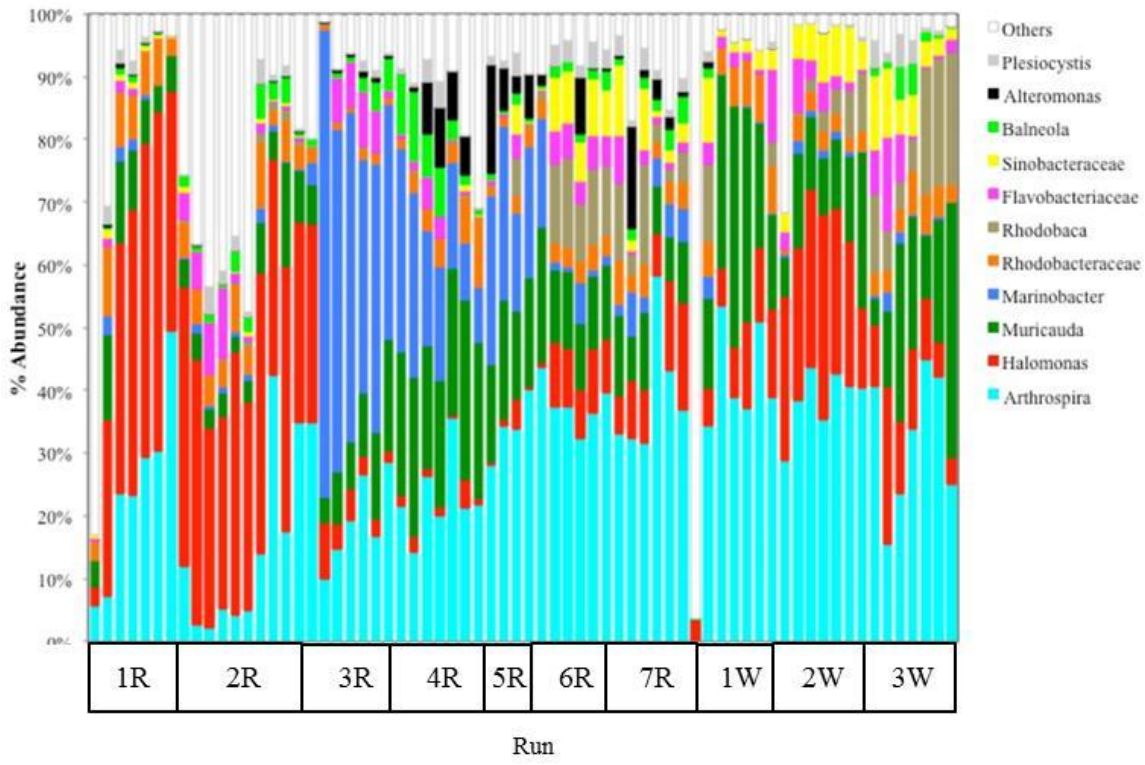

Figure 4.12. Change in microbial community composition over the batches presenting abundance of 11 most abundant species detected. Low concentration of DNA obtained in samples 1-3 in batch 5R and samples 1-2 in batch 6R means data could not be obtained for these samples.

In some batches there is noticeably a high amount of low-abundance species on inoculation, when the culture is at its lowest density. This can be seen as a high percentage of other bacteria ('others') in the first sample 1R, 3R, 1W and 2W. *Roseovarius* (*Roseobacter*), a bacterium found in saltwater was seen in low abundance under red but not under white light. In Run 3R *Marinobacter* quickly becomes abundant in the batch and this abundance of *Marinobacter* persists through subsequent batches 4R and 5R until batch 6R where *Marinobacter* is again in low abundance. In the red batches the presence of contaminant bacteria is at its lowest abundance in batches 6R and 7R indicating settling down of the system to a relatively stable microbial community. There is an abundance of *Rhodobaca* in the highest phycocyanin yielding batches 6R and 7R at levels not seen in earlier red batches. This *Rhodobaca* is also present abundantly in batch 2W and 3W cultured under white light. There is no obvious difference in the microbial communities of batch 5R compared with batch 6R, where autoflocculating properties of *Arthrospira* were observed. There is a higher diversity of species present under red light compared with white. The presence of *Alteromonas* in the majority of red batches, and abundantly in the later red batches 4-7R is not seen under white light.

4.4 Discussion

4.4.1 Main findings

Carotenoid and Chl*a* yield was 10 % and 7 % higher respectively, but not significantly higher, under red light compared with white light; however, without any significant differences or obvious trends, it is difficult to speculate on such data. In all batches the carotenoid to Chl*a* ratio remained constant demonstrating no obvious significant nutrient limitation and associated effects. There was a positive correlation between phycocyanin and Chl*a* concentration; however, such effects did not contribute significantly to the increase in phycocyanin yield observed under red light in Chapter 3. A blueshift in the second Chl*a* peak (~662 nm) in the spectra of the extracts from those batches cultured under white light was also observable. Mass spectrometry analysis revealed differences in common *m/z* peaks of biomass cultured under the different light conditions. Common peaks *m/z* 5681, *m/z* 4389 and *m/z* 2800 were higher under white light, while common peaks *m/z* 7767, *m/z* 9733 and *m/z* 9863 were higher in biomass cultured under red light, with a peak *m/z* 5157 present under white light, but absent under red light. These differences in observed mass spectra and common peaks suggests changes in protein expression during culturing under the two light sources.

When suspended in water, phycocyanin leaches more efficiently from *Arthrospira* biomass cultured under red light compared with white, and results indicated a significant difference in leaching properties of the cells caused by culturing under red light.

Autoflocculation properties were also observed in batch 6R, one of the later batches cultured under red light, which looked to be caused by a possible build-up of extracellular polysaccharides. These properties disappeared in the final batch 7R, suggesting such observations were likely not caused by red-light induced stress, through continued culturing and acclimation as was initially hypothesised.

4.4.2 Pigments

There was a positive correlation between phycocyanin and Chl*a* concentration in the biomass. A similar relationship also existed in the size and ratio of the Chl*a* and phycocyanin peaks in the extract absorbance spectra in batches 6R and 7R. For example, the spectra for 7R, which had the highest phycocyanin absorbance peak, also had the highest first Chl*a* peak as well as the most significant trough at around 530 nm. However, this relationship nor a consistant pattern is demonstrated in all batch spectra. In batches 4R and 5R (batches showing some of

the highest phycocyanin yields), the phycocyanin absorbance peak is relatively low compared with the high Chl*a* peak and trough oberved at 530 nm. A relationship between Chl*a* and phycocyanin absorbance peaks, where both high phycocyanin and Chl*a* absorbance peaks are observed in the spectra, can suggest that light limitation was a factor in increasing levels of phycocyanin. It is a known response that in light-limiting conditions, microalgae and cyanobacteria increase their levels of chlorophyll, and some other pigments, to enable the capture of light for essential photosynthetic processes (Danesi, 2004, Marquez-Rocha, 1999).

It is also known that Chl*a* can decrease under high light intensities, as a feature of the photoprotective mechanisms in photoautotrophs (Richmond, 2004, Kumar, 2011b). It is possible that the white light may have been more photodamaging than the red light. This is a plausible theory given the physics behind light wavelength and energy. A longer wavelength photon carries less energy than a photon at a shorter wavelength according to Planks Law (Equation 4.5):

Equation 4.5: $\text{Energy} = \frac{hc}{\lambda}$

Where h is Plank's constant (6.63×10^{-34} joules per second) and c is constant light velocity (3×10^{8} meters per second), demonstrating wavelength is inverse to energy.

The higher energy of photons in the shorter wavelengths causing photodamage may have contributed to lower levels of pigments in those batches cultured under white light, including a lower yield of phycocyanin and Chl*a*. However, this would not explain the decrease in carotenoids under white light as *Arthrospira* are known to increase carotenoid production under certain conditions of stress such as nitrogen starvation, high salinity (Sujatha and Nagarajan, 2013) and high light intensity (Olaizola and Duerr, 1990). As previously mentioned, light limitation under red light can also contribute to increased phycocyanin levels. Photons in longer wavelengths of light (such as in the red region of the electromagnetic spectrum) are of lower energy, meaning photon flux is lower under red light compared with white light for photosynthesis. This could prompt a physiological reaction of increased pigment production (both chlorophyll and phycocyanin) under red light. The positive correlation between phycocyanin and Chl*a* concentration in the biomass demonstrates that such effects were present, although it is difficult to say whether such affects result from photoinhibition under white light or light limitation under red light. Even so, such described effects were shown not to contribute significantly to the increase in phycocyanin yield in *Arthrospira* under red light.

If Chl*a* level increase (or decrease) matched the increase (or decrease) in phycocyanin, then the phycocyanin:Chl*a* ratios for batches cultured under both red and white light should be constant. However, the phycocyanin:Chl*a* ratio under red light is consistently higher, demonstrating that although Chl*a* concentration under red light was typically higher, the change in Chl*a* was not proportional to phycocyanin level. Therefore, the increases in phycocyanin under red light observed during the experiments were not caused by the effects of light limitation nor photoinhibition.

4.4.3 MS analysis

Whole-cell MALDI-TOF-MS has shown to be a valuable tool for the identification of microalgal strains (Emami, 2015, Barbano, 2015), demonstrating stable strain-specific fingerprints, even under variable conditions of culture age, growth-stage and microbial contamination. This tool was extended into the studies of this thesis for use in the analysis of *Arthrospira* whole-cell spectra and comparison under the two light conditions. Although spectra from the same strains are considered largely unaffected by growth conditions, as dominant peaks represent ribosomal and house-keeping proteins which generally do not change (Pineda, 2003, Teramoto, 2007), it is thought that large condition-induced proteome changes can be captured in spectra (Valentine, 2005, Salaun, 2010).

Differences in the spectral fingerprints of the biomass cultured under the two light conditions demonstrated significant variations in the proteome. The main differences were in the intensity of dominant peaks, revealing increased and decreased expression levels of regular proteins. There was also a single pronounced peak present under white light, but absent under red light, suggesting that expression of a particular protein ceased under red light. Although comment cannot be made on the identity of specific proteins, substantial changes in the *Arthrospira* proteome under λ_{max} 680 nm light are determined.

4.4.4 Auto-flocculation characteristics

The auto-flocculating properties of batch 6R were initially thought to be caused through continual environmental ‘stresses’ during acclimation to red light such as an increase in the extracellular polysaccharide layer which increased ‘clumping’ of the filaments and the stickiness capturing crystalised components of the media. However, auto-flocculation was not observed in later batches during red light culture. Auto-flocculation properties of *Arthrospira* have been associated with increased pH, causing salt ions to precipitate together with the biomass (Bux, 2013). Specifically noted for these affects are positively charged magnesium,

phosphate, calcium and carbonate ions, which are typically present in the culture medium and interact with negatively charged cell surfaces at a pH of above 10.5. As the pH of the auto-flocculating batch (6R) was typically lower than the other batches cultured under red light, high pH is unlikely to have been a cause of the auto-flocculation observed. Flocculation has also been observed by pH decrease (Liu, 2014), although not in *Arthrospira* cultures.

Additionally, there is another type of flocculation observed in *Arthrospira* cultures: bio-flocculation, mediated by extracellular biopolymers produced by the cyanobacterial cells when under stress. This has been observed under conditions of phosphorus limitation and has been related to increased carbohydrate content and decreased Chl*a* levels in *Arthrospira* (Markou, 2012). It is feasible that accumulation of extracellular polymeric substances in batch 6R caused the flocculation effects, as salt crystals were observed to coat the trichomes which would indicate a sticky substance excreted by the cells. However, there is little definitive indication of why flocculation only occurred in this particular batch. The only unique feature about batch 6R was the lower average pH, making it difficult to speculate whether the observation was pH induced auto-flocculation or stress induced bio-flocculation, or perhaps a result of bacterial infection

4.4.5 Leaching

It is known that phycocyanin will leach from *Arthrospira* biomass (either wet or dry) when suspended in distilled water (Siegelman, 1978). This water-extraction process can be used for *Arthrospira* biomass, but is slow and is therefore not applicable to large scale production (Sarada, 1999). Although phycocyanin is relatively stable across a pH range of 5-7.5 at room temperature (Sarada, 1999), the protein-pigment complexes can destabilise. This destabilisation is a consequence of the high chemical reactivity of phycocyanin, which is a free-radical scavenger, and the therapeutic benefits of this activity have been widely reported (Romay, 2003, Bhat and Madyastha, 2000). Free-radical scavenging is a result of the covalently linked phycocyanobilin chromophore. Chromophores are also well known producers of ROS chain reactions, as a result of their chemical fluorescent properties, which enables them to participate in free radical reactions (Jacobson, 2008). Such ROS-producing activity was demonstrated in Pardhasaradhi et al. (2003), where phycocyanin was considered as a potential chemotherapeutic agent showing apoptosis-inducing activity against tumour cells through ROS production. Phycocyanin can switch from ground to excited high energy states during photosynthetic processes, which normally occurs in a controlled environment inside intact cells

(Halliwell, 2006, Gratão, 2005, Foyer and Noctor, 2005). In the event of a small amount of cell death and release of phycocyanin into the culture, phycocyanin in an excited energy state can cause uncontrollable damage through ROS generation in the culture. This reaction results in the production of singlet oxygen, which can begin a chain reaction producing ROS (various free radicals), which can further interact with other biological molecules resulting in cellular damage (Das and Roychoudhury, 2014, Gill and Tuteja, 2010, Mittler, 2002). This chemistry means phycocyanin is susceptible to photodamage and sensitive to heat and will precipitate or bleach as a result of changes in the protein structure and denaturation (Fukui, 2004). Although there are many factors that can affect the yield and quality of pigment obtained during extraction, water-extraction is known as a consistent method when used on a small laboratory scale; therefore, the high variability in phycocyanin concentrations observed during the leaching experiments is unexpected, and such variability cannot be explained through pigment degradation as treatment of the samples was consistent.

Despite the variability in the dataset, the ratio of extracted : leached phycocyanin yield from biomass under red light was significantly different to that of the ratio of extracted : leached phycocyanin yield from biomass under white light. This indicates increased leaching characteristics of *Arthrospira* biomass when cultured under λ_{max} 680 nm red light. Such characteristics may come about through physiological changes in the cell structures, such as a more porous cell wall. Such changes could be beneficial for downstream processing.

4.4.7 Changes in microbial community

The high abundance of contaminating *Marinobacter* in run 3R relates to the poor growth of *Arthrospira* observed in this batch. This poor growth was originally thought to be the result of reversed acclimation after storage of the culture under different light conditions before being used as an inoculant. During the longer-than-normal storage period between batches 2R and 3R, *Marinobacter* looks to have taken a hold. The poor growth seen in 3R may therefore be due to the bacterial infection with *Marinobacter*, or perhaps a combination of reversed acclimation and infection. *Marinobacter* is typically found with a range of microalgae, and would likely have been present in the *Arthrospira* culture obtained from CCMP. *Marinobacter* has previously been noted in algae-bacteria mutually beneficial interactions including increasing iron bioavailability (Amin, 2009). *Muricauda* and *Halomonous*, both of which had a strong presence in the *Arthrospira* cultures, are also widely found in microalgae cultures, with *Muricauda* and *Halomonous* seen in cultures of filamentous cyanobacteria including *Arthrospira* (Choi, 2008, Hube, 2009). Additionally, *Halomonous* has notable synergistic

effects in microalgae cultures in providing vitamin B12 (Croft, 2005). The presence of *Roseovarius* and *Rhodobaca* have also been observed before in filamentous marine cyanobacteria cultures (Hube, 2009). *Roseovarius* and *Rhodobaca* are producers of bacteriochlorophyll *a*, a pigment which absorbs light at around 770 nm, meaning they can derive energy from light in this region of the spectrum (Buchan, 2005, Takaichi, 2001, Milford, 2000, Biebl, 2005). Although *Rhodobaca* abundance was highest under red light in the two highest phycocyanin yielding batches, *Rhodobaca* was also present under white light. The curious presence of *Roseovarius* only in cultures exposed to red light and the presence of *Alteromonas* also predominantly in the later batches cultured under red light raises the questions as to the selection effects of culturing under particular wavelengths of light on not only the microorganism of interest (in this case *Arthrospira*), but also any other microorganisms present in the microbial community. This is particularly important as cultures of microalgae/cyanobacteria are rarely axenic and usually contain a community of other microorganisms, which can be known to have mutually beneficial effects on growth. This highlights the importance of being aware of potential changes in the rest of the microbial community, and the unintended promotion of growth of potentially harmful species under particular conditions. This is something to particularly be aware of if microalgae will be used in products for human consumption.

Chapter 5. Application of Long Wavelength Red Light Emitting Diodes to Industrial Photobioreactor Systems

5.1 Introduction

5.1.1 The Light Emitting Diode (LED)

LEDs have seen increasing use over the past few decades because of their greater power-to-light efficiency compared with incandescent bulbs; where uptake has been driven by greener environmental legislation including new building efficiency regulations (McKinsey and Company, 2012). LEDs require at least 75 % less energy than incandescent bulbs to produce the same light levels (U.S. Department of Energy, 2013) giving out less waste heat. LEDs also have a 25-times longer working life compared with incandescent bulbs (ENERGY.GOV Energy Saver), so substantial cost-benefits are delivered in a number of ways; however, the initial cost or capital expenditure (CAPEX) of LED systems can offset these financial benefits. Even so, these features not only make LEDs attractive in domestic and commercial lighting systems, but also for application in artificially illuminated photobioreactors (PBRs).

LEDs are comprised of a light-emitting chip (Figure 5.1a) which is a p-n junction formed from two types of semiconductor materials (positive p-type and negative n-type) in contact (Khanna, 2014). Current flows from the p-type anode to the n-side cathode and in the electron-depleted junction, electrons meet electron holes and fall into a lower energy level thereby releasing energy as photons in the phenomenon of electroluminescence (Figure 5.1b).

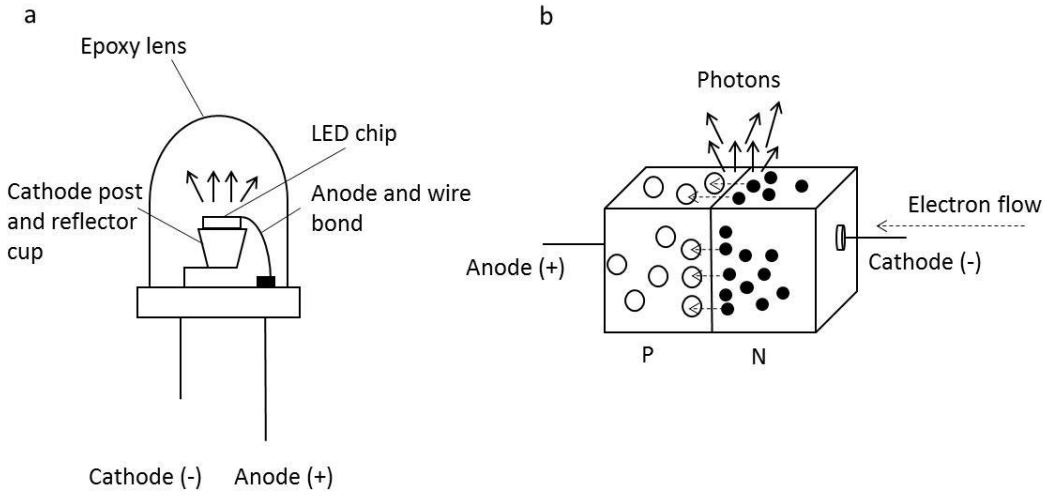

Figure 5.1. Schematic of a typical LED (a) and p-n junction (b).

LEDs emitting different wavelengths of light from ultra violet (UV) to infra-red (IR) are produced using various semi-conductor materials and compositions. LEDs emitting UV (250-360 nm) are typically produced using gallium nitrite (GaN) or aluminum gallium nitrite (AlGaN) semi-conductor materials (Dahl, 2008). Wavelengths in the visible part of the spectrum (395-645 nm) from blue-green to yellow-red are typically produced using indium gallium nitride (InGaN) and aluminium gallium indium phosphide (AlGaInP) respectively. LEDs emitting deep red – near infra-red (660-900 nm), as used in this thesis, are produced using aluminium gallium arsenide (AlGaAs) or gallium arsenide (GaAs) semi-conductor materials (Sparavigna, 2014). White LEDs are produced using blue LEDs combined with a phosphor which broadens the emission spectrum (Mueller-Mach, 2002).

Pre-dating LEDs, fluorescent lighting has been used as artificial lighting sources for microalgae cultivation, as the wavelengths of light emitted closely reflect that of natural sunlight (Carvalho, 2011). Fluorescent tubes are manufactured using glass containing mercury vapour and an inert gas (typically argon) at low pressure. The mercury vapour ionizes on application of an electric current and photons of UV wavelength are emitted when mercury electrons drop back down to ground state. UV is converted to visible light with a phosphor coating on the inner walls of the tube (Carvalho, 2011). Fluorescent tubes have a lifetime of around 10,000 hours compared with the 35,000-50,000 hours lifetime of an LED (Carvalho, 2011) and the light output from a fluorescent tube would expect to depreciate by 20 % over its lifetime, mainly through degradation of the phosphor coating and build up light-absorbing deposits in the tubes (Azevedo, 2009). Luminous efficiency is similar to that of LEDs at around 35-100 lm/W (dependent on operating power) (Carvalho, 2011), as is the whole system efficiency as ballasts/drivers and fixtures required in both fluorescence and LED systems have similar efficiencies (typically 65-95 % for the ballast/driver and 40-95 % for the fixture) (Azevedo, 2009). LEDs can achieve a higher light output (W/m^2) and an LED lens can be cheaply modified and manufactured to direct light into a PBR. Additionally, fluorescent tubes contain environmentally-hazardous mercury and are overall a less ‘green’ option than LEDs (Scholand, 2012). Overall, LED systems can be two to ten times as expensive as fluorescent tubes (Carvalho, 2011); however the price of LED lighting systems is falling rapidly. This is as a result of the falling cost of LEDs or, more accurately, the per-lumen price of LEDs known as Haitz’s Law (Haitz, 1999, Haitz and Tsao, 2011), which falls by around 25 % every decade, and also general market trends where new technology price falls as production volume increases.

Notwithstanding the benefits of LEDs as mentioned above, there are in fact other important reasons why LEDs are most attractive for PBR artificial lighting compared with fluorescent tubes. LEDs, because of their small size compared with fluorescent tubing, can be produced in many lamp configuration geometries to fit with various PBR designs and therefore offer much more design flexibility (Glemser, 2015). More importantly, LEDs can produce narrow wavelengths (20-30 nm bandwidth) of light. As studies of photosynthetic efficiency and microalgae productivity and product yield reveal wavelengths or mixtures of wavelengths that can be used to increase process efficiency, this knowledge can be applied to optimise commercial systems using LED lighting. This has already been seen with commonly available arrays of red and blue LEDs providing specific wavelengths absorbed by microalgae (Darko, 2014, Sabzalian, 2014, Illumitex, 2015). Such narrow bandwidths are not achievable with fluorescent tubes without the use of a filter, where the majority of light emitted would be absorbed and wasted.

Although ideally the use of natural illumination for the production of microalgae is preferred, the use of artificial illumination offers a higher level of process control in a closed production system and opens up industry based on microalgae production in countries which experience low-levels of sunlight. Despite numerous small-scale studies, there is a lack of independently verifiable information on the application of LED illumination in commercial algae cultivation systems. The cost of artificial LED illumination rather than sunlight is calculated to double the production cost of biomass in closed PBR systems (Blanken, 2013), which can be viable if producing high value products. Expected extra operational expenditure (OPEX) on electricity of \$19.3 per kg dry weight (kg DW^{-1}) and CAPEX on LEDs of \$7.4 kg DW^{-1} see a total CAPEX/OPEX of \$26.7 kg DW^{-1} added to any closed PBR system (Blanken et al., 2013). With future developments in LED technology, improving efficiency and reducing manufacturing costs, the CAPEX/OPEX for LED PBR illumination could fall by 60 % to \$16 kg DW^{-1} (Blanken, 2013), improving the economics of artificially illuminated closed PBRs.

The narrow and higher wavelength red LEDs used in the experiments presented in this thesis are costly in comparison to standard red or white LEDs as the lack of high-volume applications and demand means they are not widely commercially available. However, applications using these specific wavelength LEDs are being developed, examples include; anti-aging light treatment skin therapy (λ_{max} 680 nm) (Viravaidya-Pasuwat, 2014), and surface wound healing

(for comprehensive review see (Chaves, 2014). With an increasing number of products now on the market, the cost of λ_{max} 680 nm LEDs should come down.

5.1.2 Heating effects of long wavelength LEDs

All bulbs release heat through inefficiencies in the conversion of power to light. Although the heat generated from a bulb is dependent on numerous factors including wavelength spectrum emitted and fittings, the heat released from a bulb can be estimated using knowledge of the efficiency, where power not converted to light (the inefficiency) is assumed to be lost as heat. Table 5.1 shows the heat output of commonly used light sources calculated from comparative data generated in a study by Khan and Abas (2011).

Table 5.1. Heat output of commonly used light sources

Bulb	**Power (W)**	**Mean Efficiency (%)**	**Heat output (W)**
Incandescent	100	2.25	97.75
Fluorescent tube	18	12	15.84
Compact Fluorescent	23	9.5	20.82
LED	15	21	11.85

*Light output for each bulb is 1692-1702 Lumens. Heat output (W) is calculated as *Power (W) – (Power (W) x Efficiency (%) as a fraction)*.

From Table 5.1 incandescent bulbs consume the most energy and are the most inefficient, with nearly 98 % of the energy released as heat, therefore producing the most heat in comparison to other light sources. The low energy consumption of fluorescent and compact fluorescent lighting, even with a relatively low efficiency means heat generated is over 400 % less than that of an incandescent bulb. Although halogen lamps were not included in the study by Khan and Abas, halogen lamps are known to generate a considerable amount of heat, sometimes 4-times that of an incandescent bulb (Consumer Energy Centre, 2017). The low energy consumption of LEDs combined with their higher efficiency compared with other light sources results in LEDs having the lowest heat output of the commonly used light sources.

The wavelength of light is inversely proportional to energy according to Planks Law, as discussed in Chapter 4. Accordingly, longer wavelength LEDs emit light (photons) at lower

energy. A consequence of lower energy photons is a heating effect. This is illustrated by electrical heaters and toasters utilising infra-red light. The heating effect is produced through radiation. Lower energy photons of longer wavelengths cannot penetrate materials as much as higher energy photons; they move shorter distances through materials before they are absorbed. Therefore, absorption of energy and the vibration of molecules within materials (heating) is more efficient with shorter wavelengths of light.

If long wavelength LEDs were applied at larger-scale in PBRs, heating effects may have to be considered. Experiments in this chapter begin to assess the extent of heating problems caused by the use of longer wavelength LEDs.

5.2 Experimental Details and Method

5.2.1 Heating effect of long wavelength LEDs

The temperature of 2.75 L of tap water in the STPBR was measured along with the external air temperature in 10 minute intervals over stepped increases in the power/ intensity of λ_{max} 680 nm LEDs (for details of LEDs see Chapter 3). Light intensity was controlled through increasing percentage power from the driver transformer to the LED using the Iris Parallel Bioprocess Control Software. At 8-80 % power, light intensity to the culture would range linearly from 44-346 µmol m^{-2} s^{-1}. Water temperature was measured by the STPBR temperature probe. External air temperature was monitored externally using Tinytag Aquatic 2 data loggers (Gemini Data Loggers Ltd, West Sussex). The fluid in the STPBR was agitated at 200 rpm, and pH control, aeration and temperature control were turned off. LED light intensity was increased through increasing LED operating power in daily increments of 8 % from 8 % to 80 % power over 10 days. The difference between the STPBR water temperature and external air temperature was calculated by subtracting the air from water temperature to calculate the increase in temperature caused by the heating effect of the LEDs at different power levels. Prior to the difference calculation, temperature values for the external air temperature were off-set by +100 minutes to account for a slower response in air compared with water. The mean difference was calculated from a minimum of 133 temperature readings over 1330 minutes and used as the temperature increase at LED power/illumination levels. Error was calculated as standard deviation of the mean differences.

5.2.2 Dissolved oxygen probes

Dissolved oxygen (DO) data was collected in the batch experiments of Chapters 3 and 4. DO was recorded every 10 minutes by a DO probe (Finesse, Switzerland) as a percentage relative to starting DO. PreSens equipment (Precision Sensing GmbH, Germany) was used in Batch 2W as a secondary method of DO monitoring alongside the standard Finesse DO probe. The PreSens detector spot was glued to the inside of the vessel wall 3 cm below the calculated medium level, using a small amount of SG-1 silicone glue (Precision Sensing GmbH, Germany), and allowed to dry for 12 hours. The glass vessel was then filled with medium and sterilised as described in Chapter 3 3.2.1 with the PreSens spot in place. Before inoculation, the PreSens optical fibre was aligned with the spot and strapped in place using a Velcro fastener (Adaptor for Round Containments or ARC as provided) with tape for extra security (Figure 5.2a). Data from the PreSens optical fibre was recorded using an OXY-4 mini data logger (Precision Sensing GmbH, Germany) and OXY-4 mini Software version 2.30FB (Figure 5.2b). The PreSens optical fibre was carefully fed through the gap in the top of the LED jacket. PreSens data was filtered using the Moving Average Filter as described in Chapter 4 at Power 100 (using 100 data points for average calculation) in Microsoft Excel 2007.

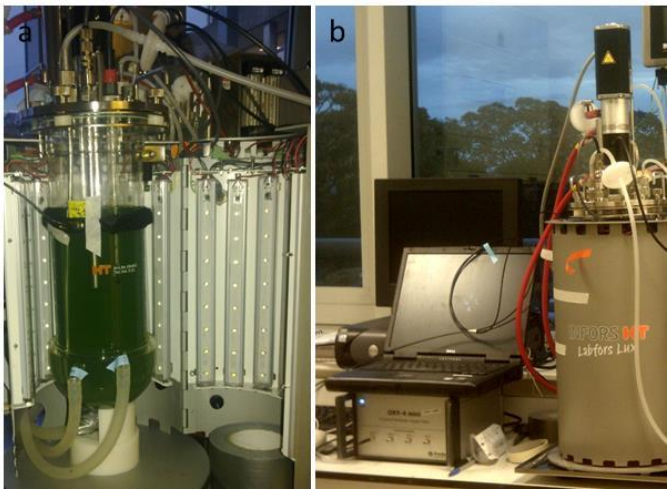

Figure 5.2. PreSens DO monitoring set-up of optical fibre (a) and data logger with STPBR system (b).

5.3 Results

5.3.1 Heating effect of long wavelength LEDs

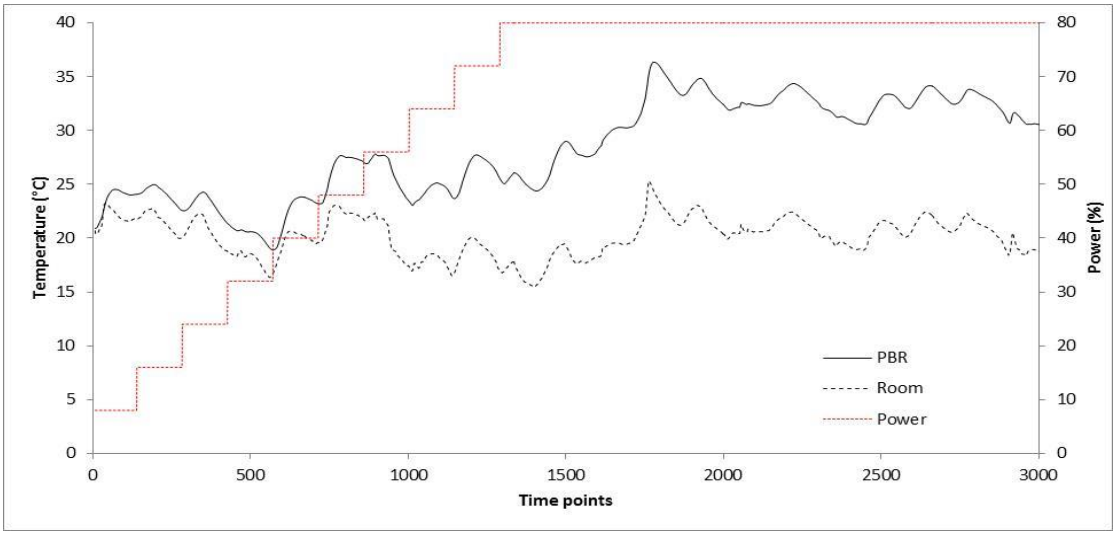

Figure 5.3. Temperature of STPBR (internal) and room (external) over increasing LED power levels. Noise is representative of normal diurnal temperature fluctuations. One time point represents 10 minutes, the interval for which temperature was recorded.

In Figure 5.3, power levels above 25 % led to an increasing deviation between STPBR and room temperature, indicating a heating effect caused by the LEDs. When the temperature difference was calculated (Figure 5.4) the heating effect became clear, with an approximate 11 ˚C rise when LEDs were operated at 80 % power (346 µmol m^{-2} s^{-1} light intensity).

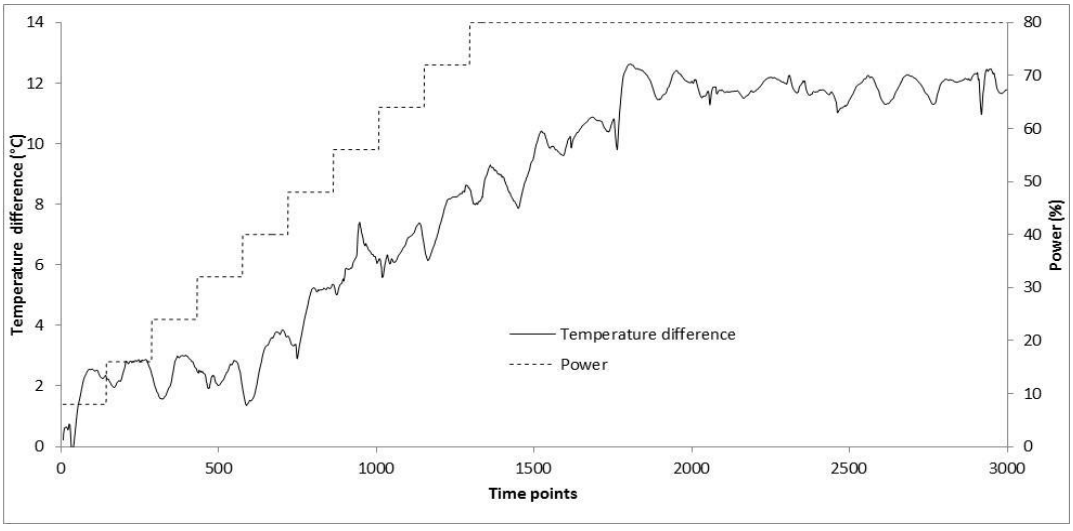

Figure 5.4. Temperature difference between STPBR and room plotted against LED power level. One time point represents 10 minutes, the interval for which temperature was recorded.

It is difficult to pick out accurate temperature differences from the noisy temperature data, as seen in Figure 5.3 and Figure 5.4. The noise (Figure 5.3), caused by diurnal cycles in temperature, interestingly, is still present in the difference calculations (Figure 5.4), when it would be expected that a simple subtraction should remove diurnal noise, which should occur the same in both STPBR and room temperature traces. Noise is still present when the temperature difference is calculated as there is a slight lag in diurnal temperature cycles in the STPBR (Figure 5.5) and the room. The lag is a result of a slower temperature change in the STPBR as a result of the volume of water with a greater heat capacity than the surrounding air, which takes more energy (and time) to heat and cool.

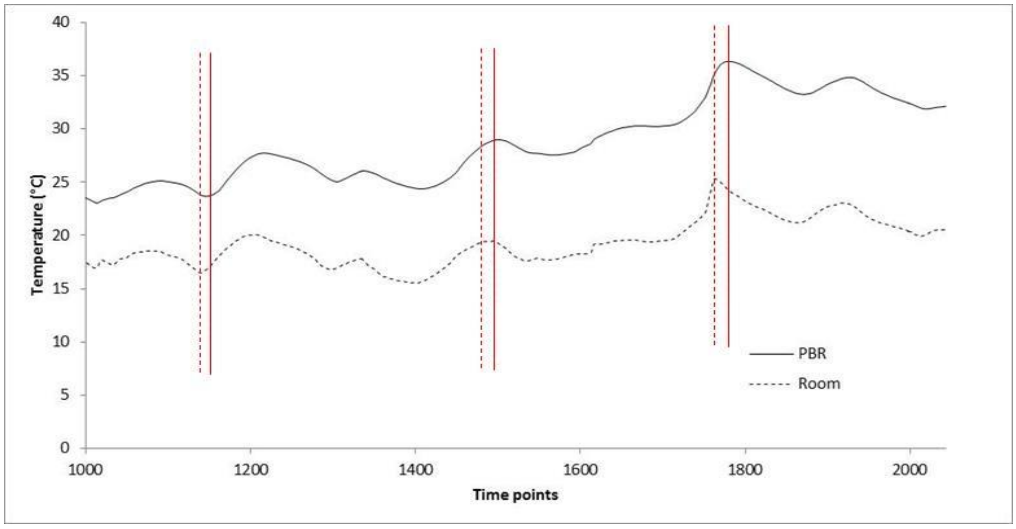

Figure 5.5. STPBR and room temperature readouts over 1000 time points showing response lag in STPBR data to normal diurnal temperature fluctuations compared with room temperature, indicated by red vertical lines. Solid red line shows peak and troughs of room temperature and dotted red line indicates lagged peaks and troughs of STPBR data. One time point represents 10 minutes, the interval for which temperature was recorded.

To reduce the lag and noise in the temperature difference calculations the temperature difference was calculated from room temperature readings offset by 10 time points (100 minutes). The offset value was calculated through selecting 5 numerical differences in peaks and troughs (as in Figure 5.5), and using these value ranges to test the visual difference on the temperature difference curve during different offset values. Offsetting by 100 minutes gave the smoothest temperature difference curve (Figure 5.6) and these offset temperature differences were used to calculate mean temperature difference under the different illumination levels (LED power) (Figure 5.7).

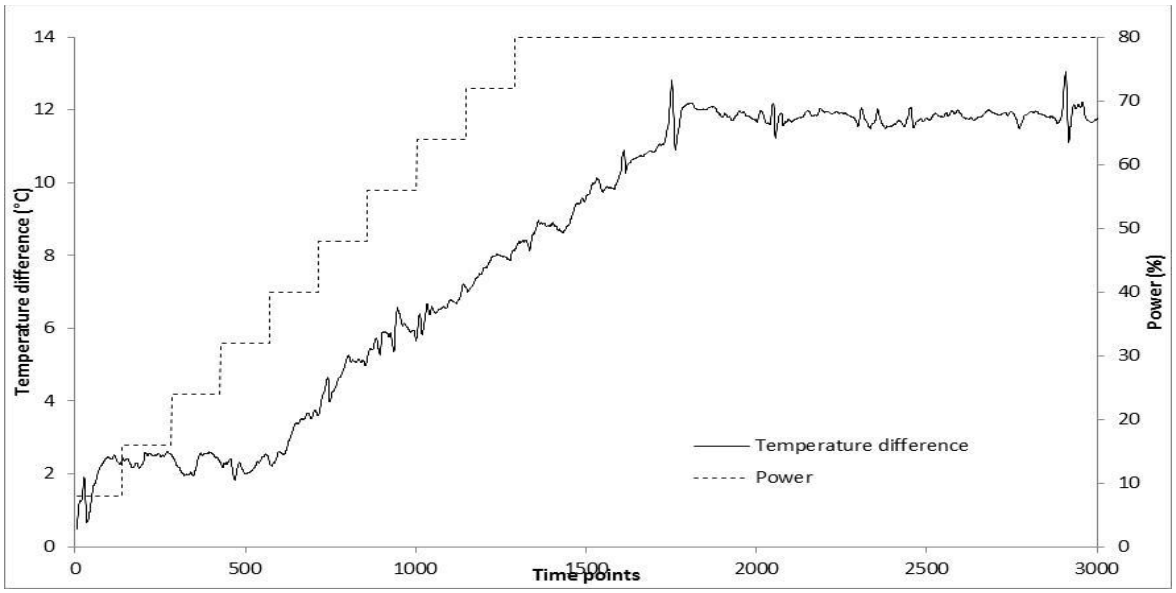

Figure 5.6. Temperature difference of STPBR and room after offset alteration of 100 minutes plotted against LED power. One time point represents 10 minutes, the interval for which temperature was recorded.

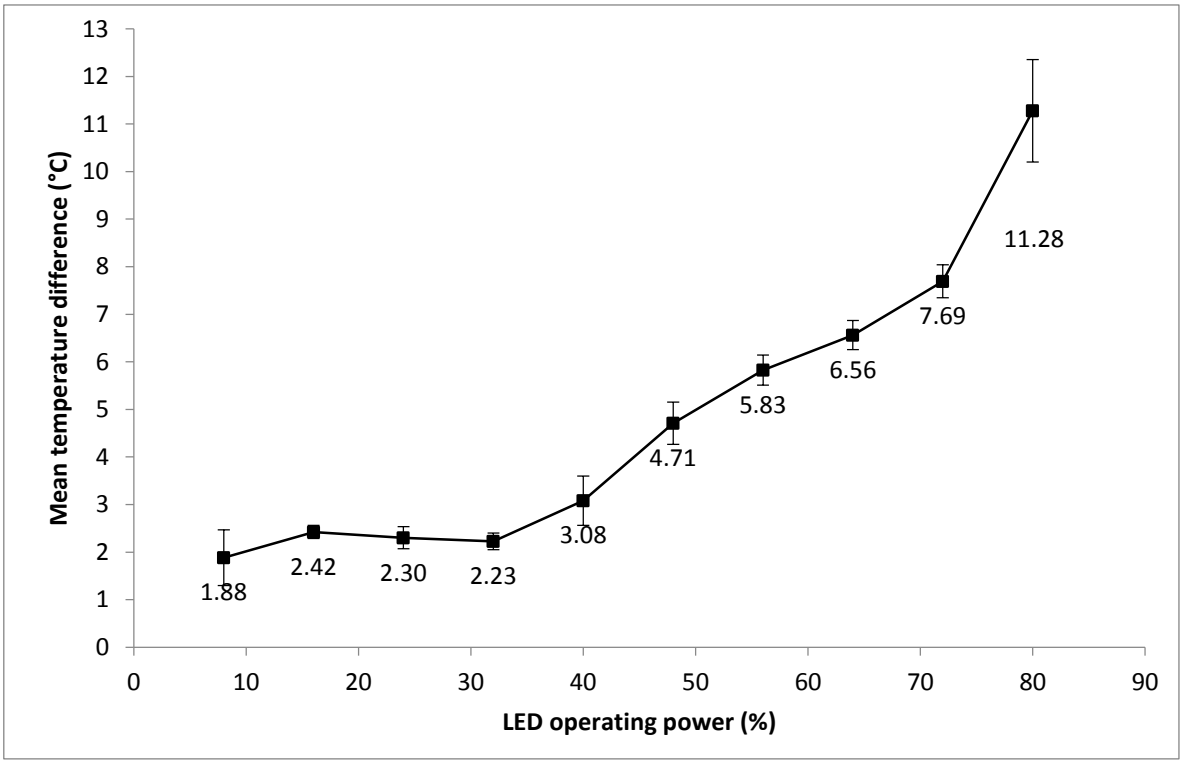

Figure 5.7. Mean temperature increase at LED power levels calculated from a minimum of 133 temperature readings over 1330 minutes. Error bars represent ± 1 standard deviation of the mean.

Operating the LEDs at 80 % power (346 µmol m^{-2} s^{-1} light intensity) increased the temperature of the water in the STPBR by an average 11.11 ˚C. There was a stable 2 ˚C increase in

temperature in the STPBR below 40 % power, indicating that there were likely no significant heating effects operating below 40 % power.

5.3.2 Interference with probe measurements

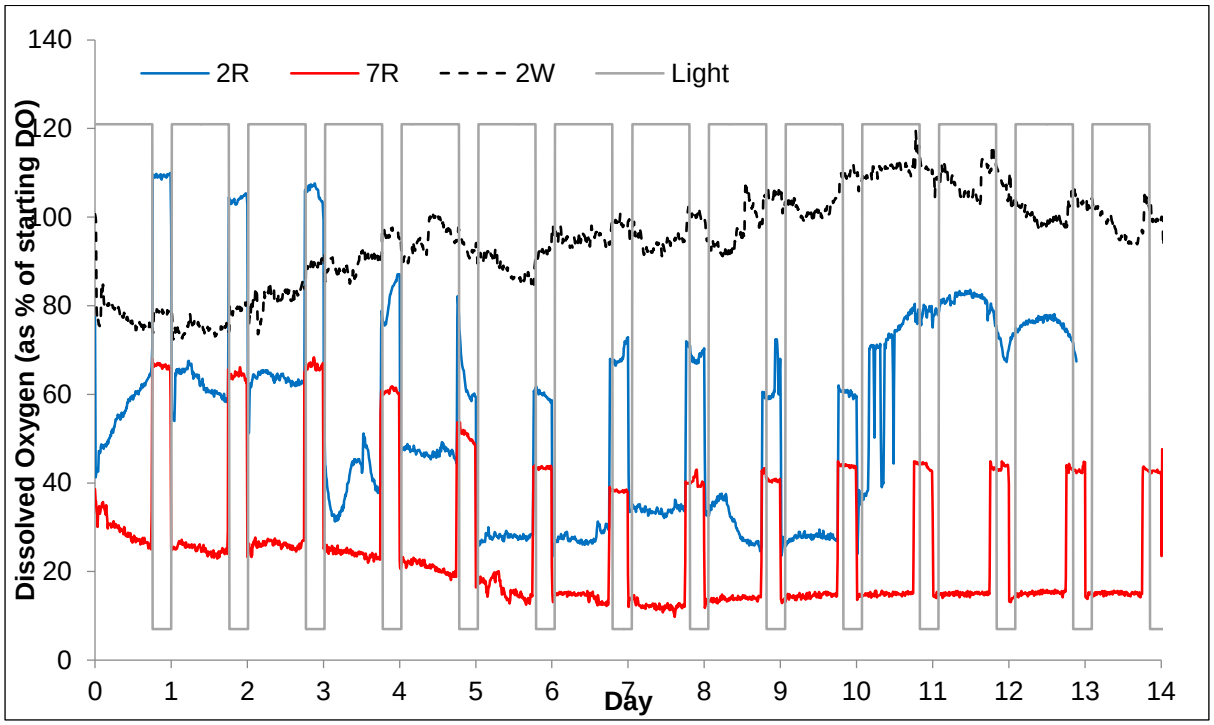

Figure 5.8. Dissolved oxygen (DO) traces of three batches as measured by the Finesse probe shown during illumination and dark periods, demonstrating interference of the red light, but not the white light with DO measurement. DO data was collected in the experiments of Chapter 3 for the 10 *Arthrospira* batches. Data shown in this figure is from batches 2R and 7R which were cultured under red (λ_{max} 680 nm) light and 2W cultured under standard white light. For batch details see Chapter 3 (3.3.2).

In Figure 5.8 the DO of the red light cultures 2R and 7R dropped instantly during illumination periods. This was not observed in white light culture 2W. The data shows the red light causes erroneous readings in the DO probe. Additionally, upon testing a new non-invasive optical DO probe by PreSens - Precision Sensing GmbH (Germany) in the STPBR under white light, again interference during illumination periods was observed creating a lot of noise in comparison to the typical invasive (Finesse) probe used for the experiments (Figure 5.9). No trend could be seen even after filtering.

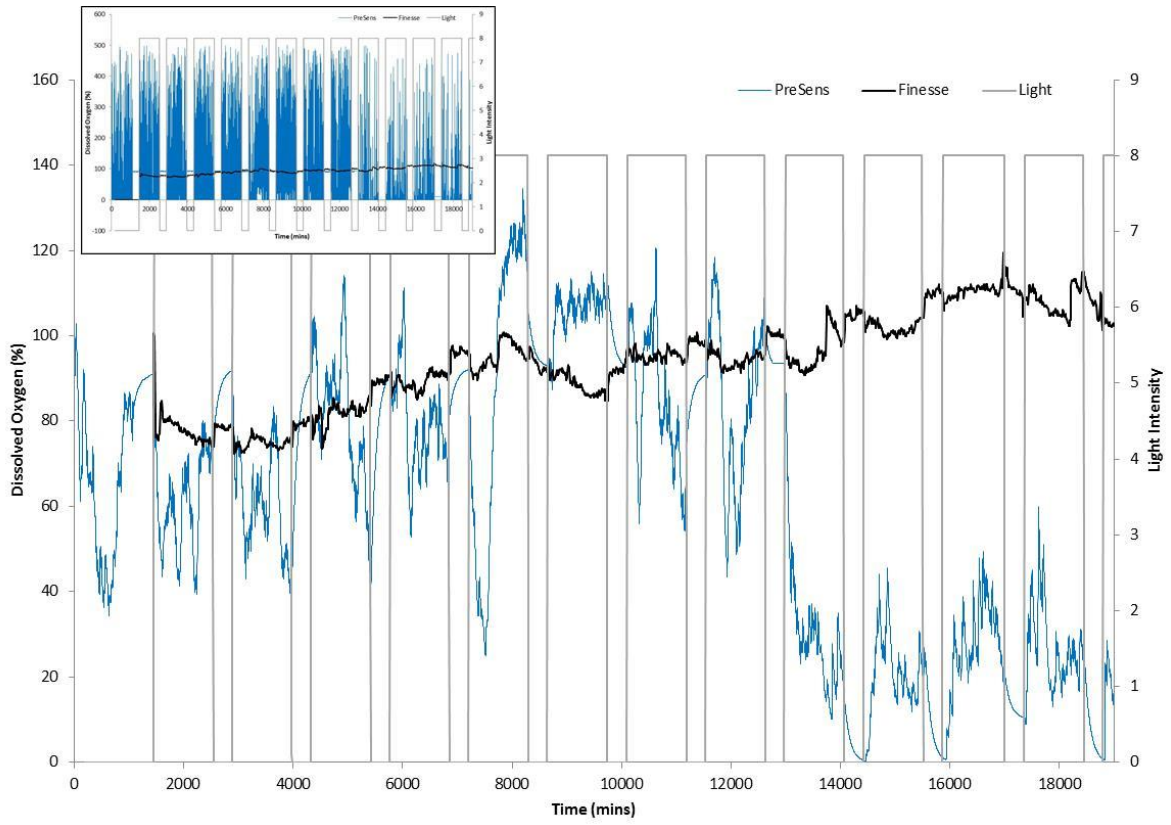

Figure 5.9. Dissolved oxygen levels measured by Finesse standard optical probe and the PreSens non-invasive optical system after filtering. Top left window shows un-filtered PreSens data.

5.4 Discussion

5.4.1 Heating

The use of longer wavelength LEDs in PBR systems will cause heating effects, but only if used at higher power levels (as seen in these experiments above 40 %). Depending on the higher power levels selected, heating effects may only be a few degrees increase in temperature of the culture and therefore unproblematic. The 2 ˚C increase seen below 40% power in the experiment could be caused by the insulating environment provided to the water by the materials of the STPBR (glass vessel plus plastic shell) rather than any heating effects caused by the LEDs. In this case the heating effect at 80 % LED power would be around 9 °C.

Given that the LED powers and intensities used in the Chapters 3 and 4 experiments were 5-times lower than 40 % (the value at which heating effects occur), it is highly probable that long wavelength LEDs may not be used at such intensities/powers and densities industrially to cause problematic heating effects and therefore would not contribute to major additional CAPEX or

OPEX costs for additional cooling requirements. As day-night daily outside temperature variations can be 3-5 °C as seen in these experiments and as UK outside temperatures can vary by around 11.3 °C over the year (Perry and Golding, 2011), any artificially illuminated PBR system should already be built with the capabilities to manage a 10 °C variation in temperature (if the culture is susceptible to temperature changes). Also heating effects of the LEDs may even be beneficial to maintain culture temperature.

Although heating effects on the culture will likely not be an issue, heating is still an issue in the LED itself. Red LEDs (and particularly IR LEDs), for the same reasons explained above, are susceptible to heating. Heating reduces the efficiency and lifetime of the LED (Yanagisawa, 1998, Nelson and Bugbee, 2014), with red LEDs being highly susceptible, sometimes requiring twice as much power at higher temperatures to produce the required light intensity (Azar, 2012). Heating can also change the peak wavelength emission of the LED which is emphasised in red LEDs in comparison to blue and green LEDs, changing by 1.6-2 nm per 10 °C (Chhajed, 2005, Shi, 2011). This problem is most commonly noted in solid state lighting systems where white light made from mixed red, green, and blue LEDs moves from warm white to cool white when red LEDs lose efficiency (Narendran, 2001, Shi, 2011), but should not be problematic in PBRs. Control of LED temperature and maintenance of LED efficiency, particularly for longer red LEDs, is therefore essential in artificially-illuminated industrial PBR systems. A doubling of these energy costs could reduce the profitability of business. Effective LED panel design with good thermal management systems to dissipate heat generated would be required even more so for PBR systems using long-wavelength LEDs.

The results, observations and thoughts from the heating study were fed-back to the company to inform the design of a scale-up facility at the Roslin Institute, Edinburgh. Interestingly, during early equipment trials large arrays of λ_{max} 680 nm LEDs did produce considerable heat, however this wasn't problematic for culture temperature, rather the problem was with the heat reducing bulb lifetime. The company therefore trialled a PBR design whereby LED panels in waterproof casing were used as submersible, internal illumination in stainless steel vessels. Submersion of the LED panels in the culture acted as a cooling system helping to keep LED panels below a 40 °C operating temperature as recommended by the manufacturer. This avoided the requirements for additional LED cooling systems. Dissipation of heat throughout the culture has also helped in maintaining culture temperature, as suggested, reducing electric heater usage and associated energy costs.

5.4.2 Interference

DO data has also highlighted how the use of longer wavelengths of light (approaching near-infrared – outside of the visible spectrum) for microalgae cultivation can cause probe interference and malfunction, limiting equipment choice. Probe types used for measurement must be carefully selected to ensure they are not affected by light or the particular wavelengths of light used for cultivation.

In the experiments using the Finesse DO probe the red light overlaps with the light wavelengths used in the probe's optical measurement system, therefore readings jump during the illumination period and the level of DO indicated does not accurately reflect the DO of the culture. In an optical DO probe a gas-permeable, water-impermeable material containing a phosphor is excited by blue light (provided by an optical fibre in the probe) (Figure 5.10a). When this material is in contact with dissolved oxygen, oxygen quenching of the excited phosphor results in the emission of red light through a phase shift. The emission frequency and duration of red light detected and measured in the probe indicates dissolved oxygen concentration. Interference of the red LED light used for illumination in the STPBR with the red LED light used in the DO sensor system demonstrated optical probes cannot be used.

Additionally, next-generation optical probe systems which work similarly on luminescence cannot function in PBRs. New optical probes such as the non-invasive optical oxygen sensor by PreSens - Precision Sensing GmbH (Germany) (Information available at: http://www.presens.de/), use a small (approximately 1 cm diameter) chemically-reactive phosphor-containing stick-on spot placed inside the walls of a transparent vessel (Figure 5.10b), and an optical sensor strapped directly opposite the spot outside the vessel. The system works as described above where oxygen quenches the blue light excited phosphor in the spot and red light is emitted. Reduction in red light detected through an optic is proportional to the presence of oxygen (Klimant, 2004). The method by which the sensors function means the patch is sensitive to photo-decomposition, therefore such systems cannot be applied to PBRs, not only because certain wavelengths of light may interfere with the measurement of fluorescence by the optic in the system, but also because light at any wavelength causes rapid decomposition of the indicators in the patch. It was demonstrated that these advanced systems cannot function in PBRs with the wavelengths of red light used in these experiments. Other optical probe types such as pH sensors will likely suffer the same interferences under λ_{max} 680 nm red LED.

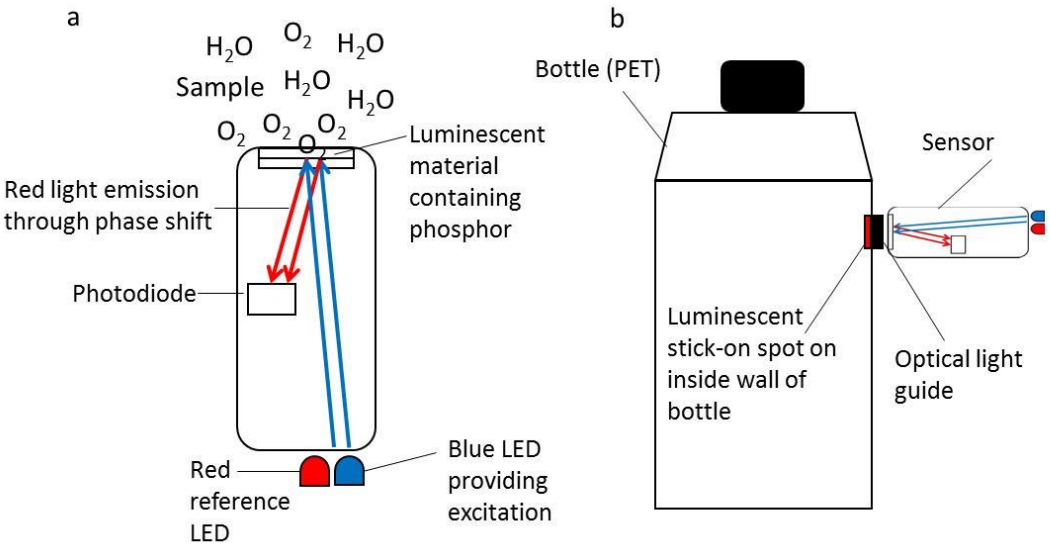

Figure 5.10. Schematic of how a typical optical dissolved oxygen sensor works (a) and the PreSens non-invasive system (b).

It is possible to use electrochemical DO probes which do not operate on optical measurement systems in PBRs where longer near-IR wavelengths of light are used for cultivation. Electrochemical probes are formed from two electrodes: typically a platinum cathode and silver anode submerged in a potassium chloride electrolyte solution with an oxygen-permeable membrane between the electrodes/electrolyte and sample to be measured (Figure 5.11) (Kanwisher, 1959). Oxygen from the sample diffuses through the membrane into the electrolyte solution where a chemical redox reaction occurs with reduction of oxygen and oxidation of the silver anode generating a small measurable electrical current. DO of the sample is proportional to oxygen diffusion into the probe and current generated. The lack of optics in these types of DO probes would avoid the interference seen with the optical probe systems. However, electrochemical probes tend to require higher maintenance and frequent calibration and are therefore less-preferred for long-term monitoring applications (YSI Incorporated, 2009). Electrochemical probes are also susceptible to interference from gases such as chlorine, hydrogen sulphide, sulphur dioxide and nitrous and nitric oxides (YSI Incorporated, 2009).

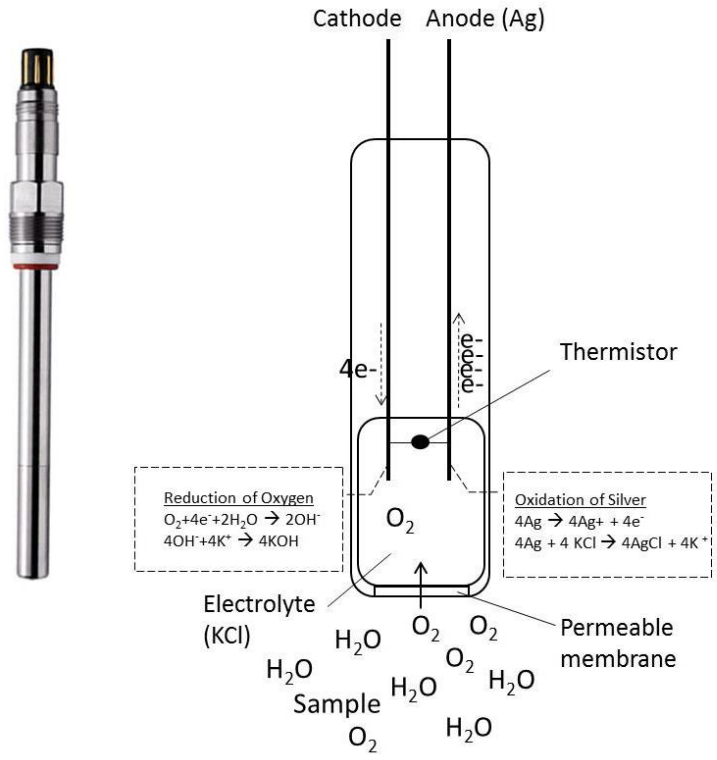

Figure 5.11. Schematic of a polarographic dissolved oxygen sensor. Redox reactions occurring at the cathode and anode are shown in dashed boxes. A thermistor is typically built-in for temperature compensation. Image of dissolved oxygen probe taken from http://www.bioprocessonline.com/doc/oxygen-sensor-inpro6800-gas-0003.

5.4.3 Comparative modelling

A simple comparative model was built to compare phycocyanin production under λ_{max} 680 nm red LEDs with standard white LEDs using data from experiments in Chapter 3 and applied to the current Scottish Bioenergy PBRs in the company's scale-up facility at Roslin Institute, Edinburgh. The model incorporates biomass, phycocyanin yield and LED power and light specifications from the STPBR and is applied to a 1000 L batch module of the larger-scale Scottish Bioenergy production system at a module cost of £1,500.

This models a PBR operated with a 14-day residence time and dry biomass output of 87.1 g/day based on 1.22 g/L maximum average batch end culture density achieved during the experiments, and assumed for both red and white LED illuminated cultures as there was no significant difference in growth rates during the experiments.

The growth medium was f/2 with additional nitrate of 2.5 g/L (although notably this would be simplified for use on a larger commercial scale). LED energy OPEX were calculated using 150 bars of 8 LEDs, reflecting the Scottish Bioenergy PBR. The red and white LED driver settings

of 8 % and 3 % used in the experiments were applied proportionally to the standard 50 % operating power used in the Scottish Bioenergy system, which is selected to achieve maximum LED lifetime. This is to reflect a commercial system where the lowest number of LEDs would be operated at a maximum selected power (50 % in this case) to keep LED CAPEX low. Here the 8 % red LED laboratory-scale driver setting represents a 50 % red LED large-scale driver setting and associated power consumption. White LED driver setting was adjusted using the ratio calculation in Equation 5.1.

Equation 5.1: $\left(\frac{\mathrm{RSD}}{\mathrm{RLD}}\right) \times \mathrm{WLD} = \mathrm{WSD}$

Where RSD is the red large-scale driver setting (%), RLD is the red LED lab-scale driver setting (%), WLD is the white LED lab-scale driver setting (%) and WSD is the white LED large-scale driver setting (%).

From LED product specification sheets LED maximum power requirements for red (Muevo-Technik) and white (LUMITRONIX) LEDs were 1.6 and 0.28 Watts (W) respectively. As light output was linear with power for red LEDs (Figure 5.12) operating power of the LED array to achieve a light intensity of 45 $\mu m^{-1}\, m^2\, s^{-1}$ was calculated using Equation 5.2.

Equation 5.2: $\mathrm{TP} = \mathrm{P} \times \mathrm{N} \times (\frac{\mathrm{LD}}{100})$

Where TP is total power consumption of operational LED array (Watts), P is Maximum LED power (Watts) assumed when the driver is set to 100 %, N is number of LEDs in the array, LD is large-scale driver setting (%).

However, light output was non-linear when ramping power for white LEDs (Figure 5.12) because the driver used was designed for dimming through pulse width modulation (PWM) specifically for the red LEDs (Poplawski, 2012). Therefore, upper and lower bounds were calculated for total power consumption of the white LED array operating at an equivalent 3 % lab-scale driver setting in the model. The bounds were calculated by a) assuming linearity that the 3 % lab-scale driver setting corresponded to 3 % of the maximum LED power requirement at a 100 % lab-scale driver setting (lower bound) and b) that a 30 % lab-scale driver setting as calibrated against light intensity in Figure 5.12 corresponds to a 100 % actual lab-scale driver setting (upper bound). These upper and lower bounds were applied to Equation 5.1 to calculate an upper and lower bound for white LED power consumption on a large-scale. Calculations were based on an electricity unit price of 9 pence per kWh.

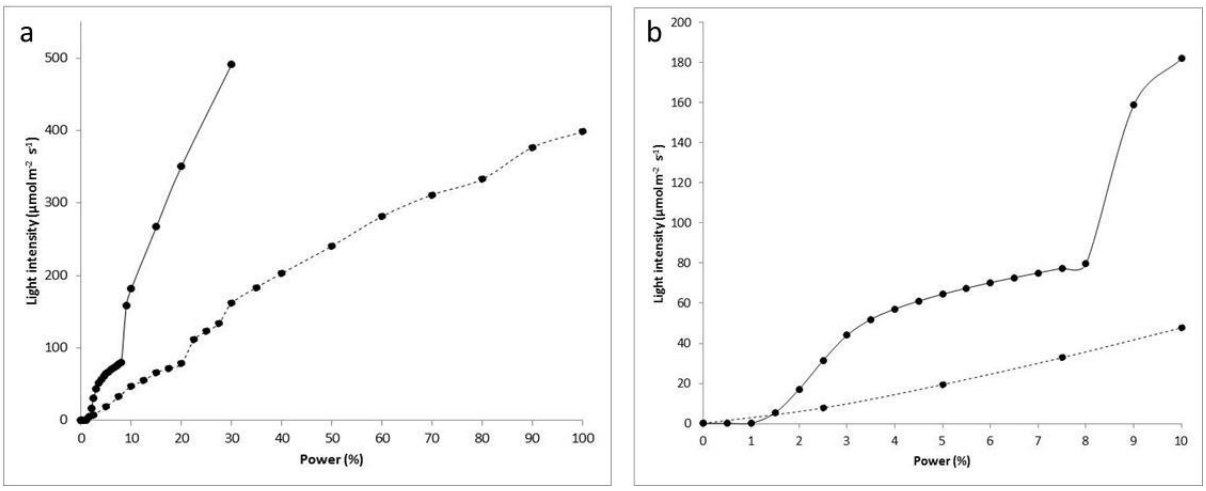

Figure 5.12. Light intensity-power curves for white (solid lines) and red (dashed lines) LEDs in the Infors STPBR as read by LI-250 light meter (LI-COR). (a) Light intensity curves for power outputs of up to 100 % for red and 30 % for white LEDs. (b) Light intensity curves for power outputs up to 10 % for both red and white LEDs. Points are means of triplicate readings. Error bars not shown as they were negligible. Relationship between light intensity and driver power was non-linear for white LEDs and light intensity reading jumped to 3000 µm m^{-2} s^{-1} above 30 % driver power and remained stable between 30-40 % power.

Mixing energy requirement was estimated using knowledge of similar systems (Doran, 2005) which would be expected small in a comparative model. Medium component costs were calculated based on lowest cost from Sigma Aldrich website (https://www.sigmaaldrich.com/) although on a larger commercial scale discount purchase on bulk chemicals would apply. LED price was calculated using cheapest current supplier quotes for 400 bars of 8 LEDs inclusive of all required equipment, VAT and shipment cost and scaled linearly (red LED £1.50, White LED £0.1, LED driver and fittings £1.88 per LED).

It was assumed that 0.0599 g of phycocyanin is extractable from 1.22 g of red LED produced dry biomass (based on average highest biomass and phycocyanin yield achieved in the experiments across all of the red batches 1-7R), which is nearly 400 % lower under white LEDs (based on the average phycocyanin yield achieved in batches 1-3W). It should be noted however, that the biomass and phycocyanin production in a commercial system would be expected to be higher as culture density was acceptably low in this experiment to achieve a small 14-day batch time in the experimental schedule, and a crude phycocyanin extraction method was used. Extraction efficiency for phycocyanin from *Arthrospira* biomass is estimated at 80 % based on contract manufacturing consultation (Biopharma, Winchester http://biopharma.co.uk/). Sale price of phycocyanin is based on achieving a freeze-dried powder and pigment of reactive grade purity 2< (Rito-Palomares, 2001) through purification

at £2000 per gram based on conversations with potential customers and also larger manufacturers in the East. Only upstream costs are considered in the comparative model, excluding any downstream processing (DSP) costs as accurate costs do not currently exist for basis and these costs are assumed equal for biomass produced under both light conditions.

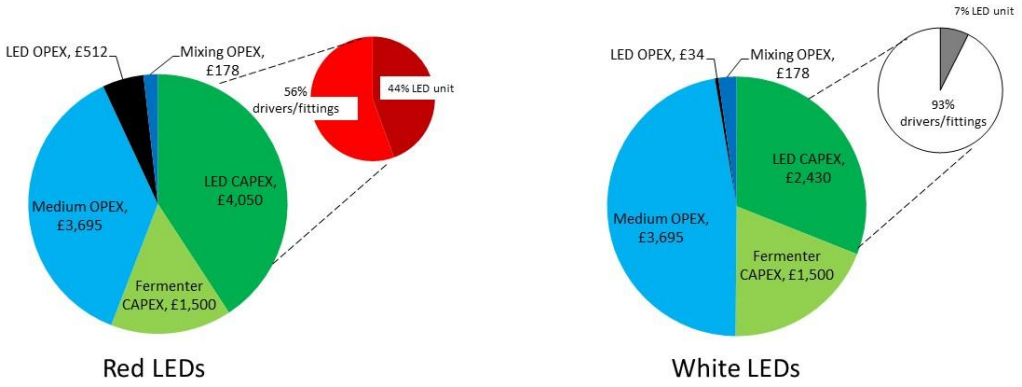

Figure 5.13. CAPEX (green) and OPEX (blue and black) upstream for 1000 L Scottish Bioenergy PBR system illuminated with red and white LEDs. Miniature pie charts display breakdown of LED CAPEX.

Looking at the upstream CAPEX and OPEX in Figure 5.13, although λ_{max} 680nm LEDs are 10-times more expensive than standard white LEDs, the substantial cost of LED driver and fitting equipment similarly required for both LED types means overall the cost of red LED arrays are 67 % higher than white LED arrays. Using the upper bounds of energy consumption for white LEDs adds £78 a year to white LED OPEX, and at such a small value it is not deemed necessary to consider both upper and lower bound white LED energy costs. Lower bounds for white LED OPEX are therefore considered only. λ_{max} 680nm LEDs consume over 15-times more energy than standard white LEDs, however energy costs make-up only a small percentage (1 % for white LEDs, 5 % for red LEDs) of the total combined CAPEX and OPEX and therefore the additional costs of energy operating under red LEDs would be insignificant to the business model.

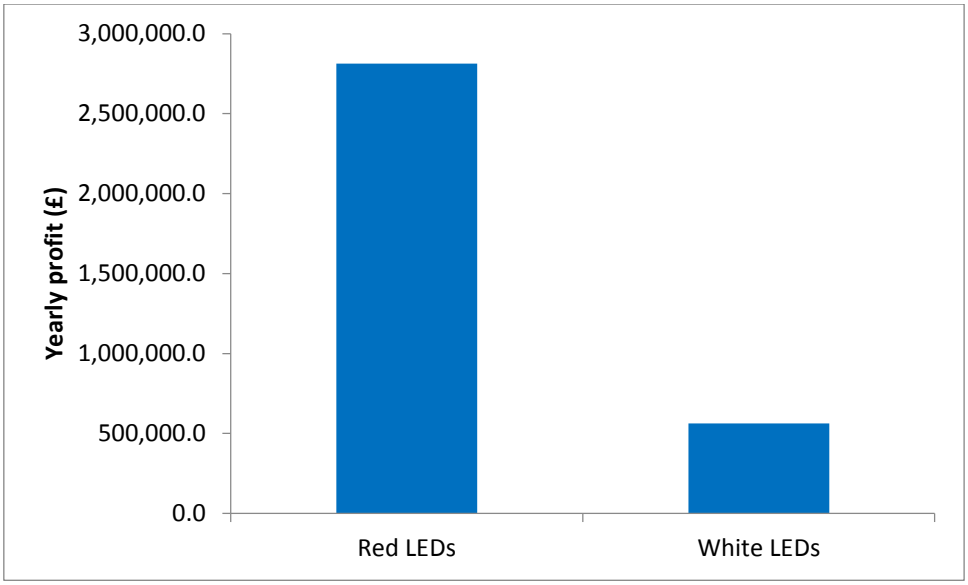

Figure 5.14. Yearly profit with PBR systems illuminated with red and white LEDs. Profits exclude DSP costs.

With a small increase in CAPEX of £1620 and increased OPEX of £478 per 1000 L PBR module per year and producing phycocyanin under red LEDs will make for a near 400 % more profitable business (Figure 5.14). The model demonstrates that, even with both the increased CAPEX and OPEX for a red LED PBR system, the significant increases in phycocyanin yield under red LEDs and associated higher profit margins easily justifies the additional costs of red LED illumination.

Chapter 6. Directed Microevolution of Arthrospira for Growth on High Copper Wastewater - a Feasibility Study

6.1 Introduction

Prenote

In this chapter resistance and tolerance are used interchangeably, but here resistance is used to describe a tolerance which has a genetic basis. Adaptation incorporates both phenotypic and genetic changes for an organism to adapt to survive in an environment. Acclimatisation describes an adaptive phenotypic (physiological or behavioural) change within an organism in response to its *natural* environment. Acclimation, a term which is used in Chapter 3, is an adaptive phenotypic (physiological or behavioural) change within an organism in response to an *artificially induced* environment.

6.1.1 Bioremediation and recovery

Bioremediation is the use of biological agents to remove wastes from the environment. Bioremediation by microorganisms for the removal of pollutants is considered an environmentally safe, inexpensive and efficient decontamination technology (Alexander, 1999). The process involves biodegradation, wherein the microorganism metabolises compounds in enzyme-driven biochemical reactions into harmless compounds; or biotransformation, wherein the molecular structure of the target compound is modified to an extent that it is rendered less toxic. Bioremediation has been demonstrated for numerous chemical mixtures including petroleum and crude oil (Vinothini and Ravikumar, 2015) and pesticides such as organophosphates (Karpouzas, 2005, Singh and Walker, 2006).

Recently there has been increasing interest in the use of plants for bioremediation – also known as phytoremediation. Microalgae can degrade toxic organic compounds such as synthetic dyes (El-Kassas and Mohamed, 2014) and certain pesticides (Jin, 2012, Zhang, 2011, Gattullo, 2012, Sethunathan, 2004) as well as inorganic compounds such as inorganic nitrate and phosphate for reduction of biochemical and chemical oxygen demand (BOD/COD) as described in Chapter 1. They can also accumulate compounds including polychlorinated biphenyls (PCBs), which concentrate in lipid stores (Lynn, 2007, Berglund, 2001). Microalgae are notable for accumulating metals (have a high biosorption capacity) through several mechanisms (Rai and Gaur, 2001) including chelation using phytochelatins. Combined with their large surface area to volume ratio, and the potential to manipulate strains to enhance these current properties –

either through genetic modification or artificial selection (Chekroun, 2014), mark microalgae as promising phytoremediation tools.

These properties indicate that microalgae may be efficient metal scavengers for use in the removal or recovery of metal contaminants from water sources. Such waters can sometimes contain high levels of precious and expensive metals of finite resource; for example, palladium is used in the electronics industry and contaminates wastewater from the plating process, and gold and platinum can be found within their respective mining wastewaters (Umeda, 2011). These industries are seeking ways to clean-up their waste streams and recover particular metals for reuse.

Microalgae and cyanobacteria require metals such as manganese, iron, cobalt, nickel, copper and zinc in trace quantities (Rai and Gaur, 2001). These metals are important for metabolic processes such as electron transport and the acquisition and assimilation of carbon, nitrogen and phosphates. However in high concentration these metals can be toxic. A number of microalgae species have been demonstrated to uptake high metal concentrations including zinc, cadmium, lead, nickel and copper (Halder, 2014). Biosorption of cadmium, chromium and copper by *Arthrospira* is reported by Chojnacka et al. (2005) and Doshi et al. (2007).

6.1.2 *Adaptation in microalgae*

Algae have the ability to rapidly adapt to a wide range of pollutants (Rai and Gaur, 2001). There are two ways in which algae can change to cope with the surrounding environment. Physiological acclimatisation (also known as phenotypic plasticity) involves changes in phenotype through gene expression at both the transcriptome and proteome levels (Schlichting and Smith, 2002). However, in more extreme conditions where physiological acclimatisation cannot provide tolerance, survival is dependent on adaptive microevolution, where random spontaneous genetic mutations confer resistance (Bradshaw, 1989, Cairns, 1988, Sniegowski, 2005). Here the mutation is pre-selective (exists before exposure to the 'selection' conditions), and is not induced by the conditions. Microevolution can therefore change the genotype and phenotype of a whole microalgae population on a short time scale, over a small number of generations. Although acclimatisation is a beneficial feature of algae cultures, it is reversible and only offers limited physiological changes for survival (Alpert and Simms, 2002). Microevolution in algae has been shown to produce culture strains resistant to a number of toxic compounds including trinitrotoulene (TNT) (García-Villada, 2002), the herbicide lindane (Lopez-Rodas, 2001), cadmium (Collard and Matagne, 1990) and some antibiotics (Gillham, 1965, Wurtz, 1979). Such strains, arising from genetic change, maintain their resistance when

conditions are interchangeable. Therefore cultures with stable resistance can be created through directed microevolution.

6.1.3 *Mechanisms of metal tolerance*

It can be difficult to determine whether adaptation has arisen by phenotypic or genetic changes, however there are a number of common mechanisms through which metal tolerance can arise in microalgae (summarised in Figure 6.1). Tolerance may be a result of the deployment of more than one of these mechanisms.

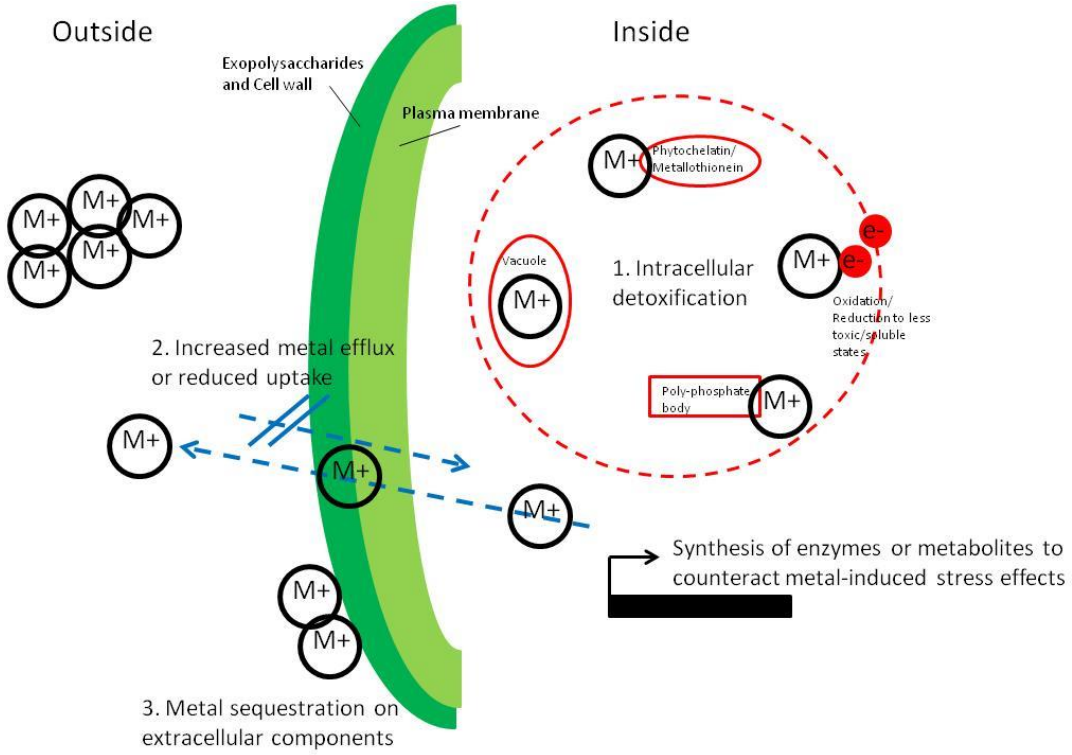

Figure 6.1. Schematic of common mechanisms of metal tolerance in microalgae adapted from Rai and Gaur (2001) including intracellular detoxification, extracellular complexation and uptake.

Intracellular detoxification mechanisms shown in Figure 6.1 (1.) inside the red circle can contribute to metal tolerance. Metal tolerance can occur through sequestration of metals intracellularly using chelators such as metallothioneins and phytochelatins (Rauser, 1990, Steffens, 1990). These chelators bind metals to form large, complex structures. Polyphosphate bodies, accumulated in the cell under conditions of surplus phosphates, can also be intracellular sites for metal complexation (Rai, 1981). The polyanionic properties of these phosphate polymers sequester cations; however, subsequent phosphate deficiency leading to mobilisation of intercellular stored phosphate can lead to the release of high concentrations of metal ions previously chelated within the cell. Metal ions have also been shown to be sequestered and

compartmentalised in the vacuole (Heuillet and Puiseux-Dao, 1986), which is a well-known mechanism in higher plants. Additionally, metal ions can also be oxidised/reduced in the cell to less soluble (precipitated) and less toxic states.

Reduced uptake and increased efflux (Figure 6.1 (2.)) from the cell can also enable metal tolerance. Reduced influx can be regulated by alterations in the permeability of the cell membrane to metal ions and possible modifications within the cell wall such as thickening for protection. Active transport of metal ions out of the cell, or secretion of chelated metal complexes from the cell can be effective. Such systems have been widely reported in novel resistant bacterial strains (Silver, 1996). Extracellular components of algae cell walls can bind metal ions, reducing bioavailability, lowering intracellular accumulation and decreasing toxicity (Figure 6.1 (3.)). Metal ions can also be chelated by metal-complexing ligands secreted from the cell, reducing bioavailability.

Although only trace quantities of metals such as copper are required for normal metabolic functions, *Arthrospira* has been shown to tolerate up to 4 mg/L of copper (Nalimova, 2005). This is done by binding copper to the cell wall in a process known as chemisorption. Peptidoglycans and polysaccharides present on the cell wall display negatively charged carboxylic, hydroxyl and phosphate functional groups which bind Cu(II) by cation exchange, deprotonating copper (Chojnacka, 2005). Deprotonation and therefore the biosorption process is strongly dependent on pH. Some copper is also taken into the cell and forms complexes with amino acids, peptides and proteins (Cavet, 2003). Cellular copper can be secreted (or precipitated) as biologically unreactive complexes after reduction of Cu(II) to Cu(I), and copper ions accumulated on the cell wall can be reduced and released. Beyond this copper concentration the cell membrane is damaged (Nalimova, 2005) and is generally lethal. Although microalgae are known to develop resistance to copper, copper is still used as the basis of many algaecides because of its toxicity to microalgae (Hrudey, 1999). Resistance to copper-based algaecides is commonly overcome by more frequent use and use of higher quantities of algaecides which can lead to accumulation of copper in the environment, causing other effects on the ecosystem (Christenson, 2014, Das and Khangarot, 2011, Karan, 1998).

6.1.4 The use of Genetically Modified Microorganisms

The genetic modification (GM) of microalgae is where DNA is modified through the use of non-natural genetic engineering tools, modifying, removing or adding genes. GM has the potential to overcome many current limitations in microalgae biotechnology such as low product yields and sensitivity to particular conditions. This realisation has created huge interest

in synthetic biology within the research community. Synthetic biology is a promising opportunity for the development of the UK algae biotechnology industry, given the current synthetic biology knowledgebase. The positives of genetically modified microorganisms (GMMs) however are not fully supported by the public. Considerable effort, investment and marketing are needed to inform and change public opinion if GMMs are to be accepted, although some markets such as personal care will not tolerate GM (Basshir, 2014). GM regulations have to be followed if GMMs are used in microalgae systems to lessen any risks of GMMs being released and disrupting the ecosystem. The hazards associated with GMMs, whether released GMMs could survive in the natural environment, and the chance of genes then transferring to other organisms depend on the traits that have been modified or introduced (Figure 6.2) (Enzing, 2012).

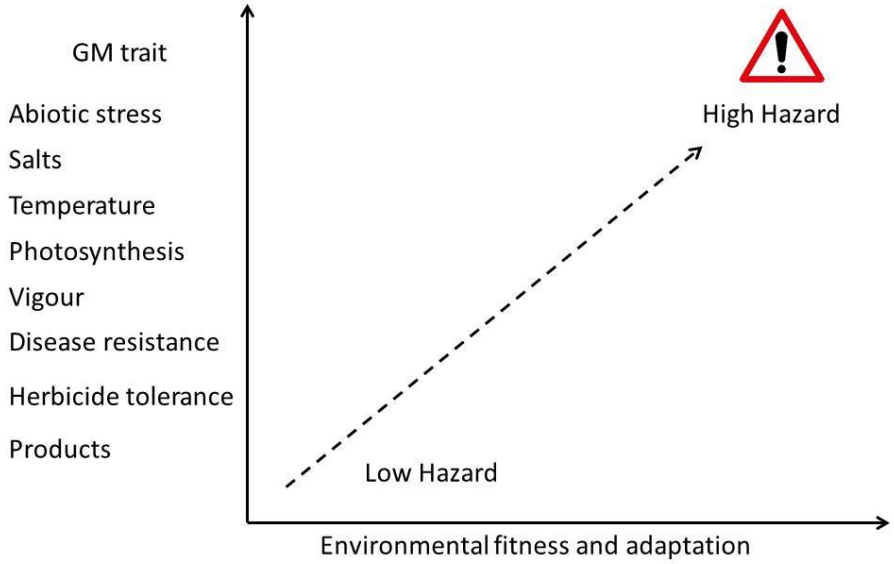

Figure 6.2. The environmental hazard of GM algae depends on the impacts of the modified trait and strain. Adapted from Sweet (2014). Image sourced from www.stocksigns.co.uk.

Using GM algae strains in the UK involves seeking approval from the Government Department for Environmental Food and Rural Affairs (DEFRA) (under Directive 2001/18/EC (European Parliament, 2001) and Directive 2009/41/EC (European Parliament, 2009) and scrutiny by the Advisory Committee on Releases to the Environment (ACRE) (Sweet, 2014). For commercial use of GM algae strains, an application has to be made to the European Commission Directorate-General for Health and Consumers (*DG SANCO*) where detailed science is collected on a case-by-case basis for risk assessment by *European Food Safety Authority* (*EFSA*), sometimes involving *The European Medicines Agency* (*EMEA*). Not only does gaining approval for use come at a substantial administrative cost, running a GM algae

facility can involve higher equipment costs (CAPEX) to improve containment together with further costs for continuous monitoring during operation (OPEX).

6.1.5 Feasibility of directed microevolution in algae biotechnology

In the Scottish Bioenergy photobioreactor (PBR) system installed at the Glen Turret Distillery, microalgae were grown on pot ale, a wastewater from the whisky distilling process. The microalgae used the ammonia and nitrate in the wastewater for growth, reducing the environmentally hazardous high BOD/COD of the wastewater, which typically makes pot ale costly to dispose of. Additionally, microalgae were shown to remove copper from the wastewater, present from the copper whisky stills (Graham, 2012). The system was also utilising waste CO_2 and heat. Not only was the system achieving treatment of pot ale to lower the BOD/COD and copper concentrations to allow release into rivers and the sea, but microalgae biomass was produced. The high protein biomass could be used as a feed to supplement the diet of young pigs which have a high copper dietary requirement (Jacela, 2010). Although the biomass was an additional revenue stream in the business model, the feed product was still low value. A new focus on higher value extracts in the research programme then, developed with the company considering growing *Arthrospira* on pot ale. Depending on the processing method used there was the possibility to purify a higher value phycocyanin product, leaving behind a high copper biomass thereupon creating more than one product revenue stream. However, the *Arthrospira* strain being experimented with could not tolerate the high copper concentrations present in pot ale. There was a requirement to identify a strain that could tolerate higher copper concentrations. It was equally important that the strain should survive the typical variability of copper levels in pot ale and be sufficiently stable to retain its tolerance under variable conditions.

Acclimation, as reversible changes (like those observed in the LED experiments of Chapter 3) would not produce the stable strain required in bioremediation systems where there is variability in the wastewater used as a feedstock. Another way to do this would be GM but it was important to the company to avoid GM and the associated environmental safety concerns, regulatory complications and costs. This was particularly important in the bioremediation system as treated wastewater leaving the PBR would likely contain GM microalgae and would be classified as a Category 4 GMM (products containing GMMs) - the highest risk category.

The process of directed microevolution was of interest as a solution to arrive at a stable non-GM strain. It wasn't known whether or how easily this could be done. Although stable resistant cultures can be created through microevolution, this cannot be induced; pre-selective mutations

must be selected using statistical methods. Working with the example of *Arthrospira* grown on pot ale in this chapter, the feasibility of using Luria–Delbrück experiment-style selection (Luria and Delbrück, 1943) or fluctuation analysis to identify a 'microevolved' copper-resistant *Arthrospira* strain was tested. Proving the feasibility of such a technique would identify a method by which the company could create non-GM strains from different commercially interesting microalgae for use in a number of systems using a variety of feedstocks. This could open up opportunities for further development of the company's multi-process PBR systems which could expand the business opportunities.

6.2 Experimental Details and Method

6.2.1 Experimental design based on theory

Figure 6.3 is a schematic of the experimental process which will be briefly outlined in the next paragraph followed by a fuller description in the subsequent paragraphs of 6.2.1. The experimental process was based on the method of (Gonzalez, 2012).

The culture was cloned through isolation of a single cyanobacterium to avoid the inclusion of previous spontaneous mutations, followed by propagation. With the cloned culture, toxicity assays were completed to assess the toxicity of copper (Cu(II)) to *Arthrospira*; these are explained in 6.2.2. Toxicity assays combined with the known concentrations of Cu(II) in pot ale informed the concentrations used for selection. When the cultures reached a particular filament density they were split into two sets. One set (Set 1) was split into tubes and the culture continued to propagate in the tubes. The other (Set 2) continued to propagate in a flask, and on reaching a particular filament density was then split into tubes. Copper sulphate ($CuSO_4$) solution was added to both Set 1 and Set 2, where sub-sets of Set 1 and Set 2 received different concentrations of $CuSO_4$ and the tubes were incubated. During this incubation period resistant mutant filaments can generate enough progeny to be detected. Afterwards, fluctuation analysis was performed to identify those cultures which developed resistance through microevolution, which is explained in 6.2.3. Identified Cu(II) resistant strains were propagated in standard medium and tested for their toxicity to Cu(II) and compared with the toxicity in the original culture to assess the extent of resistance acquired.

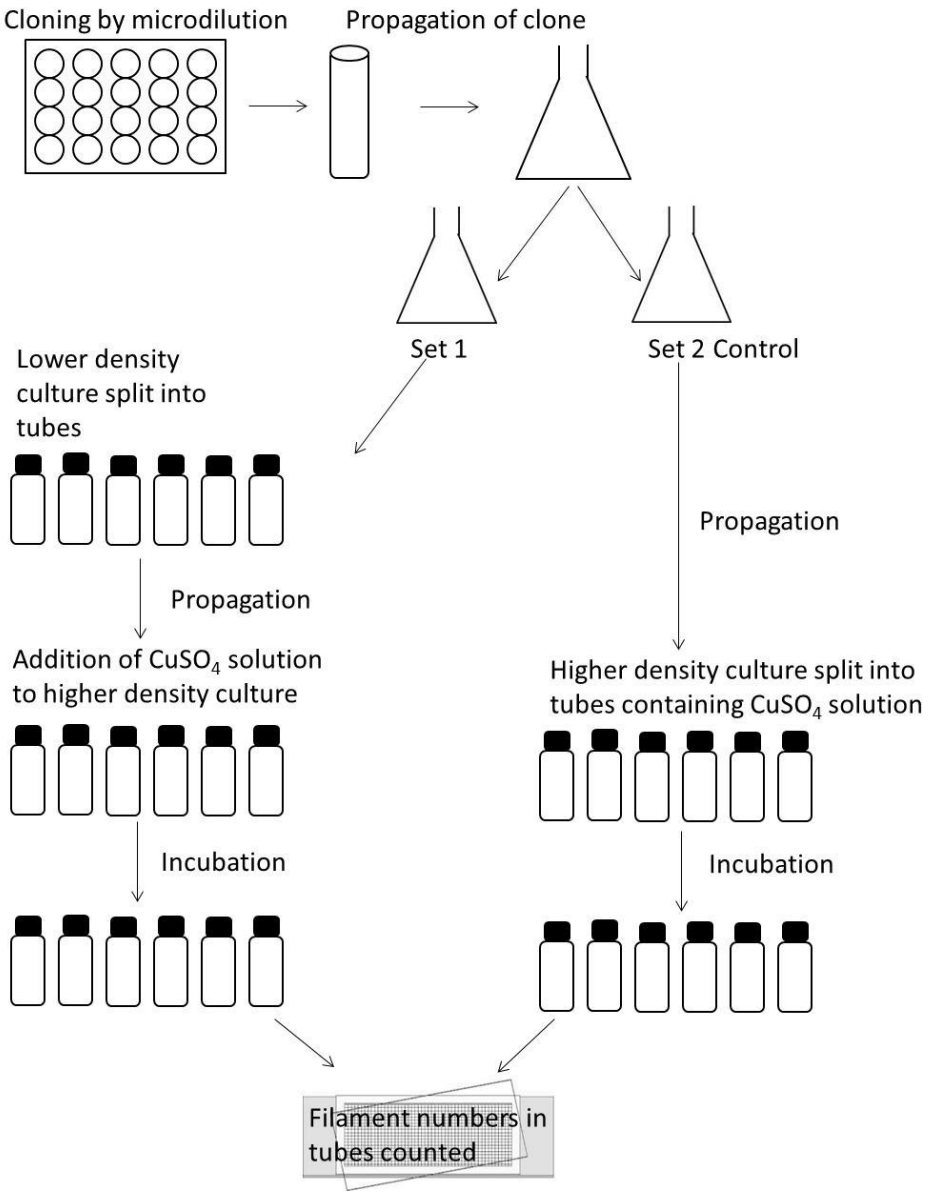

Figure 6.3. The experimental process from cloning of *Arthrospira* to selection and fluctuation analysis, based on the method by Gonzalez et al. (2012).

Cloning was performed through microdilution (Andersen, 2005) in a 96-well plate under aseptic conditions. Sterile f/2 Medium (Guillard and Ryther, 1962) supplemented with 29.4 mM/ 2.5 g/L $NaNO_3$ (Raoof, 2006) and adjusted to pH 8 was used for all dilutions. Media was made with 1 µm filtered, UV sterilised natural seawater and autoclaved. *Arthrospira platensis* (CCMP 1295) was obtained from the Provasoli-Guillard National Centre for Marine Algae and Microbiota (NCMA; https://ncma.bigelow.org/). During microdilution the *Arthrospira* culture was diluted to a filament density of 1 filament per 200 µL, and 200 µL of diluted culture pipetted into each well of the plate; thereby statistically providing a single filament in each well. The plates were incubated in a constant temperature room 18°C ± 1°C, with an average light intensity of 97 µmol m^{-2} s^{-1} with 8:16 dark:light cycle. Growth in the plate wells was monitored

under a microscope (Olympus BH-2 brightfield) until the presence of filaments could be seen by eye, after which a selection of well samples were each transferred to fresh sterile f/2 Medium supplemented with 29.4 mM/ 2.5 g/L $NaNO_3$ in 50 mL conical flasks with foam stoppers. Propagation of the cloned cultures was performed using sub-culturing in increasing volume conical flasks with foam stoppers in a constant temperature room (18°C ± 1°C, 97 µmol m^{-2} s^{-1}, 8:16 dark:light cycle) until a culture density of 100 filament per mL was reached. Filament counts were performed from triplicate 50 µL samples in a Sedgewick rafter counting cell, diluting if necessary for samples with higher numbers of filament. A single flask of clones was selected for the experiment.

The cloned culture was split into two sets representing Set 1 and Set 2, as described above. Aliquots of 3.63 mL from Set 1 were split into 200 10 mL tubes (average 363 filaments per tube), while Set 2 culture (same density as in Set 1 of 100 filaments per mL) was maintained in the flask and densities in the Set 1 tubes and Set 2 flask allowed to propagate to approximately 25,000 filaments per tube. Upon reaching this density in Set 1, concentrated $CuSO_4$ solutions ($CuSO_4$ sourced from Sigma-Aldrich) in sterile f/2 Medium supplemented with 29.4 mM/ 2.5 g/L $NaNO_3$ (3.63 mL volume) were added to create subset concentrations of 0.3, 0.6, 1, 2 and 4 mg/L Cu(II), 40 tubes for each concentration. In Set 2, the culture was split into 100 tubes and similarly, as with Set 1, $CuSO_4$ was added to create subset concentrations of Cu(II), 20 tubes for each concentration, total volume in each tube 7.26 mL. This part of the experiment, as with the cloning, was performed under aseptic conditions. Tubes were incubated for 60 days under the same propagation conditions as used for cloning, each tube lightly mixed for five seconds on a vortex every two days to prevent settlement. After 60 days filament counts were taken from each tube using the same counting method as described above. Fluctuation analysis was performed to identify those cultures in which resistance had arisen through microevolution.

6.2.2 Toxicology

Toxicology assays and EC_{50} (the half maximal effective concentration) calculations for Cu(II) were performed on *Arthrospira platensis* before and after the micro-evolution process to monitor shifts in EC_{50}. Assessments were performed under aseptic conditions. EC_{50} calculations, before directed microevolution, were carried out in two stages. First, through an initial range-finding assay *Arthrospira* were grown in $NaNO_3$ supplemented sterile f/2 Medium containing different concentrations of $CuSO_4$ (0.003-20 mg/L Cu(II)) to home in on the region of Cu(II) concentrations where toxicity becomes apparent by approaching the lethal concentration on Cu(II) (data not shown). Filament counts (filaments/mL) were taken at 0, 24, 48 and 96 hours using a microscope to count filaments in 50 µL samples, diluting if necessary

for samples with higher numbers of filament. For the range-finding assay, each well of a 24 well-plate containing various concentrations of $CuSO_4$ solution were inoculated with *Arthrospira* to a starting concentration of approximately 500 filaments per mL (total volume 1.7 mL). This range-finding assay showed that after 48 hours a concentration of 2.5 mg/L Cu(II) was lethal and that toxic effects could be observed between 0.3-2.5 mg/L Cu(II). The toxicology assay was therefore focused on Cu(II) concentrations within this range to generate accurate growth and EC_{50} dose-response curves. Here, similarly, *Arthrospira* were grown in 24 well plates in $NaNO_3$ supplemented f/2 Medium containing $CuSO_4$ concentrations ranging between 0.03-4.3 mg/L Cu(II), total volume in each well of 1.7 mL, with three repeats for each concentration. $NaNO_3$ supplemented f/2 Medium without additional $CuSO_4$ (effectively 0.003 mg/L Cu(II)) was used as a control. Filament counts were taken at 0, 24, 48, 72 hours following British Standard BS EN ISO 10253:2006 (British Standards Institution, 2006) where EC_{50} is calculated as a reduction in growth rate relative to control cultures grown under identical conditions (0.003 mg/L Cu(II)). This same range (0.003-4.3 mg/L Cu(II) and method was used to re-test the EC_{50} of *Arthrospira* after the directed microevolution process. Statistical analysis was performed using GraphPad Prism version 6.07 for Windows. Gradient values were normalised to activity at 0 inhibition (0.003 mg/L Cu(II)) and analysed by non-linear transform log(agonist) vs. response – variable response function (GraphPad Software, San Diego California USA, www.graphpad.com). Statistical analysis were performed using a paired two-tailed t-test with P values <0.05 considered statistically significant. Any morphological changes to the cultures during the course of the toxicology assay seen under the microscope were also noted.

6.2.3 Fluctuation analysis

A modified Luria-Delbrück analysis was performed, described in Lopez-Rodas et al. (2001) and shown in Figure 6.4. The importance of the experimental design in Set 1 and Set 2 is to generate the statistical test to identify microevolution. Set 2 is a control and sets the benchmark for normal distribution of propagation after exposure to Cu(II), which can be thought of as a Poisson Model. A Poisson Model is a discrete probability distribution describing the probability of a given number of events (in this case a mutation conferring resistance) occurring in a fixed time period (in this case during propagation and incubation) where events occur with a known average rate and independently of time since the last event. Such a distribution well describes mutations (Foster, 2006). Here, in Set 2, variation is caused by random sampling and the variance (σ^2) should be equal to the mean (μ) and therefore represents fluctuation consistent with the Poisson Model.

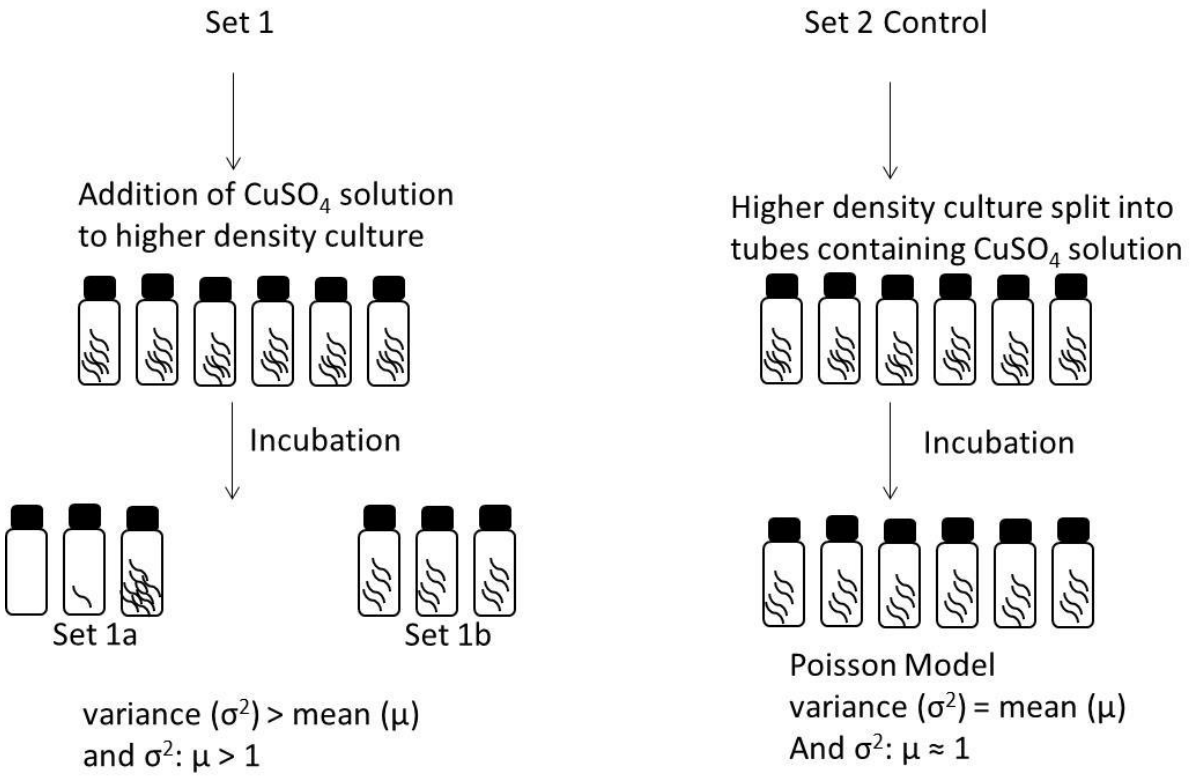

Figure 6.4. A schematic of fluctuation analysis, based on the Lopez-Rodas et al. (2001) modification of the classic 1943 Luria-Delbrück method.

Set 1 is discriminated against the normal distribution of Set 2, to identify tubes where pre-selective mutations occurred before exposure for resistance to Cu(II), indicating microevolution. A higher variance (tube-to-tube variation) in Set 1 compared with Set 2 where variance>mean, inconsistent with the Poisson Model, indicates resistance arising from a random spontaneous mutation in Set 1 before exposure, and therefore microevolution. A similar variance:mean ratio in both sets indicates post-selective adaptation. A variance:mean ratio of Set 1 significantly higher than that of Set 2 indicates resistance arising from a random spontaneous mutation before exposure - microevolution. Further, Set 1 tubes with variance:mean ratio > Set 2 with high filament numbers suggests a mutation occurring early in the propagation phase. Oppositely, a low filament number suggests mutations in late propagation phase conferring resistance to Cu(II). A lack of filaments in any of the tubes indicates no adaptation, either pre or post-selective. Statistically significant differences between variance: mean ratios of Set 1 and Set 2 are determined using the Pearson's chi-squared test where p=0.92.

6.3 Results

6.3.1 Pre-exposure Arthrospira Cu(II) toxicity

Mean EC_{50} of Cu(II) (mg/L) for *Arthrospira* was calculated at 0.2032 (95 % confidence interval 0.085-0.483 Cu(II) mg/L with an R squared value of 0.838) (Figure 6.5). Visual observations showed trichome fragmentation, bleaching and entanglement on exposure to Cu(II) at the four highest concentrations (Figure 6.6 and Figure 6.7).

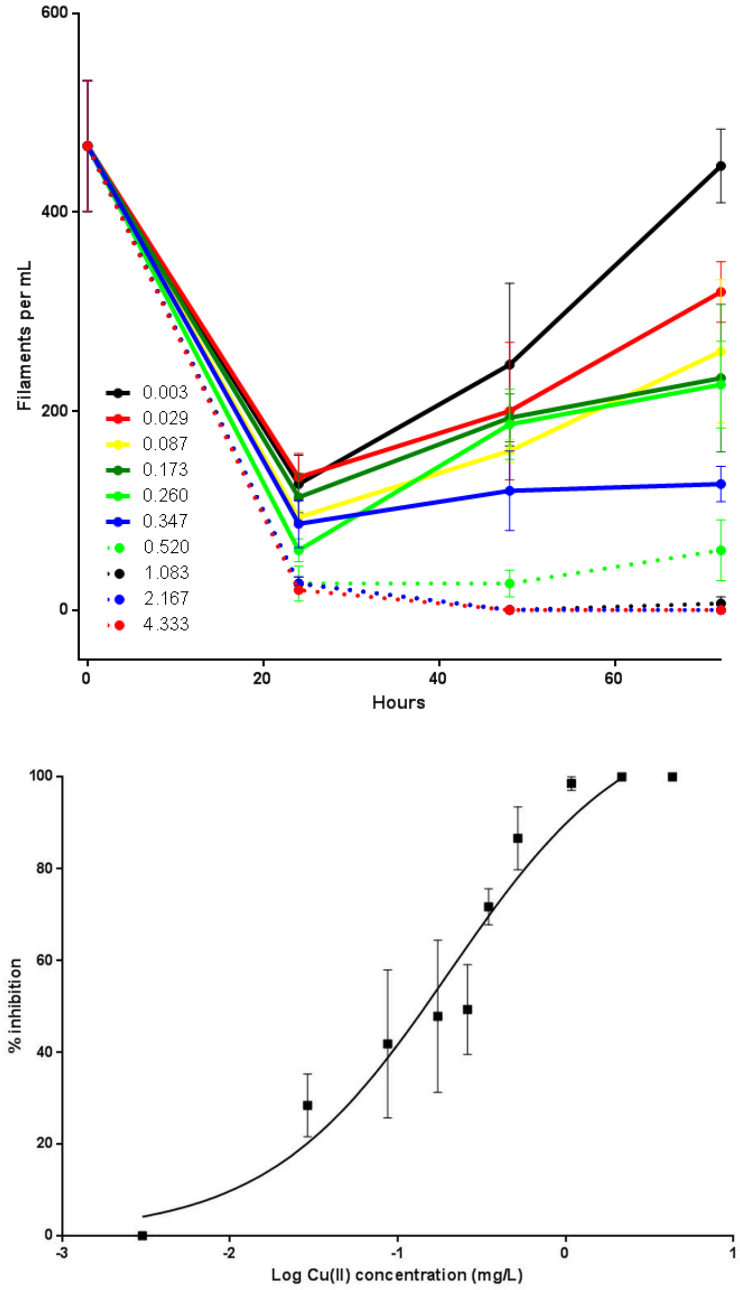

Figure 6.5. Above: Growth curves of *Arthrospira* exposed to increasing Cu(II) concentrations measured over 72 hours, below: EC_{50} dose-response curve of *Arthrospira* to Cu(II). Error bars represent standard error of the mean. At higher Cu(II) concentrations, represented by dotted lines, bleaching, fragmentation and filament shrinkage was observed.

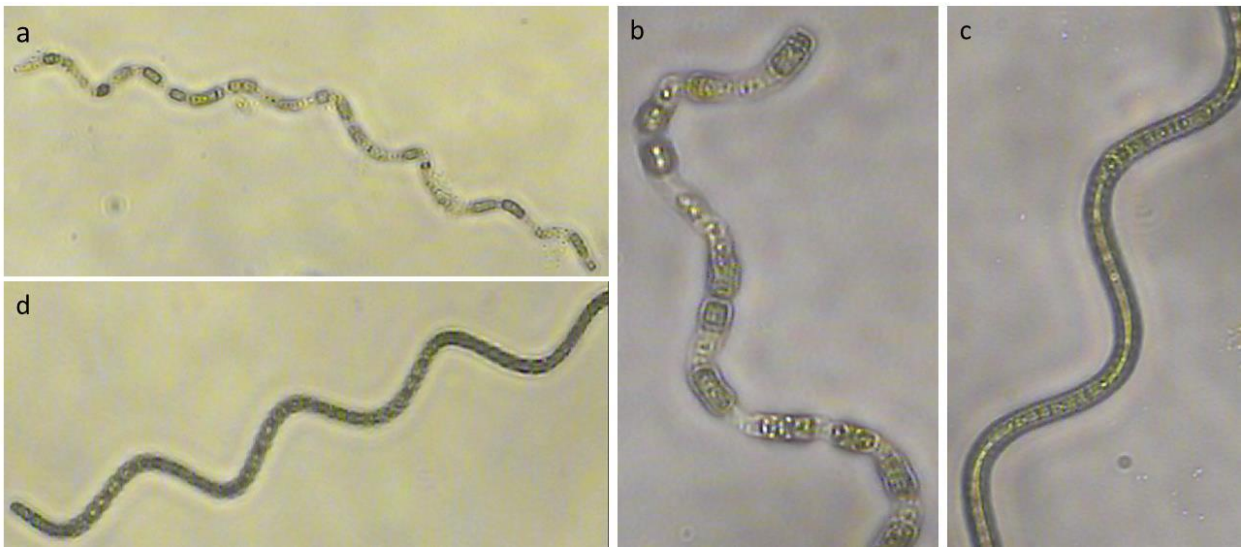

Figure 6.6. Microscope images showing morphological changes during exposure of *Arthrospira* to higher Cu(II) concentrations. After 24 hours in 0.52 mg/L Cu(II) pigment bleaching in the cells of the filaments and the beginning of fragmentation of the trichomes was observed (a&b) compared with control (0.003 mg/L Cu(II)) (c&d). At 48 and 72 hours the extent of pigment bleaching and fragmentation made the *Arthrospira* cells difficult to see and capture under the microscope. Trichomes also became prone to entanglement.

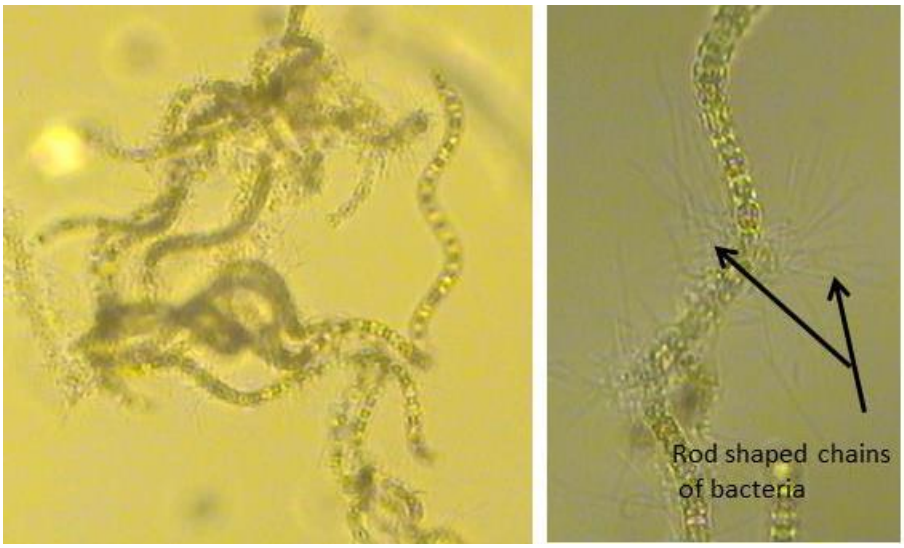

Figure 6.7. *Arthrospira* at 48 hours in 0.52 mg/L Cu(II). At 48 and 72 hours the extent of pigment bleaching and fragmentation made the *Arthrospira* difficult to see and capture under the microscope. Trichomes also became prone to entanglement (left) and bacterial breakdown of cellular material was observed (right).

Given the results of the toxicology test, five Cu(II) concentrations were selected for exposure during the directed microevolution process. These were 0.3, 0.6, 1, 2 and 4 mg/L Cu(II). Cu(II) concentration in pot ale varies from around 2-5 mg/L (Graham, 2012).

6.3.2 Post-exposure fluctuation analysis

No resistant filaments were seen in the three higher Cu(II) concentrations 1,2 and 4 mg/L Cu(II) tested after the 60 day incubation demonstrating that mutations or adaptations could not confer resistance at such high concentrations. Resistance was detected at Cu(II) concentrations of 0.3 and 0.6 mg/L Cu(II) by *Arthrospira* propagation (Table 6.1).

Table 6.1. Summary of resistance to Cu(II) concentrations observed in *Arthrospira*

Cu(II) concentration (mg/L)	**Adaptation**
0.3	Resistance (acclimation)
0.6	Resistance (RSM)
1	No resistance detected
2	No resistance detected
4	No resistance detected

Although filaments were detected in all the Set 1 and Set 2 tubes at 0.3 mg/L Cu(II), and in Set 2 at 0.6 mg/L Cu(II), there were only filaments detected in 25 % of the Set 1 tubes at 0.6 mg/L Cu(II) (Figure 6.8).

The higher variance in both Set 1 for 0.3 mg/L Cu(II) and Set 1 for 0.6 mg/L Cu(II) compared with the variance in Set 2 can be seen from the distribution in the histograms of Figure 5.8.

Looking at Figure 6.8, fluctuation analysis for concentration 0.3 mg/L Cu(II) showed a 6-fold higher variance in Set 1 compared with the Set 2 control. However, the variance in Set 2 is nearly 7-fold lower than the mean, giving a variance:mean ratio of 0.13, much lower than the variance: mean ratio of around 1 expected in a Poisson Model. This indicates a more uniform than random distribution in the control. Additionally, even though the variance is higher in Set 1 compared with Set 2, the variance:mean ratio of Set 1 represents the Poisson Model at 1.02, indicating microevolution did not occur. The variance:mean ratio is 7-fold higher in Set 1 than the Set 2 control which isn't significantly different ($p=0.92$ using chi-squared test as a measure of goodness of fit) suggesting that resistance in Set 1 could not have arisen through pre-selective random spontaneous mutation.

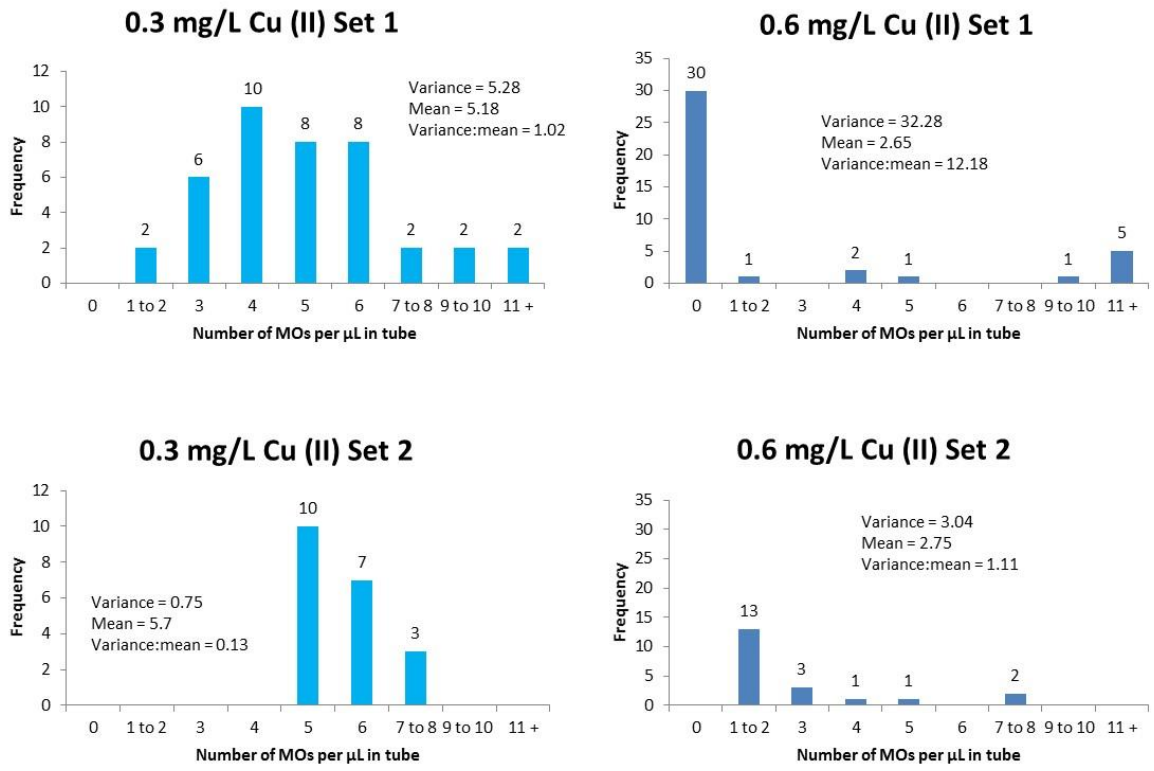

Figure 6.8. Histograms of the numbers of resistant microorganisms (MOs) in the tubes of both Sets 1 and 2 (Control) at 0.3 and 0.6 mg/L Cu(II) concentrations. Frequency represents the number of tubes containing a particular range of resistant MO numbers. Variance, mean and variance:mean ratio statistics are displayed for each set.

Fluctuation analysis for concentration 0.6 mg/L Cu(II) showed a high Set 1 variance in comparison to the mean giving a high variance:mean ratio of 12.18 compared with the Poisson-like distribution in Set 2 where variance was similar to the mean giving a variance:mean ratio of 1.11. A significantly higher variance:mean ratio in Set 1 compared with the Set 2 control ($p \sim 0$ using chi-squared test as a measure of goodness of fit) indicates that the resistance in the tubes of Set 2 arose by rare spontaneous mutation before selection.

All tubes in Set 2 at 0.6 mg/L Cu(II) contained small densities of *Arthrospira*. Of the ten Cu resistant mutant microevolved strains identified in Set 1 at the 0.6 mg/L Cu(II) concentration, there were four tubes containing low numbers of filaments (1-5 filaments per µL) (Figure 6.8) demonstrating a spontaneous random mutation which must have occurred late on in the propagation phase, giving rise to a small number of MOs with resistance before exposure to the high Cu concentration. There were also two tubes with high numbers of filaments (20 and 21 filaments per µL) demonstrating a spontaneous random mutation which must have occurred

early on in the propagation phase, giving rise to a larger number of MOs with resistance resulting in a higher number of filaments surviving exposure to the high Cu(II) concentration. Three resistant strains were selected (the two high density tubes and a low density tube), propagated and re-tested for toxicity to Cu(II).

6.3.3 Cu(II) toxicity of micro-evolved Arthrospira

Dose-response curves are shown for the highest EC_{50}-shifting strain in Figure 6.9. Mean EC_{50} of Cu(II) (mg/L) for the microevolved *Arthrospira* strain was calculated at 0.5084 (95 % confidence interval of 0.3063-0.8440 Cu(II) mg/L with an R squared value of 0.95). This is a significant 150 % increase in EC_{50} ($p=0.0028$) through directed microevolution.

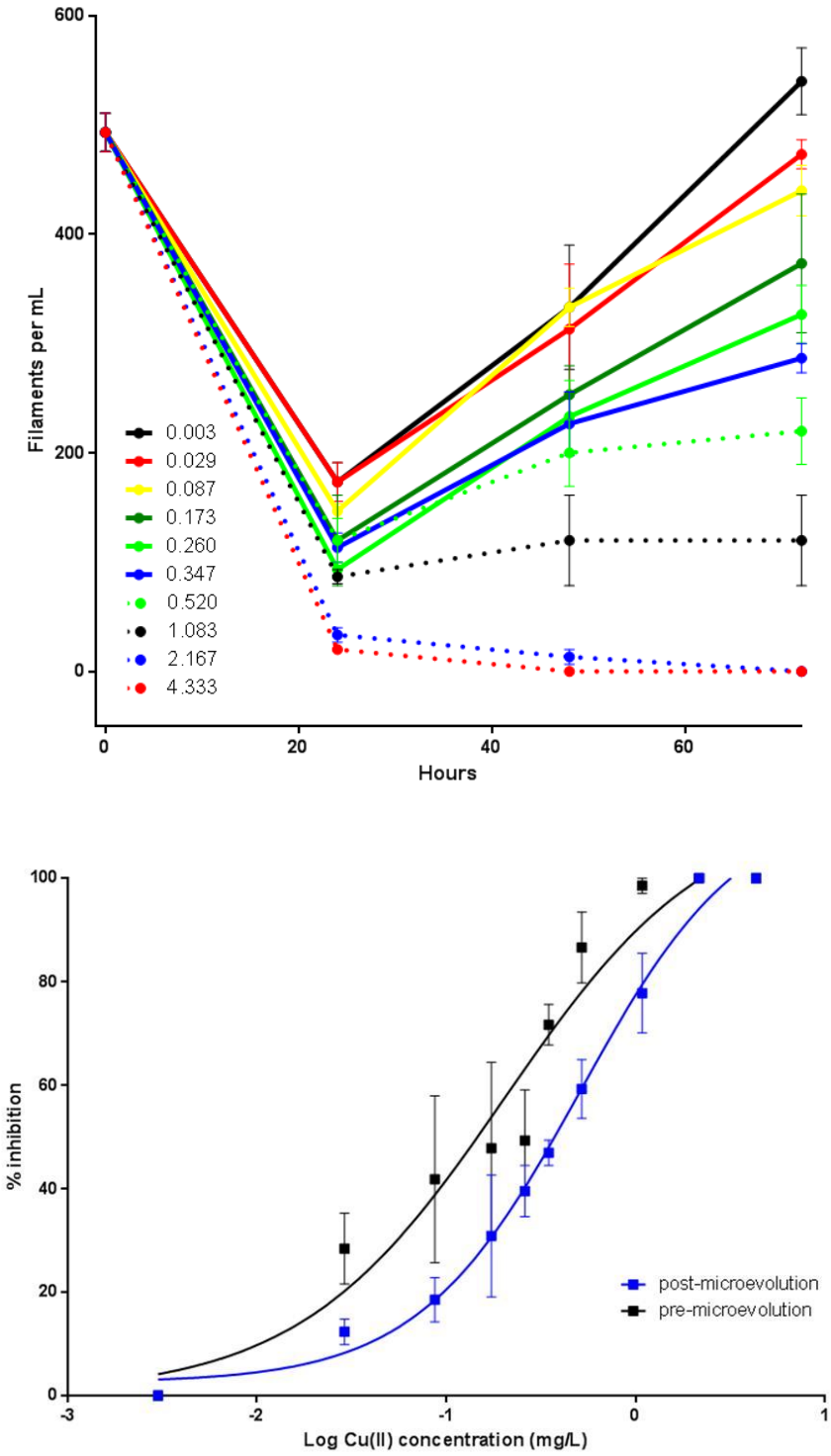

Figure 6.9. Above: Growth curves of microevolved *Arthrospira* exposed to increasing Cu(II) concentrations measured over 72 hours, below: EC_{50} dose-response curves of post-microevolution *Arthrospira* to Cu(II) compared with pre-microevolution *Arthrospira*. Error bars represent standard error of the mean.

6.4 Discussion

6.4.1 Directed microevolution and the extent and stability of resistance

A lack of any surviving *Arthrospira* after incubation at the three highest concentrations tested demonstrates adaptation (or any pre-selective RSM) could not confer resistance at such high concentrations. Fluctuation analysis showed that pre-selective spontaneous random mutations were not responsible for the resistance seen at the lowest copper concentration. Here, given that a copper concentration of 0.3 mg/L Cu(II) didn't completely kill *Arthrospira* in any of the Set 1 tubes, it is likely that the selection pressure (copper) wasn't enough to 'select'. This is supported by the pre-exposure toxicity assay which showed that although exposure to a Cu(II) concentration of 0.3 mg/L caused an instantaneous reduction in *Arthrospira* filament number, *Arthrospira* culture density gradually began to recover after 24 hours. Microevolution however was confirmed through fluctuation analysis at a copper concentration of 06 mg/L Cu(II). As 75 % of the Set 1 tubes tested at this copper concentrations showed no growth, it was obvious that this concentration was high enough to completely kill *Arthrospira*, and that the growth in 25 % of the tubes in Set 1, some reaching high density, must have been caused by an rare event – a spontaneous random mutation.

The strain generated in these experiments, arising through microevolution, can tolerate 0.6 mg/L of copper, a 200-fold increase in the optimal concentration of copper (in f/2 Medium). However, the copper concentration of pot ale varies from around 2-5 mg/L (Graham, 2012). This concentration (even at its lowest) is over 3-fold higher than the concentration of copper tolerated by the resistant strain generated in these experiments. To attempt to achieve this level of resistance, the resistant strain can undergo additional rounds of selection using the same experimental method. Each time it may be possible to select for a strain with a higher level of copper resistance. During each round a strain may be produced with a narrow window (or range) of resistance (see Figure 6.10).

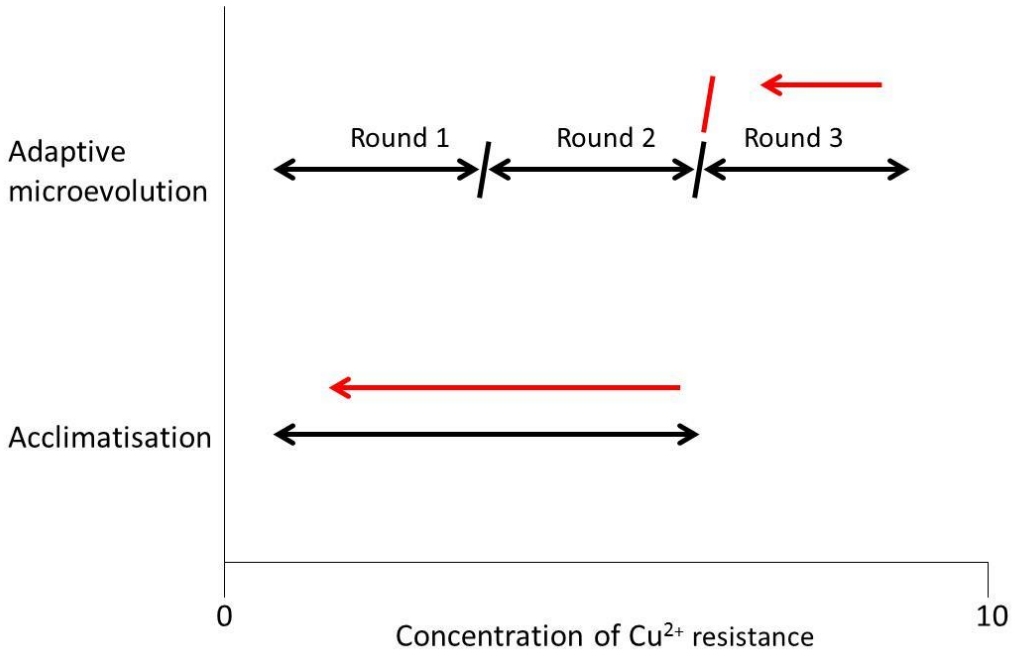

Figure 6.10. Schematic comparing adaptive microevolution (top) to acclimatisation (bottom). Black arrows represent an achievable concentration of copper resistance. Slashes represent a boundary to which copper resistance cannot move below or above. Red arrows represent the extent to which the strain can revert back to a lower concentration of copper resistance.

Through microevolution, if conditions change and the strain is then exposed to lower concentrations of copper, theoretically the resistance range won't be lost, preserving the extent of acquired resistance. This is indicated by the bounds within Figure 6.10 and is the reasoning behind increased strain stability in microevolution compared with acclimatisation. In acclimatisation, which can be achieved through gradually increasing and prolonging exposure to higher copper concentrations, the range of copper resistance can be increased. However, if a resistant strain is then exposed to lower copper concentrations the resistance range will likely be lowered (demonstrated by larger red arrow in Figure 6.10). Here, in resistant strains created and arisen through acclimatisation, resistance is not bound within a particular range, and therefore strains can revert back to lower copper resistances and are not as stable.

Tolerance to metals through acclimatisation is well known, particularly in polluted environments. Many microalgae strains have been isolated with higher than normal tolerances to metals. Twiss (1990) reported a strain of *Chlamydomonas acidophila* isolated from copper-contaminated soils with tolerances 20-125-times higher than laboratory strains. Strains with higher than normal tolerances to copper have also been produced in the lab through increasing copper concentrations in media (Bossuyt and Janssen, 2004). But the rapid loss of copper tolerance arising through acclimation once the environmental concentration of copper decreases, as described in the previous paragraph, has also been widely observed. Stokes and

Dreier (1981) reported a copper-tolerant *Scenedesmus* maintained over seven years on high-copper medium, lost its tolerance over 10 generations in copper-deficient medium. Therefore, to acquire a stable copper-resistant strain for industrial use requires the identification of a strain arisen by genetic mutation rather than acclimation, where resistance can quickly be reversed.

Although theoretically resistance acquired through genetic mutation is more stable than through acclimatisation, tolerance to metals in microalgae is quickly achievable through acclimatisation. Acclimatisation can occur rapidly to build tolerance to metals. In the experiments previously described by Stokes and Dreier copper tolerance (0.5 mg/L Cu(II)) through acclimation was seen after three generations in *Scenedesmus*. And in experiments by Sandmann and Boger (1980) acclimation of *Scenedesmus* to copper was seen in the first 24 hours of exposure. It would be interesting to test the stability of a copper-acclimatised strain compared with a microevolved strain with a similar level of resistance to attempt to evaluate the difference in stability. This would provide a better understanding of the extent of benefits offered by microevolution for development of strains for use in variable feed-stock bioremediation system.

6.4.2 Reliability of the process

Despite the limited extent of resistance achieved through directed microevolution in this experiment, the opportunity to increase resistance through subsequent rounds suggests the feasibility of possibly producing a pot-ale-copper-level resistant strain. However, as the directed microevolution process is time-consuming, any additional rounds required will extend the time taken to produce a usable strain through microevolution. The recognition of stages in the directed microevolution process, where problems can be encountered also opens up the risk of multiple stages where the method can fail when numerous rounds are required. Potential fail points in the process are highlighted in Figure 6.11 and explained.

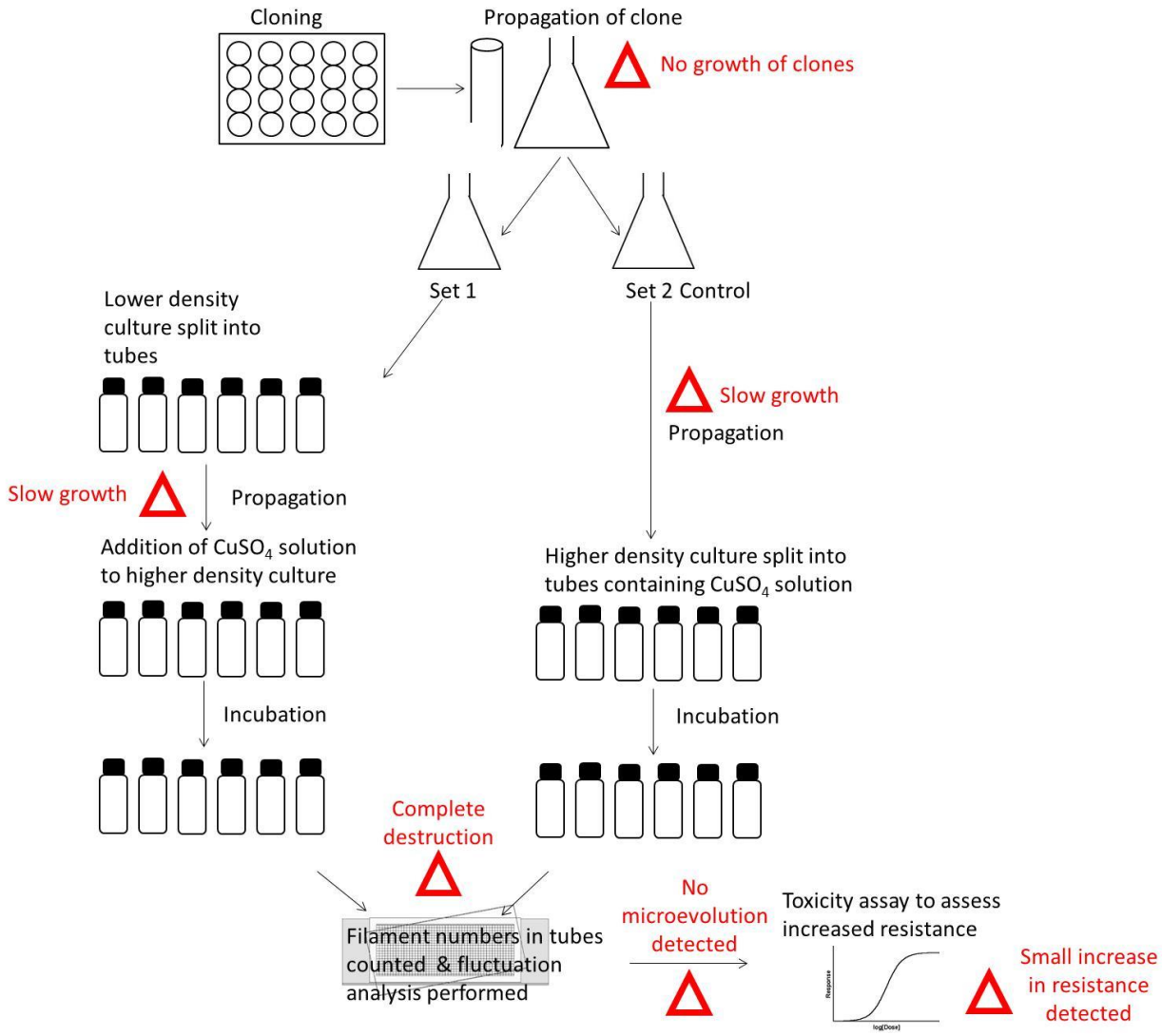

Figure 6.11. Failure points in the directed microevolution process shown by red triangles.

The process itself is lengthy and extensive. The theoretical time-scale of this particular experiment was five months; however, through experience with no guarantee of success at each stage, the process can take much longer. Additionally, because identification relies on the statistical technique of fluctuation analysis, many tubes are required in the experiment. Throughout there are stages where the process can fail. Firstly, the isolation of a single microorganism for the production of a cloned culture at the start of the process can take time. A number of microalgae do not grow well on solid medium, so isolation during cloning must be performed through microdilution, which can be unreliable; microdilution had to be repeated three times here before a cloned culture was successfully obtained. The propagation of a culture from one clone in a small volume to a density observable by the human eye can take over one month. Propagation of a small population of clones to reach the stage at which two sets can be obtained for the experiment can take another month.

During the propagation phase achieving the desired cell density can take time. It is important here too that equal growth rates are achieved in the unselective medium as unequal growth rates can skew final number of filaments at the end of the experiment after exposure. Obtaining resistant cultures in the exposure step is also not guaranteed. Complete destruction of the culture can occur. Even if resistant cultures are obtained, these may not have arisen by microevolution. Moreover, if resistant strains arising from microevolution are identified, the resistance level may only be a small increase upon the original strain. In this case multiple rounds of microevolution will likely be required to achieve a strain with the desired resistance level.

This whole process took nine months from cloning to obtaining a microevolved strain with a known toxicity/resistance increase. During these nine months a strain with resistance to 200-fold the normal medium concentration of copper was created. However, a resistance over 700-fold higher was required for commercial use. Even at the generous estimate of 4 rounds (assuming resistance can be increased by 0.597 mg/L Cu(II) in each round) required to achieve a commercially useful resistant strain, this would likely take three years. An additional risk, during the rounds of directed microevolution, is that limits may be reached where further increases in resistance cannot be achieved. Here the selection pressure (high copper concentration) would be so enormous that mutations cannot provide the resistance required for survival. Not knowing when this limit will be reached contributes to the unreliability of the process for selecting strains with particular resistance levels. This infeasibility defeats any arguments that this process avoids use of a GM-strain falling under regulatory conditions.

6.4.3 Fitness-cost

Experiments involving acclimation and microevolution of organisms to generate resistant populations have observed effects on reduced fitness. In similar experiments on microalgae, Lopez-Rodas (2001) found lower growth rates and maximum cell densities in resistant cultures obtained through microevolution. Other similar observations were also reported by García-Villada et al. (2002). This is known as the "fitness-cost" (Gonzalez, 2012). Such fitness-costs are well known also for bacterial antibiotic resistance (Melnyk, 2015, Schulz zur Wiesch, 2010) and in GM plants (Burdon and Thrall, 2003). It has also been proposed that such fitness-costs could cause resistant cultures to be susceptible to a non-resistant population outcompeting if the selection pressure is reduced, although the reversibility would be slow (Andersson and Hughes, 2010). It may be that any effects reducing growth rates (and perhaps even nutritional content or production of products of interest) may offset the benefits of a GM-free resistance obtained through directed microevolution for use in industrial multi-process bioremediation systems.

6.4.4 Improvements and alternatives

Mutation rates in different organisms are extremely low, vary between organisms and even from gene to gene (Klug and Cummings, 1997). It might be possible to increase mutation rate through the introduction of a mutagen such as UV light exposure, chemicals or atmospheric and room temperature plasmas (Fang, 2013). Using mutagens during the directed microevolution process could increase the number of RSM leading to higher resistances. This may be one way to increase the efficiency of the process.

Genetic transformation has been achieved in over thirty algae species (Enzing, 2012). *Chlamydomonas reinhardtii* has become the model species in microalgae (eukaryotic) molecular biology (Harris, 2009). Although there is a growing understanding of genes involved with metal resistance in microalgae, including copper (Giner-Lamia, 2015, Giner-Lamia, 2012), current main targets in GM of microalgae are focused on increasing growth, particular products or inserting genes for production of new products. There is good knowledge of the *Arthrospira platensis* genome achieved through sequencing (Cheevadhanarak, 2012), but difficulties exist with GM of *Arthospira*. Low stability in transformants and efficiency of foreign gene expression have been reported obstacles (Habib and Parvin, 2008). Given the current science it would be difficult to produce a copper resistant *Arthrospira* strain through GM. Consequently, the generation of a copper resistant strain for industrial use currently must rely on acclimation or the directed microevolution method.

In summary the directed microevolution process explored in this chapter for the development of a copper-resistant *Arthrospira* did achieve a strain with resistance to 200-fold normal medium copper concentration, nevertheless the target resistance of 700-fold was not achieved. The low extent of resistance obtained, significant number of potential failure points throughout the process, the long length of time required and requirement to perform numerous rounds of directed microevolution to get to a target resistance and the unknown fitness of any strain developed, I conclude, make this process impractical for industrial use for generation of resistant *Arthrospira* strains.

Chapter 7. Conclusions and the Future

This chapter concludes the portfolio of projects in this thesis and suggests additional work to explore the findings of this thesis and commercial application. The impact the EngD project has had on the company is explained and the future direction and vision of the company is shared.

Nitrate is an important nutrient for microalgae growth and limitation can cause slowed growth and depletion of particular products of interest. Conditions of nitrate starvation can also cause accumulation of carbohydrates and commercially valuable lipids. It is therefore necessary in aquaculture to monitor nitrate levels in microalgae cultures for purposes of control and optimisation of production. Typical nitrate measuring techniques involve lengthy colorimetric titration, imprecise colour indicator field test kits or more expensive equipment such as nitrate electrodes. Such methods are not applicable for small-scale experimentation involving multiple batches and frequent sampling with limited sample volume. UV absorbance by nitrate had previously been shown to form the basis of a spectroscopic test for microalgae cultures and the first small project validated this approach for two common freshwater and saltwater growth media. A rapid, simple and relatively low-cost technique based on UV absorbance for measurement of nitrate was demonstrated in batches of *Chlorella*, measuring nitrate concentration as low as 40 μM and requiring only a 2 mL sample for three repeat readings. Although inferior in accuracy and sensitivity to colorimetric titration methods, the simplicity and speed of the spectroscopic technique, and requirement for small sample volumes makes it a useful alternative if it meets the accuracy and sensitivity requirements for certain applications. The technique met the company's requirements for a nitrate test that is simple, fast, requires low sample volumes and where costs are low, given the current equipment the company has access to, but which also had the accuracy and sensitivity for use with the concentration ranges of nitrate in common microalgae media. Further experimentation using various alternative filtering techniques to remove organic matter may assist in understanding the extent to which organic matter contributes to inaccuracy caused by interference, leading to appropriate filtering methods to improve the accuracy of the technique, whilst maintaining speed and simplicity.

Microalgae and cyanobacteria are increasingly utilised as natural and sustainable sources of nutraceuticals (nutritional pharmaceuticals). Due to their beneficial bioactive properties these nutraceuticals are used in a wide range of applications ranging from health supplements and skin creams, to foods and animal feeds. Phycocyanin, an anti-oxidising phycobiliprotein, is increasingly used as a natural blue food colouring. The bulk of commercial phycocyanin

production is from the filamentous cyanobacterium *Arthrospira* (*Spirulina*) *platensis*. The second large project evaluated the effects of an unconventional, narrow spectrum Light Emitting Diode (LED) with a maximum wavelength (λ_{max}) of 680 nm for culturing *A. platensis* for phycocyanin production. Compared with standard white LED light, culturing at λ_{max} 680 nm light produced a substantial mean over 250 % increase in phycocyanin yields with no significant difference in growth rate; however, the cultures initially required an extended photoacclimation period, absent in subsequent culture cycles. λ_{max} 680 nm light also increased the extent of phycocyanin leaching from the biomass, which may prove beneficial for downstream processing. The company is now experimenting with different intensities of λ_{max} 680 nm light company to determine the optimum intensity for phycocyanin production in *A. platensis*. Further work will explore the genetic changes occurring under λ_{max} 680 nm light to better understand the mechanisms of acclimation in *Arthrospira* which are still not well understood. Changes in gene expression, indicated by differences in MALDI-TOF mass spectra, can be investigated by microarray technology and changes in the energetics of the photosynthetic apparatus caused by re-modelling could be explored using techniques such as fluorometry. The interesting observations surrounding different leaching properties of biomass cultured under red and white light is also being explored to understand why this is and how this may benefit down-stream processing. Any preservative effects of culturing under a longer wavelength (lower energy) red light on phycocyanin could be investigated through measurement of reactive oxygen species. Finally, and importantly the extent to which phycocyanin yield can be increased through continuing acclimation is being determined and the stability of cultures undergoing continuous acclimation in a commercial system is increasingly being understood.

The use of λ_{max} 680 nm LEDs in photobioreactorsystems was also considered. A simple comparative model demonstrated that despite a small increase in capital and operational expenditure, the use of these LEDs could increase profitability by 400%, thereby making a powerful commercial case for the switch to longer wavelength red LED illumination in artificially lit *Arthrospira* phycocyanin production systems. There are, however, additional design implications associated with using longer wavelength red LEDs. Careful choice of probes in PBR systems will be needed as longer wavelength red light can interfere with optical sensors operating on LED optics. Although heating effects associated with longer wavelength red LEDs did not cause temperature control problems, there are limitations and cost-implications in the design of large long-wavelength LED arrays for large-scale systems due to increased LED cooling requirements. However, the problems of heat generation can potentially

be solved by using submerged internal illumination, which may have additional benefits in maintaining a stable culture temperature. Submerged internal illumination with λ_{max} 680 nm LEDs is currently being trialled by the company.

The third project was a feasibility study. Microalgae are promising microorganisms for bioremediation of contaminated wastewaters and recovery of precious metals, given their ability to accumulate and tolerate metal burdens. Resistance to metals can occur through acclimatisation (reversible phenotypic changes) or microevolution (permanent genetic changes) where resistance is more stable. Techniques exist to identify resistance arising through microevolution in microalgae. The feasibility of selecting a 'microevolved' strain of *Arthrospira* with high resistance to copper was investigated, using a Luria–Delbrück-style experiment and fluctuation analysis. Such a strain could be used to bioremediate pot ale, a high copper wastewater produced from whisky distilling. Further, microevolution avoids regulations concerning the use of genetically modified organisms. Resistant *Arthrospira* were not obtained for Cu(II) concentrations above 1 mg/L. Conversely, for concentrations of 0.3 mg/L fluctuation analysis showed that pre-selective spontaneous random mutations were not responsible for the observed resistance. Microevolution was confirmed at 0.6 mg/L, 200-fold of the optimal copper concentration. This concentration was over 3-fold lower than the resistance required for pot ale bioremediation. The low extent of resistance obtained and length and unreliability of the process, including possible fitness-costs concluded the process to be impractical for industrial use in generating resistant *Arthrospira* strains. However, it is possible that the technique could be better applied in situations where lower-level resistance is required and when microorganism numbers can be counted using automated techniques such as flow cytometry.

The projects of this thesis have provided a nitrate measurement methodology to assist the company in future research and development, tested the feasibility of a strain development technique and provided valuable knowledge on the effects of culturing *Arthrospira* under a longer wavelength LED. The most important outcome of the whole EngD project has been the identification of a new business opportunity for the company for production of a high-value product, phycocyanin, in artificially illuminated PBR systems. The exploration early in the project through a period of desk-based research achieved a clearer understanding of microalgae biotechnology, microalgae-derived products and emerging markets for those products. During this time expertise from within the University and wider networks was drawn upon. This research identified *Arthrospira* as an organism of interest and phycocyanin as a product of increasing interest with growing markets. The high value of the pigment and available existing

information on growth and processing of the organism made it a good prospect for a new research focus and business direction at a time when a new business direction was needed.

The unexpected discovery of long wavelength red light having effects of significantly increasing the phycocyanin content of *Arthrospira* generated new protectable intellectual property, which became a valuable asset for the company for which a new business could be built upon. Two patent applications were filed as a result of the EngD project WO2014102551A1 (Van Alstyne, 2014) and WO15110844A1 (Brain, 2015). Protection is being sought at National Phase in a number of territories aligning with key markets for phycocyanin including China, Japan, US, Europe, Australia and Korea.

In May 2015 the company moved into the Roslin BioCentre at the University of Edinburgh and set up a pilot-plant facility to begin developing their up-stream and down-stream production processes for production of phycocyanin in *Arthospira.* After successful pilot-scale studies at 14,000 L and business model validation the company will soon be moving to bigger premises in BioCity Scotland to set-up a 98,000 L production facility. This facility will allow the commercial production of phycocyanin in a controlled clean laboratory environment.

As the ever growing demand for phycocyanin has seen production facilities world-wide reach capacity and where supply is struggling to keep up with demand, this has created a timely opportunity for the company. The company has been working on sourcing and securing their equipment supply lines and developing their business plan based on a negotiated market price of phycocyanin at the purity achievable. The company is currently in talks with a number of major food and drink manufacturers who are looking for a supply of phycocyanin and have investment secured for the next stage of scale-up. The company is currently valued at £1.5 million, has won a number of large grants and has developed further collaborations, including with The University of Cambridge to explore the potential of synthetic biology. The current focus of Scottish Bioenergy is the supply of phycocyanin for the food and drink industry with a future eye on achieving Current Good Manufacturing Practice (cGMP) compliance for higher-purity, higher-value phycocyanin supply for pharmaceutical applications. Out of the pilot-scale studies has also developed a higher phycocyanin producing strain, well adapted to growth under long wavelength red light and established to the conditions of the current production system, which is another valuable asset to the company.

David Van Alstyne, the CEO of Scottish Bioenergy, believes the EngD project has been critical to the survival and now growing achievements of the company. The EngD project is a tremendously positive example of an industry-academia collaboration from which not only has

incredibly interesting scientific findings arisen, but also which has provided a lifeline and new business opportunities to a UK SME. The company continues to build and maintain collaborations with UK universities and has high ambitions to become a leading global supplier of traceable nutritional and pharmaceutical ingredients.

References

AASEN, A. J., EIMHJELLEN, K.E., LIAAEN-JENSEN, S. 1969. An extreme source of beta-carotene. *Acta Chemica Scandinavica,* 23**,** 2544-2545.

ABUGHAZALEH, A. A., POTU, R.B., IBRAHIM, S. 2009. Short communication: the effect of Substituting fish oil in dairy cow diets with docosahexaenoic acid-micro algae on milk composition and fatty acids profile. *Journal of Dairy Science,* 92**,** 6156-6159.

AKIMOTO, S., YOKONO, M., HAMADA, F., TESHIGAHARA, A., AIKAWA, S. & KONDO, A. 2012. Adaptation of light-harvesting systems of Arthrospira platensis to light conditions, probed by time-resolved fluorescence spectroscopy. *Biochimica et Biophysica Acta (BBA) - Bioenergetics,* 1817**,** 1483-1489.

ALBERT, C. M., HENNEKENS, C.H., O'DONNELL, C.J., AJANI, U.A., CAREY, V.J., WILLETT, W.C., RUSKIN, J.N., MANSONM, J.E. 1998. Fish consumption and risk of sudden cardiac death. *Journal of the American Medical Association,* 279**,** 23-28.

ALUWIHARE, L. I., REPETA, D.J. 1999. A comparison of the chemical characteristics of oceanic DOM and extracellular DOM produced by marine algae. *Marine Ecology-Progress Series,* 186**,** 105-117.

ALBERTS, B., JOHNSON, A., LEWIS, J., RAFF, M., ROBERTS, K., WALTER, P. 2002. *Molecular biology of the cell,* New York, Garland Science.

ALEXANDER, M. 1999. *Biodegradation and Bioremediation,* San Diego, Academic Press.

ALGAE INDUSTRY MAGAZINE 2015. Natural food color demand boosting spirulina sales [Online]. Available: http://www.algaeindustrymagazine.com/natural-food-color-demand-boosting-spirulina-sales/).

ALI, S. K. & SALEH, A. M. 2012. Spirulina - an overview. *International Journal of Pharmacy and Pharmaceutical Sciences,* 4**,** 9-15.

ALLEN, M. M. & SMITH, A. J. 1969. Nitrogen chlorosis in blue-green algae. *Archiv für Mikrobiologie,* 69**,** 114-120.

ALPERT, P. & SIMMS, E. L. 2002. The relative advantages of plasticity and fixity in different environments: when is it good for a plant to adjust? *Evolutionary Ecology,* 16**,** 285-297.

AMIN, S. A., GREEN, D.H., HART, M.C., KÜPPER, F.C., SUNDA, W.G., CARRANO, C.J. 2009. Photolysis of iron-siderophore chelates promotes bacterial-algal mutualism. *Proceedings of the National Academy of Sciences of the United States of America,* 106**,** 17071-1707.

ANDERSEN, R. 2005. *Algal culturing techniques,* London, Academic Press.

ANDERSSON, D. I. & HUGHES, D. 2010. Antibiotic resistance and its cost: is it possible to reverse resistance? *Nature Reviews Microbiology,* 8**,** 260-271.

AZAR, K. 2012. *Lighting the way for LED development* [Online]. Available: http://www.designworldonline.com/lighting-the-way-for-led-development/#.

AZEVEDO, I. L., MORGAN, M.G., MORGAN, F. 2009. The transition to solid-state lighting. *Proceedings of the IEEE* 97**,** 481-510.

AZOV, Z. 1982. Effect of pH on inorganic carbon uptake in algal cultures. *Applied and Environmental Microbiology,* 43**,** 1300-1306.

BABU, T. S., KUMAR, A., VARMA, A.K. 1991. Effect of light quality on phycobilisome components of the cyanobacterium Spirulina platensis. *Plant Physiology,* 95**,** 492-497.

BARBANO, D., DIAZ, R., ZHANG, L., SANDRIN, T., GERKEN, H. & DEMPSTER, T. 2015. Rapid characterization of microalgae and microalgae mixtures using Matrix-Assisted Laser Desorption Ionization Time-Of-Flight Mass Spectrometry (MALDI-TOF MS). *PLoS One,* 10**,** e0135337.

BARBER, J. 2008 Photosynthetic generation of oxygen. *Philosophical Transactions of the Royal Society of London B Biological Sciences,* 363**,** 2665–2674.

BARBOSA, M. J., JANSSEN, M., HAM, N., TRAMPER, J., WIJFFELS, R.H. 2003. Microalgae cultivation in air-lift reactors: modeling biomass yield and growth rate as a function of mixing frequency. *Biotechnology and Bioengineering,* 82**,** 170-179.

BASSHIR, N. 2014. From lab-scale to scale-up: Commercialising products from microalgae-challenges and opportunities. Phyconet (BBSRC NIBB) symposium, April 14th, London.

BECKER, E. W. 1994. *Microalgae: Biotechnology and Microbiology,* Cambridge, Cambridge University Press.

BEKASOVA, O. D., SHUBIN, L. M. & EVSTIGNEEV, V. B. 1979. Phycobilisomes from the blue-green algae Aphanizomenon flos-aquae and Anabaena variabilis. *Biology Bulletin of the Academy of Sciences of the USSR,* 6**,** 164-72.

BELAY, A. 2002. The potential application of Spirulina (Arthrospira) as a nutritional and therapeutic supplement in health management. *The Journal of the American Nutraceutical Association,* 5**,** 27-48.

BEN-AMOTZ, A., KATZ, A., AVRON, M. 1982. Accumulation of β-carotene in halotolerant algae: Purification and characterization of β-carotene rich globules from Dunaliella bardawil (Chlorophyceae). *Journal of Phycology,* 18**,** 529-537.

BEN-AMOTZ, A., AVRON, M. 1983. Accumulation of metabolites by halotolerant algae and its industrial potential. *Annual Review of Microbiology,* 37**,** 95-119.

BEN-AMOTZ, A., LEVY, Y. 1996. Bioavailability of a natural isomer mixture compared with synthetic all-trans β-carotene in human serum. *American Journal of Clinical Nutrition,* 63**,** 729-734.

BENEDETTI, S., BENVENUTI, F., PAGLIARANI, S., FRANCOGLI, S., SCOGLIO, S. & CANESTRARI, F. 2004. Antioxidant properties of a novel phycocyanin extract from the blue-green alga Aphanizomenon flos-aquae. *Life Sciences,* 75**,** 2353-2362.

BENEMANN, J. 2013. Microalgae for biofuels and animal feeds. *Energies,* 6**,** 5869-5886.

BENNETT, A. & BOGORAD, L. 1973. Complementary chromatic adaptation in a filamentous blue-green alga. *The Journal of Cell Biology,* 58**,** 419-435.

BERGLUND, O., LARSSON, P., EWALD, G., OKLA, L. 2001. The effect of lake trophy on lipid content and pcb concentrations in planktonic food webs. *Ecology,* 82**,** 1078-1088.

BHAT, V. B. & MADYASTHA, K. M. 2000. C-phycocyanin: a potent peroxyl radical scavenger in vivo and in vitro. *Biochemical and Biophysical Research Communications,* 275**,** 20-25.

BIEBL, H., ALLGAIER, M., LUNSDORF, H., PUKALL, R., TINDALL, B. J. & WAGNER-DOBLER, I. 2005. Roseovarius mucosus sp. nov., a member of the Roseobacter clade with trace amounts of bacteriochlorophyll a. *International Journal of Systematic and Evolutionary Microbiology,* 55**,** 2377-83.

BJÖRN, L., PAPAGEORGIOU, G., BLANKENSHIP, R. & GOVINDJEE. 2009. A viewpoint: why chlorophyll a? *Photosynthesis Research,* 99**,** 85-98.

BLANKEN, W., CUARESMA, M., WIJFFELS, R. H. & JANSSEN, M. 2013. Cultivation of microalgae on artificial light comes at a cost. *Algal Research,* 2**,** 333-340.

BOGORAD, L. 1975. Phycobiliproteins and complementary chromatic adaptation. *Annual Review of Plant Physiology,* 26**,** 369-401.

BOROWITZKA, L. J., BOROWITZKA, M.A. 1989. B-carotene (Provitamin A) production with algae. *In:* VANDAMME, E. J. (ed.) *Biotechnology of vitamins, pigments and growth factors.* London: Elsevier Applied Science.

BOSSUYT, B. T. & JANSSEN, C. R. 2004. Long-term acclimation of Pseudokirchneriella subcapitata (Korshikov) Hindak to different copper concentrations: changes in tolerance and physiology. *Aquatic Toxicology,* 68**,** 61-74.

BOUSSIBA, S. & RICHMOND, A. E. 1979. Isolation and characterization of phycocyanins from the blue-green alga Spirulina platensis. *Archives of Microbiology,* 120**,** 155-159.

BRADSHAW, A. D., HARDWICK, K. 1989. Evolution and stress—genotypic and phenotypic components. *Biological Journal of the Linnean Society,* 37**,** 137-155.

BRAIN, C. M., CALDWELL, G.S. 2015. 'Improvements in the Synthesis of Phycocyanins' published as WO2015110844A1 on 30th July 2015. https://www.google.co.uk/webhp?sourceid=chrome-instant&ion=1&espv=2&ie=UTF-8#q=WO+number+patent&*.

BREUER, G., LAMERS, P. P., MARTENS, D. E., DRAAISMA, R. B. & WIJFFELS, R. H. 2012. The impact of nitrogen starvation on the dynamics of triacylglycerol accumulation in nine microalgae strains. *Bioresource Technology,* 124**,** 217-226.

BRITISH STANDARDS INSTITUTION 2006. Water quality. Marine algal growth inhibition test with Skeletonema costatum and Phaeodactylum tricornutum, British Standard BS EN ISO 10253:2006.

BUCHAN, A., GONZALEZ, J. M. & MORAN, M. A. 2005. Overview of the marine roseobacter lineage. *Applied and Environmental Microbiology,* 71**,** 5665-5677.

BURDON, J. J. & THRALL, P. H. 2003. The fitness costs to plants of resistance to pathogens. *Genome Biology,* 4**,** 227.

BURKE, S. 2001. Regression and calibration. LC-GC Europe online supplement statistics and data analysis. 13-18.

BUX, F. 2013. *Biotechnological applications of microalgae: biodiesel and value-added products,* Florida, CRC Press.

CAIRNS, J., OVERBAUGH, J., & MILLER, S. 1988. The origin of mutants. *Nature,* 335**,** 142-145.

CARR, N. G. 1988. *Nitrogen reserves and dynamic reservoirs in cyanobacteria,* Oxford, Clarendon Press.

CARVALHO, A. P., SILVA, S. O., BAPTISTA, J. M. & MALCATA, F. X. 2011. Light requirements in microalgal photobioreactors: an overview of biophotonic aspects. *Applied Microbiology and Biotechnology,* 89**,** 1275-1288.

CAVET, J. S., BORRELLY, G. P. & ROBINSON, N. J. 2003. Zn, Cu and Co in cyanobacteria: selective control of metal availability. *FEMS Microbiology Reviews,* 27**,** 165-181.

CHAIKLAHAN, R., CHIRASUWAN, N. & BUNNAG, B. 2012. Stability of phycocyanin extracted from Spirulina sp.: Influence of temperature, pH and preservatives. *Process Biochemistry,* 47**,** 659-664.

CHAVES, M. E., ARAÚJO, A. R., PIANCASTELLI, A. C., & PINOTTI, M. 2014. Effects of low-power light therapy on wound healing: LASER x LED *Anais Brasileiros de Dermatologia,* 89**,** 616-623.

CHEEVADHANARAK, S., PAITHOONRANGSARID, K., PROMMEENATE, P., KAEWNGAM, W., MUSIGKAIN, A. ET AL. 2012. Draft genome sequence of Arthrospira platensis C1 (PCC9438). *Standards in Genomic Sciences,* 6**,** 43-53.

CHEKROUN, K. B., SANCHEZ, E., BAGHOUR, M. 2014. The role of algae in bioremediation of organic pollutants. *International Research Journal of Public and Environmental Health,* 1**,** 19-32.

CHEN, H.-B., WU, J.-Y., WANG, C.-F., FU, C.-C., SHIEH, C.-J., CHEN, C.-I., WANG, C.-Y. & LIU, Y.-C. 2010a. Modeling on chlorophyll a and phycocyanin production by Spirulina platensis under various light-emitting diodes. *Biochemical Engineering Journal,* 53**,** 52-56.

CHEN, M., SCHLIEP, M., WILLOWS, R. D., CAI, Z. L., NEILAN, B. A. & SCHEER, H. 2010b. A red-shifted chlorophyll. *Science,* 329**,** 1318-1319.

CHHAJED, S., XI, Y., GESSMANN, T., XI, J.-Q., SHAH, J. M., KIM, J. K. & SCHUBERT, E. F. Junction temperature in light-emitting diodes assessed by different methods. SPIE Proceedings 25th March 2005 California, USA. 16-24.

CHIU, H.-F., YANG, S.-P., KUO, Y.-L., LAI, Y.-S. & CHOU, T.-C. 2006. Mechanisms involved in the antiplatelet effect of C-phycocyanin. *British Journal of Nutrition,* 95**,** 435-440.

CHOI, G. G., BAE, M. S., AHN, C. Y. & OH, H. M. 2008. Induction of axenic culture of Arthrospira (Spirulina) platensis based on antibiotic sensitivity of contaminating bacteria. *Biotechnology Letters,* 30**,** 87-92.

CHOI, G., AHN, C., OH, H. 2012. Phylogenetic relationships of arthrospira strains inferred from 16S rRNA gene and cpcBA-IGS sequences. *Algae,* 27**,** 75-82.

CHOJNACKA, K., CHOJNACKI, A. & GORECKA, H. 2005. Biosorption of Cr3+, Cd2+ and Cu2+ ions by blue-green algae Spirulina sp.: kinetics, equilibrium and the mechanism of the process. *Chemosphere,* 59**,** 75-84.

CHRISTENSON, T. A., HORTON, M. E., JACKSON, B. C., SMITH, G. R. & RETTIG, J. E. 2014. Effects of Cutrine-Plus® algaecide and predators on wood frog (Lithobates sylvaticus) tadpole survival and growth. *Environmental Science and Pollution Research,* 21**,** 12472-12478.

COHEN, Y., JØRGENSEN, B.B., REVSBECH, N.P., POPLAWSKI, R. 1986. Adaptation to hydrogen sulfide of oxygenic and anoxygenic photosynthesis among cyanobacteria. *Applied and Environmental Microbiology,* 51**,** 398–407.

COLLARD, J. M., & MATAGNE, R. F. 1990. Isolation and genetic analysis of Chlamydomonas reinhardtii strains resistant to cadmium. *Applied and Environmental Microbiology,* 56**,** 2051–2055.

COLLOS, Y. & BERGES, J. A. 2009. Nitrogen metabolism in phytoplankton. *In:* DUARTE, C. M., HELGUERAS, L.M. (ed.) *Marine Ecology.* Oxford: EOLSS.

COLLOS, Y., MORNET, F., SCIANDRA, A., WASER, N., LARSON, A. & HARRISON, P. J. 1999. An optical method for the rapid measurement of micromolar concentrations of nitrate in marine phytoplankton cultures. *Journal of Applied Phycology,* 11**,** 179-184.

COMETTA, A., ZUCCHELLI, G., KARAPETYAN, N. V., ENGELMANN, E., GARLASCHI, F. M. & JENNINGS, R. C. 2000. Thermal behavior of long wavelength absorption transitions in Spirulina platensis photosystem I trimers. *Biophysical Journal,* 79**,** 3235-3243.

CONSUMER ENERGY CENTRE. 2017. California Energy Comission. Incandescent, LED, Fluorescent, Compact Fluorescent and Halogen Bulbs [Online]. Available: http://www.consumerenergycenter.org/lighting/bulbs.html.

CRAWFORD, E. 2015. Demand for natural colors increases as 80% of parents cite artificial color safety concerns, survey finds [Online]. Available: http://www.foodnavigator-usa.com/R-D/Natural-color-demand-increases-as-parents-site-safety-concerns.

CROFT, M. T., LAWRENCE, A. D., RAUX-DEERY, E., WARREN, M. J. & SMITH, A. G. 2005. Algae acquire vitamin B12 through a symbiotic relationship with bacteria. *Nature,* 438**,** 90-93.

DAHL, R. 2008. *Light-Emitting Diodes: A Primer in Photonics Handbook* [Online]. Available: http://www.photonics.com/EDU/Handbook.aspx?AID=36706.

DANESI, E. D. G., RANGEL-YAGUI, C. O., CARVALHO, J. C. M. & SATO, S. 2004. Effect of reducing the light intensity on the growth and production of chlorophyll by Spirulina platensis. *Biomass and Bioenergy,* 26**,** 329-335.

DARKO, E., HEYDARIZADEH, P., SCHOEFS, B. & SABZALIAN, M. R. 2014. Photosynthesis under artificial light: the shift in primary and secondary metabolism. *Philosophical Transactions of the Royal Society of London B: Biological Sciences,* 369**,** 20130243.

DAS, K. & ROYCHOUDHURY, A. 2014. Reactive oxygen species (ROS) and response of antioxidants as ROS-scavengers during environmental stress in plants. *Frontiers in Environmental Science,* 2**,** 1-13.

DAS, S. & KHANGAROT, B. S. 2011. Bioaccumulation of copper and toxic effects on feeding, growth, fecundity and development of pond snail Lymnaea luteola L. *J Hazard Mater,* 185**,** 295-305.

DAVIGLUS, M. L., STAMLER, J., ORENCIA, A.J., DYER, A.R., LIU, K., GREENLAND, P., WALSH, M.K., MORRIS, D., SHEKELLE, R.B. 1997. Fish consumption and the 30-year risk of fatal myocardial infarction. *New England Journal of Medicine,* 336**,** 1046-1053.

DE JESUS RAPOSO, M. F., DE MORAIS, R. M. S. C. & DE MORAIS, A. M. M. B. 2013. Health applications of bioactive compounds from marine microalgae. *Life Sciences,* 93**,** 479-486.

DE LOURA, I. C., DUBACQ, J. P. & THOMAS, J. C. 1987. The effects of nitrogen deficiency on pigments and lipids of cyanobacteria. *Plant Physiology,* 83**,** 838-843.

DEGNAN, P. H. & OCHMAN, H. 2012. Illumina-based analysis of microbial community diversity. *International Society for Microbial Ecology Journal,* 6**,** 183-94.

DEUBLEIN, D., STEINHAUSER, A. 2011. *Biogas from waste and renewable resources: an introduction,* Weinheim., Wiley-VCH.

DIONISI, D., BRUCE, S.S., BARRACLOUGH, M.J. 2012. Effect of pH adjustment, solid-liquid separation and chitosan adsorption on pollutants' removal from pot ale wastewaters. *Journal of Environmental Chemical Engineering,* 2**,** 1929-1936.

DISMUKES, G. C., CARRIERI, D., BENNETTE, N., ANANYEV, G.M., POSEWITZ, M.C. 2008. Aquatic phototrophs: efficient alternatives to land-based crops for biofuels. *Current Opinion in Biotechnology,* 19**,** 235-240.

DOMINGUEZ, H. 2013. *Functional ingredients from algae for foods and nutraceuticals,* Cambridge, Woodhead Publishing.

DORAN, P. M. 2005. *Bioprocess Engineering Principles,* London, Academic press.
DOSHI, H., RAY, A. & KOTHARI, I. L. 2007. Bioremediation potential of live and dead Spirulina: spectroscopic, kinetics and SEM studies. *Biotechnology and Bioengineering,* 96**,** 1051-1063.
DUCRET, A., SIDLER, W., WEHRLI, E & FRANK, G. Isolation, characterisation and electron microscopy analysis of a hemidiscoidal phycobilisome type from the cyanobacterium Anabaena sp. PCC 7120. *The FEBS Journal,* 236**,** 1010-1024.
EL-KASSAS, H. Y. & MOHAMED, L. A. 2014. Bioremediation of the textile waste effluent by Chlorella vulgaris. *The Egyptian Journal of Aquatic Research,* 40**,** 301-308.
EMAMI, K., HACK, E., NELSON, A., BRAIN, C. M., LYNE, F. M., MESBAHI, E., DAY, J. G. & CALDWELL, G. S. 2015. Proteomic-based biotyping reveals hidden diversity within a microalgae culture collection: an example using Dunaliella. *Scientific Reports,* 5**,** 10036.
ENERGY.GOV ENERGY SAVER. *LED lighting* [Online]. Available: http://energy.gov/energysaver/led-lighting.
ENGELMANN, T. W. 1902. Uber experimentelle erzeugung zwechmassiger anderung der farbung pflanzlicher chromophylle durch farbiges Licht. *Archiv für Anatomie und Physiologie,* 333.
ENZING, C., NOOIJEN, A., EGGINK, G., SPRINGER, J.,WIJFFELS, R. 2012. Algae and genetic modification: Research, production and risks. CGM 2012-05 Onderoeksrapport.
EPSRC 2011. The EPSRC Industrial Doctorate Centre Scheme Good Practice Guidance.
ERIKSEN, N. 2008. The Technology of Microalgal Culturing. *Biotechnology Letters,* 30**,** 1525-1536.
EUROPEAN COUNCIL 1991. Council Directive 91/676/EEC of the of 12 December 1991 concerning the protection of waters against pollution caused by nitrates from agricultural sources. Official Journal L 375, 31.12.1991, p. 1-8.
EUROPEAN PARLIAMENT 2000. Directive 2001/18/EC 2000/60/EC of the European Parliament and of the Council of 23 October 2000 on establishing a framework for the Community action in the field of water policy. Official Journal L 327, 22.12.2000, p. 1-73.
EUROPEAN PARLIAMENT 2001. Directive 2001/18/EC of the European Parliament and of the Council of 12 March 2001 on the deliberate release into the environment of genetically modified organisms and repealing Council Directive 90/220/EEC - Commission Declaration. Official Journal L 106, 17.4.2001, p. 1–39.
EUROPEAN PARLIAMENT 2009. Directive 2009/41/EC of the European Parliament and of the Council of 6 May 2009 on the contained use of genetically modified micro-organisms. Official Journal L 125, 21.5.2009, p. 75–97.
EVANS, J. D. 1996. *Straightforward statistics for the behavioral sciences,* Pacific Grove, California, Brooks/Cole Publishing.
FALKOWSKI, P. G. & RAVEN, J. A. 2007. *Aquatic photosynthesis,* New Jersey, Princeton University Press.
FANG, M., JIN, L., ZHANG, C., TAN, Y., JIANG, P., GE, N. ET AL. 2013. Rapid mutation of Spirulina platensis by a new mutagenesis system of atmospheric and room temperature plasmas (ARTP) and generation of a mutant library with diverse phenotypes. *PLoS ONE,* 8**,** e77046.
FARGES, B., LAROCHE, C., CORNET, J.-F. & DUSSAP, C.-G. 2009. Spectral kinetic modeling and long-term behavior assessment of Arthrospira platensis growth in photobioreactor under red (620 nm) light illumination. *Biotechnology Progress,* 25**,** 151-162.
FEDLER, C. B. 2006. Potential Biomass Production from Recycled Wastewater. *BioCycle,* 47**,** 46-50.
FOSTER, P. L. 2006. Methods for determining spontaneous mutation rates. *Methods in Enzymology,* 409**,** 195-213.
FOYER, C. H. & NOCTOR, G. 2005. Redox homeostis and antioxidant signaling: a metabolic interface between stress perception and physiological responses. *Plant and Cell Physiology,* 17**,** 1866-1875.
FRANKLIN, S. T., MARTIN, K.R., BAER, R.J., SCHINGOETHE, D.J., HIPPEN, A.R. 1991. Dietary marine algae (Schizochytrium sp.) increases concentrations of conjugated linoleic, docosahexaenoic and transvaccenic acids in milk of dairy cows. *Journal of Nutrition* 129**,** 2048-2054.

FUKUI, K., SAITO, T., NOGUCHI, Y., KODERA, Y., MATSUSHIMA, A., NISHIMURA, H. & INADA, Y. 2004. Relationship between color development and protein conformation in the phycocyanin molecule. *Dyes and Pigments,* 63**,** 89-94.

FUTURE MARKET INSIGHTS 2016. Spirulina extracts market: global industry analysis and opportunity assessment 2015-2025 [Online]. Available: http://www.futuremarketinsights.com/reports/spirulina-extracts-market.

GAN, F., ZHANG, S., ROCKWELL, N.C., MARTIN, S.S., LAGARIAS, J.C., & BRYANT, D. A. 2014. Extensive remodeling of a cyanobacterial photosynthetic apparatus in far-red light. *Science***,** 1312-1317.

GARCÍA-VILLADA, L., LÓPEZ-RODAS, V., BAÑARES-ESPAÑA, E., FLORES-MOYA, A., AGRELO, M., MARTÍN-OTERO, L. & COSTAS, E. 2002. Evolution of microalgae in highly stressing environments: An experimental model analyzing the rapid adaptation of dictyosphaerium chlorelloides (chlorophyceae) from sensitivity to resistance against 2,4,6-trinitrotoluene by rare preselective mutations. *Journal of Phycology,* 38**,** 1074-1081.

GATTULLO, C. E., BAHRS, H., STEINBERG, C. E. & LOFFREDO, E. 2012. Removal of bisphenol A by the freshwater green alga Monoraphidium braunii and the role of natural organic matter. *The Science of the Total Environment,* 416**,** 501-506.

GERSHWIN, M. E. & BELAY, A. 2007. *Spirulina in human nutrition and health,* Florida, CRC Press.

GILL, S. S. & TUTEJA, N. 2010. Reactive oxygen species and antioxidant machinery in abiotic stress tolerance in crop plants. *Plant physiology and biochemistry,* 48**,** 909-30.

GILLHAM, N. W. 1965. Induction of chromosomal and nonchromosomal mutations in chlamydomonas reinhardi with n-methyl-n'-nitro-n-nitrosoguanidine. *Genetics,* 52**,** 529-537.

GINER-LAMIA, J., LÓPEZ-MAURY, L., REYES, J. C., FLORENCIO, F. J. 2012. The CopRS two-component system is responsible for resistance to copper in the cyanobacterium Synechocystis sp. PCC 6803. *Plant Physiology,* 159**,** 1806-1818.

GINER-LAMIA, J., LOPEZ-MAURY, L. & FLORENCIO, F. J. 2015. CopM is a novel copper-binding protein involved in copper resistance in Synechocystis sp. PCC 6803. *MicrobiologyOpen,* 4**,** 167-185.

GLAZER, A. N. 1982. Phycobilisomes: structure and dymanics. *Annual Review of Microbiology,* 36**,** 173-198.

GLAZER, A. N. 1985. Light harvesting by phycobilisomes. *Annual Review of Biophysics and Biophysical Chemistry,* 14**,** 47-77.

GLEMSER, M., HEINING, M., SCHMIDT, J., BECKER, A., GARBE, D., BUCHHOLZ, R. & BRUCK, T. 2015. Application of light-emitting diodes (LEDs) in cultivation of phototrophic microalgae: current state and perspectives. *Applied Microbiology and Biotechnology,* 100**,** 107-1088.

GODFREY, P. 2012. The Engineering Doctorate (EngD): Developing Leaders for Tomorrow with Industry, in CLAIU – EU (Council of Association of long-cycle Engineers, of a university or higher school of engineering of the European Union), Madrid.

GOLDMAN, J. C., AZOV, Y., RILEY, C.B., DENNETT, M.R. 1982. The effect of pH in intensive microalgal cultures. I. Biomass regulation. *Journal of Experimental Marine Biology and Ecology,* 57**,** 1-13.

GONZALEZ, R., RODRIGUEZ, S., ROMAY, C., GONZALEZ, A., ARMESTO, J., REMIREZ, D. & MERINO, N. 1999. Anti-inflammatory activity of phycocyanin extract in acetic acid-induced colitis in rats. *Pharmacological Research,* 39**,** 55-59.

GONZALEZ, R., GARCÍA-BALBOA, C., ROUCO, M., LOPEZ-RODAS, V. & COSTAS, E. 2012. Adaptation of microalgae to lindane: a new approach for bioremediation. *Aquatic Toxicology,* 109**,** 25-32.

GORDON, J., POLLE, J. 2007. Ultrahigh bioproductivity from algae. *Applied Microbiology and Biotechnology,* 76**,** 969-975.

GRAHAM, J., PETER, B., WALKER, G.M., WARDLAW, A., CAMPBELL, E. 2012. Characterisation of the pot ale profile from a malt whisky distillery. *Distilled Spirits: Science and Sustainability* Nottingham: Nottingham University Press.

GRATÃO, P. L., POLLE, A., LEA, P. J. & AZEVEDO, R. A. 2005. Making the life of heavy metal-stressed plants a little easier. *Functional Plant Biology,* 32**,** 481-494.

GRIFFITHS, M. J., GARCIN, C., VAN HILLE, R. P. & HARRISON, S. T. L. 2011. Interference by pigment in the estimation of microalgal biomass concentration by optical density. *Journal of Microbiological Methods,* 85**,** 119-123.

GRIGOROVA, S. 2005. Dry biomass of fresh water algae of Chlorella genus in the combined forages for laying hens. *Central European Agriculture,* 6**,** 625-630.

GROSSMAN, A. R., SCHAEFER, M.R., CHIANG, G.G., & COLLIER, J. L. 1993. The phycobilisome, a light-harvesting complex responsive to environmental conditions. *Microbiology Reviews,* 57**,** 725-749.

GUIKEMA, J. A. & SHERMAN, L. A. 1983. Organization and function of chlorophyll in membranes of cyanobacteria during iron starvation *Plant Physiology,* 73**,** 250–256.

GUILLARD, R. R. L. & RYTHER, J. H. 1962. Studies on marine planktonic diatoms. I. Cyclotella nana Hustedt, and Detonula confervaceae (cleve) Gran. *Canadian Journal of Microbiology,* 8**,** 229-239.

GULBRANDSEN, M. & SLIPERSÆTER, S. 2007. The third mission and the entrepreneurial university model. *In:* BONACCORSI, A. & DARAIO, C. (eds.) *Universities and strategic knowledge creation: specialization and performance in europe.* Cheltenham: Edward Elgar.

GUPTA, P. L., LEE, S. M. & CHOI, H. J. 2015. A mini review: photobioreactors for large scale algal cultivation. *World Journal of Microbiology & Biotechnology,* 31**,** 1409-1417.

HABIB, M. A. B., PARVIN, M. 2008. A review on culture, production and use of Spirulina as food for humans and feeds for domestic animals and fish. (FAO Fisheries and Aquaculture Circular no. 1034). Food and Agriculture Organisation (FAO) of the United Nations.

HAITZ, R., F. KISH, J. TSAO, & J. NELSON. 1999. The case for a national research program on semiconductor lighting. Annual forum of the Optoelectronics Industry Development Association. Washington, D.C.

HAITZ, R. & TSAO, J. Y. 2011. Solid-state lighting: the case 10 years after and future prospects. *Physica Status Solidi (a),* 208**,** 17-29.

HALDER, S. 2014. Bioremediation of heavy metals through fresh water microalgae: a review. *Scholars Academic Journal of Biosciences,* 2**,** 825-830.

HALLIWELL, B. 2003. Free radicals and other reactive species in disease. *eLS.*

HALLIWELL, B. 2006. Reactive species and antioxidants. Redox biology is a fundamental theme of aerobic life. *Plant Physiology,* 141**,** 312-322.

HAMMOUDA, O., GABER, A., ABDELRAOUF, N. 1995. Microalgae and wastewater treatment. *Ecotoxicology and Environmental Safety,* 31**,** 205-210.

HARRIS, E. H., STERN, D.B., WITMAN, G.B. 2009. *The Chlamydomonas Sourcebook,* Oxford, Academic Press.

HARRISON, P. J., WATERS, R.E., & TAYLOR, F. J. R. 1980. A broad spectrum artificial seawater medium for coastal and open ocean phytoplankton. *Journal of Phycology,* 16**,** 28-35.

HAYASHI, O., ONO, S., ISHII, K., SHI, Y., HIRAHASHI, T. & KATOH, T. 2006. Enhancement of proliferation and differentiation in bone marrow hematopoietic cells by Spirulina (Arthrospira) platensis in mice. *Journal of Applied Phycology,* 18**,** 47-56.

HEUILLET, E., MOREAU, A., HALPREN, S., JEANNE, N., & PUISEUX-DAO, S. 1986. Cadmium binding to a thiol molecule in vacuoles of Dunaliella bioculata contaminated with CdCl2: electron probe microanalysis. *Biology of the Cell,* 58**,** 79-86.

HOUSE OF COMMONS SCIENCE AND TECHNOLOGY SELECT COMMITTEE 2013. Bridging the valley of death: improving the commercialisation of research.

HRUDEY, S., BURCH, S., BURCH, M., DRIKAS, M., GREORGY, R. 1999. Remedial measures. *In:* CHORUS, I., BARTRAM, J (ed.) *Toxic cyanobacteria in water: a guide to their public health consequences, monitoring and management. WHO.* London: E & FN Spon.

HUBE, A. E., HEYDUCK-SÖLLER, B. & FISCHER, U. 2009. Phylogenetic classification of heterotrophic bacteria associated with filamentous marine cyanobacteria in culture. *Systematic and Applied Microbiology,* 32**,** 256-265.

ILLUMITEX. 2015. *Is full-spectrum light necessary for plant growth?* [Online]. Available: https://www.illumitex.com/full-spectrum-light-plant-growth/.

ITOH, S., OHNO, T., NOJI, T., YAMAKAWA, H., KOMATSU, H., WADA, K., KOBAYASHI, M. & MIYASHITA, H. 2015. Harvesting far-red light by chlorophyll f in photosystems I and II of unicellular cyanobacterium strain KC1. *Plant and Cell Physiology,* 56**,** 2024-2034.

JACELA, J. Y., DEROUCHEY, J.M., TOKACH, M.D., ET AL. 2010. Feed additives for swine: Fact sheets – high dietary levels of copper and zinc for young pigs, and phytase. *Journal of Swine Health and Production,* 18**,** 87-91.

JACOBSON, K., RAJFUR, Z., VITRIOL, E. & HAHN, K. 2008. Chromophore-assisted laser inactivation in cell biology. *Trends in Cell Biology,* 18**,** 443-450.

JIN, Z. P., LUO, K., ZHANG, S., ZHENG, Q. & YANG, H. 2012. Bioaccumulation and catabolism of prometryne in green algae. *Chemosphere,* 87**,** 278-284.

JODO, M., KAWAMOTO, K., TOCHIMOTO, M., & COVERLY, S. C. 1992. Determination of nutrients in seawater by segmented–flow analysis with higher analysis rate and reduced interference on ammonia. *The Journal of Automatic Chemistry,* 14**,** 163-167.

JOHNSON JR, J. C., NEWTON, G. L. & BUTLER, J. L. Recycling liquid dairy cattle waste to sustain annual triple crop production of forages. 28th Annual Florida Dairy Production Conference, 1991 Gainesville, Florida.

JONES, M. N. 1984. Nitrate reduction by shaking with cadmium. *Water Research,* 18**,** 643-646.

KANWISHER, J. 1959. Polarographic oxygen electrode. *Limnology and Oceanography,* 4**,** 210-217.

KARAN, V., VITOROVIC, S., TUTUNDZIC, V. & POLEKSIC, V. 1998. Functional enzymes activity and gill histology of carp after copper sulfate exposure and recovery. *Ecotoxicol Environ Saf,* 40**,** 49-55.

KARAPETYAN, N. V., BOLYCHEVTSEVA, Y. V., YURINA, N. P., TEREKHOVA, I. V., SHUBIN, V. V. & BRECHT, M. 2014. Long-wavelength chlorophylls in photosystem I of cyanobacteria: origin, localization, and functions. *Biochemistry (Moscow),* 79**,** 213-220.

KARPOUZAS, D. G., FOTOPOULOU, A., MENKISSOGLU-SPIROUDI, U. & SINGH, B. K. 2005. Non-specific biodegradation of the organophosphorus pesticides, cadusafos and ethoprophos, by two bacterial isolates. *FEMS Microbiology Ecology,* 53**,** 369-378.

KEHOE, D. M. 2010. Chromatic adaptation and the evolution of light color sensing in cyanobacteria. *Proceedings of the National Academy of Sciences of the United States of America,* 107**,** 9029-9030.

KHAN, N. & ABAS, N. 2011. Comparative study of energy saving light sources. *Renewable and Sustainable Energy Reviews*, 15**,** 296-309.

KHANNA, V. K. 2014. *Fundamentals of solid-state lighting. LEDs, OLEDs, and their applications in illumination and displays,* Florida, CRC Press.

KIRK, J. O. T. 2000. *Light and photosynthesis in aquatic systems,* Cambridge, Cambridge University Press.

KLIMANT, I. 2004. 'Method and device for referencing fluorescence intensity signals' published as US6770220B1.

KLUG, W., CUMMINGS, M.R. 1997. *Concepts of genetics,* Englewood Cliffs, NJ, Prentice Hall.

KUMAR, K., DASGUPTA, C. N., NAYAK, B., LINDBLAD, P. & DAS, D. 2011a. Development of suitable photobioreactors for CO2 sequestration addressing global warming using green algae and cyanobacteria. *Bioresource Technology,* 102**,** 4945-4953.

KUMAR, M., KULSHRESHTHA, J., & SINGH, G. P. 2011b. Growth and biopigment accumulation of cyanobacterium Spirulina platensis at different light intensities and temperature. *Brazilian Journal of Microbiology,* 42**,** 1128–1135.

LAU, R. H., MACKENZIE, M.M., & DOOLITTLE, W. F. 1977. Phycocyanin synthesis and degradation in the blue-green bacterium Anacystis nidulans. *Journal of Bacteriology* 132**,** 771-778.

LAWTON, L., MARSALEK, B., PADISAK, J., & CHORUS, I. 1999. Chapter 12. Determination of cyanobacteria in the laboratory. *In:* CHORUS, I., BARTRAM, J. (ed.) *Toxic Cyannobacteria in Water: A guide to their public health consequences, monitoring and management (WHO).* London: E & FN Spon.

LEE, R. E. 2008. *Phycology. Fourth Editition,* Cambridge, Cambridge University Press.

LEVIN, G., Mokady, S. 1994. Antioxidant activity of 9-cis compared to all-trans β-carotene in vitro. *Free Radical Biology and Medicine,* 17**,** 77-82.

LI, Y. & CHEN, M. 2015. Novel chlorophylls and new directions in photosynthesis research. *Functional Plant Biology,* 42**,** 493-501.

LICHTENTHALER, H. K. 1987. Chlorophylls and carotenoids - pigments of photosynthetic biomembranes. *Methods in Enzymology,* 148**,** 350–382.
LIU, J., TAO, Y., WU, J., ZHU, Y., GAO, B., TANG, Y., LI, A., ZHANG, C. & ZHANG, Y. 2014. Effective flocculation of target microalgae with self-flocculating microalgae induced by pH decrease. *Bioresource technology,* 167**,** 367-375.
LOPEZ-RODAS, V., AGRELO, M., CARRILLO, E., FERRERO, L. M., LARRAURI, A., MARTIN-OTERO, L. & COSTAS, E. 2001. Resistance of microalgae to modern water contaminants as the result of rare spontaneous mutations. *European Journal of Phycology,* 36**,** 179-190.
LUMITRONIX. *High power SMD leiste technisches datenblatt (53802)* [Online]. Available: http://www.leds.de/out/media/techn__Datenblatt.a82fe626.pdf.
LURIA, S. E. & DELBRÜCK, M. 1943. Mutations of bacteria from virus sensitivity to virus resistance. *Genetics,* 28**,** 491–511.
LYNN, S. G., PRICE, D. J., BIRGE, W. J. & KILHAM, S. S. 2007. Effect of nutrient availability on the uptake of PCB congener 2,2',6,6'-tetrachlorobiphenyl by a diatom (Stephanodiscus minutulus) and transfer to a zooplankton (Daphnia pulicaria). *Aquatic Toxicology,* 83**,** 24-32.
MA, Z. & GAO, K. 2010. Spiral breakage and photoinhibition of Arthrospira platensis (Cyanophyta) caused by accumulation of reactive oxygen species under solar radiation. *Environmental and Experimental Botany,* 68**,** 208-213.
MAEDA, K., OWADA, M., KIMURA, N., OMATA, K. & KARUBE, I. 1995. CO2 fixation from the flue gas on coal-fired thermal power plant by microalgae. *Energy Conversion and Management,* 36**,** 717-720.
MARKOU, G. 2014. Effect of various colors of light-emitting diodes (leds) on the biomass composition of arthrospira platensis cultivated in semi-continuous mode. *Applied Biochemistry and Biotechnology,* 172**,** 2758-2768.
MARKOU, G., CHATZIPAVLIDIS, I. & GEORGAKAKIS, D. 2012. Carbohydrates production and bio-flocculation characteristics in cultures of Arthrospira (Spirulina) platensis: improvements through phosphorus limitation process. *BioEnergy Research,* 5**,** 915-925.
MARQUEZ-ROCHA, F. 1999. Reassessment of the bioenergetic yield of Arthrospira platensis using continuous culture. *World Journal of Microbiology and Biotechnology,* 15**,** 235-238.
MARQUEZ, F., SASAKI, K., NISHIO, N. & NAGAI, S. 1995. Inhibitory effect of oxygen accumulation on the growth of Spirulina platensis. *Biotechnology Letters,* 17**,** 225-228.
MASAMOTO, K., ZSIROS, O. & GOMBOS, Z. 1999. Accumulation of zeaxanthin in cytoplasmic membranes of the cyanobacterium Synechococcus sp. strain PCC7942 grown under high light condition. *Journal of Plant Physiology,* 155**,** 136-138.
MASSA, G. D., KIN, H.H., WHEELER, R.M., & MITCHELL, C. A. 2008. Plant productivity in response to LED lighting. *HortScience,* 43**,** 1951-1956.
MATTHIJS, H. C. P., BALKE, H., VAN HES, U. M., KROON, B. M. A., MUR, L. R. & BINOT, R. A. 1996. Application of light-emitting diodes in bioreactors: flashing light effects and energy economy in algal culture (Chlorella pyrenoidosa). *Biotechnology and Bioengineering,* 50**,** 98-107.
MCKINSEY & COMPANY 2012. Lighting the way: perspectives on the global lighting market. Second ed.
MELNYK, A. H., WONG, A., KASSEN, R. 2015. The fitness cost of antibiotic resistance mutations. *Evolutionary Applications,* 8**,** 273-283.
MILFORD, A. D., ACHENBACH, L. A., JUNG, D. O. & MADIGAN, M. T. 2000. Rhodobaca bogoriensis gen. nov. and sp. nov., an alkaliphilic purple nonsulfur bacterium from African Rift Valley soda lakes. *Archives of Microbiology,* 174**,** 18-27.
MILLÁN-OROPEZA, A., TORRES-BUSTILLOS, L. G. & FERNÁNDEZ-LINARES, L. 2015. Simultaneous effect of nitrate (NO3-) concentration, carbon dioxide (CO2) supply and nitrogen limitation on biomass, lipids, carbohydrates and proteins accumulation in Nannochloropsis oculata. *Biofuel Research Journal,* 2**,** 215-221.
MITSUHASHI, S., FUJIMOTO, M., MURAMATSU, H. & TANISHITA, K. 1994. Effect of simple shear flow on photosynthesis rate and morphology of micro algae. *Acta Astronautica,* 33**,** 179-187.

MITSUHASHI, S., HOSAKA, K., TOMONAGA, E., MURAMATSU, H. & TANISHITA, K. 1995. Effects of shear flow on photosynthesis in a dilute suspension of microalgae. *Applied Microbiology and Biotechnology,* 42**,** 744-749.

MITTLER, R. 2002. Oxidative stress, antioxidants and stress tolerance. *Trends in Plant Science,* 7**,** 405-410.

MIYASHITA, H., IKEMOTO, H., KURANO, N., ADACHI, K., CHIHARA, M. & MIYACHI, S. 1996. Chlorophyll d as a major pigment. *Nature,* 383**,** 402-402.

MOHANA, S., ACHARYA, B. K. & MADAMWAR, D. 2009. Distillery spent wash: treatment technologies and potential applications. *Journal of Hazardous Material,* 163**,** 12-25.

MORAES, C. C., SALA, L., CERVEIRA, G. P. & KALIL, S. J. 2011. C-phycocyanin extraction from Spirulina platensis wet biomass. *Brazilian Journal of Chemical Engineering,* 28**,** 45-49.

MORALES-SÁNCHEZ, D., MARTINEZ-RODRIGUEZ, O. A., KYNDT, J. & MARTINEZ, A. 2015. Heterotrophic growth of microalgae: metabolic aspects. *World Journal of Microbiology and Biotechnology,* 31**,** 1-9.

MORRIS, A. W. & RILEY, J. P. 1963. The determination of nitrate in seawater. *Analytica Chimica Acta,* 29**,** 272-279.

MORROW, R. C. 2008. LED lighting in horticulture. *Hortscience,* 43**,** 1947-1950.

MOSTOFA, K. M. G., LIU, C-Q., MOTTALEB, M.A., WAN, G., OGAWA, H., VIONE, D., YOSHIOKA, T., & WU, F. 2013. Dissolved organic matter in natural waters. *In:* MOSTOFA, K. M. G. (ed.) *Photobiogeochemistry of organic matter, Environmental science & engineering.* Berlin: Springer-Verlag.

MUELLER-MACH, R., MUELLER, G.O., KRAMES, M.R., TROTTIER, T. 2002. High-power phosphor-converted light-emitting diodes based on III-Nitrides. *IEEE Journal of Selected Topics in Quantum Electronics***,** 339-345.

MUEVO-TECHNIK. *High power top LED SMB680-1100-02-I specifications* [Online]. Available: http://www.ir-led.de/fileadmin/Specification/smb_leds/SMB680-1100-02-I.pdf.

MULLINEAUX, C. W. 1992. Excitation energy transfer from phycobilisomes to Photosystem I in a cyanobacterium. *Biochimica et Biophysica Acta (BBA) - Bioenergetics,* 1100**,** 285-292.

NALIMOVA, A. A., POPOVA, V.V., TSOGLIN, L.N., & PRONINA, N. A. 2005. The effects of copper and zinc on Spirulina platensis growth and heavy metal accumulation in its cells. *Russian Journal of Plant Physiology,* 52**,** 229-234.

NARENDRAN, N., MALIYAGODA, N., DENG, L. & PYSAR, R. Characterizing LEDs for general illumination applications: mixed-color and phosphor-based white sources. *In:* FERGUSON, I. T., PARK, Y. S., NARENDRAN, N. & DENBAARS, S. P., eds. Solid State Lighting and Displays, 5th December 2001 California, USA. SPIE Proceedings, 137-147.

NELSON, J. A. & BUGBEE, B. 2014. Economic analysis of greenhouse lighting: light emitting diodes vs. high intensity discharge fixtures. *PLoS ONE,* 9**,** e99010.

NEMEROW, N. L. 2007. *Industrial waste treatment: contemporary practice and vision for the future,* Oxford, Elsevier.

NISHIYAMA, Y., ALLAKHVERDIEV, S. & MURATA, N. 2005. Inhibition of the repair of Photosystem II by oxidative stress in cyanobacteria. *Photosynthesis Research,* 84**,** 1-7.

NNFCC 2011. Newsletter - Issue 21. Incentives for Bioenergy.

NOMSAWAI, P., TANDEAU DE MARSAC, N., THOMAS, J.C., TANTICHAROEN, M., & CHEEVADHANARAK, S. 1999. Light regulation of phycobilisome structure and gene expression in *Spirulina platensis* C1 (*Arthrospira* sp. PCC 9438). *Plant and Cell Physiology,* 40**,** 1194-1202.

OBERNOSTERER, I. & HERNDL, G. J. 1995. Phytoplankton extracellular release and bacterial growth: dependence on the inorganic N:P ratio. *Marine Ecology Progress Series,* 116**,** 247-257.

OGBONNA, J. C., YADA, H. & TANAKA, H. 1995. Effect of cell movement by random mixing between the surface and bottom of photobioreactors on algal productivity. *Journal of Fermentation and Bioengineering,* 79**,** 152-157.

OLAIZOLA, M. & DUERR, E. 1990. Effects of light intensity and quality on the growth rate and photosynthetic pigment content of Spirulina platensis. *Journal of Applied Phycology,* 2**,** 97-104.

ÖQUIST, G. 1971. Changes in pigment composition and photosynthesis induced by iron-deficiency in the blue-green alga Anacystis nidulans. *Physiologia Plantarum,* 25**,** 188-191.
ORGANIC MONITOR 2015. The Asian market for natural and organic cosmetics [Online]. Available: http://www.organicmonitor.com/500160.htm.
PALOZZA, P. & KRINSKY, N. 1992. Antioxidant effects of carotenoids in vivo and in vitro: an overview. *Methods in Enzymology,* 213**,** 403-420.
PARDHASARADHI, B. V., ALI, A. M., KUMARI, A. L., REDDANNA, P. & KHAR, A. 2003. Phycocyanin-mediated apoptosis in AK-5 tumor cells involves down-regulation of Bcl-2 and generation of ROS. *Molecular Cancer Therapeutics,* 2**,** 1165-1170.
PARNABY, J. 1990. The Engineering Doctorate. A SERC working party report to the Engineering Board of the Science and Engineering Research Council.
PERRY, M., GOLDING, N. 2011. Range of environmental temperature conditions in the United Kingdom. For: Department of Transport. Met Office.
PHILLIPS JR, J. N. & MYERS, J. 1954. Growth rate of chlorella in flashing light. *Plant Physiology,* 29**,** 152-161.
PINEDA, F. J., ANTOINE, M. D., DEMIREV, P. A., FELDMAN, A. B., JACKMAN, J., LONGENECKER, M. & LIN, J. S. 2003. Microorganism identification by matrix-assisted laser/desorption ionization mass spectrometry and model-derived ribosomal protein biomarkers. *Analytical Chemistry,* 75**,** 3817-3822.
PIÑERO ESTRADA, J. E., BERMEJO BESCÓS, P. & VILLAR DEL FRESNO, A. M. 2001. Antioxidant activity of different fractions of Spirulina platensis protean extract. *Il Farmaco,* 56**,** 497-500.
PIORRECK, M., BAASCH, K.H., POHL, P. 1984. Biomass production, total protein, chlorophylls, lipids and fatty acids of freshwater green and blue-green algae under different nitrogen regimes. *Phytochemistry,* 23**,** 207-216.
PISAL, D. S., LELE, S.S. 2005. Carotenoid production from microalga, *Dunaliella salina*. *Indian Journal of Biotechnology,* 4**,** 476-483.
POPLAWSKI, M. 2012. LED dimming: what you need to know for U.S. Department of Energy. Energy efficiency & renewable energy. DOE SSL Program.
POSTEN, C. 2009. Design principles of photo-bioreactors for cultivation of microalgae. *Engineering in Life Sciences,* 9**,** 165-177.
PUDDU, A., ZOPPINI, A., FAZI, S., ROSATI, M., AMALFITANO, S. & MAGALETTI, E. 2003. Bacterial uptake of DOM released from P-limited phytoplankton. *FEMS Microbiology Ecology,* 46**,** 257-268.
RAI, L. C. & GAUR, J. P. 2001. *Algal adaptation to environmental stresses: phsiological, biochemical and molecular mechanisms,* Berlin, Springer-Verlag.
RAI, L. C., GAUR, J.P., & KUMAR, H. D. 1981. Protective effects of certain environmental factors on the toxicity of zinc, mercury, and methylmercury to Chlorella vulgaris. *Environmental Research,* 25**,** 250-259.
RAJA, R., HEMAISWARYA, S. & RENGASAMY, R. 2007. Exploitation of Dunaliella for β-carotene production. *Applied Microbiology and Biotechnology,* 74**,** 517-523.
RAKHIMBERDIEVA, M. G., BOICHENKO, V.A., KARAPETYAN, N.V., STADNICHUK, I.N. 2001. Interaction of phycobilisomes with photosystem II dimers and photosystem I monomers and trimers in the cyanobacterium Spirulina platensis. *Biochemistry,* 40**,** 15780-15788.
RAOOF, B., KAUSHIK, B. D. & PRASANNA, R. 2006. Formulation of a low-cost medium for mass production of Spirulina. *Biomass and Bioenergy,* 30**,** 537-542.
RATHA, S. K. & PRASANNA, R. 2012. Bioprospecting microalgae as potential sources of "green energy" - challenges and perspectives (review). *Prikl Biokhim Mikrobiol,* 48**,** 133-149.
RAUSER, W. E. 1990. Phytochelatins. *Annual Review of Biochemistry,* 59**,** 61-86.
RAVEN, J. A., WOLLENWEBER, B., & HANDLEY, L. L. 1993. The quantitive role of ammonia/ammonium transport and metabolism by plants in the global nitrogen cycle. *Physiologia Plantarum,* 89**,** 512-518.

REID, B., SISSONS, ANDREW, BRINKLEY, I., LEVY, C., ALBERT, A., HOLLOWAY,C. 2010. Technology Innovation Centres: Applying the Fraunhofer model to create an effective Innovation Ecosystem in the UK, Science and Technology Select Committee.

RESEARCH COUNCILS UK 2014. Impact Report 2014.

RICHMOND, A. 2004. Environmental effects on cell composition. *In:* HU, Q. (ed.) *Handbook of microalgal culture: biotechnology and applied phycology.* Oxford: Blackwell Science.

RITO-PALOMARES, M., NUNES, L., AMADOR, D. 2001. Practical application of aqueous two-phase systems for the development of a prototype process for c-phycocyanin recovery from spirulina maxima. *Journal of Chemical Technology and Biotechnology,* 76**,** 1273-1280.

ROBERTSON, D., JACOBSON, S., MORGAN, F., BERRY, D., CHURCH, G., AFEYAN, N. 2011. A New Dawn for Industrial Photosynthesis. *Photosynthesis Research,* 107**,** 269-277.

ROBINSON, L. F., MORRISON, A.W. 1993. 'Improvements relating to biomass production' published as EP0239272B1.

ROMAY, C., ARMESTO, J., REMIREZ, D., GONZALEZ, R., LEDON, N. & GARCIA, I. 1998. Antioxidant and anti-inflammatory properties of C-phycocyanin from blue-green algae. *Inflammation Research,* 47**,** 36-41.

ROMAY, C., GONZALEZ, R., LEDON, N., REMIREZ, D. & RIMBAU, V. 2003. C-phycocyanin: a biliprotein with antioxidant, anti-inflammatory and neuroprotective effects. *Current Protein & Peptide Science,* 4**,** 207-216

ROSENTHAL, M. 2011. Not Your Father's Algae. *Biomass Magazine.*

ROY, K. R., NISHANTH, R. P., SREEKANTH, D., REDDY, G. V. & REDDANNA, P. 2008. C-Phycocyanin ameliorates 2-acetylaminofluorene induced oxidative stress and MDR1 expression in the liver of albino mice. *Hepatology Research,* 38**,** 511-520.

RUBIO, F. C., CAMACHO, F.G., SEVILLA, J.M.F., CHISTI, Y., GRIMA, E.M. 2003. A mechanistic model of photosynthesis in microalgae. *Biotechnology and Bioengineering,* 81**,** 459-473.

SABZALIAN, M. R., HEYDARIZADEH, P., ZAHEDI, M., BOROOMAND, A., AGHAROKH, M., SAHBA, M. R. & SCHOEFS, B. 2014. High performance of vegetables, flowers, and medicinal plants in a red-blue LED incubator for indoor plant production. *Agronomy for Sustainable Development,* 34**,** 879-886.

SALAUN, S., KERVAREC, N., POTIN, P., HARAS, D., PIOTTO, M. & LA BARRE, S. 2010. Whole-cell spectroscopy is a convenient tool to assist molecular identification of cultivatable marine bacteria and to investigate their adaptive metabolism. *Talanta,* 80**,** 1758-1770.

SANDMANN, G., BÖGER, P. 1980. Copper deficiency and toxicity in Scenedesmus. *Zeitschrift fur Pflanzenphysiologie,* 98**,** 53-59.

SANDNES, J. M., RINGSTAD, T., WENNER, D., HEYERDAHL, P. H., KÄLLQVIST, T. & GISLERØD, H. R. 2006. Real-time monitoring and automatic density control of large-scale microalgal cultures using near infrared (NIR) optical density sensors. *Journal of Biotechnology,* 122**,** 209-215.

SANTOYO, S., RODRÍGUEZ-MEIZOSO, I., CIFUENTES, A., JAIME, L., GARCÍA-BLAIRSY REINA, G., SEÑORANS, F. J. & IBÁÑEZ, E. 2009. Green processes based on the extraction with pressurized fluids to obtain potent antimicrobials from Haematococcus pluvialis microalgae. *LWT - Food Science and Technology,* 42**,** 1213-1218.

SANZ-LUQUE, E., CHAMIZO-AMPUDIA, A., LLAMAS, A., GALVAN, A., & FERNANDEZ, E. 2015. Understanding nitrate assimilation and its regulation in microalgae. *Frontiers in Plant Science,* 6**,** 899.

SARADA, R., PILLAI, M. G. & RAVISHANKAR, G. A. 1999. Phycocyanin from Spirulina sp: influence of processing of biomass on phycocyanin yield, analysis of efficacy of extraction methods and stability studies on phycocyanin. *Process Biochemistry,* 34**,** 795-801.

SCHITÜTER, L., RIEMANN, B. & SØNDERGAARD, M. 1997. Nutrient limitation in relation to phytoplankton carotenoid/chiorophyll a ratios in freshwater mesocosms. *Journal of Plankton Research,* 19**,** 891-906.

SCHLARD-RIDLEY, B. 2011. Algal research in the UK. BBSRC scoping study [Online]. Available: http://www.bbsrc.ac.uk/documents/algal-scoping-study-report-pdf/.

SCHLARB-RIDLEY, B., PARKER, B. 2013. Roadmap of Algal Technologies, NERC-TSB Algal Bioenergy-SIG.
SCHLICHTING, C. D., SMITH, H. 2002. Phenotypic plasticity: linking molecular mechanisms with evolutionary outcomes. *Evolutionary Ecology,* 16**,** 189-211.
SCHOLAND, M. J., DILLON, M.E. 2012. U.S. Department of Energy. Energy efficiency & renewable energy. Building Technologies Program. Life-cycle assessment of energy and environmental impacts of LED lighting products Part 2: LED manufacturing and performance.
SCHULZ ZUR WIESCH, P., ENGELSTADTER, J. & BONHOEFFER, S. 2010. Compensation of fitness costs and reversibility of antibiotic resistance mutations. *Antimicrobial Agents and Chemotherapy,* 54**,** 2085-2095.
SCOTT, A. 2014. Blue biotechnology rises from below. *Chemical and Engineering News,* 92**,** 21-23.
SETHUNATHAN, N., MEGHARAJ, M., CHEN, Z. L., WILLIAMS, B. D., LEWIS, G. & NAIDU, R. 2004. Algal degradation of a known endocrine disrupting insecticide, alpha-endosulfan, and its metabolite, endosulfan sulfate, in liquid medium and soil. *Journal of Agricultural and Food Chemistry,* 52**,** 3030-3035.
SHARMA, K. K., SCHUHMANN, H., SCHENK, P.M. 2012. High Lipid Induction in Microalgae for Biodiesel Production. *Energies,* 5**,** 1532-1553.
SHARP, J., FRAKE, A.C., HILLIER, G.B., & UNDERHILL, P. A. 1982. Modeling nutrient regeneration in the ocean with an aquarium system. *Marine Ecology - Progress Series,* 8**,** 15-23.
SHI, J. W., KUO, F.M., LIN, C.W., & CHEN, W. 2011. Investigation of the efficiency-droop mechanism in vertical red light-emitting diodes using a dynamic measurement technique. *Photonics Technology Letters, IEEE* 23**,** 1585 - 1587.
SIEGELMAN, H.W., KYCIA, J.H. 1978. *Algal bili-proteins: handbook of phycological method,* Cambridge, Cambridge University Press.
SILVER, S., PHUNG, L.T. 1996. Bacterial heavy metal resistance: new surprises. *Annual Review of Microbiol,* 50**,** 753-789.
SINGH, B. K. & WALKER, A. 2006. Microbial degradation of organophosphorus compounds. *FEMS Microbiology Reviews,* 30**,** 428-471.
SINGH, D. P., SINGH, N. & VERMA, K. 1995. Photooxidative damage to the cyanobacterium Spirulina platensis mediated by singlet oxygen. *Current Microbiology,* 31**,** 44-48.
SKILL, S. 2013. Use of Algae in AD. ADBA R&D Forum Presentation Slides [Online]. Available: adbiogas.co.uk/wp-content/uploads/2013/11/Steve-Skill.pdf.
SMITH, C. 2010. Assessing the potential for algae in the UK. Department of Energy and Climate Change (DECC) [Online]. Available: nnfcc.co.uk/tools/assessing-the-potential-for-algae-in-the-uk
SMITH, S. W. 1997. Moving average filters. *In:* SMITH, S. W. (ed.) *The scientist and engineer's guide to digital signal processing.* California: California Technical Publishing.
SNIEGOWSKI, P. D. 2005. Linking mutation to adaptation: overcoming stress at the spa. *New Phytologist,* 166**,** 360-362.
SOLOVCHENKO, A. & CHEKANOV, K. 2014. Production of carotenoids using microalgae cultivated in photobioreactors. *In:* PAEK, K.-Y., MURTHY, N. H. & ZHONG, J.-J. (eds.) *Production of biomass and bioactive compounds using bioreactor technology.* Dordrecht: Springer Netherlands.
SPARAVIGNA, A. C. 2014. Light-emitting diodes in the solid-state lighting systems. *International Journal of Sciences,* 3**,** 9-17.
SPELLMAN, F. R. 2009. *The science of water: concepts and applications,* Florida, CRC Press.
SRIVASTAVA, A. K., RAI, A.R., & NEILAN, B. A. 2013. *Stress biology of cyanobacteria - molecular mechanisms to cellular responses,* Florida, CRC Press.
STALLINGS, C. C. 2011. Feeding cows with increasing feed prices: efficiencies, feed options, and quality control. 47th Florida Dairy Production Conference, Gainesville, Florida.
STEEN, I. 1998. Phosphorus availibility in the 21st Century: management of a non-renewable resource. *Phosphorus and Potassium,* 217**,** 25-31.
STEFFENS, J. C. 1990. The Heavy Metal-Binding Peptides of Plants. *Annual Review of Plant Physiology and Plant Molecular Biology,* 41**,** 553-575.

STOKES, P. M. & DREIER, S. I. 1981. Copper requirement of a copper-tolerant isolate of Scenedesmus and the effect of copper depletion on tolerance. *Canadian Journal of Botany,* 59**,** 1817-1823.
STRICKLAND, J. D. H. & PARSONS, T. R. 1968. Determination of reactive nitrate. *A Practical Handbook of Seawater Analysis.* Fisheries Research Board of Canada. Bulletin 167. 71-75.
SU, X., FRAENKEL, P.G., & BOGORAD, L. 1992. Excitation energy transfer from phycocyanin to chlorophyll in an apcA-defective mutant of Synechocystis sp. PCC 6803. *Journal of Biological Chemistry,* 267**,** 22944-22950.
SUDHIR, P. R., POGORYELOV, D., KOVACS, L., GARAB, G. & MURTHY, S. D. 2005. The effects of salt stress on photosynthetic electron transport and thylakoid membrane proteins in the cyanobacterium Spirulina platensis. *Journal of Biochemistry and Molecular Biology,* 38**,** 481-485.
SUJATHA, K. & NAGARAJAN, P. 2013. Optimization of growth conditions for carotenoid production from Spirulina platensis (Geitler). *International Journal of Current Microbiology and Applied Sciences,* 2**,** 325-328.
SWEET, J. 2014. GM Algae Regulation and Risk Assessment. Phyconet (BBSRC NIBB) symposium, April 14th, London.
TAKAICHI, S., JUNG, D. O. & MADIGAN, M. T. 2001. Accumulation of unusual carotenoids in the spheroidene pathway, demethylspheroidene and demethylspheroidenone, in an alkaliphilic purple nonsulfur bacterium Rhodobaca bogoriensis. *Photosynthesis Research,* 67**,** 207-214.
TAMARY, E., KISS, V., NEVO, R., ADAM, Z., BERNAT, G., REXROTH, S., ROGNER, M. & REICH, Z. 2012. Structural and functional alterations of cyanobacterial phycobilisomes induced by high-light stress. *Biochimica et Biophysica Acta,* 1817**,** 319-27.
TANDEU DE MARSAC, N. 1977. Occurrence and nature of chromatic adaptation in cyanobacteria. *Journal of Bacteriology,* 130**,** 82-91.
TERAMOTO, K., SATO, H., SUN, L., TORIMURA, M., TAO, H., YOSHIKAWA, H., HOTTA, Y., HOSODA, A. & TAMURA, H. 2007. Phylogenetic classification of Pseudomonas putida strains by MALDI-MS using ribosomal subunit proteins as biomarkers. *Analytical Chemistry,* 79**,** 8712-9.
THE ROYAL SOCIETY 2010. The scientific century: securing our future prosperity.
TOMASELLI L, G. L. & MARGHERI, M. 1981. On the mechanism of trichome breakage in Spirulina platensis and S. maxima. *Annuals of Microbiology,* 31**,** 27-31.
TORZILLO, G., BERNARDINI, P. & MASOJIDEK, J. 1998. On-line monitoring of chlorophyll fluorescence to assess the extent of photoinhibition of photosynthesis induced by high oxygen concentration and low temperature and its effect on the productivity of outdoor cultures of Spirulina platensis (Cyanobacteria). *Journal of Phycology,* 34**,** 504-510.
TORZILLO, G., PUSHPARAJ, B., MASOJIDEK, J. & VONSHAK, A. 2003. Biological constraints in algal biotechnology. *Biotechnology and Bioprocess Engineering,* 8**,** 338-348.
TSOUPEIS, D. 2009 Algae's impact on the food-versus-fuel debate. *Biodiesel Magazine.*
TURNER DESIGNS. *Trilogy laboratory fluorometer manual, application note: nitrate analysis s-0091.* [Online]. Available: http://www.turnerdesigns.com/products/laboratory-fluorometer/trilogy-laboratory-fluorometer.
TWISS, M. R. 1990. Copper tolerance of chlamydomonas acidophila (chlorophyceae) isolated from acidic, copper-contaminated soils. *Journal of Phychology,* 26**,** 655-659.
UNITED STATES GOVERNMENT PUBLISHING OFFICE. 2013. Federal Register Volume 78, Number 156 (Tuesday, August 13, 2013), Rules and Regulations, Pages 49117-49120.
U.S. DEPARTMENT OF ENERGY 2013. Energy Efficiency & Renewable Energy Building Technologies Program, Solid-State Lighting Technology Fact Sheet, Energy Efficiency of LEDs.
UMEDA, H., SASAKI, A., TAKAHASHI, K., HAGA, K., TAKASAKI, Y., SHIBAYAMA, A. 2011. Recovery and Concentration of Precious Metals from Strong Acidic Wastewater. *Materials Transactions,* 52**,** 1462-1470.
VALENTINE, N., WUNSCHEL, S., WUNSCHEL, D., PETERSEN, C. & WAHL, K. 2005. Effect of culture conditions on microorganism identification by matrix-assisted laser desorption ionization mass spectrometry. *Applied and Environmental Microbiology,* 71**,** 58-64.

VAN ALSTYNE, D. C., VAN ALSTYNE, L.E. 2009. *Systems and methods for production of Biofuel*. WO2009063296.

VAN ALSTYNE, D. C.D, BRAIN, C.M., CALDWELL, G.S. 2014. 'Micro-evolution of Microbes' published as WO2014102551A1 on 3rd July 2014. https://www.google.com/patents/WO2014102551A1?cl=en.

VINOTHINI, C., SUDHAKAR, S., & RAVIKUMAR, R. 2015. Biodegradation of petroleum and crude oil by *Pseudomonas putida* and *Bacillus cereus*. *International Journal of Current Microbiology and Applied Sciences* 4**,** 318-329.

VIRAVAIDYA-PASUWAT, K., KOAYKUL, C., WONG-IN, S. 2014. Effect of light-emitting diode wavelengths on human dermal fibroblasts for phototherapy. *Biomedical Engineering International Conference (BMEiCON).* Fukuoka, Japan: IEEE.

VONSHAK, A. 1997. *Spirulina platensis (Arthrospira): physiology, cell biology and biotechnology,* London, Taylor & Francis.

WALTER, A., CARVALHO, J. C. D., SOCCOL, V. T., FARIA, A. B. B. D., GHIGGI, V. & SOCCOL, C. R. 2011. Study of phycocyanin production from Spirulina platensis under different light spectra. *Brazilian Archives of Biology and Technology,* 54**,** 675-682.

WANG, C.-Y., FU, C.-C. & LIU, Y.-C. 2007. Effects of using light-emitting diodes on the cultivation of Spirulina platensis. *Biochemical Engineering Journal,* 37**,** 21-25.

WEBER, R. W., HOFFMAN, M., RAINE, D. A., JR. & NELSON, H. S. 1979. Incidence of bronchoconstriction due to aspirin, azo dyes, non-azo dyes, and preservatives in a population of perennial asthmatics. *Journal of Allergy and Clinical Immunology,* 64**,** 32-37.

WESSNER, C. W. 2013. *Fraunhofer-Gesellschaft: The German model of Applied Research in 21st Century Manufacturing: The Role of the Manufacturing Extension Program of the National Institute of Standards and Technology; Board on Science, Technology, and Economic Policy; National Research Council,* National Academies Press.

WIJANARKO, A. D., SENDJAYA, A., HERMANSYAH, H., WITARTO, A., GOZAN, M., SOFYAN, B., ASAMI, K., OHTAGUCHI, K., SOEMANTOJO, R. & SONG, S. 2008. Enhanced Chlorella vulgaris buitenzorg growth by photon flux density alteration in serial photobioreactors. *Biotechnology and Bioprocess Engineering,* 13**,** 476-482.

WOLLAN, M. 2016. Brand New Hue: The Quest to Make a True Blue M&M. New York Times Magazine. New York.

WOOD, E. D., ARMSTRONG, F.A.J., & RICHARDS, F. A. 1967. Determination of nitrate in sea water by cadmium-copper reduction to nitrite. *Journal of Marine Biological Association of the United Kingdom,* 47**,** 23-31.

WURTZ, E. A., SEARS, B. B., RABERT, D. K., SHEPHERD, H. S., GILLHAM, N. W. & BOYNTON, J. E. 1979. A specific increase in chloroplast gene mutations following growth of Chlamydomonas in 5-fluorodeoxyuridine. *Molecular & General Genetics,* 170**,** 235-242.

YANAGISAWA, T. 1998. The degradation of GaAlAs red light-emitting diodes under continuous and low-speed pulse operations. *Microelectronics Reliability,* 38**,** 1627-1630.

YSI INCORPORATED 2009. The Dissolved Oxygen Handbook: a practical guide to dissolved oxygen measurements.

ZEHR, J. P. 2011. Nitrogen fixation by marine cyanobacteria. *Trends in Microbiology,* 19**,** 162-173.

ZHANG, K., MIYACHI, S., KURANO, N. 2001. Evaluation of a vertical flat-plate photobioreactor for outdoor biomass production and carbon dioxide bio-fixation: effects of reactor dimensions, irradiation and cell concentration on the biomass productivity and irradiation utilization efficiency. *Applied Microbiology and Biotechnology,* 55**,** 428-433.

ZHANG, S., QIU, C. B., ZHOU, Y., JIN, Z. P. & YANG, H. 2011. Bioaccumulation and degradation of pesticide fluroxypyr are associated with toxic tolerance in green alga Chlamydomonas reinhardtii. *Ecotoxicology,* 20**,** 337-347.

ZHANG, X. 2015. Microalgae removal of CO2 from flue gas. London: IEA Clean Coal Centre.

ZHANG, Y.-M. & CHEN, F. 1999. A simple method for efficient separation and purification of c-phycocyanin and allophycocyanin from Spirulina platensis. *Biotechnology Techniques,* 13**,** 601-603.

ZHAO, K.-H., SU, P., TU, J.-M., WANG, X., LIU, H., PLÖSCHER, M., EICHACKER, L., YANG, B., ZHOU, M. & SCHEER, H. 2007. Phycobilin:cystein-84 biliprotein lyase, a near-universal lyase for cysteine-84-binding sites in cyanobacterial phycobiliproteins. *Proceedings of the National Academy of Sciences,* 104**,** 14300-14305.

Appendices

Appendix 1. Medium lists

Jaworskis Medium (JM)
Stocks per 200 ml:
(1) $Ca(NO_3)_2 \cdot 4H_2O$ 4.0 g
(2) KH_2PO_4 2.48 g
(3) $MgSO_4 \cdot 7H_2O$ 10.0 g
(4) $NaHCO_3$ 3.18 g
(5) EDTAFeNa 0.45 g
EDTANa2 0.45 g
(6) H_3BO_3 0.496 g
$MnCl_2 \cdot 4H_2O$ 0.278 g
$(NH_4)_6Mo_7O_{24} \cdot 4H_2O$ 0.20 g
(7) Cyanocobalamin 0.008 g
Thiamine HCl 0.008 g
Biotin 0.008 g
(8) $NaNO_3$ 16.0 g
(9) $Na_2HPO_4 \cdot 12H_2O$ 7.2 g
1 L of Medium: 1 mL of stock solutions 1-9, autoclave at 15 psi for 15 min.

Jaworskis Medium Modified (JMM)
Stocks per 200 ml:
(1) $CaCl_2$ 18.0 g
(2) KH_2PO_4 2.48 g
(3) $MgSO_4 \cdot 7H_2O$ 10.0 g
(4) $NaHCO_3$ 3.18 g
(5) EDTAFeNa 0.45 g
EDTANa2 0.45 g
(6) H_3BO_3 0.496 g
$MnCl_2 \cdot 4H_2O$ 0.278 g
$(NH_4)_6Mo_7O_{24} \cdot 4H_2O$ 0.20 g
(7) Cyanocobalamin 0.008 g
Thiamine HCl 0.008 g
Biotin 0.008 g
(8) $NaNO_3$ 17.44 g
(9) $Na_2HPO_4 \cdot 12H_2O$ 7.2 g
1 L of Medium: 1 mL of stock solutions 1-9, autoclave at 15 psi for 15 min.

F/2 Medium
Stocks per L:
(1) Trace metals stock solution (chelated)
- EDTANa2 - 4.360 g
- $FeCl_3 \cdot 6H_2O$ - 3.150 g
- $CuSO_4 \cdot 5H_2O$ - 0.010 g
- $ZnSO_4 \cdot 7H_2O$ - 0.022 g
- $CoCl_2 \cdot 6H_2O$ - 0.010 g
- $MnCl_2 \cdot 4H_2O$ - 0.180 g
- $Na_2MoO_4 \cdot 2H_2O$ - 0.006 g

(2) Vitamin mix stock solution
Cyanocobalamin - 0.0005 g
Thiamine HCl - 0.1 g
Biotin - 0.0005 g

1 L of Medium:
$NaNO_3$ - 0.075 g
$NaH_2PO_4.2H_2O$ - 0.00565 g
Trace metals stock solution (chelated) (1) 1.00 ml
Vitamin mix stock solution (2) 1.00 ml
Make up to 1 litre with filtered natural seawater and adjust pH to 8.0 with 1M NaOH or HCl. Autoclave at 15 psi for 15 min.

Appendix 2. Replicate MALDI-TOF mass spectra showing protein-mass spectral patterns of Arthrospira cultured under red (A) and white (B) light.

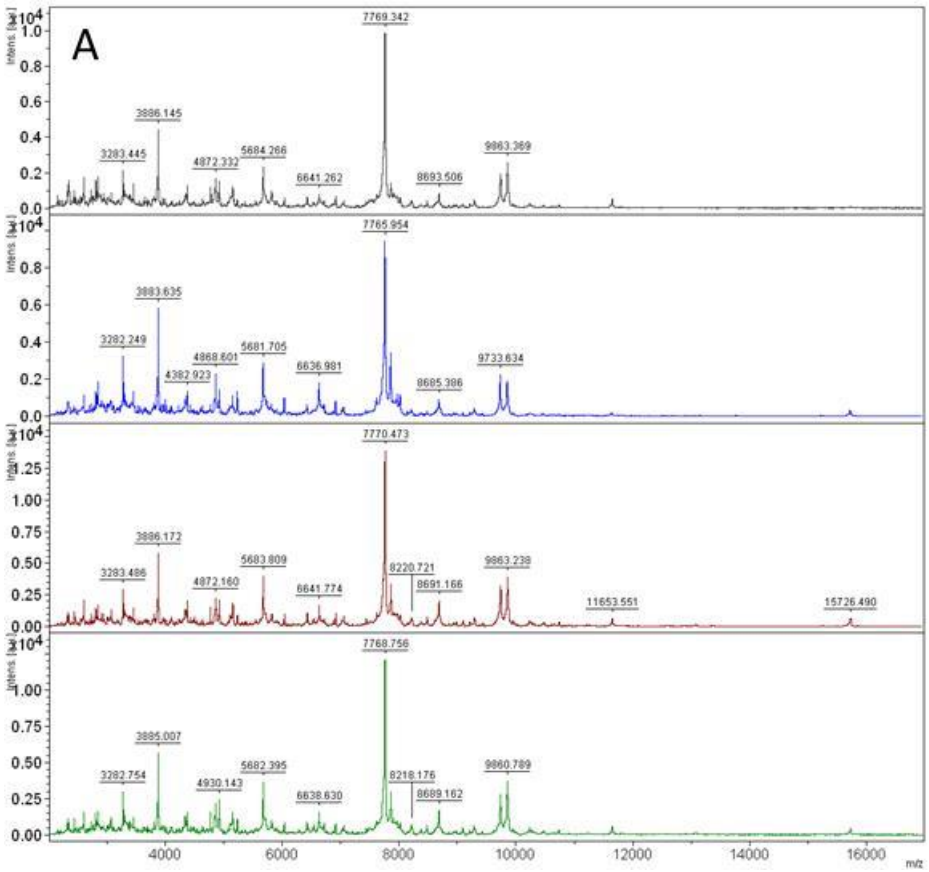

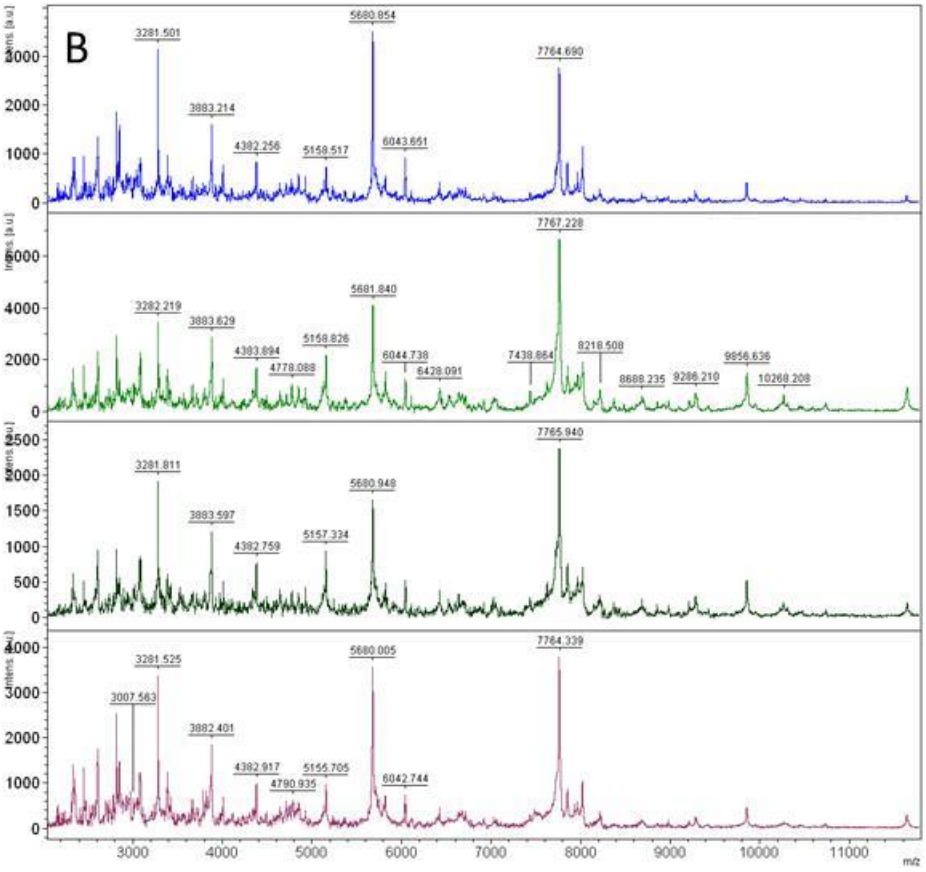
B
3281.501
5680.854
7764.690
3883.214
4382.256
5158.517
6043.651
7767.228
3282.219
5681.840
3883.629
5158.826
4383.894
4778.088
6044.738
6428.091
7438.864
8218.508
8688.235
9286.210
9856.636
10268.208
7765.940
3281.811
5680.948
3883.597
4382.759
5157.334
7764.339
3281.525
5680.005
3007.563
3882.401
4382.917
5155.705
4790.935
6042.744
3000
4000
5000
6000
7000
8000
9000
10000
11000
m/z